The Institute of Paper Chemistry

Appleton, Wisconsin

Doctor's Dissertation

The Importance of the Structure of Alkali Metal Hydroxide Solutions in Decrystallizing Cellulose I

Bruce E. Dimick

January, 1976

THE IMPORTANCE OF THE STRUCTURE OF ALKALI METAL HYDROXIDE SOLUTIONS IN DECRYSTALLIZING CELLULOSE I

A thesis submitted by

Bruce E. Dimick

B.A. 1968, Earlham College

M.S. 1972, Lawrence University

in partial fulfillment of the requirements
of The Institute of Paper Chemistry
for the degree of Doctor of Philosophy
from Lawrence University,
Appleton, Wisconsin

January, 1976

TABLE OF CONTENTS

	Page
SUMMARY	1
INTRODUCTION	4
THEORETICAL ASPECTS OF THE MERCERIZATION PROCESS	6
Introduction	6
General Theory of Polymer Swelling	6
Donnan Equilibrium Theory	8
Other Mercerization Theories	16
Temperature Effects	23
THESIS OBJECTIVES	25
EXPERIMENTAL PROGRAM	26
Selection of a Highly Crystalline Cellulose I	26
X-Ray Diffraction Procedure	27
Infrared Procedure	28
Mercerization	29
Preparation of Alkali Metal Hydroxide Solutions	29
Alkali Treatment of the Cellulose	31
Examination of the Mercerized Cellulose	32
X-Ray Diffraction	32
Laser Raman Spectroscopy	36
Raman Spectra of the Alkali Metal Hydroxides	38
Spectra of the Solutions	38
Polarization of the Band at 3610 cm^{-1}	38
Spectra of the Solids	40
Mercerization Using Mixed Electrolytes	40
Precipitation from the Dimethylsulfoxide-paraformaldehyde Cellulose Solvent System	41
Preparation of the Cellulose Solution	41
Precipitation from the Cellulose Solution	42

Page

High Temperature Wash of Fully Mercerized Cellulose 42

RESULTS AND DISCUSSION 44

Introduction 44

Evaluation of Cellulose I Crystallinity 44

X-Ray Analysis Method 45

Infrared Analysis Method 50

Results 52

Mercerization of Hydrocellulose with LiOH, NaOH, and KOH 55

Method of Analysis of the X-Ray Diffractograms of Mercerized Cellulose 55

Results of the Analysis of the X-Ray Diffractograms of Mercerized Cellulose 68

Raman Spectral Analysis of the Mercerized Hydrocellulose 78

Analysis of the Structure of the Alkali Metal Hydroxide Solutions 83

Analysis of the Raman Spectra of the Alkali Metal Hydroxide Solutions 83

Identification of the Band at 3610 cm^{-1} 87

Intramolecular Vibrational Spectrum of Water 89

Band Resolution of the Raman Spectra 91

Interpretation of the Results of the Band Resolution 92

Thermodynamic Considerations 106

Activity Coefficients of the Alkali Metal Hydroxides 106

The Water Removal Theory of Activity Coefficients 108

A Test of the Proposed Theory 115

Effect of Temperature on the Lattice Type Assumed by Cellulose Precipitated from Solution 116

Effect of Washing Mercerized Samples at High Temperature 122

SUMMARY OF RESULTS AND CONCLUSIONS 124

SUGGESTIONS FOR FUTURE RESEARCH 127

Page

ACKNOWLEDGMENTS 128

LITERATURE CITED 129

APPENDIX I. PREPARATION OF CRYSTALLINE CELLULOSE I SAMPLES 134

APPENDIX II. MOLARITIES AND MOLALITIES OF MERCERIZING SOLUTIONS 136

APPENDIX III. PREPARATION OF PRECIPITATED CELLULOSES FROM THE DMSO-PF SYSTEM 137

APPENDIX IV. X-RAY DIFFRACTOGRAMS OF THE LABORATORY STANDARDS 147

APPENDIX V. PROGRAM BAND — A COMPUTER PROGRAM TO RESOLVE OVERLAPPING BANDS USING A NONLINEAR LEAST-SQUARES PROCEDURE 151

APPENDIX VI. RESULTS OF THE BAND RESOLUTION OF THE ALKALI METAL HYDROXIDE SOLUTIONS 175

APPENDIX VII. CALCULATION OF THEORETICAL ACTIVITY COEFFICIENTS — PROGRAMS DEH3 AND DEH4 182

SUMMARY

The mercerization of cellulose is most commonly accomplished using concentrated solutions of aqueous sodium hydroxide. The process includes the swelling and decrystallization of the native fiber followed by recrystallization as the mercerizing agent is washed from the cellulose.

The main objective of this study was to determine the factors which are important in the decrystallization of native cellulose by alkali metal hydroxide. This objective was accomplished by treating highly crystalline hydrolyzed cellulose I with aqueous solutions of lithium, sodium, and potassium hydroxide over a broad range of concentrations. These three alkali metal hydroxides vary with respect to the degree of hydration of the cations and the extent of ion-pairing.

The conversion of cellulose I to cellulose II was measured as a function of alkali metal hydroxide concentration using x-ray diffraction and Raman spectroscopy.

The concentration of free hydroxide ion and a measure of its hydration were obtained through analysis of the Raman spectra of the alkali metal hydroxide solutions. A theoretical analysis of the activity coefficients of the alkali metal hydroxides provided additional information about the structure of the solutions.

Through this combined examination of both the alkali treated cellulose and the mercerizing solutions themselves, a mechanism for decrystallization was proposed. The evidence indicates that the hydroxide ion is primarily responsible for the decrystallization step in the mercerization process. Furthermore, it appears that the hydroxide ion must be partially or completely dehydrated before it can penetrate the native lattice and promote decrystallization.

The Donnan equilibrium theory has been successfully invoked in the past to explain the swelling of accessible cellulose with sodium hydroxide. Under strongly alkaline conditions cellulose would be expected to behave as a weak acid. Some of the hydroxyl groups would become deprotonated. The essence of the Donnan theory is that the concentration of cations in the immediate vicinity of the polymeric chains would be greater under most conditions than in the bulk solution as electrical neutrality must be preserved. This surplus of cations will promote an osmotic pressure differential and thus swell the polymeric network.

The evidence from this study indicates that the Donnan effect may be a factor in the decrystallization process also. At equal free hydroxide ion concentrations (i.e., where allowances for ion-pairing have been made), lithium hydroxide was found to be the most effective of the three hydroxides in decrystallizing cellulose I. Sodium hydroxide was less effective and potassium hydroxide was the least effective. However, the differences among the three hydroxides on this basis were almost insignificant.

The lithium cation would be the most highly hydrated of the three with sodium being more hydrated than potassium; therefore, the lithium cation should promote the greatest osmotic pressure differential.

One aspect of the effect of temperature on mercerization was explored by precipitating cellulose from solution at various temperatures and comparing the results of this study to observations about the mercerization process at elevated temperatures.

This investigation was accomplished by precipitating cellulose from the dimethylsulfoxide-paraformaldehyde solvent system at temperatures between -2 and 165°C. The precipitates were examined using x-ray diffraction and Raman spectroscopy.

A continuous transition from the cellulose II lattice to cellulose IV was observed as the precipitating temperature was increased. This transition was interpreted in terms of changes in the conformation of the cellulose chains.

INTRODUCTION

Mercerization is commonly defined as the conversion of cellulose I to cellulose II with concentrated alkali metal hydroxides. The mercerization of cellulose includes the swelling and partial or complete decrystallization of the native fiber. The most common agent used to effect mercerization is aqueous sodium hydroxide, although a variety of chemical agents could be used.

During the mercerization process using 12 to 18% sodium hydroxide the native fiber becomes highly swollen and opalescent, but its basic morphology is not lost. The cellulose chains do not form a true solution in a mercerizing medium. However, they do gain the necessary mobility such that the native cellulose I crystal structure may be completely disrupted under certain conditions. When the mercerizing agent is washed from the fiber, the cellulose chains recrystallize, assuming the cellulose II lattice at room temperature and below.

The phenomenon of mercerization was first discovered by Mercer in 1844 (1). In 1889 Lowe found that cellulose fibers mercerized under tension had increased luster. In 1892 Cross, Bevan, and Beadle discovered the "viscose" process in which mercerized cellulose is treated with carbon disulfide to produce cellulose xanthate which is used in the production of cellulose films and rayon (1).

Mercerization is still an important industrial process. In the textile industry cotton fibers are mercerized in order to increase their luster and dye absorption. Cellophane is an important flexible film although it has suffered in recent years from competition with petroleum based products. The first step in the production of many cellulose derivatives is mercerization. In the paper industry wood fibers are mercerized in the preparation of certain types of highly absorptive papers and paperboard.

Although cellulose is generally easily mercerized, we do not understand the mechanism. The phenomenon is rather complex. The cellulose goes through at least three distinct physical-chemical processes: it is swollen; the crystalline areas are disrupted; and when the mercerizing solution is washed out, a new crystalline lattice is formed. These three processes are all functions of the activity of the alkali metal hydroxide or other mercerizing agent.

Most prior studies have focused on only one element of the mercerization process and have viewed mercerization as a much more homogeneous entity than it really is. No one has looked closely at both how cellulose is affected over a range of concentration of alkali metal hydroxides and how the nature of the solutions themselves change as a function of concentration.

THEORETICAL ASPECTS OF THE MERCERIZATION PROCESS

INTRODUCTION

Probably no single area of cellulose chemistry has been more extensively studied than mercerization. In 1966 Warwicker, et al. (2) published a 247 page review of the topic in which they listed 1484 references. Extensive reviews on mercerization are also to be found in References (1) and (3). Despite the great volume of research done on the mercerization process, there are still many theoretical questions which are not understood. The more significant theoretical contributions will be critically examined in the following pages.

GENERAL THEORY OF POLYMER SWELLING

The mercerization of cellulose most often has been interpreted strictly as a swelling process. The Donnan theory has several times been used to explain mercerization. It will be shown that the Donnan theory can be interpreted as a special case of the general theory of polymer swelling. Since the preponderance of previous work has focused on swelling effects, a presentation of the general case should aid in putting these studies in prespective.

To speak of a polymeric material as being swollen implies that there remains a certain degree of association between the polymeric chains. Otherwise one would simply have a solution. Thus most swollen polymeric systems that are in equilibrium with an overabundance of the swelling solvent are cross-linked. Generally, solubility decreases as the melting point of the solute increases. Crystalline polymers are relatively insoluble and often dissolve only at temperatures slightly below their melting points. If equilibrium can be achieved in a polymer-solvent system, the most important term with regard to whether solubilization or

swelling of the solid polymer will occur is the enthalpy term. The entropy of mixing will always be positive (4).

The general swelling theory due to Flory and Huggins (5) puts the various parameters of interest in the proper thermodynamic perspective. The Flory-Huggins treatment for the swelling of a polymeric network uses as a model a cross-linked, completely accessible, isotropic structure such as vulcanized rubber. The underlying assumption is that at equilibrium the forces tending to cause dissolution of the polymeric network are balanced against the elastic free energy forces which tend to keep the network compact.

$$\Delta G_{swelling} = \Delta G_{mixing} + \Delta G_{elastic} \quad (1)$$

$$\Delta G_{mixing} = \Delta H_{mixing} - T\Delta S_{mixing} \quad (2)$$

$$= kT[n_1 \ln v_1 + \kappa n_1 v_2] \quad (3)$$

where k = Boltzmann's constant

n_1 = number of solvent molecules in solution

v_1 = volume fraction of solvent

v_2 = volume fraction of solute

κ = interaction parameter expressing the first neighbor interaction free energy divided by kT for the solvent with polymer

The elastic free energy term is simply equal to the entropic term.

$$\Delta G_{elastic} = T\Delta S_{elastic} \quad (4)$$

$\Delta S_{elastic}$ represents the entropy change associated with the change in configuration of the network. Flory and Huggins resolved the elastic free energy term according to Equation (5), which comes directly from the statistical theory of rubber elasticity.

$$\Delta G_{elastic} = (kT\gamma_e/2)(3\alpha^2_S - 3 - \ln \alpha^3_S), \qquad (5)$$

where γ_e = effective number of chains in the network

α_S = linear deformation factor

and

$$\alpha^3_S = V/V_o,$$

where V_o = volume of the relaxed network

V = volume of the swollen gel

These five equations represent the foundation of the Flory-Huggins theory of swelling. The complete development may be found in Reference (5).

DONNAN EQUILIBRIUM THEORY

That ionic colloidal networks should swell or exhibit osmotic pressure effects was first recognized by Donnan and Harris (6). Donnan was able to demonstrate that Congo Red, when confined by a semipermeable membrane, exerts an osmotic pressure which is dependent on the concentration of a dissolved electrolyte in the aqueous medium. The semipermeable membrane was, of course, no barrier to the electrolyte.

The Donnan equilibrium theory is quite often applied to the swelling of polyelectrolytes in aqueous solvents. Though some do not agree (7), cellulose is generally considered to be a polyelectrolyte in strong alkali solution. During the late twenties and early thirties, Neale (8) made one of the more significant contributions toward an understanding of the mercerization process through his application of the Donnan theory to the swelling of cellophane in sodium hydroxide. More recently, Pennings and Prins (9) have reexamined the application of the Donnan theory to the swelling of cellulose and found Neale's work to be essentially valid.

A simple example taken from Reference (10) will best illustrate the Donnan theory. Envision a sample cell divided by a semipermeable membrane. Initially on one side of the membrane there is an aqueous polymer solution consisting of the dissociated polymer species P^- and a suitable cation such as Na^+. On the other side of the membrane there is a solution of sodium chloride. These conditions are illustrated in Fig. 1. The C's refer to concentrations.

INITIALLY

Polymer Side 1		Solvent Side 2	
Na^+	P^-	Na^+	Cl^-
C_1	C_1	C_2	C_2

Figure 1. Initial Conditions Illustrating Donnan Equilibrium Membrane Theory

All species may diffuse through the membrane except the polymer molecules. If C_1 is greater than C_2 the electrical neutrality can only be maintained through the dissociation of water. There would then be a net flow of H^+ ions to the polymer side of the membrane, and bulk solvent would become more basic. If C_2 is greater than C_1, there will be a net flow of sodium and chloride ions from the solvent side of the cell to the polymer side until the chemical potentials or free energies of the sodium and chloride ions are equal on both sides of the membrane. Therefore, at equilibrium, the situation depicted in Fig. 2 prevails.

AT EQUILIBRIUM

Polymer Side 1			Solvent Side 2	
Na^+	P^-	Cl^-	Na^+	Cl^-
C_1+X	C_1	X	C_2-X	C_2-X

Figure 2. Final Conditions Illustrating Donnan Effect

Since the activities of the sodium and chloride ions must be equal on both sides of the membrane, Equation (6) must be valid.

$$(\gamma\pm)_1^2\ (Na^+)_1\ (Cl^-)_1 = (\gamma\pm)_2^2\ (Na^+)_2\ (Cl^-)_2 \qquad (6)$$

If the assumption can be made that the mean activity coefficients on both sides of the membrane can be considered to be equal, then the Donnan equilibrium relation becomes:

$$(Na^+)_1\ (Cl^-)_1 = (Na^+)_2\ (Cl^-)_2 \qquad (7)$$

or

$$(C_1 + X)\ (X) = (C_2 - X)^2 \qquad (8)$$

The increase in ionic concentration on the polymer side of the membrane plus the necessary water of hydration for these ions causes an osmotic pressure difference.

Cross-linking would put a restraint on a polymer system analogous to the membrane example. Therefore, a cross-linked, completely accessible, ionic polymer placed in a salt solution should swell due to the Donnan effect.

Neale applied the Donnan theory to the swelling of cellulose both theoretically and experimentally. The goal of Neale's work was to explain the mercerization process, yet most of his experimental work was done on cellophane which, of course, is much more accessible to chemical agents than the more highly crystalline native fiber. Neale was aware that his application of the Donnan theory did not adequately deal with the accessibility issue and that there was only qualitative agreement between his application of the Donnan theory to the swelling of cellulose and the mercerization of native fibers. However, it will be shown that the agreement between Neale's theoretical calculations and the swelling of accessible cellophane within a range of concentrations between 0.5 and 23 molal sodium hydroxide is impressive.

Neale assumed that the weak polyacid, cellulose, contained one acidic proton per anhydroglucose unit. An approximate dissociation constant for cellulose was then determined to be 1.84×10^{-14} at 25°C. Neale derived the following set of equations which show how the weak acid, cellulose, should swell. In this derivation the subscript 2 refers to the solvent phase and 1 refers to the constrained phase, the cellophane. A^- represents a dissociated anhydroglucose unit, while HA represents an undissociated unit. The basic relationships are given in Equations (9)-(12).

$$[Na^+]_2 = [OH^-]_2 \tag{9}$$

$$[Na^+]_1 = [A^-]_1 + [OH^-]_1 \tag{10}$$

$$[H^+]_1 \, [A^-]_1/[HA]_1 = k_A \cong 1.84 \times 10^{-14} \tag{11}$$

$$[H^+]_1 \, [OH^-]_1 = k_w \cong 1 \times 10^{-14} \tag{12}$$

Neglecting activity coefficient differences, the Donnan condition in this case would be the following:

$$[Na^+]_1 \times [OH^-]_1 = [Na^+]_2 \times [OH^-]_2 \tag{13}$$

The concentration of anhydroglucose units would be constant prior to the actual swelling process.

$$[HA] + [A^-] = C \tag{14}$$

The osmotic pressure, $\underline{P}$, which causes the swelling, would be a function of the difference in ionic concentration of the sodium hydroxide between the two phases.

$$P = f([Na^+]_1 + [OH^-]_1 - [Na^+]_2 - [OH]_2) \tag{15}$$

Neale's final solution of Equation (15) is the following.

$$P = \{C\beta[OH^-]_1/(1 + \beta[OH^-]_1) + 2[OH^-]_1 - 2[Na^+]_2\} RT, \quad (16)$$

where $\beta = \underline{k}_A/\underline{k}_w$

Figure 3, which has been taken from Neale's work, compares the calculated osmotic pressure with the experimental water absorption curve. Neale had no way of measuring the osmotic pressure directly and thus had to depend on several indirect measurements of swelling. The basic agreement of the two curves is quite convincing.

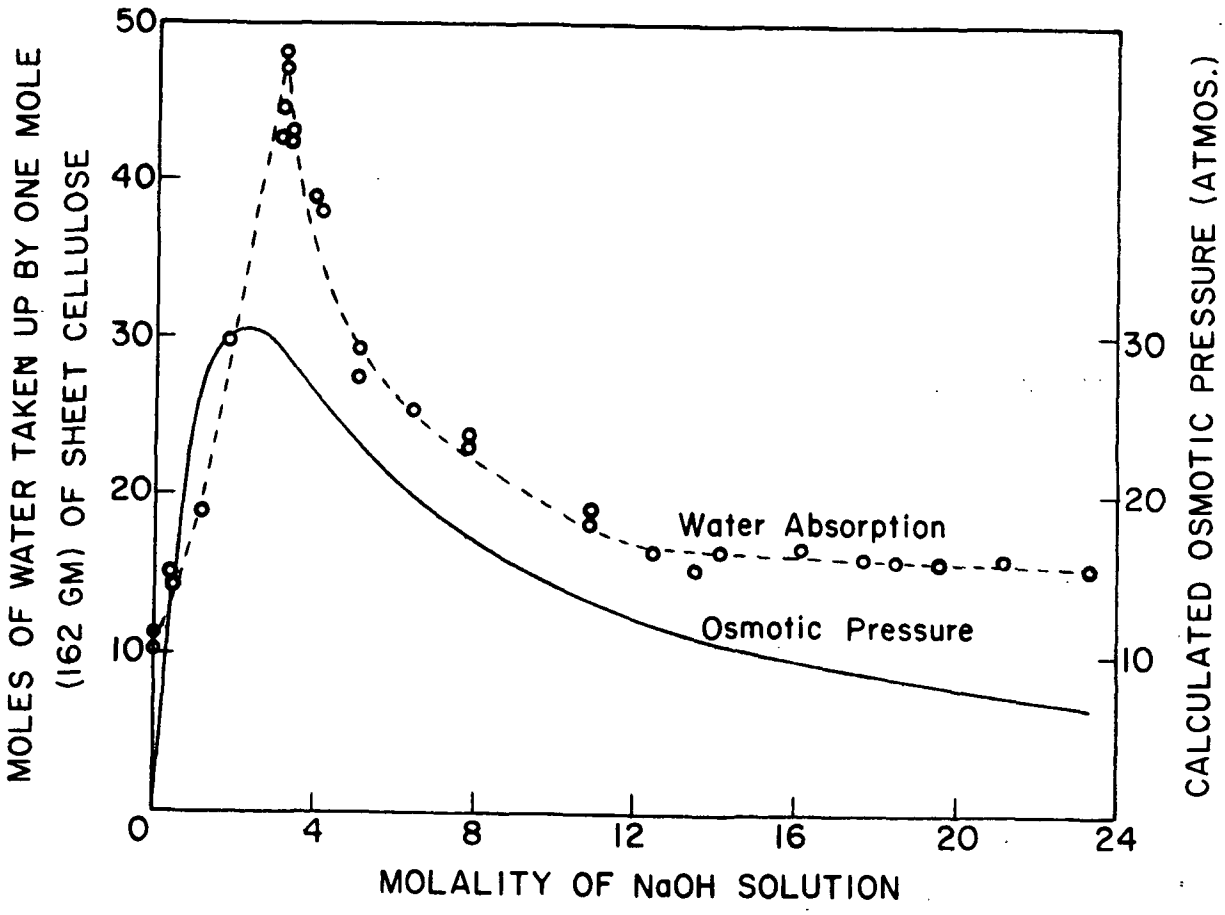

Figure 3. The Experimental Water Absorption Curve is Compared to the Theoretical Osmotic Pressure. From Neale (8)

As mentioned earlier Pennings and Prins (9) undertook a reexamination of the applicability of the Donnan equilibrium theory to the swelling of cellulose.

They were able to derive the Donnan relationship from the Flory-Huggins free energy of mixing theory.

$$\Delta G_M = -T\Delta S_M = -kT \sum_i M_i \ln \phi_i, \tag{17}$$

where $\underline{i}$ = any species present

$\phi_{\underline{i}}$ = volume fraction of species $\underline{i}$

The chemical potential of the mobile species inside and outside the cellulose gel must be equal at equilibrium. The following relationship applies to the mobile species, water, in the gel phase.

$$\mu^g{}_1 - \mu^o{}_1 = \alpha\Delta G_M/\alpha N_1 + \alpha\Delta G_{el}/\alpha N_1 + \pi v_1, \tag{18}$$

where $\mu^g{}_1$ = chemical potential in the gel phase

$\mu^o{}_1$ = standard chemical potential

$\underline{N_1}$ = number of water molecules

ΔG_{el} = elastic free energy

v_1 = molar volume of water

π = hydrostatic pressure or swelling pressure

A combination of Equations (17) and (18) yields the following series of equations which culminates with the Donnan relationship. The superscript $\underline{s}$ refers to the bulk solution.

$$RT \ln \phi_1{}^s + RT[1 - (v_1/V) \sum N_i{}^g] = RT \ln \phi_1{}^g + RT[1 - (v_1/V) \sum N_i{}^g] + v_1\alpha\Delta G_{el}/\alpha V + \pi v_1 \tag{19}$$

Simplifying, we have Equation (20).

$$(RT/v_1) \ln \phi_1{}^s/\phi_1{}^g + (RT/V) (\sum N_i{}^g - \sum N_i{}^s) = \pi + \alpha\Delta G_{el}/\alpha V \tag{20}$$

The same type of expression also applies to the other mobile species, the Na^+ and OH^- ions. Ion pairs are neglected.

$$[RT/(v+ + v-)] \ln \phi+^s \phi-^s/\phi+^g \phi-^g + (RT/V) (\sum N_i^g - \sum N_i^s) = \pi + \alpha\Delta G_{el}/\alpha V, \quad (21)$$

where $v+$ = molar volume of Na^+

$v-$ = molar volume of OH^-

$\phi+$ = volume fraction of Na^+

$\phi-$ = volume fraction of OH^-

The two preceding equations may then be combined and the result yields the Donnan relationship in terms of volume fractions.

$$[(\phi+^s \phi-^s)/(\phi+^g \phi-^g)] = (\phi_1^s/\phi_1^g)^{(v+ + v-)/v_1} \quad (22)$$

If equal molar volumes for all the mobile species are assumed, the ideal Donnan relationship is realized.

From this initial development, Pennings and Prins went on to derive an equation which is essentially the same as Neale's final relationship, Equation (16).

The importance of Pennings and Prins' derivation is that it improved the theoretical support for the application of the Donnan theory to the swelling of cellulose. The derivation also brought together the common elements of the general theory of polymer swelling and the Donnan theory. One criticism of the derivation is that the enthalpy term in the initial free energy of mixing relationship, Equation (17), was ignored. This is not a negligible term in an aqueous system of sodium hydroxide and cellulose. As an example, a 5.4 molar solution of sodium hydroxide will evolve approximately 5.4 kcal/mole of anhydroglucose units when the two are mixed (11).

Experimentally, Pennings and Prins were able to actually measure the swelling pressure as a function of alkali concentration at constant volume. They determined an average k_A for cellulose of 0.52×10^{-14}, slightly less than Neale's value. Their calculated swelling pressure was in fair agreement with the experimentally determined swelling pressure as is illustrated in Fig. 4 which was duplicated from their work.

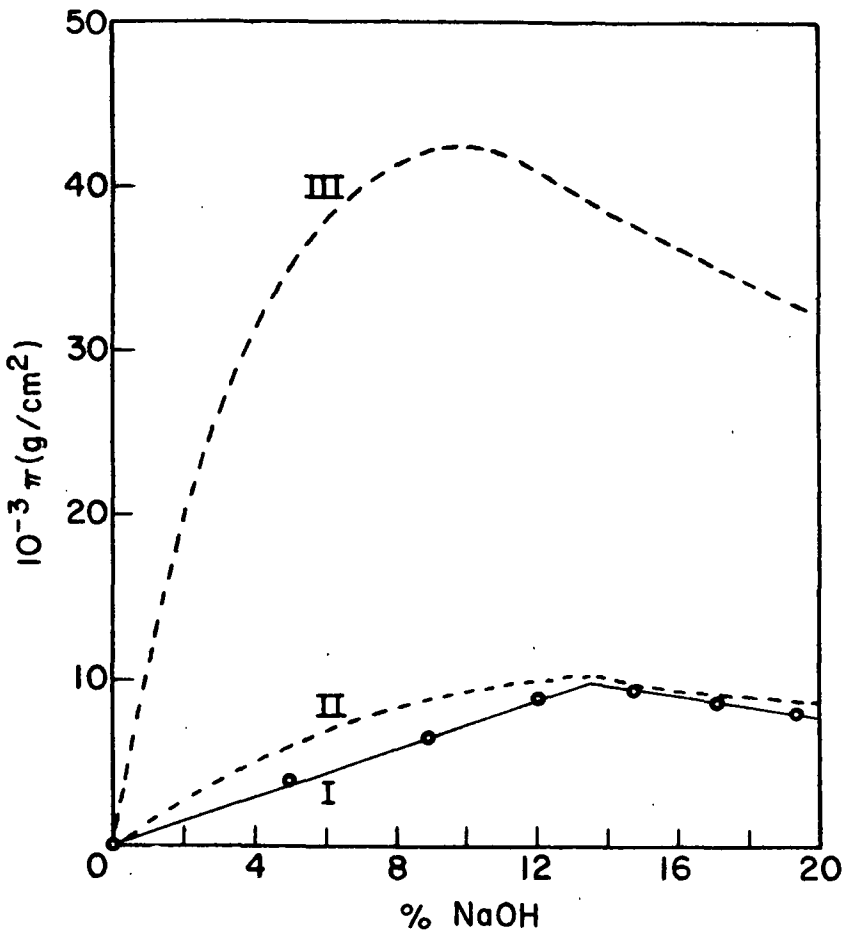

Figure 4. Donnan Pressures for Accessible Cellulose in Sodium Hydroxide Solutions: (I) Pennings and Prins' Experimental; (II) Pennings and Prins' Theoretical; (III) Neale's Theoretical. From Pennings and Prins (9)

Pennings and Prins claimed that Neale's calculated swelling pressure was four times too high due to his higher value for the k_A of cellulose. It should be pointed out here that the experimental restraint of constant volume which

Pennings and Prins imposed could decrease the accessibility of their conditioned isotropic cellulose gels. Thus, the k_A of cellulose could have been artificially depressed under these conditions.

OTHER MERCERIZATION THEORIES

Probably the biggest flaw in the application of the Donnan theory to the swelling, and by implication the mercerization, of cellulose is that native cellulose is highly crystalline. Therefore, one would expect that a fair proportion of a native fiber would not be accessible to a swelling agent until the crystal structure is somehow disrupted. Neale (8) was aware of this limitation on his theory, but some researchers have ignored his discussion of this limitation and discarded the whole application of the Donnan theory as being invalid.

Most of the alternative swelling theories have been influenced by some of the precepts of the Donnan theory. Generally most investigators have regarded the decrystallization and swelling of the crystalline areas of cellulose as a continuation of the same mechanism that swells the accessible intercrystalline areas. Vigo, et al. (12,13) have shown that the decrystallization of the crystalline areas may well proceed by a different mechanism than the swelling of the accessible areas. Vigo's important contribution will be reviewed after several of the more noted theories are examined.

Chedin and Marsaudon (7,14,15) felt that cellulose should not be treated as a weak polyelectrolyte in strong alkali solution. They were unable to experimentally detect a difference in concentration of the bulk mercerizing solution and the solution closely associated with the cellulose matrix. Therefore, they discarded the Donnan theory. Their own theory, which has gained a certain degree of acceptance, especially by Warwicker (16), Jeffries and Warwicker (17), and Warwicker and Wright (18), is that ion pairs of sodium

hydroxide complex with cellulose and cause the swelling and decrystallization which takes place. They believed that these ion pairs were hydrated but as the concentration of sodium hydroxide increased, the amount of water available for hydration decreased. The ion pairs would then substitute three hydroxyl groups from adjacent cellulose chains to complete their hydration spheres. Below 10% by weight sodium hydroxide, the authors predicted that there would be no ion pairs. It should be noted that the authors presented no experimental evidence for any of the elements of their theory.

Warwicker, et al., have rather recently presented a series of papers on the mercerization process (16-18) in which they are in substantial agreement with the theories of Chedin and Marsaudon. Through the use of x-ray diffraction measurements, they concluded that in the process of mercerization lateral disorder is produced in the fibrils along with splitting of the fibrils by cleavage in the (101) plane. Figure 5 depicts a unit cell of cellulose I in which the (101) plane is plainly indicated.

Warwicker, et al. concluded that the decrystallization of the fibrils occurred along the (101) plane in the following manner. Samples of cotton and ramie were mercerized with sodium hydroxide solutions of varying concentration and temperature. Some of these samples were washed with water while others were washed with acidified sodium chloride. Adhering solution was removed from the samples, but the x-ray diagrams were taken while the mercerized fibers were still in the wet state. Over a hundred different samples were prepared under dissimilar conditions. The d(101) spacings varied between 7.44 and 9.24 A, while the $d(10\bar{1})$ spacings only varied within the limits from 4.30 to 4.64 A; and for the d(002) spacings the variation was from 3.91 to 4.13 A. The authors (18) concluded from these data that

"... it seems clear that the true fundamental unit in these reactions is a sheet of chains and not a single chain. Such a sheet is held together chiefly by Van der Waals forces, although the possibility of hydrogen bonds between the primary hydroxyl group of one chain and the secondary hydroxyl of a neighboring chain in the (101) plane must not be overlooked."

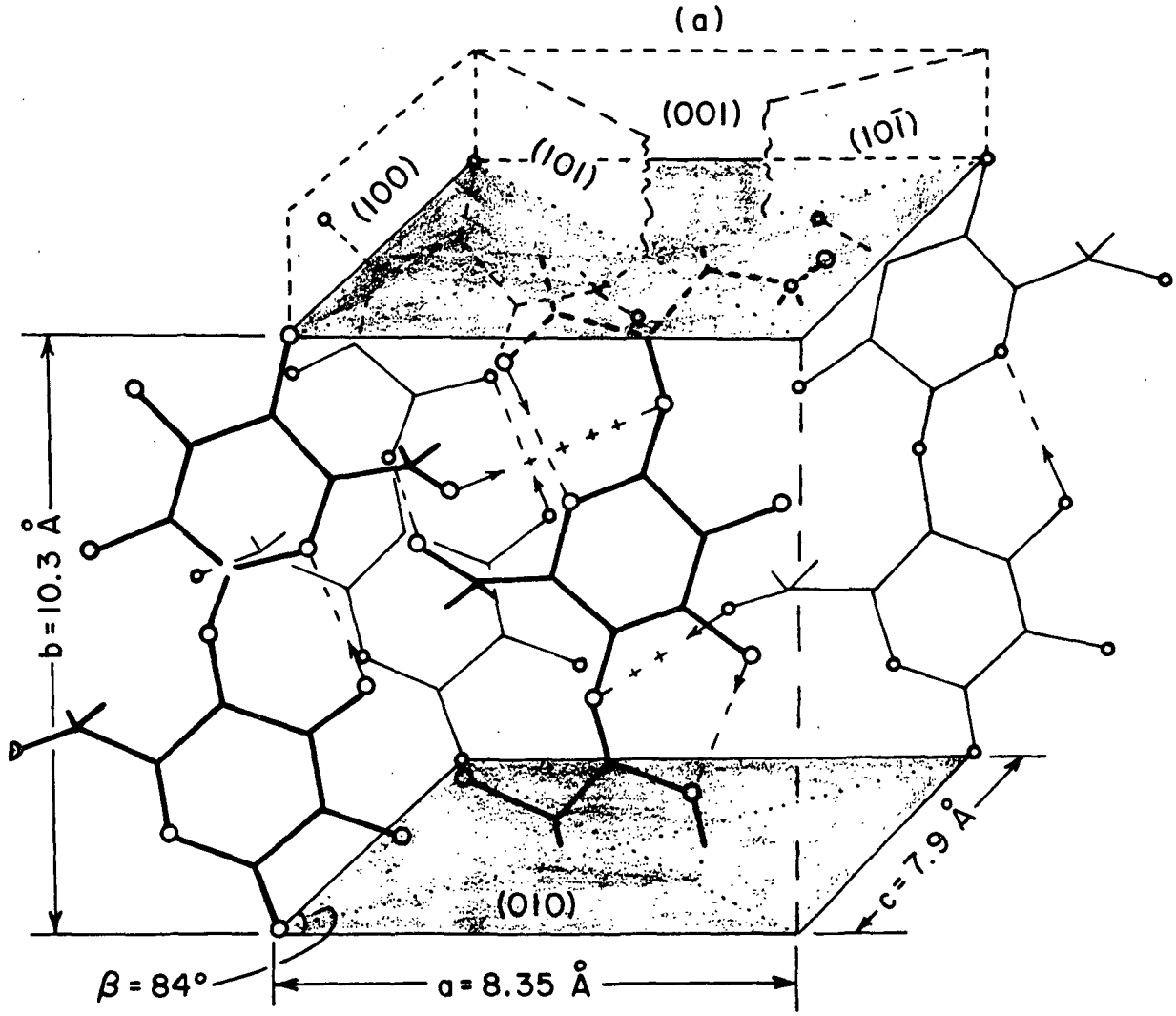

Figure 5. Unit Cell of Cellulose I Showing One Possible Hydrogen Bonding Scheme. From Liang and Marchessault (19)

The authors thought that complexes of the type described by Chedin and Marsaudon formed between the cellulose sheets. The hydrogen bonds between the sheets were disrupted through the formation of these complexes.

Denoyelle (20) has also been quite critical of Neale's theory. He mercerized a series of samples and determined the amount of "bound" sodium ion as a function of concentration. The "bound" sodium was defined as the sodium that remained associated with the mercerized cellulose after pressing or centrifugation. The amount of "bound" sodium ion increased continuously but not linearly with increasing concentration for native cellulose. From this evidence, Denoyelle deduced that mercerization involved the formation of a true alcoholate, -CHONa. He also believed that swelling in the inter- and intracrystalline regions is of a homogenous nature. His own experimental evidence suggests that just the opposite is true. The fact that the amount of bound sodium ion was not a linear function of concentration suggests that the activity of the sodium hydroxide must reach a certain level before the crystalline areas of cellulose can be disrupted.

The mercerization of cellulose has been interpreted as an exothermic phase transition by Ranby (21). Through a thermodynamic analysis, Ranby concluded that cellulose I is in a metastable or higher free energy state than is cellulose II. Ranby's conclusions may well be valid, but the following analysis of his arguments raises some doubts about the validity of his theory.

Ranby arbitrarily divided up the heat of reaction of cellulose with alkali into three elements according to the following equation.

$$\Delta H_T = \Delta H_a + \Delta H_b + \Delta H_c, \tag{23}$$

where ΔH_T = heat of transition

ΔH_a = heat of wetting the dry cellulose

ΔH_b = heat of reaction of the alkali with the wet cellulose

ΔH_c = heat of the lattice transition

ΔH_c was further divided as follows:

$$\Delta H_c = \Delta H_{c1} + \Delta H_{c2}, \tag{24}$$

where ΔH_{c1} = the actual lattice transition

ΔH_{c2} = reaction of the phases with water

Using data from the literature, Ranby showed that there is a difference in enthalpy between cellulose I and II when the two are treated with equal concentrations of sodium hydroxide. This approximately constant difference over a broad concentration range was 1.4 cal/g to 2.0 cal/g (more exothermic for cellulose II than for cellulose I). One important criticism of this type of analysis is that the size and perfection of the crystallites of a typical cellulose II are much less than for native cellulose. Therefore, unless a correction is made for these crystallinity differences, it does not appear to be valid to assign an enthalpy difference as a difference between the molecular arrangements of the lattices. At the present time there is a study underway of the thermal properties of the four polymorphs of cellulose (22). These investigators have acknowledged the need for making corrections to their thermodynamic data for differences in crystallinity between the polymorphs.

Ranby was aware of these crystallinity differences between native cellulose I and mercerized cellulose II, but he felt that these differences could all be simply included in the entropy term. The entropic term was not evaluated as it would certainly be difficult or impossible to do. Ranby mentioned that there would be an increase in entropy in going from the native structure to mercerized cellulose. Therefore, the transition would be favored by the entropy as well as enthalpy terms.

The overall implication of Ranby's analysis is that the negative free energy change which he has calculated in going from cellulose I to cellulose II is the driving force behind mercerization. But mercerization is a three step process. First the native fiber is swollen and decrystallized with caustic. Then the caustic is washed out and the polymer recrystallizes as cellulose II at room temperature and below. Swelling, decrystallization, and recrystallization appear to be distinct steps in lattice conversion (12).

As is evident from much of the preceding discussion, the swelling of accessible cellulose and the decrystallization of the crystalline areas are often regarded as being accomplished by the same type of physical or chemical action. This is probably why there is so much confusion and divergence of opinion concerning the topics of swelling and mercerization.

From a review of the literature and through their own work, Vigo, et al. (12,13) emphasized the distinction between decrystallization and swelling. Through their study of the effects of the alkali metal hydroxides on native cellulose the authors were able to show some clear differences between swelling and decrystallization. At optimum swelling concentrations by weight (9.5% LiOH, 13% NaOH, 32% KOH, 40% RbOH, and 40% CsOH) of alkali the fiber swelling order was found to be the following:

$$CsOH<RbOH<KOH<NaOH<LiOH.$$

However, the authors found that the lattice conversion order at these optimum swelling concentrations was:

$$LiOH \cong CsOH<RbOH<KOH<NaOH.$$

They also found that benzyltrimethylammonium hydroxide (BTMOH) was a highly effective swelling agent but was very ineffective in promoting lattice

conversion. However, solutions of approximately 35% by weight BTMOH and small amounts of alkali metal hydroxide were quite effective in converting the lattice from cellulose I to cellulose II. From these experimental determinations the authors concluded that there is a synergistic effect between BTMOH and the alkali metal hydroxides. They attributed the anomalous behavior of lithium hydroxide and BTMOH to the large cationic size. Lithium hydroxide has the most highly hydrated cation of the alkali metal hydroxides (23), and of course the BTMOH cation would be expected to be large although probably not hydrated. The authors went on to conclude that (12):

> "... there are stringent requirements in effecting conversion to cellulose II, and sodium hydroxide is unique in having cations of the optimum radius and coordination tendencies to cause lattice conversion."

Dobbins (24) published an interesting paper in which he discussed the various factors involved in the swelling of cellulose. He came to the conclusion that the role of the electrolyte in solution with cellulose is a secondary one, and that the primary chemical species involved in the solvation of cellulose is free, nonhydrogen-bonded, monomeric water of the description first proposed by Frank and Wen (25). According to Frank and Wen's flickering-cluster model, water is essentially a two component system; there are "icebergs" of highly structured, tetrahedrally-hydrogen-bonded aggregates in solution with monomeric water. Electrolytes have the ability to alter the balance between the two postulated species. Small, highly charged ions are credited with an ability to immobilize more water in their primary hydration shell than relatively large and less highly charged ions. Between each ion's hydration or A shell and the bulk solution, there is a transition region which is referred to as the B shell. This B shell is the buffer region between the bulk solvent and the ion and would appear to be composed mainly of monomeric water. For any given

electrolyte there should be an optimum concentration where the amount of B water is a maximum. According to Dobbins this maximum amount of B water happens to correlate rather well with the maximum ability of various electrolytes to swell cellulose.

Dobbins' theory can be criticized from several different perspectives. The main criticism is that he made no distinction between swelling and decrystallization. His paper has been mentioned in order to emphasize the controversy and diversity of opinion surrounding the mercerization process.

TEMPERATURE EFFECTS

There is frequent mention in the mercerization literature (2) that alkali metal hydroxides are less effective as mercerizing agents at elevated temperatures. As an example of this type of investigation the recent work of Jeffries and Warwicker (17) will be briefly examined.

Jeffries and Warwicker did a series of mercerizations in which they mercerized cotton at two temperatures 0 and 25°C and washed the caustic out for some samples at the mercerization temperature and for others at 100°C. Table I is reproduced from their paper. It is evident from their interpretation of their x-ray and infrared data that washing at the higher temperature resulted in a higher proportion of cellulose I. They interpreted their results in the following manner:

> "It is evident, therefore, that the presence of cellulose I in the final sample is not merely cellulose I material that has not been swollen. It must be that the intrafibrillar swelling during the initial swelling and washing was such that reconversion to cellulose I was promoted. In terms of the swelling of sheets of cellulose chains, it seems that the rearrangement necessary within the sheet to form cellulose II cannot take place unless there is sufficient swelling during the washing treatment."

TABLE I

ACALA 4-42 SCOURED COTTON TREATED WITH 5N CAUSTIC SODA

(Effect of Washing Temperature)

Treatment	Infrared-deuteration			X-ray
	H-Bond Disorder, %	Cell. II in Total, %	Cell. I in Total, %	Cell. I in Total, %
At 0°C				
Washed at 0°C	60	32	8	<1
Washed at 100°C	58	25	17	14
At 25°C				
Washed at 25°C	62	30	8	<1
Washed at 100°C	57	22	21	24

The work done on cellulose polymorphy by Atalla (26) and Attala and Nagel (27) would suggest that another interpretation of the effects observed by Jeffries and Warwicker is possible. Atalla and Nagel have demonstrated that the crystal structure of cellulose precipitated from solution may be a function of temperature. They were able to regenerate cellulose wholly in its native form at 170°C from a phosphoric acid solution. Precipitates of predominantly the cellulose IV crystal structure were regenerated over a range of lower temperatures.

These findings would imply that Jeffries and Warwicker were possibly observing a temperature effect associated with the cellulose crystal structure and not with the mercerizing solution. The x-ray diffraction patterns of cellulose I and IV are quite similar. If a cellulose II sample is intermixed with a small fraction of either polymorph, it is difficult or impossible to determine which polymorph is present as the minor constituent.

THESIS OBJECTIVES

The preceding discussion indicates that the mechanism of mercerization is not well understood. There are several general criticisms which may be made about most of the earlier theoretical interpretations of the mercerization process. The main criticism is that few investigators have perceived the possibility that there may be a difference between the swelling of accessible cellulose and the decrystallization and subsequent swelling of the crystalline areas. Another equally important criticism is that no investigators have looked other than superficially at the structure of the mercerizing solutions. This is understandable as a detailed knowledge of concentrated electrolytes is not yet available.

The main objective of this thesis work will be to advance the knowledge of the decrystallization step of the mercerization process. This will be done by taking a unique look at the mercerization process. Both the mercerizing solutions and the treated cellulose will be examined independently. Interrelationships between changes in the cellulose structure and changes in the solution structure will be deduced from such an approach.

A secondary objective of this work will be to investigate the effect of temperature on the crystal structure of cellulose precipitated from solution. It was anticipated that this work would provide fresh insights into the effect of temperature on the mercerization process.

EXPERIMENTAL PROGRAM

SELECTION OF A HIGHLY CRYSTALLINE CELLULOSE I

It was believed that a hydrocellulose with a high degree of crystallinity would be the ideal substrate for the mercerization phase of this work. A hydrocellulose would have the constraints between crystallites removed and this should facilitate the separation of swelling effects from decrystallization effects during the mercerization process. It would seem to be a logical premise that the transition from cellulose I to cellulose II should be easier to follow if the initial starting material were highly crystalline, as the x-ray diffraction peaks of cellulose I and II overlap. X-ray diffraction was to be the main analytical technique. Mercerized samples incorporating both crystal lattices were anticipated.

Searching for a highly ordered cellulose I starting material, I investigated a series of different native celluloses. The sources of the native celluloses as well as the hydrolyzing procedures and any other pertinent details are found in Appendix I. Crystallinity was assessed with standard x-ray and infrared procedures. The methods for obtaining the raw x-ray and infrared data are discussed in subsequent sections, while the analysis of the data and justification of the procedures are found in the Results and Discussion section.

Avicel*, both in the "as received" condition and hydrolyzed under various conditions, was first investigated because the patent (28) covering its production describes the process as producing "cellulose crystallites having a high degree of perfection as characterized by x-ray diffraction."

*Avicel PH 101 is a commercial microcrystalline hydrocellulose manufactured by FMC Corporation.

Other native celluloses which were investigated included two types of cotton fibers, a sample of ramie fibers, and Whatman CF1.*

Battista (29) has reported that hydrolyzing cellulose with 2.5N hydrochloric acid at 105°C for 15 minutes will reduce native fibers down to their level-off degree of polymerization (LODP). When the LODP is reached, this is a good indication that all the amorphous material has been removed, and only the crystallites are left. Nelson and O'Connor (30) have reported using more severe hydrolysis conditions in producing hydrocelluloses. They refluxed cotton for 30 minutes in 4N HCl. These reported hydrolyzing conditions were used as guidelines in the preparation of the celluloses examined in this work.

After a detailed examination of the hydrolysis of cellulose, Sharples (31) concluded that cellulose crystallites are degraded by acid only on their ends. There is no general chain scission. Thus, the crystallites are not unpredictably degraded by prolonged acid treatment, they are just shortened.

X-RAY DIFFRACTION PROCEDURE

The primary method of assessing the relative crystallinity of the various celluloses investigated was x-ray diffraction using the spectrometric powder technique. The equipment used was a Norelco diffraction unit equipped with a wide range goniometer. The x-ray tube was operated at 35 kv and 20 ma. Nickel filtered CuKα radiation was used. A 0.5° divergence slit defined the primary beam while a 0.006-inch receiving and a 0.5° scatter slit defined the diffracted beam. The intensity of the diffracted beam was measured with a proportional counting tube and recorded with a Brown recording potentiometer which was

*Whatman CF1 is a commercial highly purified high crystallinity cellulose I. The manufacturer, Reeve Angel, will not disclose the sources nor the methods of production of the Whatman cellulose products.

calibrated before every run. The diffraction spectrum was recorded from 8 to 30° 2θ. The time constant, scanning rate, chart speed and intensity amplification were varied to suit specific needs.

The sample holder was a thin rectangular piece of aluminum with a hole toward one end just large enough for the sample pellets.

All samples were conditioned in a constant temperature-constant humidity room at 50% relative humidity and 20°C for at least 24 hours. The sample pellets were prepared from 0.20 g of cellulose on a conditioned basis. The pellets were formed in a Perkin-Elmer evacuable potassium bromide die. Experimental evidence was obtained which indicated that high pressing pressures may lower the crystallinity of the cellulose. Ant-Wuorinen and Visapaa (32) have also mentioned this possibility in connection with their own x-ray studies on the crystallinity of cellulose. Therefore, a pressure of 1400 psi gage was used which was the minimum pressure found consistent with the strength requirements of the sample pellets.

INFRARED PROCEDURE

Infrared spectra were recorded and used as a secondary method of assessing the crystallinity of the native hydrocelluloses. All spectra were recorded on a Perkin-Elmer 621. The following machine settings were always used: slit program 1000, amplifier gain 4.6, attenuator 1100, scale expansion 1x and source intensity 0.8. Spectra were generally recorded over the range 3900 to 600 cm^{-1} with a scan time of 25 minutes.

Sample pellets were made from 0.0015 g of cellulose conditioned in a vacuum oven at 50-60°C for at least 4 hours. The cellulose was combined with 0.350 g of optical grade potassium bromide. The two components were thoroughly

mixed and ground together using an agate mortar and pestle. The pellets were formed at pressures of 20,000 to 22,000 psi gage using a Perkin-Elmer evacuable die and a time of 2 minutes under full pressure after a evacuation time of 3 minutes.

MERCERIZATION

PREPARATION OF ALKALI METAL HYDROXIDE SOLUTIONS

A series of solutions of lithium, sodium, and potassium hydroxide were needed for the mercerization work. Concentrated solutions of alkali metal hydroxides require special handling since they degrade glass and readily absorb carbon dioxide (33). Stock solutions of 50% by weight sodium hydroxide and potassium hydroxide and 11% lithium hydroxide were made up in boiled, distilled water.

The containers used for these stock solutions were 1-liter, thoroughly washed, polyethylene bottles. After standing for two weeks the solutions were filtered over fine sintered glass filters. Solutions of various concentrations were made from these stock solutions using freshly boiled, distilled water. All dilutions were done inside a dry-box under a carbon dioxide-free atmosphere. The diluted solutions were stored in polyethylene bottles which had drying bulbs filled with Ascarite as well as polyethylene drawing tubes attached. With this arrangement a sample of hydroxide could be removed from the stock solution bottle without exposing the solution to the atmosphere. There was a short section of Tygon tubing at the lower end of the drawing tubes where the Hoffman compressor clamps, which served to regulate the flow, were located. The short section of Tygon tubing was necessitated since polyethylene tubing is not sufficiently flexible to form a seal using a compressor clamp. The solutions

were all stored in the dry-box under a carbon dioxide-free atmosphere, as polyethylene is slightly permeable to carbon dioxide.

The hydroxide solutions were diluted approximately to the desired molarities and then standardized. Calibrated pipets and burets were used in the standardization procedure. Aliquots of hydroxide solution were added to 100 ml of boiled, distilled water, and then the stirred solution was titrated with 0.500N HCl. Three aliquots of each solution were titrated and median values were reported. A calibrated pH meter was used to determine the end point of the titrations.

It was necessary to determine the molalities of all the mercerizing solutions as well as the molarities since much of the thermodynamic work of pertinence to this study found in the literature uses the molality scale. Also, it was necessary to know the molalities of the solutions, because some of the prior work done on mercerization has been presented using molalities. Molalities can be determined from a knowledge of the molarity of a solution and its density. The densities were determined in triplicate using a calibrated 25 ml pyconometer, and mean values were used in the calculations. The observed weights were corrected for buoyancy according to the following formula; an iterative technique was used:

$$w_1 = d_{air}\, w_2(1/d_1 - 1/d_2) + w_2, \qquad (25)$$

where w_1 = corrected weight

d_{air} = density of air 0.0012 g/ml

w_2 = observed weight

d_1 = density of measured liquid

d_2 = density of the stainless steel weights in the electric balance: assumed to be 7.9 g/ml

The molarities and molalities of all the mercerizing solutions are given in Appendix II.

ALKALI TREATMENT OF THE CELLULOSE

Fifty ml of alkali metal hydroxide solution were transferred to a 2-oz polyethylene bottle inside the carbon dioxide-free dry-box. The stoppered bottles were then removed and allowed to equilibrate in a constant temperature bath at 20.0°C for a minimum of 2 hours. After the equilibration, 1 g of the crystalline hydrocellulose was added to the solution and the mixture was agitated vigorously and placed in the constant temperature bath for 30 minutes. The slurry was agitated several times during the 30 minute mercerization.

At the end of the 30 minutes, the mercerization was quenched in enough distilled water at 20°C to insure that the final molarity of the resulting solution was no more than 0.5M hydroxide. The diluted slurries were next neutralized with approximately 4N HCl to pH 7 and allowed to stand. After the mercerized hydrocellulose had settled the supernatant solution was substantially discarded and the remaining slurry was filtered, washed, and freeze dried. Mercerizations at each hydroxide concentration were done in duplicate.

Filtration of the mercerized hydrocellulose proved to be almost impossible using conventional sintered glass filters. The filters would easily clog due to the small particle size and plastic nature of the mercerized material. The final solution to the problem was to use sintered Teflon filter disks* as a replacement for the fritted glass.

The fritted glass was removed from 60 ml funnel filters and the shells were used in conjunction with the filter disks. A sandwich consisting of two

*Pall Trinity Micro Corporation, Cortland, New York.

grooved Teflon rings was used to hold and seal the filter disks in place. Viton O-rings were employed to insure good sealing between the Teflon rings and the glass shell and also between the rings and the filter disks. Stainless steel screws were used to hold the Teflon rings together. A heavy gage stainless steel screen was fitted directly below the filter disk to give it rigidity. Without this support the sintered filter disks would tend to distort under vacuum. Several larger Teflon filters were made from 600 ml fritted glass funnel filters. These larger filters required stainless steel annuli both above and below the Teflon rings, since Teflon has a tendency to "cold flow" under stress and these larger filters would lose their seal after a while. Figure 6 illustrates the design of the filter holders. The glass shell has been omitted for clarity.

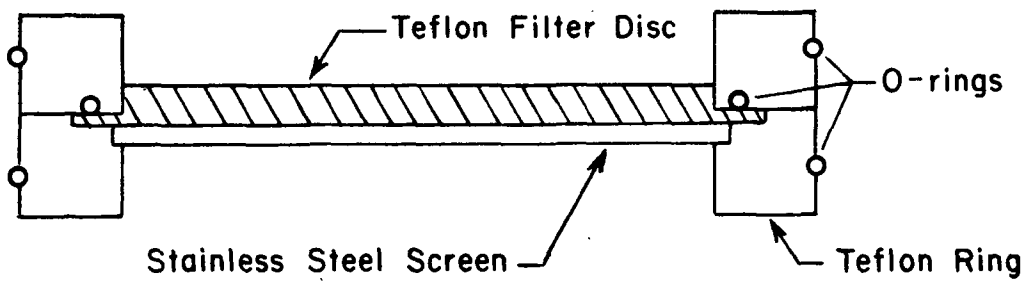

Figure 6. Sintered Teflon Filter Disk Holder

EXAMINATION OF THE MERCERIZED CELLULOSE

X-RAY DIFFRACTION

X-ray diffraction was the primary analytical method used in following the course of conversion of cellulose I to cellulose II as a function of alkali concentration. The experimental procedure was essentially the same as described previously for the x-ray determination of cellulose crystallinity. However, an internal standard, 0.012 g of TiO_2 rutile, was added to the 0.20 g of conditioned

cellulose before the pellets were pressed. This internal standard, which has a sharp peak at 27.46° 2θ due to a reflection from the (110) plane, was included in order to more accurately determine the location of the cellulose reflections. An internal standard aids in compensating for errors in the grid line spacing and sample pellet misalignment.

The x-ray diffractograms of the alkali treated samples were analyzed for their percentage cellulose II content according to a procedure which is described in detail in the Results and Discussion section. This empirical analytical method is based on a comparison of the diffractogram of the mercerized sample to laboratory standards of known composition of the two polymorphs, and of varying crystallinity. The cellulose I standards were unmodified Avicel and Whatman CF1 hydrolyzed for 30 minutes in 4N HCl. The cellulose II standards used were 22-B, a low crystallinity cellulose and a combination of two fully converted samples which had been mercerized with 4.631M NaOH. Sample 22-B was precipitated from the dimethylsulfoxide-paraformaldehyde solvent system. Its history is discussed in Appendix III.

It would have been desirable to have a cellulose II standard of higher crystallinity than the mercerized sample. Since rayon has been used by others (34) as a standard cellulose II, it was investigated as a possibility. A sample of FMC rayon* was hydrolyzed for 15 minutes in 2.5N HCl. The diffractogram of this sample is shown in Fig. 7. This hydrolyzed rayon could not possibly be 100% cellulose II, as the $(10\bar{1})$ peak intensity should be greater than the (002) peak for cellulose II. A sample of the same material was hydrolyzed more severely — 30 minutes in 4N HCl. As can be seen in Fig. 8 this treatment substantially changed the ratio of the intensities of the $(10\bar{1})$ and (002) peaks.

*FMC Regular Bright Rayon, Denier 1.5, Product Code 2485.

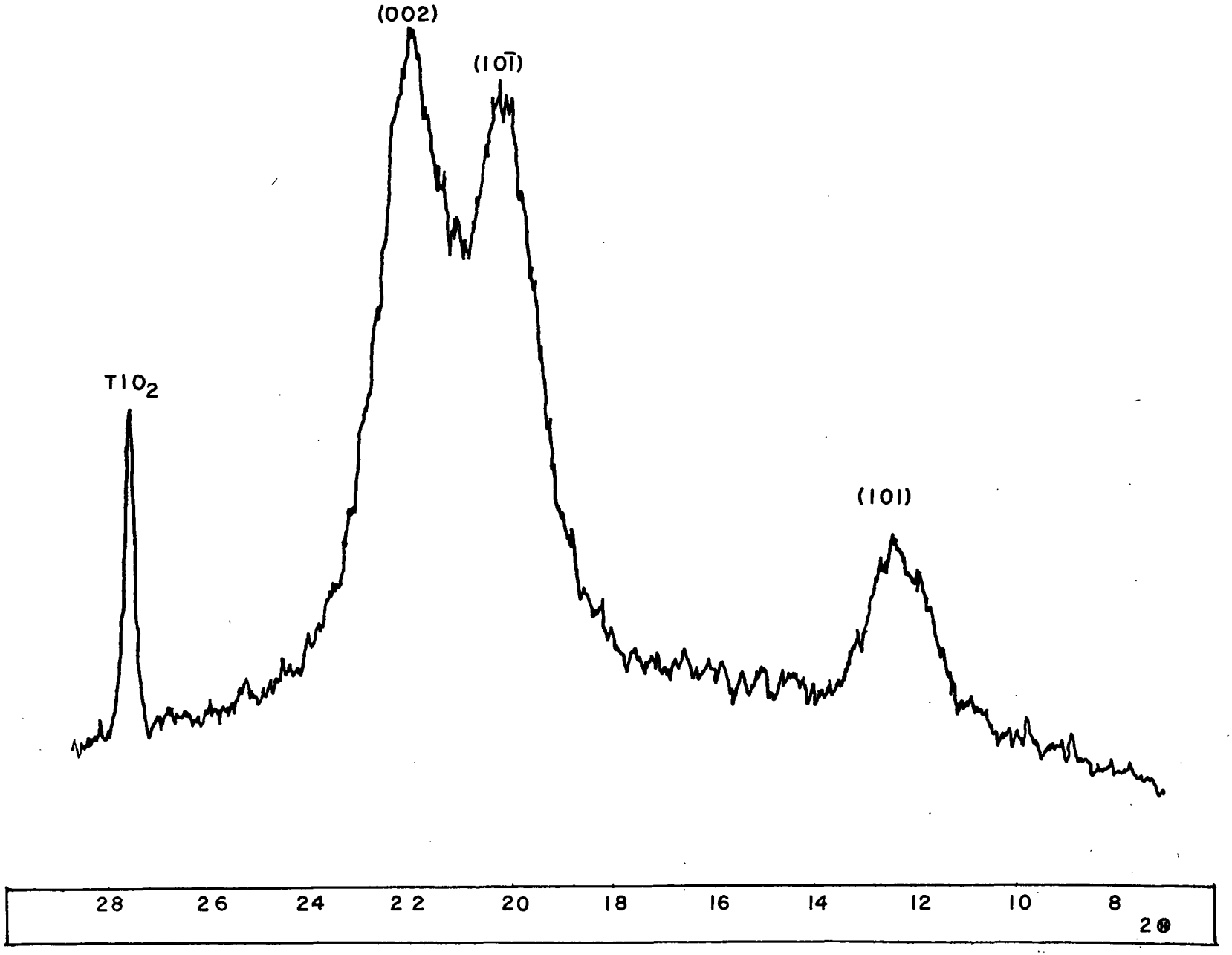

Figure 7. Powder X-ray Diffractogram of FMC Rayon Hydrolyzed for 15 Minutes in 2.5N HCl

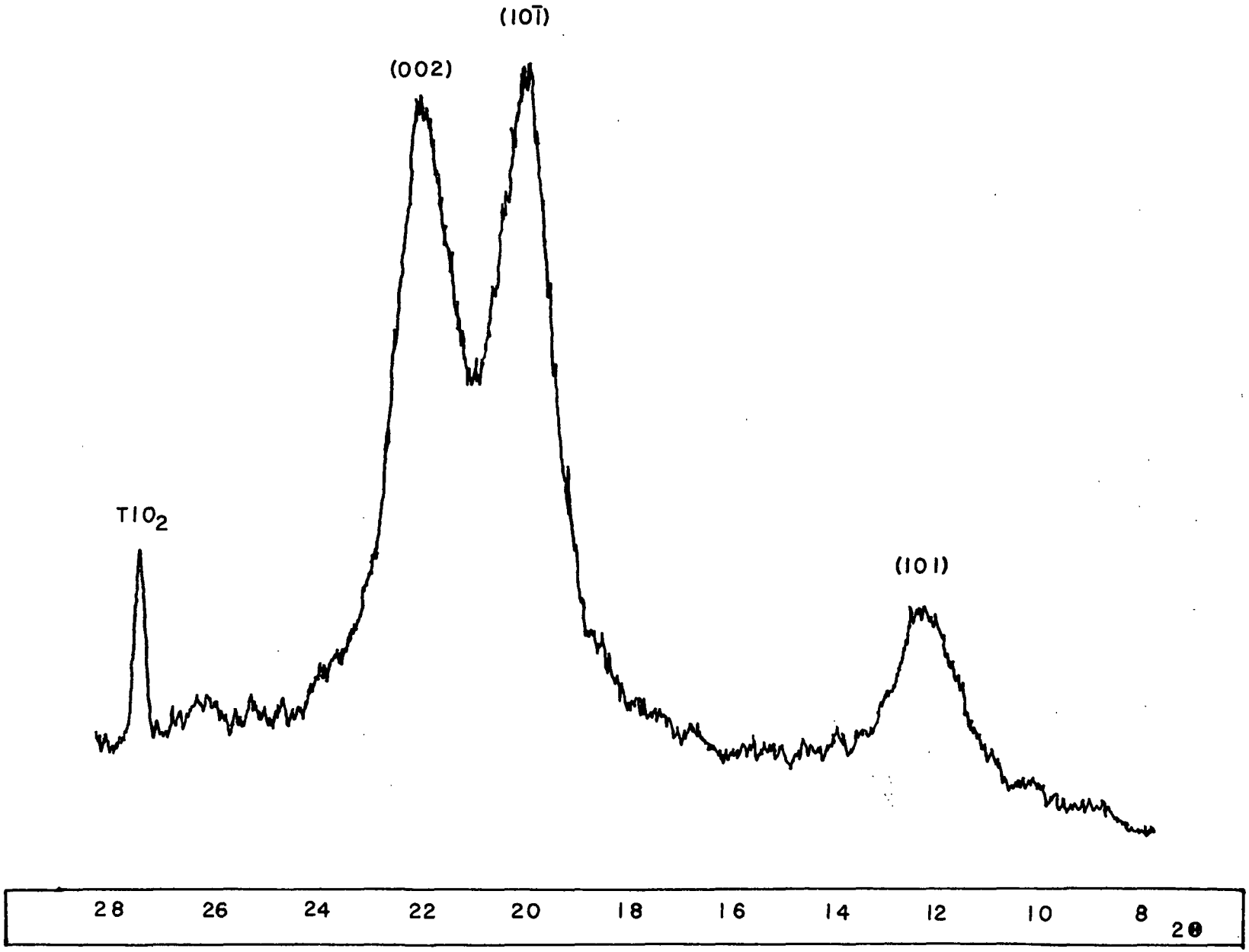

Figure 8. Powder X-ray Diffractogram of FMC Rayon Hydrolyzed for 30 Minutes in 4N HCl

It would appear that the original rayon sample was a mixture of cellulose II and either cellulose I or cellulose IV. Both cellulose I and cellulose IV have their (002) peaks in the same vicinity as the (002) peak of cellulose II. Therefore, either of these polymorphs would enhance the intensity of the apparent cellulose II (002) peak. Apparently the cellulose II fraction was more resistant to hydrolysis than the other polymorph.

This hydrolyzed rayon sample was not used as a standard due to the uncertainties about its composition.

LASER RAMAN SPECTROSCOPY

Raman spectra were recorded of most of the mercerized samples. Atalla (35) had observed some interesting differences between the vibrational spectra of celluloses I and II, especially in the low frequency region. Therefore, the Raman spectra were obtained in order to find out if these changes in the low frequency region correlated with the changes observed using x-ray diffraction and what these changes signify in terms of changes in the supermolecular structure of cellulose.

A Spex Raman spectrometer equipped with an argon ion laser as the exciting source at 5145 A was used. The slit widths of the three slits were always kept at 250 microns. The spectra were recorded using the direct current mode. The photomultiplier tube was maintained at -20°C. A narrow band interference filter was used to eliminate plasma emission lines. The time constant was 0.3 sec and the scan rate was 25 cm^{-1}/min. The spectra were recorded from 50 to 1550 cm^{-1} and 2700 to 3200 cm^{-1}.

Sample pellets were prepared in a Perkin-Elmer evacuable die using the same conditions that were used in making the x-ray pellets with the exception that no TiO_2 was included. The pellets were mounted on a 180° mount. Using this

technique the plane of the pellet is at right angles to the plane of the entrance slit. The filtered and focused laser beam impinges upon the sample pellet and the back-scattered radiation is reflected toward the entrance slit by a mirror which is at 45° to the plane of the pellet and the plane of the entrance slit. This arrangement is shown in Fig. 9.

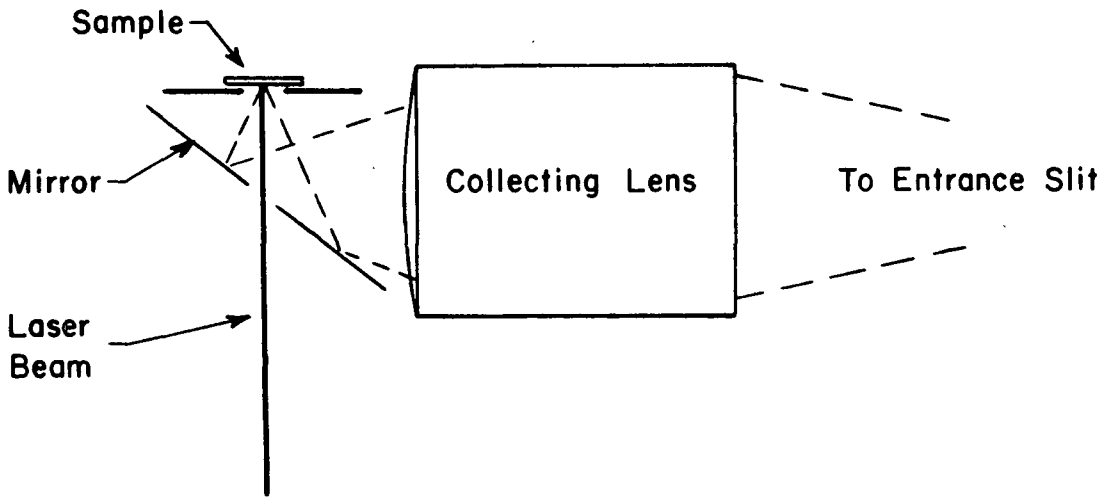

Figure 9. The Geometry of the 180° Mount

There was some problem with sample fluorescence. Generally, the fluorescence would decay with time. In order to avoid burning the cellulose, the approach was to radiate the sample with reduced intensity until the fluorescence had decayed sufficiently for analysis. The intensity of the primary radiation was reduced either by using neutral density and spike filters and defocusing the beam, or some combination thereof. It was observed that as the degree of conversion from cellulose I to II increased the fluorescence problem decreased. The implication of this observation is that the source of the fluorescence was naturally associated with the native lattice and removed by the caustic solution. Atalla and Nagel (36) have shown that laser-induced fluorescence in cellulose is caused by transition-metal ions.

RAMAN SPECTRA OF THE ALKALI METAL HYDROXIDES

SPECTRA OF THE SOLUTIONS

In order to supplement the meager information in the literature on the structure of the aqueous alkali metal hydroxides, the Raman spectra were recorded for all the mercerizing solutions. An impetus for this investigation was the discovery by Atalla (37) of a sharp band at 3610 cm^{-1} among the intramolecular vibrational bands of water in concentrated solutions of sodium hydroxide. The goal of this experimental work was to find out how the intensity of this band varied with concentration. Also, any variations of this band with respect to position or relative intensity among the three hydroxides studied would certainly be pertinent. It was expected that this band would be identified in the course of the investigation.

All the spectra were recorded using the photon counting mode at either 20 or 50°K. Large liquid quartz cells were used rather than capillaries. The cells were covered with quartz disks in order to preclude the absorption of carbon dioxide. The exciting source was the unfiltered argon laser at 5145 A. The slit widths were set at 250 microns with an entrance slit height of 20 mm. A time constant of 0.4 sec and a scan rate of 50 cm^{-1}/min were used. All the solutions were scanned from 2000 to 4000 cm^{-1}. The work was done at room temperature.

Polarization of the Band at 3610 cm^{-1}

It was suspected that the band at 3610 cm^{-1} represented the fundamental stretching frequency of the free hydroxide ion. The hydroxide ion is a linear diatomic species without a center of symmetry. It, therefore, belongs to the point group $C_{\infty,\nu}$. One can deduce that νOH^- should be polarized by consulting a character table for the point group $C_{\infty,\nu}$ (38). Therefore, the polarization of

the Raman bands of one concentrated hydroxide solution, 10.23M NaOH, was determined. If the band at 3610 cm^{-1} were not polarized then the tentative assignment of the band would unambiguously be wrong.

There are a number of ways to run depolarization ratio experiments using a laser Raman spectrometer. The method adopted in this work was to use a piece of polaroid film in a fixed position in the output optics and obtain the spectrum of the hydroxide solution twice, with and without a half-wave plate in position in the path of the laser beam in the input optic system. The laser beam is almost completely polarized. The purpose of the half-wave plate is to rotate the electric vector of the laser beam 90°. Another method which could have just as easily been used would have been to rotate the polaroid film 90° between the two spectral runs.

Carbon tetrachloride is generally the standard used in polarization work as it has a completely polarized band at 459 cm^{-1} and two completely depolarized bands at 218 and 312 cm^{-1}. The theoretical integrated depolarization ratio for a completely depolarized band when viewed at right angles to the exciting source, as was the case in this work, is 0.75, whereas the ratio for a completely polarized band is 0.0 (39). Actually the ratio for the polarized band for carbon tetrachloride at 459 cm^{-1} is 0.01 ± 0.001 due to secondary effects.

Using carbon tetrachloride as a standard, the best depolarization ratio that could be achieved was 0.71 for the depolarized bands and a more typical value was 0.70. A depolarization value of 0.0089 was achieved for the band at 459 cm^{-1} which is almost within the range cited by Tobin (39). Apparently, there was a systematic error in the optical system somewhere. However, the reproducibility using a given method was quite good. Since the band at 3610 cm^{-1} was highly

polarized, and therefore had a low depolarization ratio, the systematic error did not affect the general conclusions of the experiment.

SPECTRA OF THE SOLIDS

The Raman spectra of the solids lithium hydroxide, lithium hydroxide monohydrate, sodium hydroxide, and potassium hydroxide were obtained in order to see how different environments affect the location of the hydroxide ion fundamental stretching frequency. The spectra were run on hydroxide pellets in the "as received" condition.

The spectra were obtained using the aforementioned 180° mount. The sample pellets were placed on a glass cover slide and covered with an inverted quartz liquid sample cell. The joint between the cover slide and the inverted cylinder was sealed with silicone stopcock grease. These precautions were taken to keep the samples from hydrating during the course of the measurement.

It was discovered that to get good spectra of these pellets, the converging lens had to be in its normal position for running liquid samples and finely adjusted until the pellet glowed.

Raman spectra of these solids were taken using the photon counting mode, a time constant of 0.25 sec, and a signal amplification of from 10 to 100°K. The slit widths were 250 microns and a wide band interference filter was used.

MERCERIZATION USING MIXED ELECTROLYTES

The study involving the alkali treatment of cellulose over a broad range of concentrations indicated that there was a transition region in going from cellulose I to cellulose II in which the cellulose was progressively mercerized. The transition region proved to be a time-independent function of concentration.

A mercerizing solution of 3.19M sodium hydroxide and 1.30M sodium chloride was made in order to investigate the effect of added neutral electrolyte on the efficiency of a mercerizing solution in the transition region. The standard mercerization procedure was used with this solution.

PRECIPITATION FROM THE DIMETHYLSULFOXIDE-PARAFORMALDEHYDE CELLULOSE SOLVENT SYSTEM

PREPARATION OF THE CELLULOSE SOLUTION

The timely discovery by Nicholson (40) of the dimethylsulfoxide-paraformaldehyde (DMSO-PF) cellulose solvent system allowed for the precipitation of cellulose from solution under a variety of conditions. The advantages of this solvent system include the fact that there is no degradation of the polymer in solution (41) and that no heavy metal ions are involved which might be occluded upon precipitation.

Nicholson found that native cellulose could be solubilized in heated DMSO in the presence of paraformaldehyde. At about 120°C paraformaldehyde decomposes to the monomer. Nicholson has shown that under these conditions cellulose forms a hemiacetal with the formaldehyde. The substitution is predominantly at C_6 and the degree of substitution is one. The solvent system has little tolerance for water during the formation of the hemiacetal, but once the cellulose is in solution a fair amount of water must be added before the hemiacetal is hydrolyzed and precipitation occurs.

Numerous quantities of the cellulose solution were made during the course of the investigation using variations of the following method.

A 3% by weight/volume cellulose solution was made from Whatman CF1. The Whatman cellulose and paraformaldehyde were dried in a vacuum oven. The DMSO used was dried over molecular sieve for 6 hours.

The dissolution method used was to heat 15 g of cellulose with 500 ml of DMSO up to 120°C in a resin reaction flask with stirring and a condenser. Once the proper temperature was reached 4 or 5 g of paraformaldehyde were added. The paraformaldehyde quickly decomposed to the monomer and the cellulose went into solution. The solution was clear and rather viscous.

PRECIPITATION FROM THE CELLULOSE SOLUTION

Cellulose was precipitated from the DMSO-PF solvent under a variety of conditions. The effect of precipitating temperature on the supermolecular structure of cellulose was the primary investigation carried out using the DMSO-PF solvent. Other investigations included the effect of using various precipitating media such as alcohols and combinations of alcohol and acid on the supermolecular structure of the precipitate and the production of amorphous methylol cellulose by freeze drying the solution.

The pertinent experimental details for each of these samples are included in Appendix III, and the rationale and relevance of this work toward a greater understanding of the mercerization process and the supermolecular structure of cellulose are discussed in the Results and Discussion section.

HIGH TEMPERATURE WASH OF FULLY MERCERIZED CELLULOSE

Two fully mercerized samples were washed at high temperature: 100 and 165°C. The cellulose was mercerized with 6M sodium hydroxide for 30 minutes at 20.0°C using the standard mercerizing procedures previously explained. It had been determined that 6M sodium hydroxide completely decrystallizes the native lattice.

The mercerization slurry for one of the samples was plunged into stirred, boiling, distilled water under cover of nitrogen. The resulting slurry was neutralized with hydrochloric acid, filtered, washed, and freeze dried. The

other sample was plunged into stirred glycerol at 165 ± 2°C under nitrogen. This was a potentially dangerous experiment, and the slurry was added to the glycerol with considerable care. The resulting slurry was not neutralized but was filtered, washed, and freeze dried.

RESULTS AND DISCUSSION

INTRODUCTION

Initially a suitable grade of highly crystalline cellulose had to be found. In the course of determining how to evaluate the crystallinity of native cellulose using x-ray diffraction techniques, it was discovered that there is quite a divergence of opinion in the literature on the topic of cellulose crystallinity. Therefore, the concept of cellulose crystallinity and the methods of evaluation using x-ray techniques are examined in some detail under the heading "X-Ray Analysis Method." This discussion is not essential to the basic thrust of the dissertation, and may be omitted if one is not interested in the topic.

In the following sections the effect on native cellulose of the treatment with lithium, sodium, and potassium hydroxide solutions over a broad concentration range are discussed. Next the alkali metal hydroxide solutions are examined both experimentally, using Raman spectroscopy, and theoretically, through an examination of their activity coefficients. A theoretical interpretation of the decrystallization process is then deduced by relating the changes in the cellulose crystal structure to the changes in the solution structure.

The final topic discussed here is the effect of temperature on the supermolecular structure of cellulose precipitated from solution. The results of this precipitation work are then compared to the findings for completely mercerized cellulose which was washed at elevated temperatures.

EVALUATION OF CELLULOSE I CRYSTALLINITY

The crystallinity of cellulose has been aptly described as an "elusive" variable (42,43). Indeed the whole concept of crystallinity as applied to solid polymers is rather nebulous (43):

> "Imperfections in crystalline regions and some ordered arrangement of molecules in amorphous regions break down the clear distinction between the crystalline and amorphous regions. Differences in experimental technique can thus give rise to different estimates of crystallinity so that it is difficult to define crystallinity unambiguously."

Perhaps a satisfactory working definition of polymer crystallinity might be "the extent to which all the chains in a specimen approach the spatial distribution implied by the unit cell for the polymer."

X-RAY ANALYSIS METHOD

There are essentially two basic approaches for interpreting x-ray diagrams of polymers with respect to crystallinity. If the solid polymer is conceived of as a two-phase system, an approach that attempts to separate the scattering due to the amorphous fraction and the crystalline fraction would be used. On the other hand if the solid is thought to be a one-phase "sloppy lattice" then alternative methods of analysis may be employed.

For a two-phase system the following method is often employed using a fairly wide range of the diffraction intensity curve (44). Typically the diffraction pattern would be measured over a range of approximately 50° 2θ. Standard crystalline and standard amorphous specimens are used. Thus, this method is a relative crystallinity index, not an absolute determination. The relative crystallinity is evaluated by application of Equation (26).

$$X_{cr} = [(I_u - I_{amorph})_j - K]/(I_{cryst} - I_{amorph})_j, \qquad (26)$$

where I_u = diffraction intensity of specimen being investigated

I_{amorph} = diffraction intensity of amorphous standard

I_{cryst} = diffraction intensity of crystalline standard

j = various values of the diffraction angle

K = the intercept, should equal zero

The results of the individual calculations at each value of j are plotted on a graph with $(I_u - I_{amorph})_j$ as the ordinates, and $(I_{cryst} - I_{amorph})_j$ as the abscissae. A linear regression is performed on the plotted points and the slope of this line is the crystallinity index X_{cr}. A value of 1 would indicate a 100% crystalline sample and a slope of 0 would be a 100% amorphous sample.

In one of the more frequently cited papers on the crystallinity of cellulose, Wakelin, et al. (45) essentially applied the above method in a careful examination of a series of native celluloses. Ellefsen, et al. (46) adopted a slightly different approach. They put the diffraction curve of a ground amorphous sample tangent to the diffraction curve of the unknown specimen at approximately 18° 2θ. They then determined the "degree of amorphity" to be a ratio of two areas. The numerator was the area of the amorphous curve tangent to the unknown sample. The denominator was the total area under the diffraction curve for 100% "x-ray amorphous cellulose." According to this method of evaluation, the "degree of amorphity" of hydrolyzed surgical cotton was determined to be 0.38 on a scale of zero, for completely crystalline cellulose, to one, for completely amorphous cellulose. Thus, this approach has certain drawbacks as one would expect hydrolyzed surgical cotton to be free of any accessible amorphous fraction. Ellefsen, et al. were aware that their approach had some limitation.

As discussed by Kakudo and Kasai (47), Hosemann has developed a sophisticated approach for the analysis of the crystallinity of polymers. The underlying basic assumption is to view solid polymers as paracrystalline. Then, according to this theory, the broadening of diffraction peaks and a fraction of the background scattering are due to lattice distortions of the first and second kind. Lattice

distortions of the first kind are generally smaller than distortions of the second kind.

Lattice distortions of the first kind include thermally induced displacements from the ideal lattice points, vacancies and interstitials, small displacements from the theoretical lattice points which are "frozen in," and other small displacements which do not affect the long range order. Distortions of the first kind reduce the intensity and add to the continuous background scattering.

Distortions of the second kind are generally distortions which are larger in magnitude than distortions of the first kind. The statistical averages of the positions of the atoms do not form an ideal lattice when distortions of the second kind are present, and the long range order is affected by this class of distortions; the paracrystalline lattice factor, $\underline{Z}(\underline{b})$, is influenced. The diffraction peaks are broadened depending upon the magnitude of the defects.

The main drawback of Hosemann's theory is that it is too complicated to be readily applied. No one has yet applied it to cellulose I, but certain elements of the theory have been incorporated into a study of the crystalline perfection of a viscose cellulose II product (48). Even though the theory is much too involved to be used as a method for routine analysis, it will be introduced here as some of the ramifications of the theory are of qualitative value both in this section and elsewhere in the dissertation. Equation (27) is the expression for the diffraction intensity, $\underline{I}(\underline{b})$.

$$I(b) = \overline{N}[\langle A_{cell}{}^2\rangle - D^2 \langle A_{cell}\rangle^2] + 1/\mu\langle A_{cell}\rangle^2(D)^2 \times [Z(b)^*|S(b)|^2], \quad (27)$$

where $\underline{b}$ = vector in reciprocal space

$\overline{N}$ = total number of unit cells

$\langle A_{cell} \rangle$ = average scattering amplitude for a unit cell

$\underline{D}$ = distortion factor of the first kind (Debye factor)

μ = average volume of one unit cell

$\underline{Z}(\underline{b})$ = paracrystalline lattice factor; corresponds to the Laue function for the ideal crystal

$|\underline{S}(\underline{b})|^2$ = shape factor of the domain of the paracrystalline lattice

Gjonnes, et al. (49) and Gjonnes and Norman (50) have developed a crystallinity index which is related to lattice distortions of the second kind. They resolved the (002) reflection of cellulose I into a Cauchy distribution profile. From this analysis they were able to get a measure of the width of the peak at half height which was then used as a measure of crystallinity. According to their analysis, cellulose I "... very likely consists of aggregates of distorted crystallites, and that only small quantities of highly disordered material are present."

One very relevant aspect of the study just cited is that the authors also calculated the "degree of amorphity" as described by Ellefsen, et al. (46). Figure 10 is a plot of the width at half height vs. the "degree of amorphity" from their work. Essentially this figure indicates that the ranking of the relative crystallinities of cellulose I will be nearly in the same order using these two entirely different methods of x-ray analysis. Ellefsen, et al. based their index on the assumption that cellulose is a two-phase system while Gjonnes, et al. (49,50) assumed a homogeneous distorted lattice. Since distortions contribute to the general background scattering, it is clear why these two methods can potentially yield the same relative results.

Segal, et al. (51) proposed a widely adopted crystallinity index for cellulose I which is quite easy to apply. The index is simply a linear intensity ratio of the (002) plane reflection and the minimum between the (002) and the

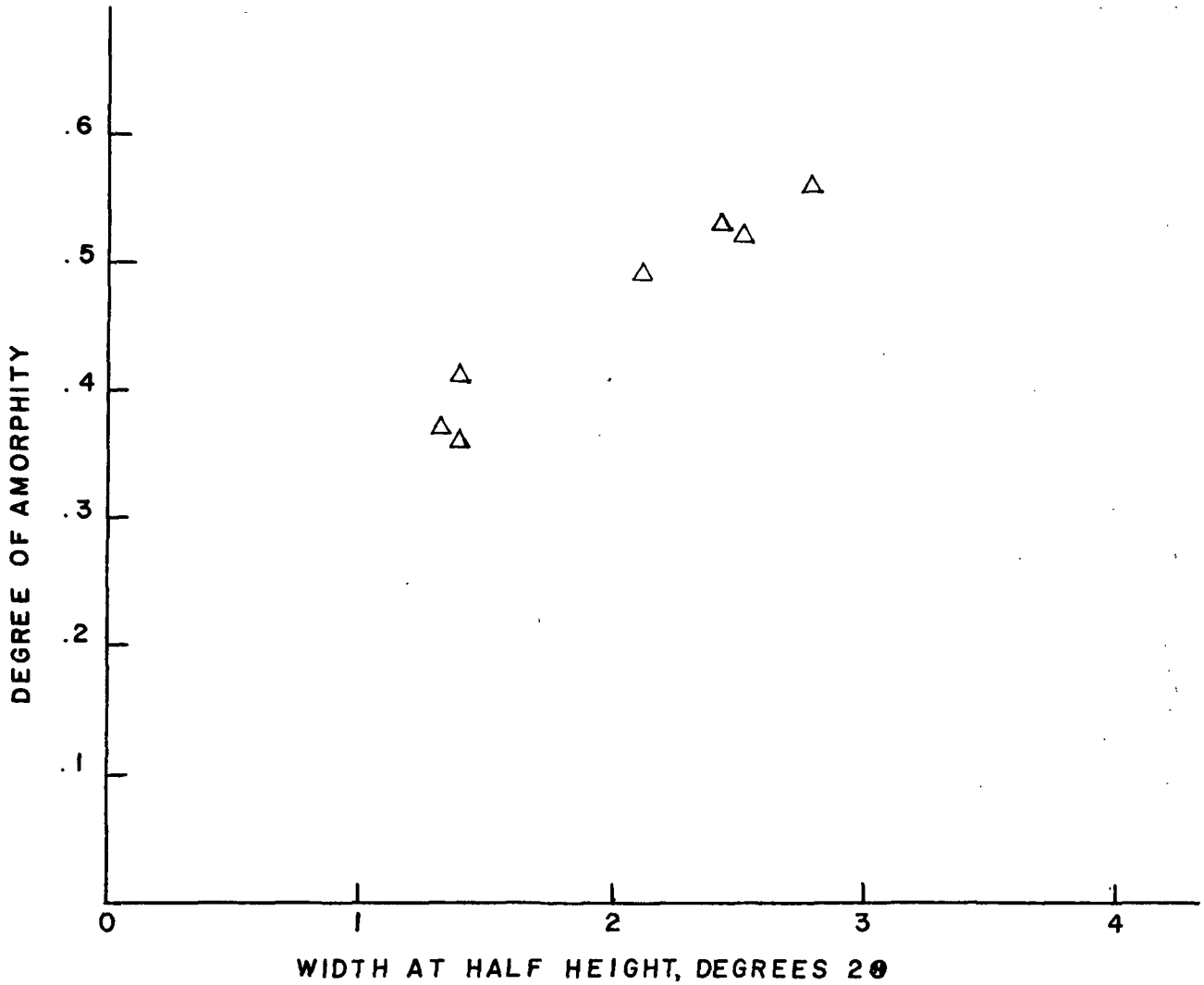

Figure 10. Degree of Amorphity vs. Width at Half Height for a Series of Cellulose I Samples (50)

$(10\bar{1})$ plane which is at about 19° 2θ for CuKα radiation. Figure 11 shows the location and measurement of these two intensities. Their crystallinity index is calculated according to Equation (28).

$$CrI = [(I_{002} - I_{am})/(I_{002})] \times 100\%, \qquad (28)$$

where CrI = crystallinity index

I_{002} = intensity at approximately 22.6° 2θ

I_{am} = intensity at approximately 19° 2θ

This crystallinity index, which is based on the two-phase model of cellulose, has no absolute theoretical significance, but it is as good as any other approach for the relative ranking of cellulose I crystallinities. The method correlates well with infrared crystallinity indices, moisture regain, and density. Nelson and O'Connor (30) have shown that the method also correlates well with the more complex Wakelin crystallinity index. Therefore, this method was used in ranking the crystallinities of the celluloses examined. The results are presented in Table II which has been deferred until after the infrared crystallinity index discussion is completed.

INFRARED ANALYSIS METHOD

The intensity ratios of various bands in the infrared have been used as a measure of cellulose crystallinity. Therefore, the infrared spectra of the investigated celluloses were recorded as a supplement to the x-ray data.

The infrared crystallinity index developed by Nelson and O'Connor (30,52) was used in this work. This method is based on the absorption ratio of two bands in the infrared spectrum of cellulose, $a_{1372\ cm^{-1}}/a_{2900\ cm^{-1}}$. Nelson and O'Connor found that the band at 2900 cm^{-1} (C-H and CH_2 stretching) is relatively invariant while the absorption band at 1372 cm^{-1} (C-H bending) is quite sensitive

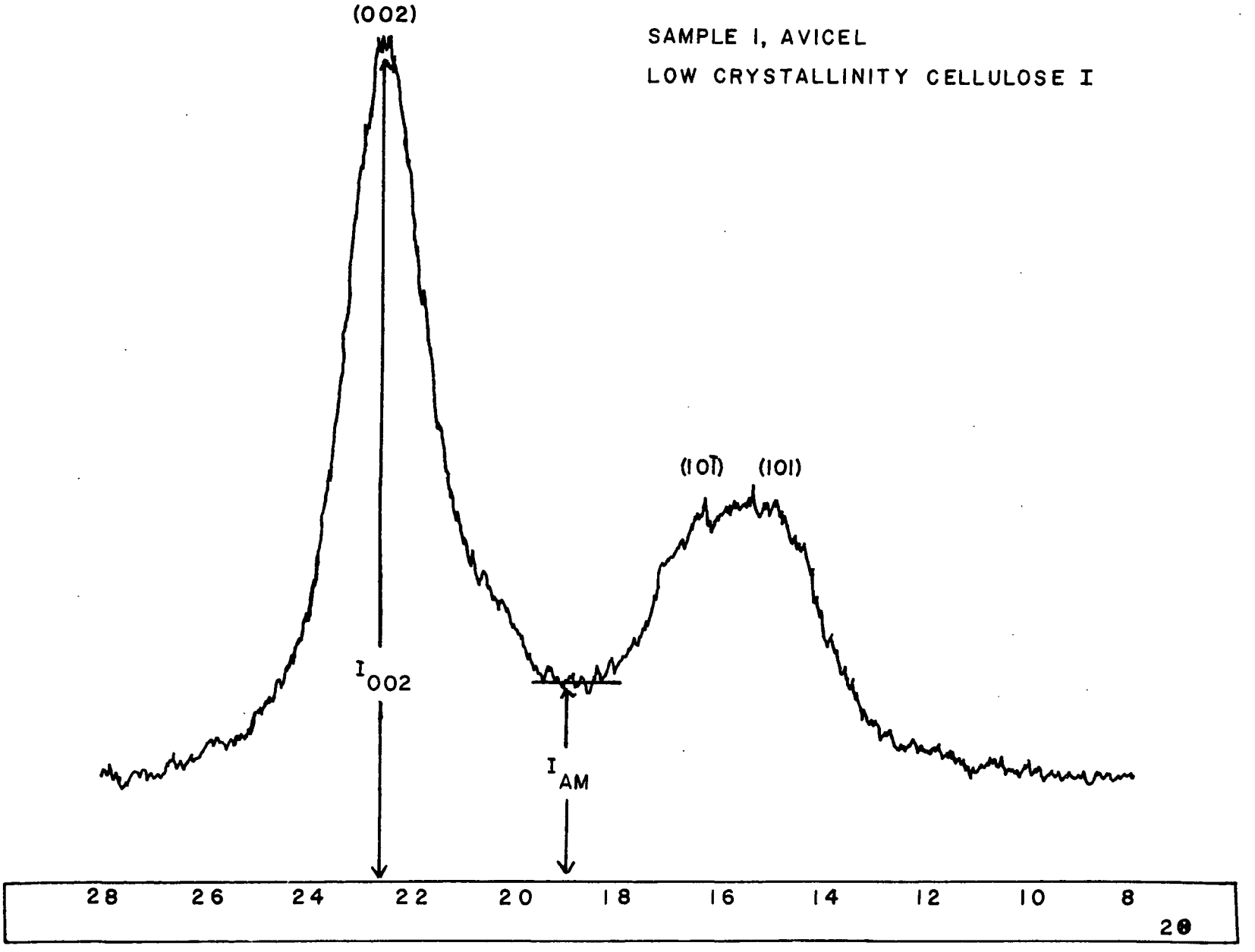

Figure 11. Method of Obtaining the Parameters for the Crystallinity Index Proposed by Segal, et al. (51)

to changes in crystallinity. One of the advantages of using the band at 1372 cm^{-1} is that it apparently is not much affected by lattice type, but only by crystallinity. Therefore, crystallinity comparisons may be made between the various polymorphs of cellulose using this index.

Figure 12 is the infrared spectrum of Sample 11, Stoneville 2B cotton hydrocellulose, in which the base lines and absorption measurements suggested by Nelson and O'Connor are indicated. Beer's law was invoked in converting the percent transmittance measurements into absorbance values.

RESULTS

The x-ray and infrared crystallinity index results are given in Table II for the celluloses investigated. As can be seen, there is not a particularly good correlation between the infrared and x-ray results. This may be due in part to the technique used in preparing the infrared pellets. To avoid excessive scattering using the potassium bromide pressed disk method, the particle size of the sample's powder must be less than 2 microns (53). No measurements or corrections were made of the particle size and there may well have been a scattering problem which could account for some of the seemingly spurious results such as the unusually high value assigned to Sample 12. Because of the uncertainty of the infrared data, the x-ray results were employed in making the final decision about which cellulose would be used.

Prolonged hydrolysis did not dramatically change the crystallinity of Avicel or markedly affect the crystallinity of the Whatman CF1. Whatman CF1 hydrolyzed for 30 minutes in 4N hydrochloric acid was adopted as the standard cellulose for use in the mercerization work. This preparation had nearly the highest x-ray crystallinity and was much easier to prepare than any of the hydrolyzed cottons. A large lot of the cellulose product was purchased so that a homogeneous supply

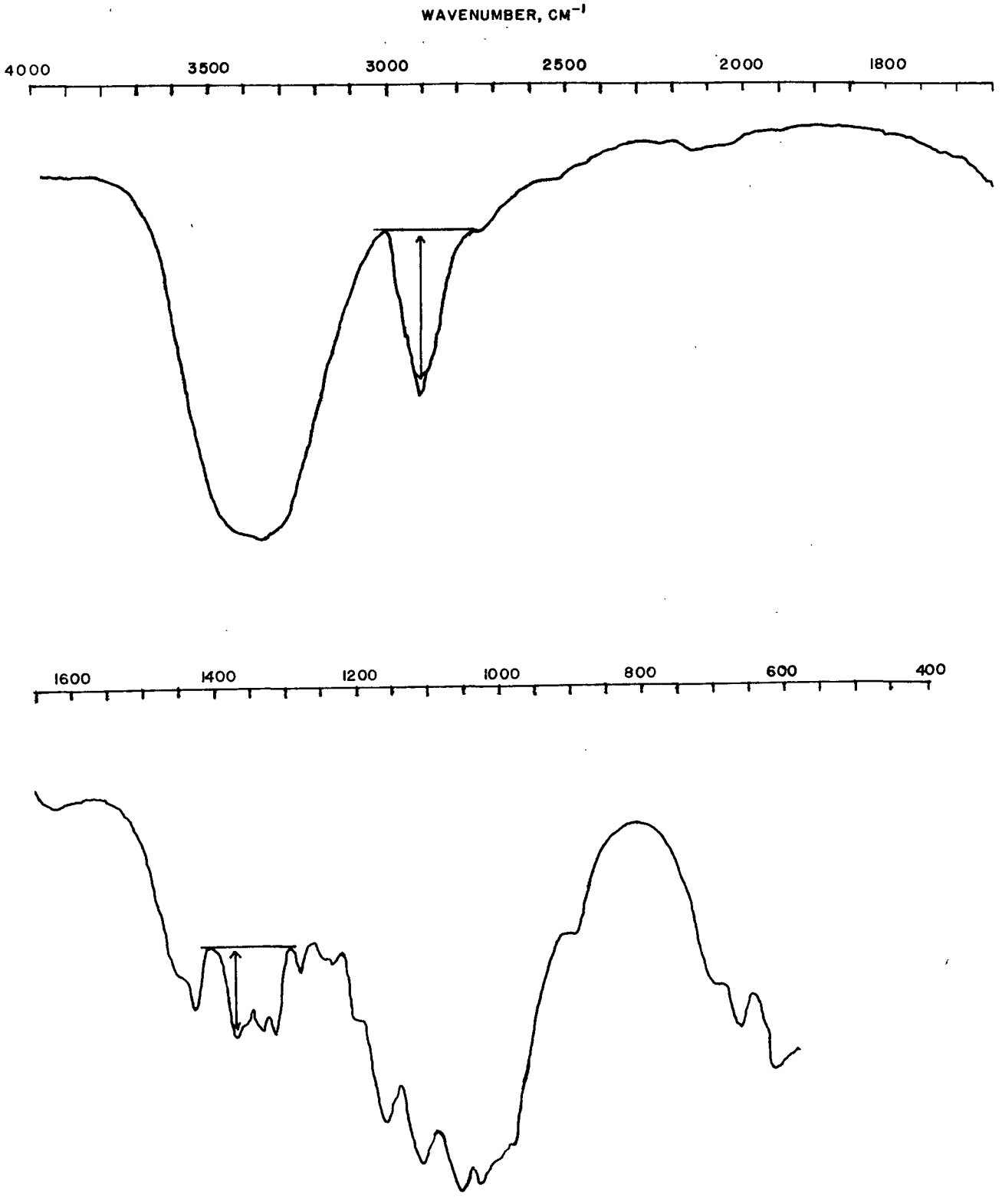

Figure 12. Infrared Spectrum of Stoneville 2B Cotton Hydrocellulose.

The method for obtaining the absorbance values used in the infrared crystallinity index is indicated

TABLE II

X-RAY AND INFRARED CRYSTALLINITY RATIOS OF THE CELLULOSES EXAMINED AS POSSIBLE MATERIALS FOR MERCERIZATION

Sample	Description	Crystallinity Index			
		N[a]	IR	N	X-ray
1	Avicel untreated	19	0.3632 ± 0.0054	19	74.94 ± 0.40%
2	Avicel hydrolyzed 1 hr in 2.4N HCl	1	0.36	1	82.0
3	Avicel hydrolyzed 4 hr in 2.4N HCl	1	0.43	1	81.4
4	Avicel hydrolyzed 8 hr in 2.4N HCl	1	0.43	1	76.9
5	Cotton hydrolyzed 15 min in 2.5N HCl	1	0.45	1	90.0
6	Cotton hydrolyzed 2 hr in 2.5N HCl	1	0.41	1	88.2
7	Avicel freeze-dried	1	0.37	1	76.3
8	Avicel solvent exchange dried	1	0.33	1	78.9
10	Ramie hydrolyzed 30 min in 2.5N HCl	1	0.43	2	83.0
11	Stoneville 2B cotton hydrolyzed 30 min in 4N HCl	1	0.50	3	86.5
--	Whatman CF1 untreated		--	1	87.5
12	Whatman CF1 hydrolyzed 15 min in 2.5N HCl	1	0.60	1	87.8
13	Whatman CF1 hydrolyzed 30 min in 4N HCl	1	0.49	1	89.1

[a] N = number of samples.

would be insured throughout the project. The hydrolysis procedure was determined to be reproducible by preparing two batches and making 10 x-ray pellets from each batch. Statistical analysis of the x-ray results indicated that the two populations were equal at the 95% confidence limits.

MERCERIZATION OF HYDROCELLULOSE WITH LiOH, NaOH, AND KOH

METHOD OF ANALYSIS OF THE X-RAY DIFFRACTOGRAMS OF MERCERIZED CELLULOSE

The primary quantitative means of following changes in the crystal structure of the native hydrocellulose as a result of alkali treatment were the x-ray diffractograms. Figure 13 includes representative diffractograms from the KOH mercerization series at various molar concentrations. The bottom diffractogram is cellulose I, whereas the top diffractogram is converted to cellulose II to the maximum extent that such a conversion may be achieved under the experimental conditions described earlier. The other diffractograms are of mixed lattices indicating intermediate conversion of cellulose I to II.

There are a host of corrections which may be applied to raw x-ray data. As mentioned earlier, Wakelin, et al. (45) did a very exacting x-ray diffraction study in the development of their cellulose crystallinity index. They applied the following corrections to the raw x-ray intensity data: (1) cosmic ray background, (2) Geiger counter dead time, (3) x-ray tube fluctuations, (4) air scattering, (5) polarization, (6) spectrometer geometry, (7) sample absorption, (8) sample moisture, and (9) incoherent radiation and curve fitting for total independent scattering of a unit mass of cellulose.

In order to get a measure of the relative importance of the corrections which Wakelin, et al. applied, the following was done: Wakelin's original, normalized crystallinity index data was plotted vs. the corrected data. This

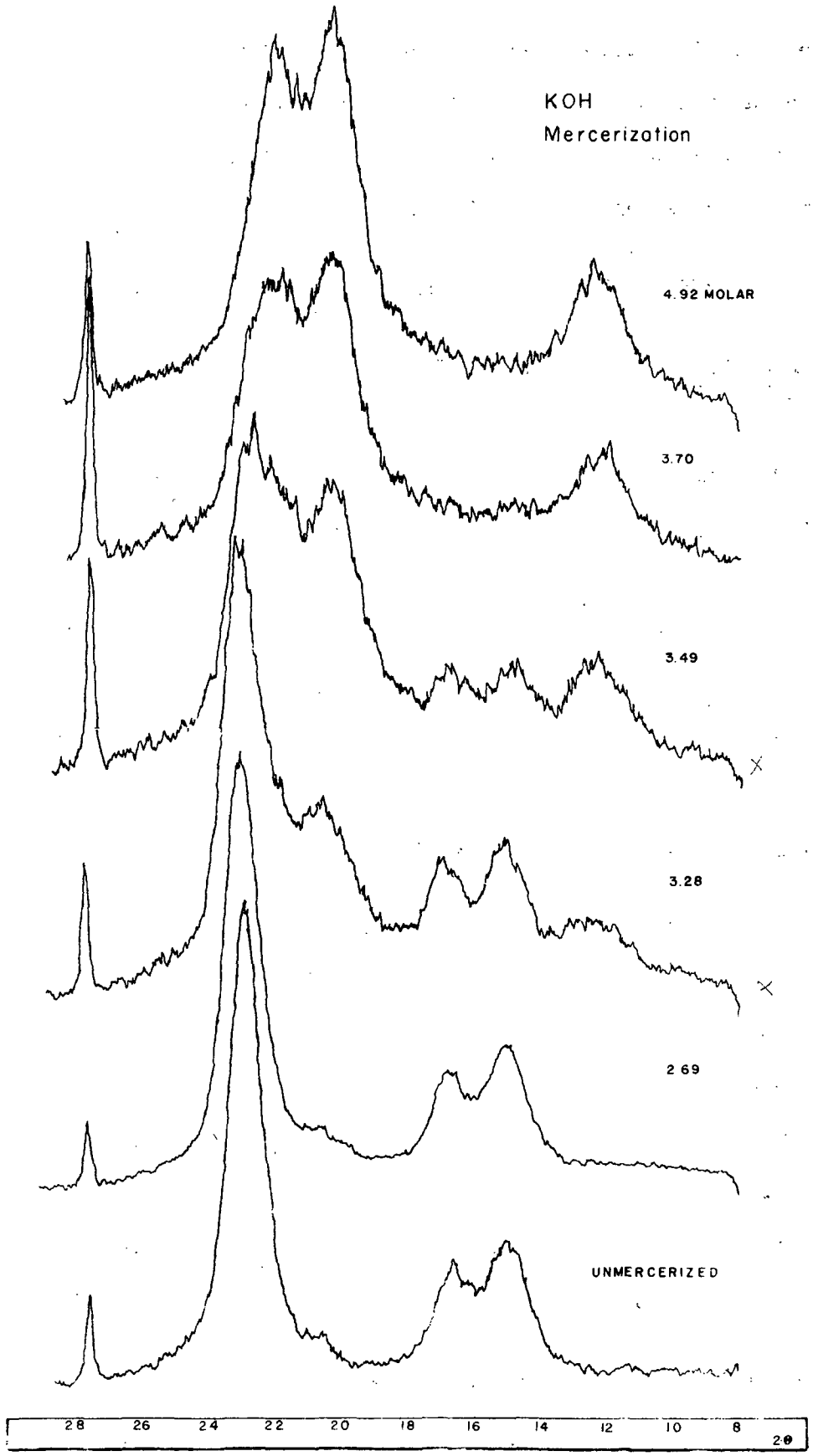

Figure 13. X-ray Diffractograms of the KOH Mercerization Series in the Transition Region.

The molarity of the mercerizing solution is indicated

plot is shown in Fig. 14, which appears to be a good linear correlation between corrected and raw x-ray data especially when the following statement by Wakelin, et al. is taken into consideration:

> "... there are no statistically significant differences between estimates of crystallinity indices for the six native cotton varieties studied."

The native cotton varieties mentioned refer to the cluster of six points in Fig. 14. From this comparison of corrected and raw x-ray data it was concluded that the corrections mentioned would not significantly alter relative x-ray measurements of cellulose. All the x-ray measurements used in this dissertation were relative rather than absolute. Comparisons were made between various cellulose samples. Since relative, rather than absolute, measurements were made in this work, no corrections were made to the raw data.

It was necessary to quantify the degree of lattice conversion as a function of concentration of alkali in order that meaningful comparisons as to the relative effectiveness of the three alkali metal hydroxides could be made. Ellefsen, et al. (46) have suggested that intensity ratios at certain specified 2θ values could be used in conjunction with known laboratory mixtures of native and mercerized cellulose in determining the degree of conversion from cellulose I to II. Gjonnes and Norman (54,55) have brought attention to the fact that simple intensity ratios are not an entirely accurate measure of the degree of conversion since there may be variations in crystallinity of either or both of the polymorphs in a mixed sample. A less crystalline sample will have broader diffraction peaks of lower integrated intensity than a more crystalline sample. It was decided that Gjonnes and Norman's approach would be adopted.

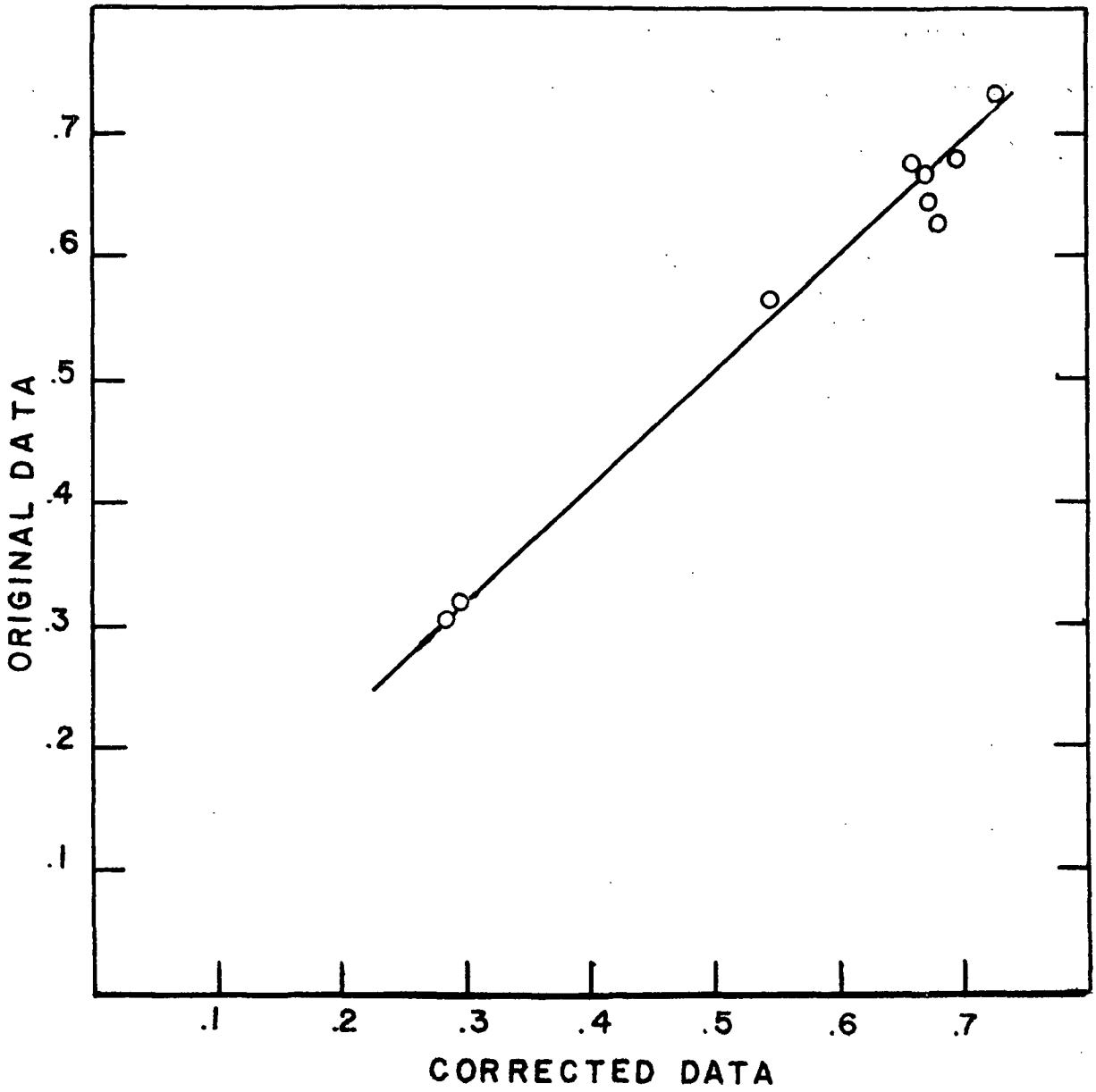

Figure 14. Linear Correlation Between Original and Corrected X-ray Crystallinity Index.

This figure depicts the linear relationship between original and corrected x-ray data with reference to the Wakelin (48) crystallinity index

Gjonnes and Norman developed an empirical method for dealing with the problem of analyzing mixed systems of cellulose I and II of varying crystallinity. They formulated a 2-parameter index. The two parameters which they used are best explained by reference to Fig. 15 which is from their publication (54).

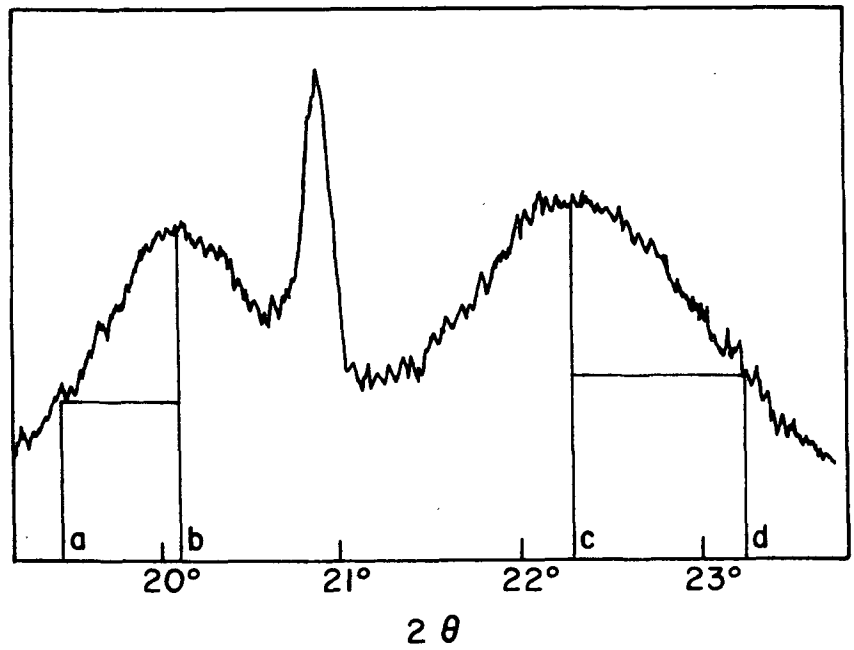

Figure 15. Microphotometer Curve for a Mixed Sample of Cellulose I and II.

The sharp peak at 2θ = 20.88° is an internal standard

The letters a and b indicate the $(10\bar{1})$ outer half value intersection and the $(10\bar{1})$ peak position for cellulose II. The letters c and d refer to the (002) peak position and outer half value intersection. The (002) peak is made up of contributions from both cellulose I and II. The $(10\bar{1})$ peak is really a combination of the (021) peak of cellulose I and the $(10\bar{1})$ peak of cellulose II. Gjonnes and Norman used the intensity ratio $\underline{I}(10\bar{1})/\underline{I}(002)$ and the (002) outer half value intersection in their 2-parameter index. Laboratory standards of known ratios of the two cellulose polymorphs of varying crystallinities were used by Gjonnes and Norman in developing a method for converting x-ray data of

partially mercerized samples into a ratio of the two polymorphs. A conversion chart based on data developed by Gjonnes and Norman could not be used as they employed a symmetrical transmission x-ray technique, while a symmetrical reflecting technique was used in this work. The relative intensities of the various diffraction peaks are not the same for the two techniques.

It is not clear from Gjonnes and Norman's papers (54,55) what criteria they used in drawing base lines. The purpose of the base line is to isolate the diffraction peaks from the background which is composed of many contributions, including Compton or incoherent scattering, and coherent background scatter due to lattice imperfections. The most reproducible method of separating the crystalline peaks from the background is to draw a smooth curve from one minimum point to the next following the general curvature of the independent scattering curve (56). Unfortunately, this cannot be reliably done for mixed lattice systems of cellulose I and II because the broad tails of the five apparent peaks obscure the points of tangency. Therefore, the base line must be tangent to the curve in areas unaffected by the peaks of cellulose I and II. The base line must also be a straight line because the x-ray diffractograms were not normalized and vary considerably in their total integrated intensities. A curved base line would have to be modified for each analysis, because the radius of curvature would be a function of the integrated intensity.

The base line resorted to in this study is illustrated in Fig. 16. It is tangent to the diffractogram at 27.46° 2θ which is the position of the (110) peak of the internal standard, TiO_2. The other point of tangency is at 10° 2θ.

Seven parameters were obtained from the x-ray data. These include the peak position of the (002) peak of celluloses I and II and the peak position of the $(10\bar{1})$ peak of cellulose II. The method of determining the peak positions was to

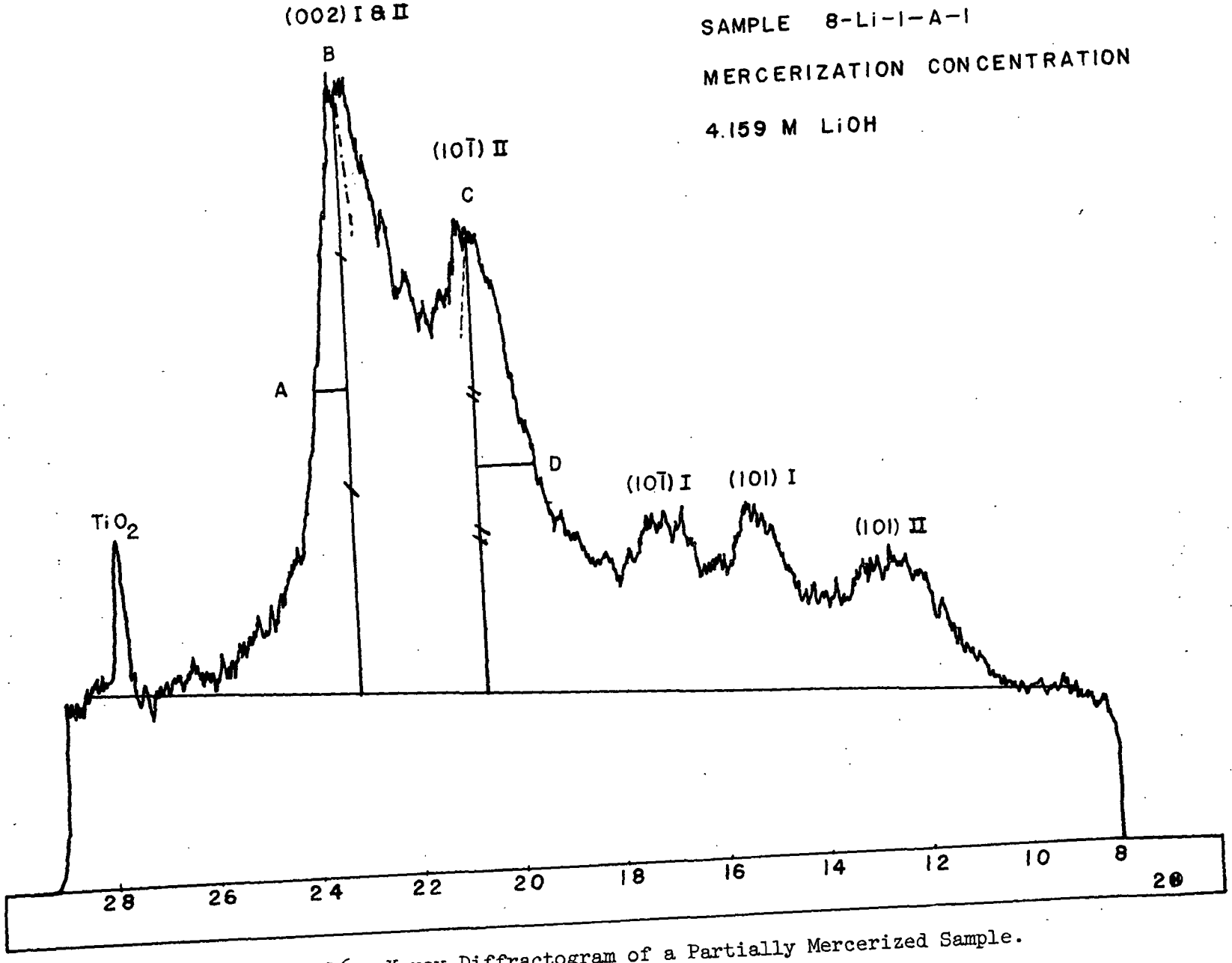

Figure 16. X-ray Diffractogram of a Partially Mercerized Sample.

The base line and method of determining the x-ray parameters are illustrated

draw several horizontal chords near the apex of the peak and bisect these chords. A line was then drawn through the chord bisections. The intersection of this line with the diffractogram was then determined to be the apex or position of the peak. This approach had to be used as the peaks of interest are not symmetrical since they overlap each other. The heights of the (002) and $(10\bar{1})$ peaks were measured from the apex to the base line as shown in Fig. 16. The ratio of the intensities was then calculated from these measurements. The outer half height intersections were determined by bisecting the peak heights and running a horizontal line through the bisection to the outer boundary of the peak. These intersections are marked A and D in the figure. The width at half height (whh) parameters in degrees 2θ were calculated by taking the difference between the peak position and the half height intersection and multiplying by two. These parameters should represent the width of a peak at half its height if no other peaks interfered.

Of the seven parameters which have been mentioned three were found to be most useful and reproducible. These three are the intensity ratio $\underline{I}(10\bar{1})/\underline{I}(002)$ and the 2θ outer intersections for the (002) and $(10\bar{1})$ peaks.

Laboratory mixtures of the two polymorphs were prepared from samples of low and high crystallinity celluloses I and II. The history of the samples used in the preparation of these laboratory mixtures is discussed in the Experimental Program section. The laboratory mixtures were prepared on an oven-dry weight basis. The four celluloses used are listed in Table III. The x-ray parameters for all the standards and mixtures used are reported in Table IV.

In addition to the celluloses used in the mixtures, a series of cellulose I and II samples are included which were used to define the 100% cellulose I and 100% cellulose II parameters. Samples 17, 19, and 20 are all Whatman CF1

hydrolyzed for 30 minutes in 4N hydrochloric acid. Sample 11 is described in Appendix I. The series of samples listed after 22-B-2 are all mercerized samples that have been converted to cellulose II to the full extent that this can be done using alkali metal hydroxide mercerizing agents. The x-ray diffractograms of the mixtures are found in Appendix IV.

TABLE III

STANDARDS USED IN PREPARED MIXTURES

Sample Designation	Lattice	History	Moisture Content, %
1	I	Avicel unmodified	5.97
16	I	Whatman CF1 hydrolyzed 30 min in 4N HCl	5.00
22-B	II	Precipitated from DMSO-PF	6.35
8-Na-1-2	II	Mercerized in 4.631M NaOH	11.19

Figures 17 and 18 are the two parameter plots used in converting the raw x-ray mercerization data into proportions of celluloses I and II. The ordinate of Fig. 17 is the 2θ outer half height intersection of the $(10\bar{1})$ peak of cellulose II and the abscissa is the intensity ratio of the $(10\bar{1})$ peak of cellulose II and the (002) peak of celluloses I and II. The way to use this figure is to position an unknown partially mercerized sample according to the values of the two designated x-ray parameters and determine the value by interpolation. Since the percent composition lines are not parallel, the interpolation becomes a ratio of the shortest distances of the experimental point from each of the two labeled composition lines which bound the area in which the experimental point is found. As an example, suppose that an unknown sample point was somewhere in the area bounded by the 60% II composition line and the 80% II composition line of Fig. 17. Let the distance from the unknown to the

TABLE IV

STANDARDS TABLE — X-RAY DATA

Sample Designation	Composition	2θ (002)	whh (002)	2θ Inter (002)	2θ ($10\bar{1}$)	whh ($10\bar{1}$)	2θ Inter ($10\bar{1}$)	$\frac{I(10\bar{1})}{I(002)}$
19-A-3	100% I	22.73	1.14	23.31	--	--	--	0.0772
19-A-4	"	22.73	1.10	23.28	--	--	--	0.0774
11-B-4	"	22.71	1.28	23.35	--	--	--	0.0947
1-I-5	"	22.57	1.78	23.46	--	--	--	0.1955
20-A-1	"	22.76	1.18	23.35	--	--	--	0.1010
17-E-1	"	22.72	1.20	23.32	--	--	--	0.0804
	80% I/20% II							
Standard B	80% 1/20% 22-B	22.58	1.84	23.50	--	--	--	0.2355
Standard G	80% 16/20% 22-B	22.76	1.18	23.35	--	--	19.44	0.1650
Standard K	80% 16/20% 8-Na	22.73	1.22	23.34	20.53	2:10	19.48	0.2007
	60% I/40% II							
Standard C	60% 1/40% 22-B	22.53	1.84	23.45	20.37	2.54	19.10	0.3860
Standard H	60% 16/40% 22-B	22.73	1.16	23.31	20.42	2.02	19.41	0.2219
Standard L	60% 16/40% 8-Na	22.70	1.24	23.32	20.26	1.52	19.50	0.3310
	40% I/60% II							
Standard D	40% 1/60% 22-B	22.42	1.98	23.41	20.38	2.54	19.11	0.5449
Standard I	40% 16/60% 22-B	22.69	1.30	23.34	20.29	2.10	19.24	0.404
Standard M	40% 16/60% 8-Na	22.69	1.24	23.31	20.20	1.78	19.31	0.520
	20% I/80% II							
Standard E	20% 1/80% 22-B	22.23	2.02	23.24	19.93	1.68	19.09	0.797
Standard J	20% 16/80% 22-B	22.46	1.70	23.31	20.01	1.90	19.06	0.766
Standard N	20% 16/80% 8-Na	22.59	1.46	23.32	20.13	1.72	19.27	0.891
22-B-2	100% II	21.66	2.14	22.73	20.09	2.16	19.01	1.040
8-Na-1-A-2[a]	"	21.74	1.92	22.70	20.10	1.62	19.29	1.223
8-Na-2-A-2	"	21.83	1.66	22.66	20.04	1.50	19.29	1.182
9-Na-1-A-2	"	21.75	1.92	22.71	20.07	1.68	19.23	1.151
9-Na-2-A-2	"	21.62	2.20	22.72	20.07	1.70	19.22	1.194
10-Na-1-A-2	"	21.61	2.14	22.68	20.07	1.66	19.24	1.122
10-Na-2-A-3	"	21.72	1.92	22.68	20.16	1.90	19.21	1.172
11-Na-1-A-1	"	21.71	1.94	22.68	20.14	1.88	19.20	1.178
11-Na-2-A-A	"	21.61	2.28	22.75	20.16	1.94	19.19	1.157
12-Na-1-A-1	"	21.74	1.94	22.71	20.13	1.78	19.24	1.179
12-Na-2-A-2	"	21.69	2.04	22.71	20.10	1:74	19.23	1.180
9-K-1-A-2	"	21.85	1.72	22.71	20.08	1.76	19.20	1.120
9-K-2-A-2	"	21.76	2.32	22.82	20.14	1.96	19.16	1.152
10-K-1-A-2	"	21.76	1.96	22.74	20.09	1.72	19.23	1.144
10-K-2-A-2	"	21.76	1.86	22.69	20.04	1.54	19.27	1.144
11-K-2-A-2	"	21.76	1.94	22.73	20.07	1.76	19.19	1.138
11-K-1-A-2	"	21.93	1.58	22.72	20.10	1.70	19.25	1.207

[a]Sample Designation explanation: Example, 8-Na-1-A-2 would refer to a sample mercerized by NaOH solution 8. The 1 refers to this being the first sample mercerized by solution 8. The A refers to this being the first x-ray pellet and the final 2 means that this information refers to the second x-ray diffractogram run on pellet A.

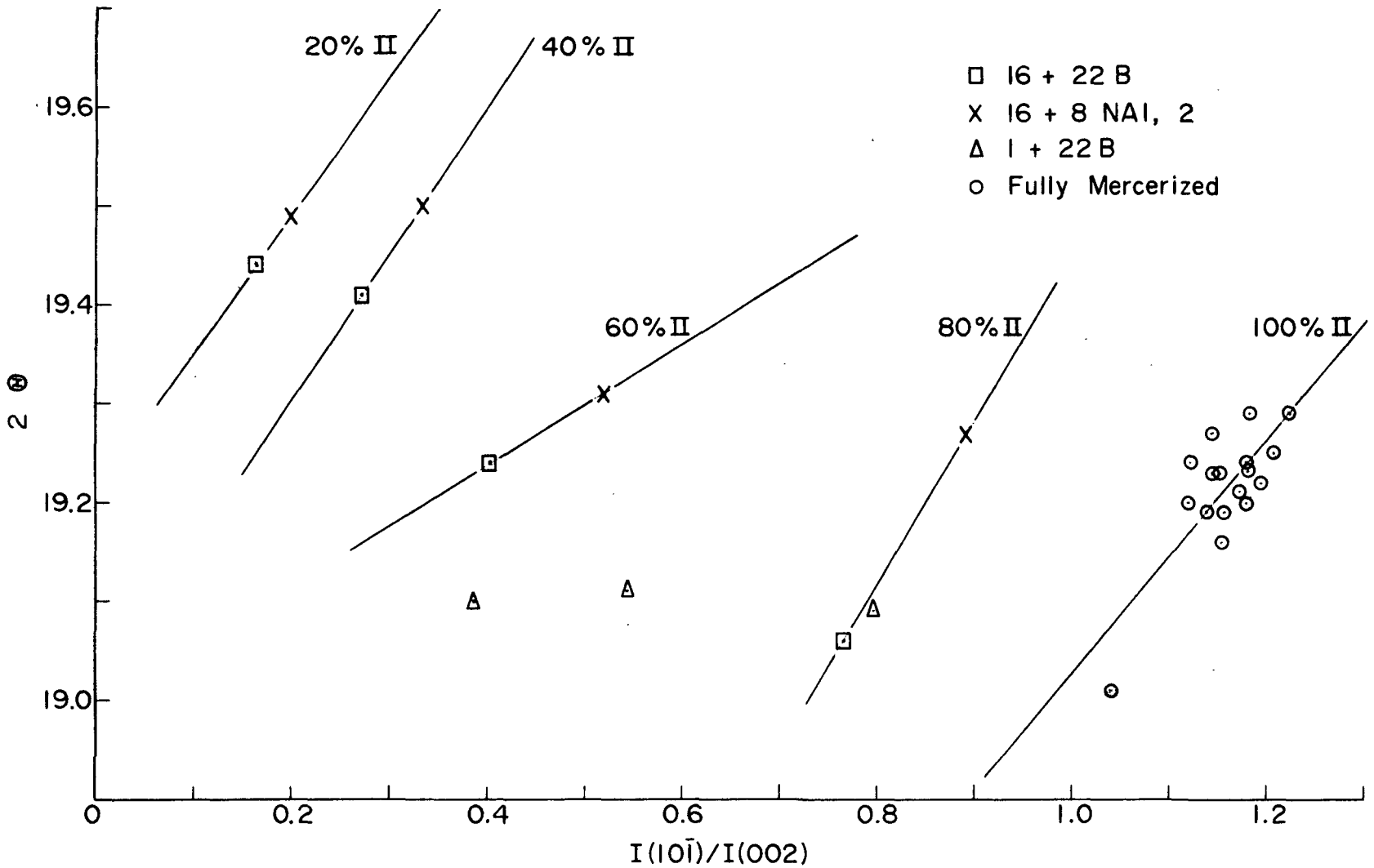

Figure 17. Two-parameter Plot Used in Converting the X-ray Data from Partially Converted Systems into Proportions of Cellulose I and II.

The y-axis represents the 2θ outer half-height intersection of the (10$\bar{1}$) peak of cellulose II. This is point D of Fig. 16. The x-axis is the height ratio of the two major peaks

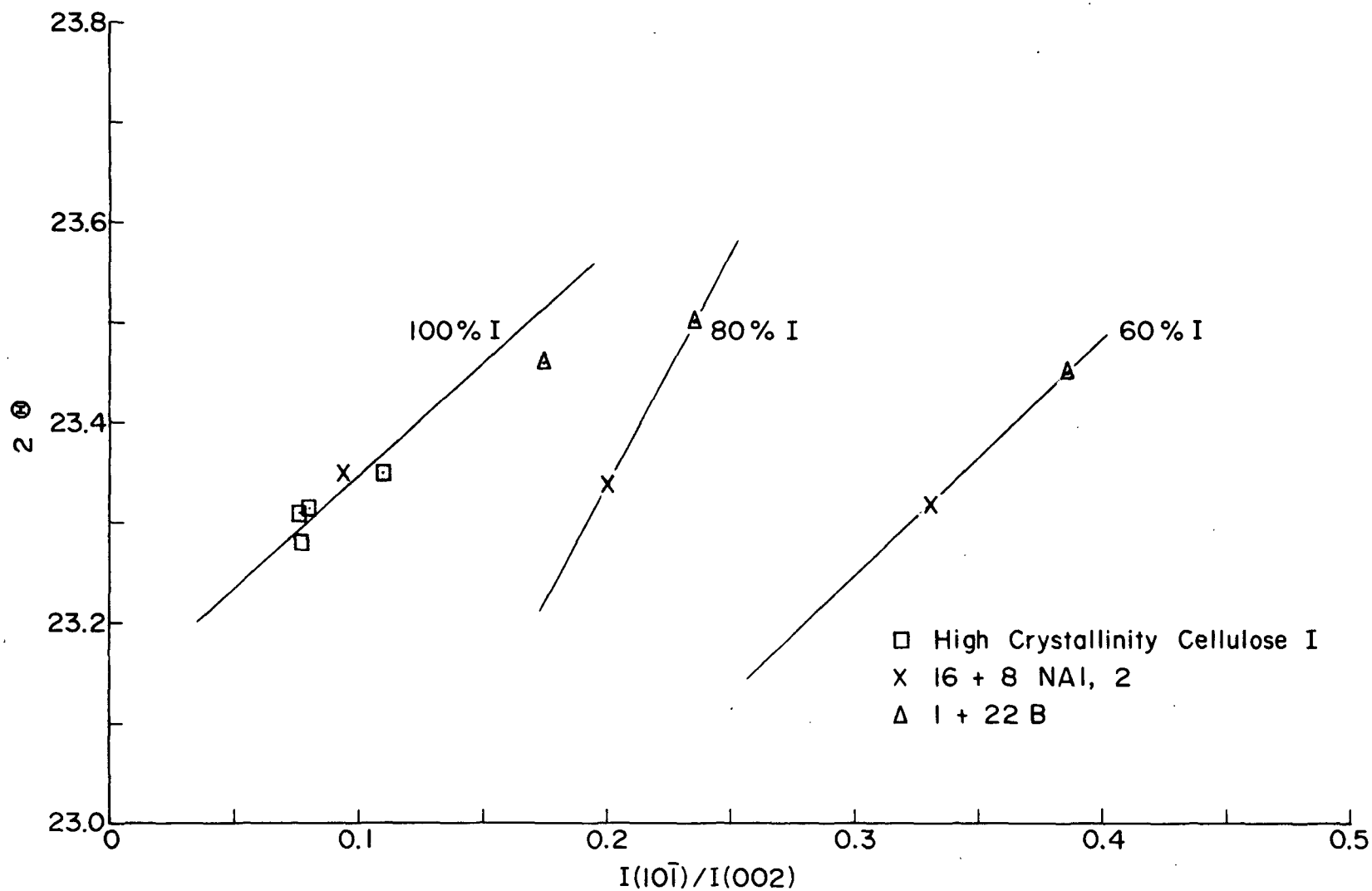

Figure 18. Two-parameter Plot Similar to Fig. 17 Except that the y-Axis Represents the 2θ Half-height Intersection of the (002) Peak.

This is Point A of Fig. 16. This conversion plot must be used at low concentrations of cellulose II

60% II line be A and the distance from the 80% line be B. The percent cellulose II composition of the unknown, partially mercerized, sample would then be: 60% + [A/(A + B)] x (20%).

Figure 17 could not be used in converting mercerized samples with less than 20% cellulose II in them since the 2θ outer half-height intersection for the combination (021) and ($10\bar{1}$) of celluloses I and II, respectively, cannot be accurately determined in this range. Therefore, Fig. 18 was constructed using the 2θ outer width at half-height intersection of the (002) peak in conjunction with the intensity ratio. In this case, the standards employing the lower crystallinity cellulose I had to be employed. For this reason the mercerized samples which were analyzed using Fig. 18 were probably less accurately determined than those which were analyzed in conjunction with Fig. 17.

In the course of the development of these two parameter plots it was found that samples made up of the lower crystallinity cellulose I, Avicel, and the low crystallinity cellulose II did not fall on the percent composition lines determined by the high crystallinity cellulose I and the high and low crystallinity cellulose II. The magnitude of the deviation can be seen in Fig. 17 for the 40, 60, and 80% composition lines. From an inspection of the x-ray diffractograms of the mercerized samples it was concluded that the fraction of cellulose I not converted to cellulose II is not measurably altered in crystallinity. Therefore, it should be more accurate to base the percent composition lines on the laboratory mixtures made from Sample 16 and high and low crystallinity cellulose II. Sample 16 was made from the same material used in the mercerization experiments. The 100% cellulose II line is a regression line of 16 mercerized samples which were deemed to be wholly converted to cellulose II and Sample 22. The essence of this two-parameter conversion procedure is that variations in the crystallinity of the cellulose II fraction of mixed samples, and the

effect of this variation on the $\underline{I}(10\bar{1})/\underline{I}(002)$ intensity ratio, are accounted for. The variation in crystallinity of the cellulose II fraction was slight. In fact, it was found that simple relative intensity calculations lead to the same conclusions as did this method, which accounts for variations in crystallinity.

RESULTS OF THE ANALYSIS OF THE X-RAY DIFFRACTOGRAMS OF MERCERIZED CELLULOSE

All the mercerization runs were done in duplicate. The x-ray data for all the mercerization work is presented in Table V. The average values for the x-ray parameters for both samples at each alkali metal concentration were used in conjunction with the conversion plots mentioned in the previous section in determining the percent conversion to cellulose II. The percent conversion to cellulose II as a function of concentration is reported in tabular form in Table VI. Figures 19 and 20 present the information graphically. The percent conversion data are presented as a function of both molarity and molality. This was done as some of the information on the solutions to be discussed in later sections must necessarily be done in the context of one or the other of these concentration scales.

The percent conversion to cellulose II *vs.* concentration for the three alkali metal hydroxides are all quite similar. There is an initial plateau followed by a transition region. The curves then level off at what has been assumed to be complete conversion to cellulose II.

These figures indicate that the Donnan equilibrium swelling theory is not the key to the decrystallization step of the mercerization process. The Donnan theory does not predict the threshold effect which is quite apparent for each of the three alkali metal hydroxide systems studied. This threshold effect for

TABLE V

X-RAY MERCERIZATION DATA

Sample Designation	Mercerization Concentration, M	2θ (002)	whh (002)	2θ Inter (002)	2θ (10$\bar{1}$)	whh (10$\bar{1}$)	2θ Inter (10$\bar{1}$)	$\frac{I(10\bar{1})}{I(002)}$
1-Na-1-A-2	0.851 ± 0.002	22.74	1.12	23.30	--	--	--	0.0761
1-Na-1-B-2	"	22.77	1.08	23.31	--	--	--	0.0707
1-Na-2-B-2	"	22.71	1.18	23.30	--	--	--	0.0861
1-Na-2-A-1	"	22.75	1.12	23.31	--	--	--	0.0728
Average	"	22.74	1.125	23.305	--	--	--	0.0764
2-Na-1-A-1	1.795 ± 0.002	22.74	1.14	23.31	--	--	--	0.0742
2-Na-2-A-2	"	22.73	1.12	23.29	--	--	--	0.0808
2-Na-1-A-4	"	22.74	1.14	23.31	--	--	--	0.0732
Average	"	22.74	1.13	23.30	--	--	--	0.0761
3-Na-1-A-2	2.297 ± 0.002	22.74	1.14	23.31	--	--	--	0.0802
3-Na-2-A-5	"	22.74	1.18	23.33	--	--	--	0.0788
Average	"	22.74	1.16	23.32	--	--	--	0.0795
4-Na-1-A-1	2.793 ± 0.002	22.73	1.14	23.30	--	--	--	0.0843
4-Na-2-A-2	"	22.75	1.12	23.31	--	--	--	0.0922
Average	"	22.74	1.13	23.305	--	--	--	0.0883
5-Na-1-A-3	3.163 ± 0.002	22.75	1.16	23.33	--	--	--	0.1953
5-Na-2-A-3	"	22.71	1.16	23.29	--	--	--	0.1735
Average	"	22.73	1.16	23.31	--	--	--	0.1844
7-Na-1-A-2	3.644 ± 0.002	22.65	1.32	23.31	20.10	1.72	19.24	0.784
7-Na-2-A-2	"	22.65	1.34	23.32	20.12	1.68	19.28	0.868
Average	"	22.65	1.33	23.315	20.11	1.70	19.26	0.826
8-Na-1-A-2	4.631 ± 0.002	21.74	1.92	22.70	20.10	1.62	19.29	1.223
8-Na-2-A-2	"	21.83	1.66	22.66	20.04	1.50	19.29	1.182
Average	"	21.785	1.79	22.68	20.07	1.56	19.29	1.203
9-Na-1-A-2	5.228 ± 0.002	21.75	1.92	22.71	20.07	1.68	19.23	1.151
9-Na-2-A-2	"	21.62	2.20	22.72	20.07	1.70	19.22	1.194
Average	"	21.685	2.06	22.715	20.07	1.69	19.225	1.1725
10-Na-1-A-2	6.243 ± 0.002	21.61	2.14	22.68	20.07	1.66	19.24	1.122
10-Na-2-A-3	"	21.72	1.92	22.68	20.16	1.90	19.21	1.172
Average	"	21.665	2.03	22.68	20.115	1.78	19.225	1.147
11-Na-1-A-1	7.771 ± 0.014	21.71	1.94	22.68	20.14	1.88	19.20	1.178
11-Na-2-A-1	"	21.61	2.28	22.75	20.16	1.94	19.19	1.157
Average	"	21.66	2.11	22.715	20.15	1.91	19.195	1.1675

TABLE V (Continued)

X-RAY MERCERIZATION DATA

Sample Designation	Mercerization Concentration, M	2θ (002)	whh (002)	2θ Inter (002)	2θ (10$\bar{1}$)	whh (10$\bar{1}$)	2θ Inter (10$\bar{1}$)	$\frac{I(10\bar{1})}{I(002)}$
12-Na-1-A-1	10.233 ± 0.002	21.74	1.94	22.71	20.13	1.78	19.24	1.179
12-Na-2-A-2	"	21.69	2.04	22.71	20.10	1.74	19.23	1.180
Average	"	21.715	1.99	22.71	20.115	1.76	19.235	1.1795
1-K-1-A-2	0.862 ± 0.003	22.75	1.14	23.32	--	--	--	0.0725
1-K-2-A-3	"	22.77	1.14	23.34	--	--	--	0.0853
Average	"	22.76	1.14	23.33	--	--	--	0.0814
2-K-1-A-2	1.572 ± 0.001	22.74	1.36	23.42	--	--	--	0.0836
2-K-2-A-2	"	22.77	1.18	23.36	--	--	--	0.0778
Average	"	22.755	1.27	23.39	--	--	--	0.0807
3-K-1-A-2	2.216 ± 0.004	22.74	1.26	23.37	--	--	--	0.0882
3-K-2-A-2	"	22.76	1.22	23.37	--	--	--	0.0787
Average	"	22.75	1.24	23.37	--	--	--	0.0835
4-K-1-A-1	2.692	22.76	1.22	23.37	--	--	--	0.1116
4-K-2-A-1	"	22.75	1.16	23.33	--	--	--	0.1158
Average	"	22.755	1.19	23.35	--	--	--	0.1137
5-K-1-A-1	3.282	22.73	1.20	23.33	20.22	2.10	19.17	0.397
5-K-2-A-1	"	22.74	1.22	23.35	20.32	2.52	19.06	0.401
Average	"	22.735	1.21	23.34	20.27	2.31	19.115	0.399
6-K-2-A-2	3.492	22.65	1.38	23.34	20.22	2.10	19.17	0.805
6-K-1-A-2	"	22.59	1.56	23.37	20.23	2.00	19.23	0.802
Average	"	22.62	1.47	23.355	20.225	2.05	19.20	0.804
7-K-1-A-2	3.695 ± 0.002	21.97	2.22	23.08	20.10	1.72	19.24	1.074
7-K-2-A-2	"	21.92	2.34	23.09	20.07	1.72	19.22	1.084
Average	"	21.95	2.28	23.09	20.09	1.72	19.23	1.079
8-K-1-A-3	3.959	21.70	2.52	22.96	20.11	1.76	19.23	1.114
8-K-2-A-2	"	21.78	2.56	23.06	20.10	1.54	19.27	1.092
Average	"	21.74	2.54	23.01	20.11	1.65	19.25	1.103
9-K-1-A-2	4.919	21.85	1.72	22.71	20.08	1.76	19.20	1.120
9-K-2-A-2	"	21.76	2.32	22.82	20.14	1.96	19.16	1.152
Average	"	21.81	2.02	22.77	20.11	1.86	19.18	1.136

TABLE V (Continued)

X-RAY MERCERIZATION DATA

Sample Designation	Mercerization Concentration, M	2θ (002)	whh (002)	2θ Inter (002)	2θ ($10\bar{1}$)	whh ($10\bar{1}$)	2θ Inter ($10\bar{1}$)	$\frac{I(10\bar{1})}{I(002)}$
10-K-1-A-2	5.808	21.76	1.96	22.74	20.09	1.72	19.23	1.144
10-K-2-A-2	"	21.76	1.86	22.69	20.04	1.54	19.27	1.144
Average	"	21.76	1.91	22.725	20.07	1.63	19.25	1.144
11-K-2-A-2	9.677	21.76	1.94	22.73	20.07	1.76	19.19	1.138
11-K-1-A-2	"	21.93	1.58	22.72	20.10	1.70	19.25	1.207
Average	"	21.85	1.76	22.725	20.09	1.73	19.22	1.1725
1-Li-1-A-2	1.059	22.75	1.18	23.34	--	--	--	0.0916
1-Li-2-A-2	"	22.74	1.14	23.31	--	--	--	0.0916
Average	"	22.75	1.16	23.33	--	--	--	0.0916
2-Li-1-A-1	2.083	22.74	1.22	23.35	--	--	--	0.0883
2-Li-2-A-1	"	22.77	1.14	23.34	--	--	--	0.0881
Average	"	22.76	1.18	23.35	--	--	--	0.0882
4-Li-1-A-3	3.296	22.78	1.16	23.36	--	--	--	0.1968
4-Li-2-A-2	"	22.76	1.20	23.36	--	--	--	0.1342
Average	"	22.77	1.18	23.36	--	--	--	0.1655
7-Li-4-A-2	3.7315	22.77	1.16	23.35	20.46	2.38	19.27	0.2103
7-Li-3-D-1	"	22.74	1.26	23.37	20.54	2.68	19.20	0.2515
Average	"	22.755	1.21	23.36	20.50	2.53	19.235	0.2309
7-Li-1-A-2	3.7315	22.73	1.24	23.35	20.34	2.44	19.12	0.2965
7-Li-2-A-2	(merc. for	22.76	1.18	23.35	20.37	1.90	19.42	0.2940
Average	23 hr)	22.745	1.21	23.35	20.355	2.17	19.27	0.2953
8-Li-1-A-2	4.159	22.74	1.18	23.33	20.20	1.84	19.28	0.766
8-Li-2-A-2	"	22.75	1.20	23.35	20.16	2.00	19.16	0.627
Average	"	22.75	1.19	23.34	20.18	1.92	19.22	0.697
10-Li-1-D-1	4.881	21.97	2.14	23.04	20.11	1.80	19.21	1.151
10-Li-2-A-2	"	22.00	2.50	23.25	20.17	1.96	19.19	1.131
Average	"	21.985	2.32	23.145	20.14	1.88	19.20	1.141
9-Li-1-A-2	5.061	21.82	2.54	23.09	20.12	1.86	19.19	1.174
9-Li-2-A-2	"	21.95	2.64	23.27	20.16	2.04	19.14	1.128
Average	"	21.885	2.59	23.18	20.14	1.95	19.165	1.151

TABLE VI

THE CONVERSION OF HYDROCELLULOSE TO CELLULOSE II
AS A FUNCTION OF ALKALI CONCENTRATION

Sample Designation	Mercerization Concentration, M	% Cellulose II
	NaOH	
1-Na (Average)	0.851	0
2-Na "	1.795	0
3-Na "	2.297	0
4-Na "	2.793	1.03
5-Na "	3.163	17.63
7-Na "	3.644	76.02
8-Na "	4.631	100
9-Na "	5.228	100
10-Na "	6.243	100
11-Na "	7.771	100
12-Na "	10.223	100
	KOH	
1-K (Average)	0.862	0
2-K "	1.572	0
3-K "	2.216	0
4-K "	2.692	1.86
5-K "	3.282	62.89
6-K "	3.492	77.16
7-K "	3.695	94.45
8-K "	3.959	95.43
9-K "	4.919	100
10-K "	5.808	100
11-K "	9.677	100
	LiOH	
1-Li (Average)	1.059	0
2-Li "	2.083	0
4-Li "	3.296	10.40
7-Li "	3.732	48.47
8-Li "	4.159	65.45
10-Li "	4.881	100
9-Li "	5.061	100

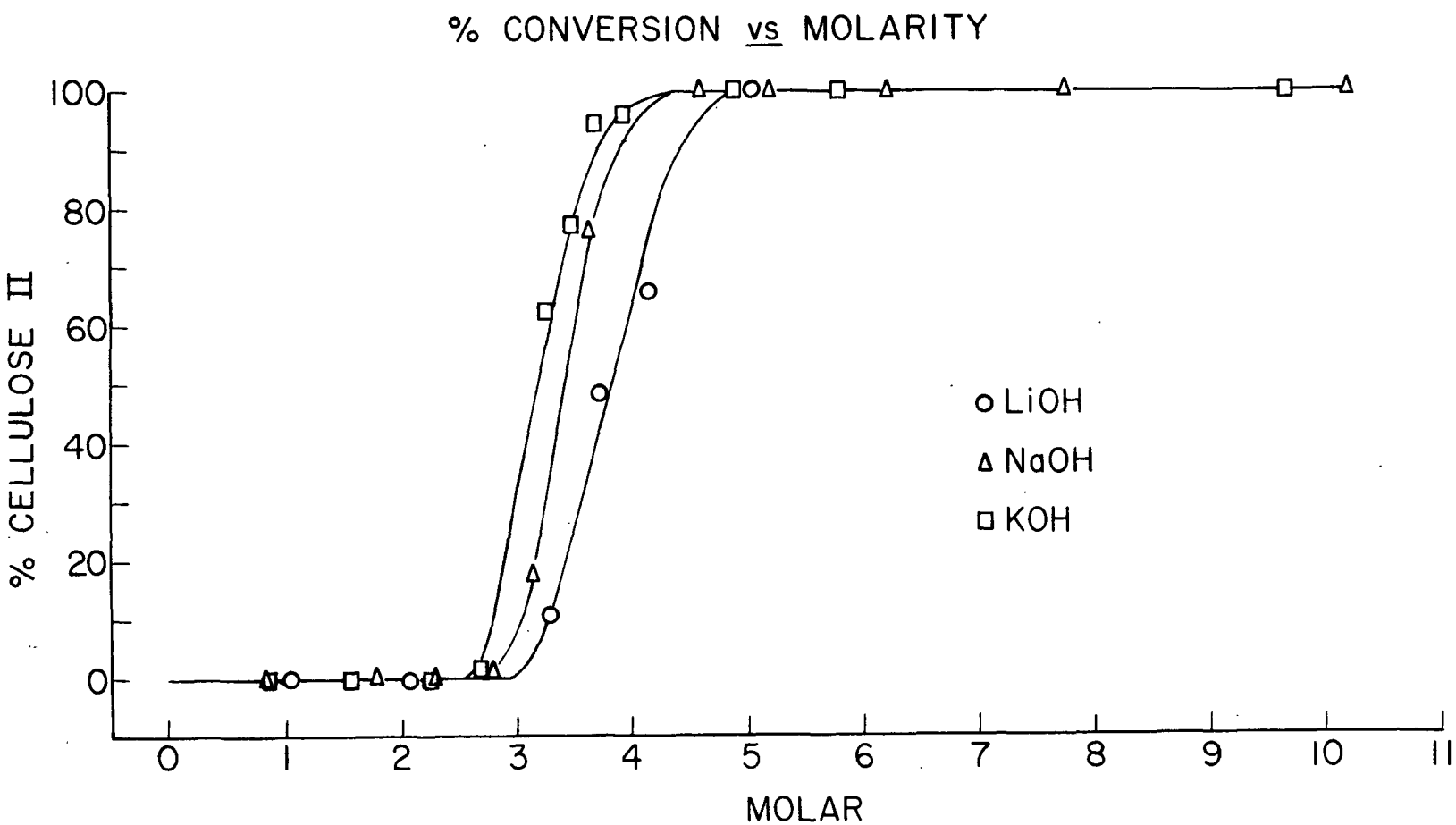

Figure 19. Conversion of Cellulose I to Cellulose II as a Function of Molarity

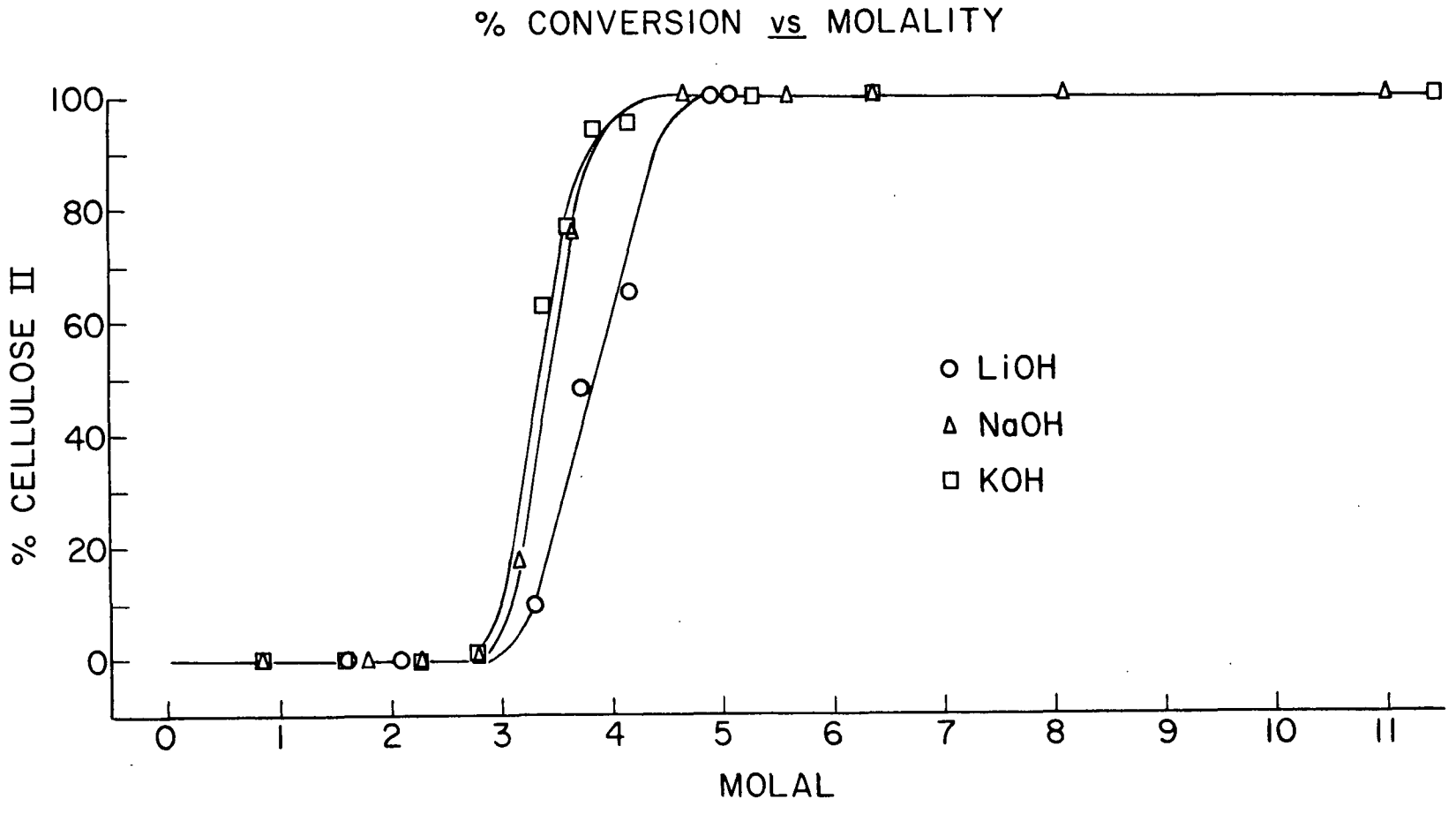

Figure 20. Conversion of Cellulose I to Cellulose II as a Function of Molality

the conversion of the lattice from I to II has been noted by others involved in following the mercerization process through x-ray diffraction methods (21,57).

The differences among the three alkali metal hydroxides studied in their ability to decrystallize cellulose I are not great. On the molality concentration scale it is difficult to distinguish the difference between sodium and potassium hydroxide. The transition region in which lattice conversion commences at about 2.7M and is complete by about 4.5M in the case of NaOH is of considerable interest.

The sample points in the transition region do not represent a time dependent phenomenon. One sample solution in the transition region, 3.732M LiOH, was used to treat two samples for the usual time span of 30 minutes and another two samples for 23 hours. The difference in conversion to cellulose II between these two sets of samples was only 2.5%. The breadth and stability of the transition region must be explained before the mercerization process is completely understood.

Ranby (21) and Ranby and Mark (58), among others, have noted that cellulose samples of different origin require different minimum concentrations of sodium hydroxide to initiate and complete mercerization. One can infer from their work that cellulose specimens of lower crystallinity, such as wood cellulose, can be mercerized at lower sodium hydroxide concentrations than can celluloses of higher crystallinity such as cotton linters. Since their results imply that there is a relationship between cellulose crystallinity and minimum mercerization concentration, the breadth of the transition region may indicate that cellulose from a given source does not have homogeneous crystalline domains. The less well-ordered crystalline regions are predicted to be more susceptible to decrystallization with aqueous alkali metal hydroxides than the more ordered areas.

Vigo, et al. (12) have reported that the lattice conversion order for the alkali metal hydroxides is:

LiOH<CsOH<RbOH<KOH<NaOH

whereas the swelling order was determined to be the following:

CsOH<RbOH<KOH<NaOH<LiOH

In contrast to this, it was found in this study that potassium hydroxide is a slightly more effective decrystallizing agent than sodium hydroxide at equal molar and molal concentrations. This discrepancy may be related to the fact that Vigo, et al. carried out their investigations using cotton fibers while hydrocellulose was used in this work. However, some of the work done by Zeronian and Cabradilla (59) using cotton fibers is in agreement with the ranking of the alkali metal hydroxides found in this study. Zeronian and Cabradilla found that at equal concentrations in the transition region, the level-off degree of polymerization (LODP) is most rapidly diminished by KOH. The LODP is a measure of the accessbility of cellulose. The fraction of native cellulose which would have been converted to the less crystalline cellulose II would be expected to be more accessible to the hydrolyzing acid. NaOH was less effective and LiOH was the least effective as can be seen from Fig. 21 which was taken from their paper.

Zeronian and Cabradilla also studied the sorption ratio as a function of alkali metal hydroxide concentration. The sorption ratio was defined as the ratio of moisture content of a treated cellulose sample to that of the starting material conditioned at the same relative humidity and temperature. The trends were almost the same as were found for the LODP case.

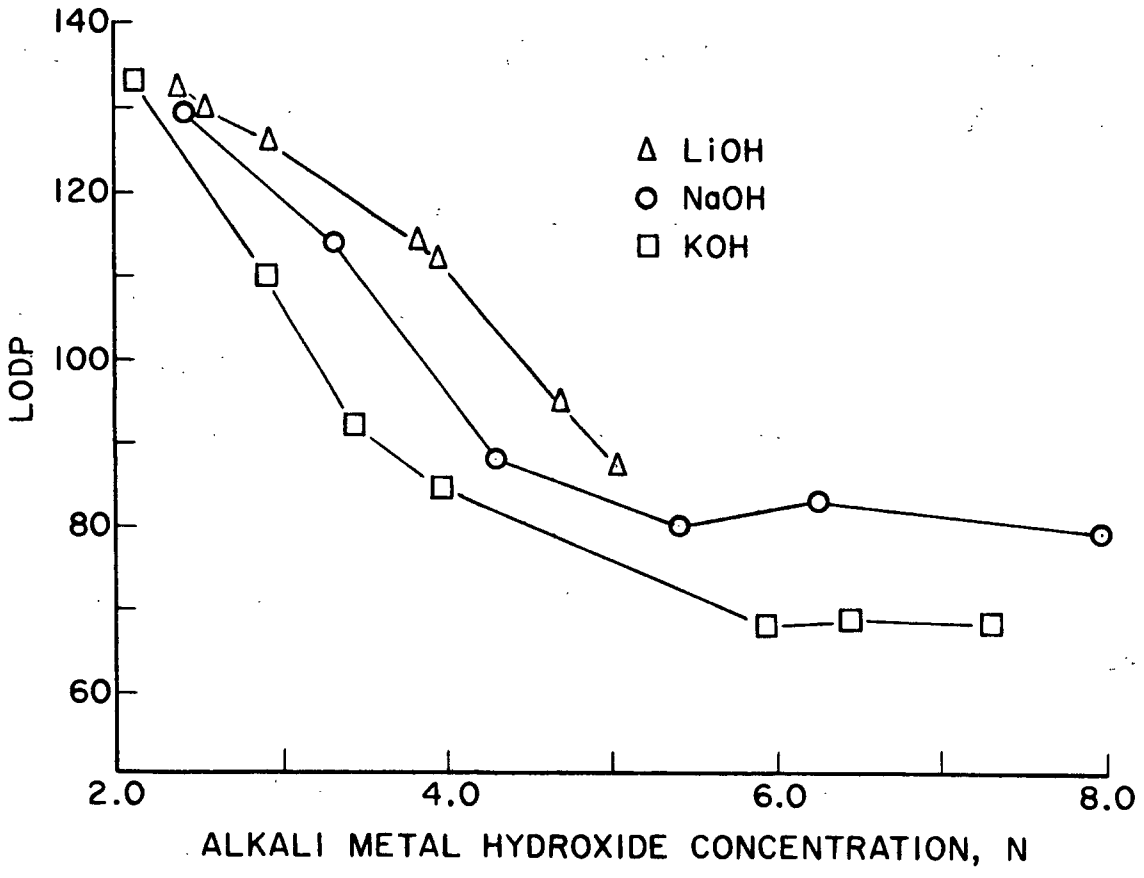

Figure 21. The Level-off Degree of Polymerization of Cotton as a Function of Alkali Metal Hydroxide Concentration, Temperature 21°C (59)

The ranking of the alkali metal hydroxides as to their effectiveness as decrystallizing agents found in this study and supported by experimental evidence developed by Zeronian and Cabradilla suggests that the activity of the hydroxide ion may be more important to the decrystallizing step of mercerization than the nature of the cation. The rationale for this statement is that the lattice conversion order found in this study is in the same order as are the dissociation constants of these three alkali metal hydroxides. Lithium hydroxide has a reported dissociation constant of about 0.65 and sodium hydroxide a dissociation constant of about 5.9. Potassium hydroxide is considered to be completely dissociated (60,61).

Another equally important rationale for the hypothesis mentioned above is that the cations for these three hydroxides are hydrated considerably differently, yet the differences among the mercerizing curves are not great.

RAMAN SPECTRAL ANALYSIS OF THE MERCERIZED HYDROCELLULOSE

Figure 22 presents the Raman spectra of the potassium hydroxide mercerization series in the transition region. These spectra are of the same series of samples as are the x-ray diffractograms shown in Fig. 13. The Raman spectra of all the alkali-treated samples were obtained.

The major changes in the spectra as the transition proceeds from cellulose I to cellulose II are the significant increase in intensity of the band centered at 895 cm^{-1} and the radical changes in the low frequency region below 600 cm^{-1}. Note, for instance, the decrease in intensity of the band at 375 cm^{-1} and the simultaneous emergence of a band centered at approximately 350 cm^{-1} as the proportion of cellulose II increases.

The band at 895 cm^{-1} is believed to be a vibrational mode involving C_1 and the four attached atoms (30,52). Suitably normalized, this band has served as an indication of mercerization in infrared studies and potentially can be quantified in the Raman as well.

Atalla (26) and Atalla and Dimick (62) have deduced that the changes in the low frequency region are associated with a change in the conformation of the cellulose chain with respect to the glycoside linkage. Studies of the vibrational spectra of simple saccharides (63,64) have established that bands found in the region below 700 cm^{-1} are associated with skeletal and ring bending modes, some ring stretching, and ring torsions. Thus changes in this region of the magnitude illustrated in Fig. 22 can only be accounted for by a realignment of the

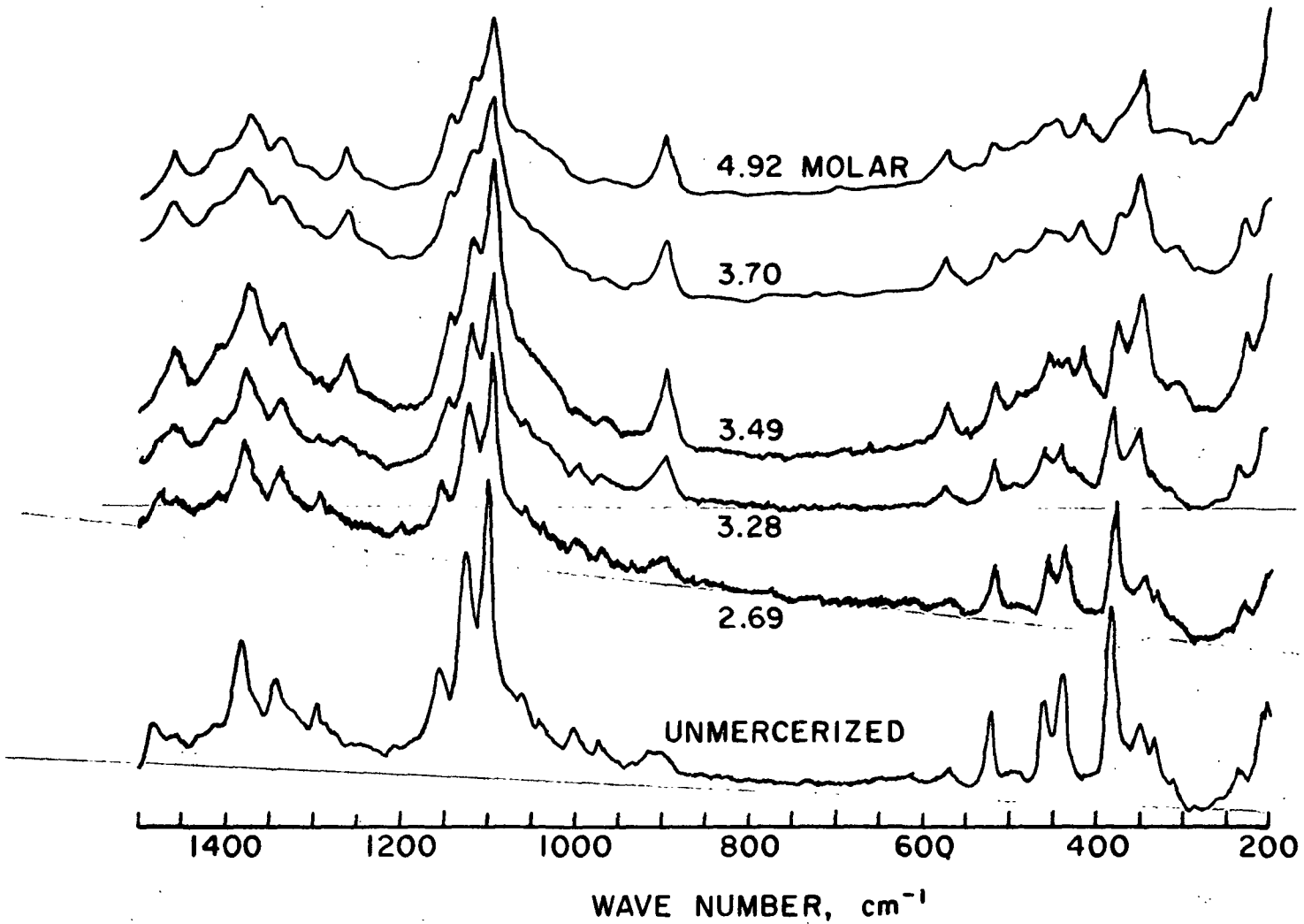

Figure 22. Raman Spectra of the Potassium Hydroxide Mercerization Series in the Transition Region

anhydroglucose units with respect to each other. This realignment leads to different coupling patterns which in turn produce a different set of vibrational bands in the low frequency region.

The interpretation of the low frequency region and the manner in which the change in chain conformation relates to an overall understanding of cellulose polymorphy will be further developed in a later section of the thesis.

Four integrated intensity ratios were calculated for the lithium hydroxide mercerization series in order to see if the Raman spectra might reveal any other new information not apparent from the x-ray diffraction studies or already discussed.

The integrated intensities were obtained using a method of limited accuracy because a mechanical integrator, a Technicon Integrator/Calculator, was used. Overlapping peaks such as in the case of the bands at 350 and 375 cm^{-1} were rather arbitrarily resolved. The linear base line for the two aforementioned peaks was drawn tangent to the spectra at the minimum at approximately 330 and 390 cm^{-1}. The bands at 895 and 1375 cm^{-1} were much easier to isolate as they are not so badly overlapped. The band at 1375 cm^{-1} (1372 cm^{-1} in the infrared) was discussed in connection with the infrared crystallinity index. It should be sensitive to crystallinity changes but not to crystal type. The possibility of using a more sophisticated approach such as the computerized band resolution technique described in Appendix V and applied to the Raman spectra of the mercerizing solutions was considered. However, the approach used was sufficiently accurate to follow trends in the mercerization process.

Table VII includes the calculated results of the four integrated intensity ratios. These four computed ratios are graphically illustrated in Fig. 23. Although the analysis was not as precise as potentially it could be due to the

TABLE VII

INTEGRATED RAMAN INTENSITY RATIOS
FOR THE LiOH MERCERIZATION SERIES

Spectra No.	M	$\underline{I}_{350}/\underline{I}_{375}$	$\underline{I}_{895}/\underline{I}_{1375}$	$\underline{I}_{895}/\underline{I}_{375}$	$\underline{I}_{350}/\underline{I}_{350}+\underline{I}_{375}$
1-Li-1-A-1	1.059	0.1827	0.2514	0.1933	0.1545
1-Li-2-A-1	1.059	0.1804	0.3138	0.2149	0.1529
Average		0.1816	0.2826	0.2041	0.1537
2-Li-1-A-2	2.083	0.1844	0.3609	0.2681	0.1557
2-Li-2-A-1	2.083	0.1683	0.3003	0.2355	0.1475
Average		0.1764	0.3306	0.2518	0.1516
4-Li-1-A-1	3.296	0.2296	0.3506	0.2562	0.1867
4-Li-2-A-1	3.296	0.2246	0.4021	0.2998	0.1834
Average		0.2271	0.3764	0.2780	0.1851
7-Li-3-A-1	3.7315	0.5084	0.6819	0.6514	0.3371
7-Li-4-A-1		0.3934	0.6021	0.5437	0.2823
Average		0.4509	0.6420	0.5976	0.3097
8-Li-1-A-1	4.159	1.3715	0.8241	0.9739	0.5794
8-Li-2-A-2	4.159	0.7629	0.8592	0.8620	0.4328
Average		1.0702	0.8417	0.9179	0.5061
10-Li-1-A-1	4.8815	2.2173	1.0512	1.5875	0.6892
10-Li-2-A-1	4.8815	1.4712	1.0679	1.3438	0.5953
Average		1.8442	1.0595	1.4656	0.6423
9-Li-1-A-1	5.061	1.607	1.114	1.3607	0.6165
9-Li-2-A-1	5.061	1.257	1.084	1.0993	0.5571
Average		1.441	1.099	1.2300	0.5868

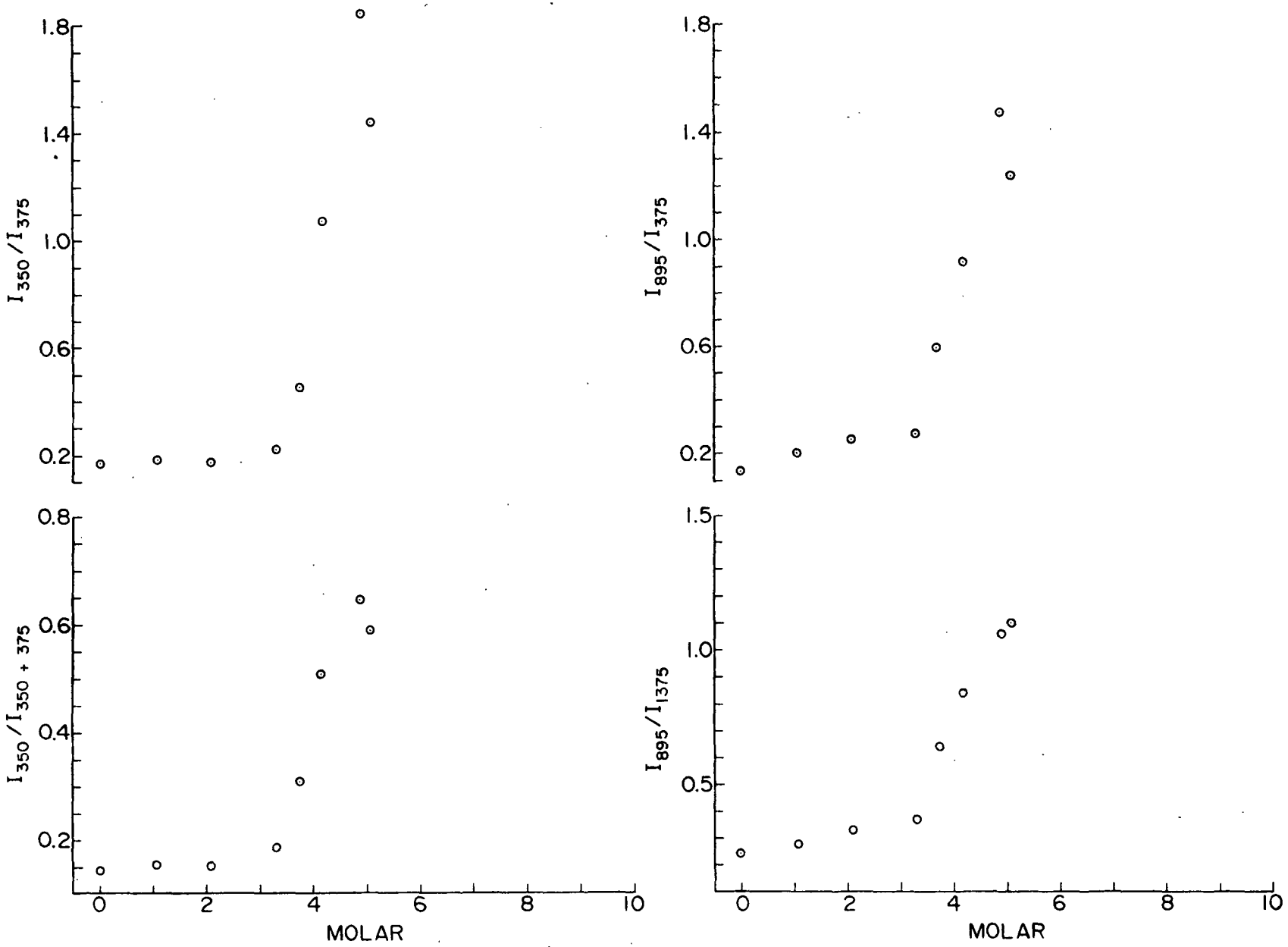

Figure 23. Four Integrated Intensity Ratios from the Raman Spectra of the Lithium Hydroxide Mercerization Series

reasons already mentioned, some interesting trends have emerged. The $\underline{I}_{350}/\underline{I}_{375}$ ratio would suggest that these two bands could quite conceivably be used as a quantitative measure of the relative amounts of cellulose I and II present in a partially mercerized sample. The $\underline{I}_{350}/(\underline{I}_{350} + \underline{I}_{375})$ intensity ratio suggests the same result. The other two intensity ratios which involve the band at 895 cm^{-1} reveal that there is some slight change in the cellulose before the chains actually achieve the mobility to assume the cellulose II conformation. This subtle change could not be picked up in the x-ray diffraction study. The two ratios which involve only those bands in the low frequency region do not show any discernible changes prior to the transition region. Apparently the chain conformation is not affected prior to the transition region, but there are some changes in the crystal structure.

ANALYSIS OF THE STRUCTURE OF THE ALKALI METAL HYDROXIDE SOLUTIONS

The structure of the alkali metal hydroxides was investigated both experimentally and theoretically. The results of these investigations were then related to the decrystallization process.

ANALYSIS OF THE RAMAN SPECTRA OF THE ALKALI METAL HYDROXIDE SOLUTIONS

The Raman spectra of all the mercerizing solutions are illustrated in Fig. 24, 25, and 26. The spectrum of water is included for comparative purposes in Fig. 24. The relatively sharp band at approximately 3610 cm^{-1} is obviously a function of the alkali metal hydroxide concentration. An analysis of this band is presented below.

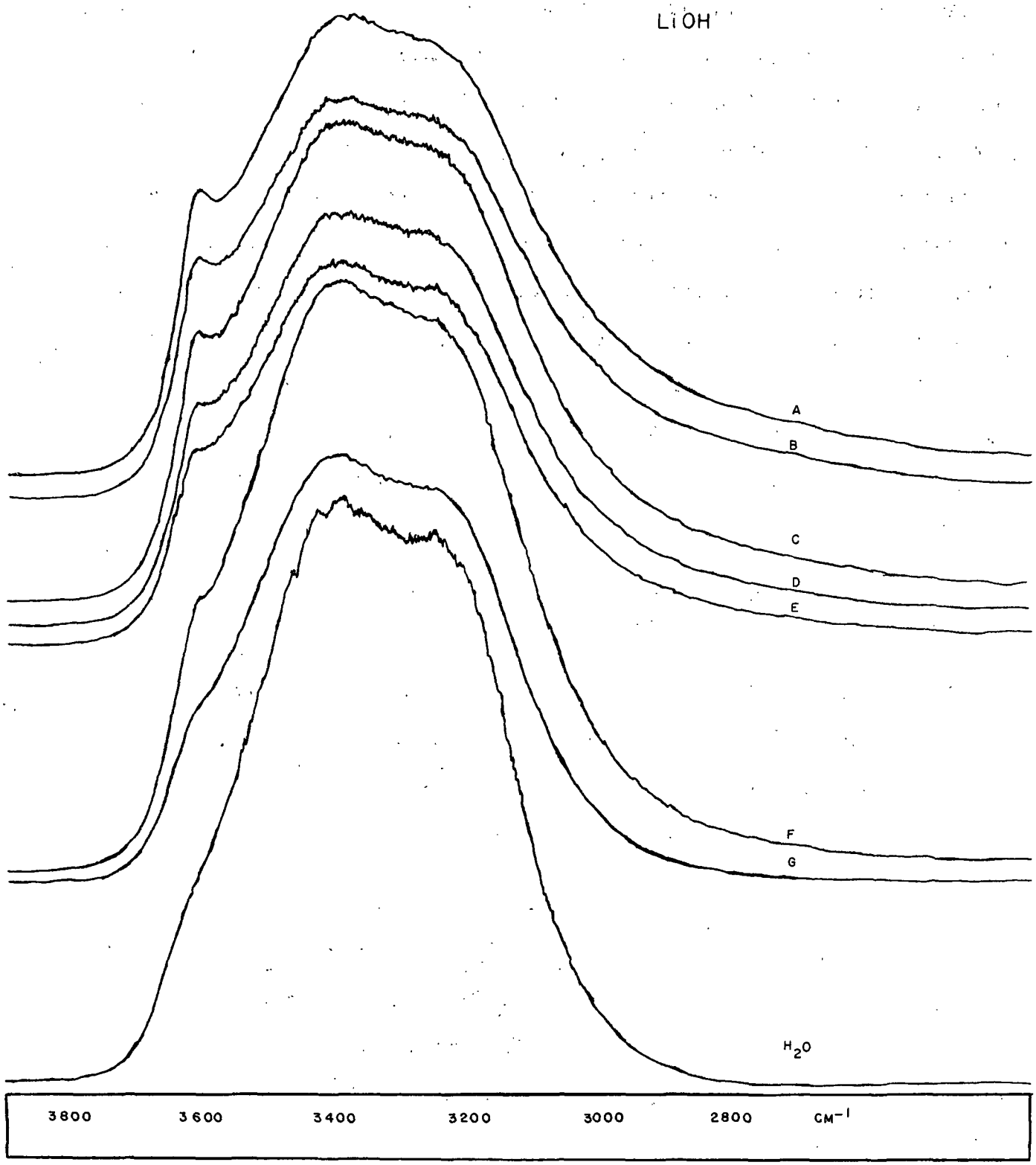

Figure 24. Raman Spectra of the LiOH Solutions Used in the Mercerization Studies. The Molarities Are: A = 5.061, B = 4.882, C = 4.159, D = 3.732, E = 3.296, F = 2.083, and G = 1.059

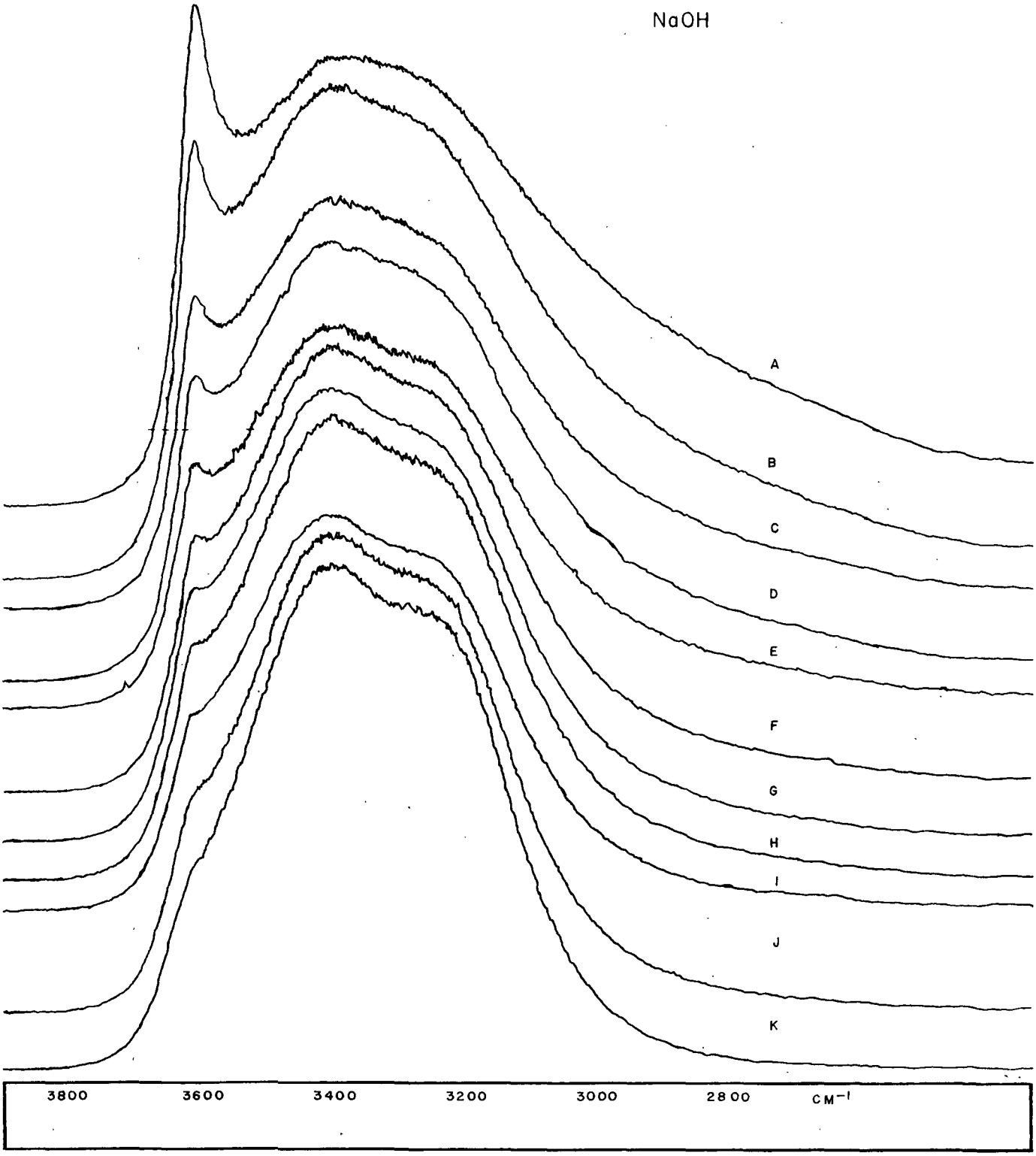

Figure 25. Raman Spectra of the NaOH Solutions Used in the Mercerization Studies. The Molarities Are:
A = 10.233, B = 7.771, C = 6.243,
D = 5.228, E = 4.631, F = 3.644,
G = 3.163, H = 2.793, I = 2.297,
J = 1.795, and K = 0.851

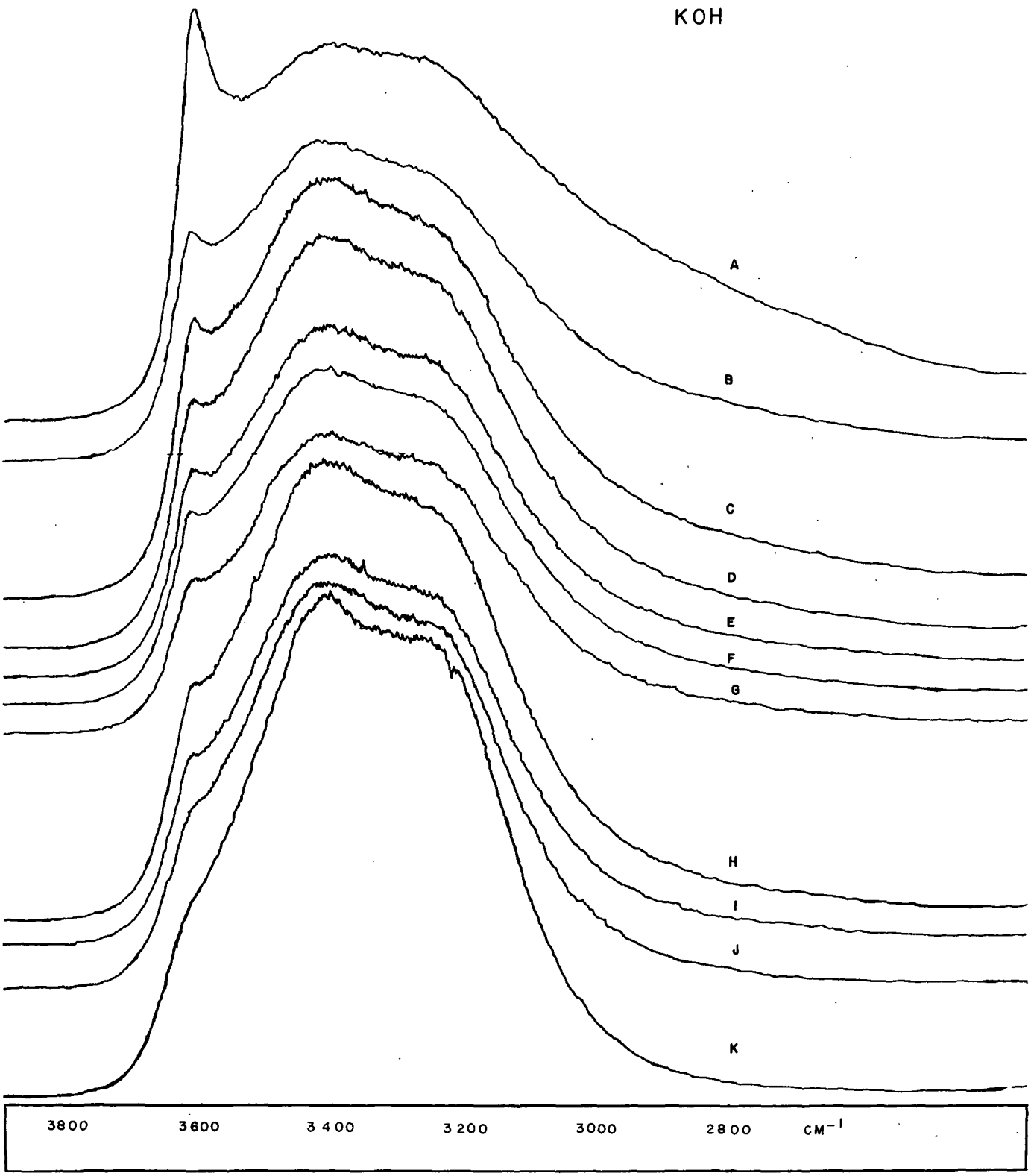

Figure 26. Raman Spectra of the KOH Solutions Used in the Mercerization Studies. The Molarities Are:
A = 9.677, B = 5.808, C = 4.919,
D = 3.959, E = 3.695, F = 3.492,
G = 3.282, H = 2.692, I = 2.216,
J = 1.572, and K = 0.862

Identification of the Band at 3610 cm^{-1}

The Raman spectra of the solid alkali metal hydroxides were obtained and compared to values found in the literature. One would expect the frequency of the hydroxide ion to be in nearly the same location in both the ionic solid and in solution. These values are given in Table VIII.

TABLE VIII

FUNDAMENTAL HYDROXIDE ION STRETCHING FREQUENCIES

Solid Hydroxide	OH^- Raman (experimental), cm^{-1}	Raman OH^- Ref.	Infrared OH^- Ref.
LiOH	3665	3664 (65)	3678 (66)
$LiOH \cdot H_2O$	3563	3563 (67)	3574 (66)
NaOH	3630	3630 (68)	3637 (69)
KOH	3596	3597 (70)	3600 (71)

It is most interesting to note that the values in Table VIII for the fundamental stretching frequencies of the hydroxide ion bracket the apparent value of 3610 cm^{-1} for the hydroxide ion in solution.

The interpretations of the variations found in the solid state should provide some insights about the solution properties. The difference in frequency between the lithium hydroxide and lithium hydroxide-monohydrate has been explained as the result of strong hydrogen bonds in the monohydrate (66,72). The oxygen-oxygen distance in the monohydrate is only 2.68 A which would indicate that hydrogen bonds should be present. The distance of closest approach between hydroxyl groups for anhydrous lithium hydroxide is 3.05 A which should preclude hydrogen bonding.

The difference between the two fundamentals in the infrared and Raman for sodium hydroxide has been interpreted as due to coupling between adjacent hydroxyl ions (69). The symmetric stretching vibration would be Raman active while the antisymmetric stretching mode would be active in the infrared. The difference between the two is a measure of the strength of the coupling. This line of reasoning implies a unit cell containing two sodium hydroxide units which must be antiparallel or nearly so. No hydrogen bonding was predicted and the small split between the infrared and the Raman fundamentals indicate that the coupling is weak.

The crystal structure of potassium hydroxide is different from that of lithium and sodium hydroxide (71). The hydroxide ions are able to participate in weak hydrogen bonding. By using mixtures of KOH and KOD the authors determined that there is also coupling between hydroxide ions (71).

None of the spectroscopic studies referenced above placed any significance on any sort of cation-anion interaction with respect to the location of νOH^- in the solid alkali metal hydroxides. Walrafen came to the same conclusion about the effect of the cations Li^+, Na^+, and K^+ with respect to their ability to affect the OH and OD stretching vibrations of aqueous perchlorate solutions (73).

The locations of the fundamental OH^- stretching vibration in the solid alkali metal hydroxides certainly suggest that the band at 3610 cm^{-1} has been properly assigned. In addition, the location of the νOH^- in solution would suggest that the hydroxide ion is not hydrogen bonded; if it were, it should have a lower frequency. In further support of this interpretation, Turnbull (74) found the νOH^- of small concentrations of NaOH in a potassium nitrate-sodium nitrite melt at 150°C to be located at 3619 cm^{-1} in the infrared. Turnbull concluded that the hydroxide ion was not hydrogen bonded to the nitrate or nitrite

ions. Turnbull found the width at half height of the νOH^- band to be between 60-80 cm^{-1}. The significance of this parameter will be mentioned in a later section.

The polarization of the band at 3610 cm^{-1} was also investigated. The hydroxyl ion is a linear diatomic molecule without a center of symmetry. It, therefore, belongs to the point group $C_{\infty,\nu}$. From symmetry considerations it may be deduced that the fundamental symmetric vibration of the hydroxyl ion should be polarized (75). Figure 27 includes two Raman spectra of 10.233N NaOH. The top scan was run without the half-wave plate in position in the input optic system while the half-wave plate, which rotates the electric vector of the laser beam 90°, was in position for the bottom scan. Obviously, the band at 3610 cm^{-1}, as well as the intramolecular bands of water, are highly, but not completely, polarized.

Intramolecular Vibrational Spectrum of Water

A quantitative analysis of the band at 3610 cm^{-1} demands that the intramolecular spectrum of water be examined, as the water bands overlap the band at 3610 cm^{-1} significantly.

The infrared spectrum of water vapor has three fundamental absorption bands centered at 1595, 3652, and 3756 cm^{-1}. The two lower frequency bands correspond to symmetric modes while the band at 3756 cm^{-1} is the antisymmetric vibration (76).

The spectrum of the liquid state is a bit more complicated due to interactions with neighboring molecules. Walrafen (77) has conducted extensive spectral investigations of liquid water and come to the conclusion that the evidence supports a mixture model for water. This conclusion was largely based on Walrafen's computer analysis of the Raman spectrum of the intramolecular valence region from 2000 to 4000 cm^{-1}. This region of the spectrum was resolved into four major Gaussians located approximately at 3225, 3415, 3565, and 3640 cm^{-1}

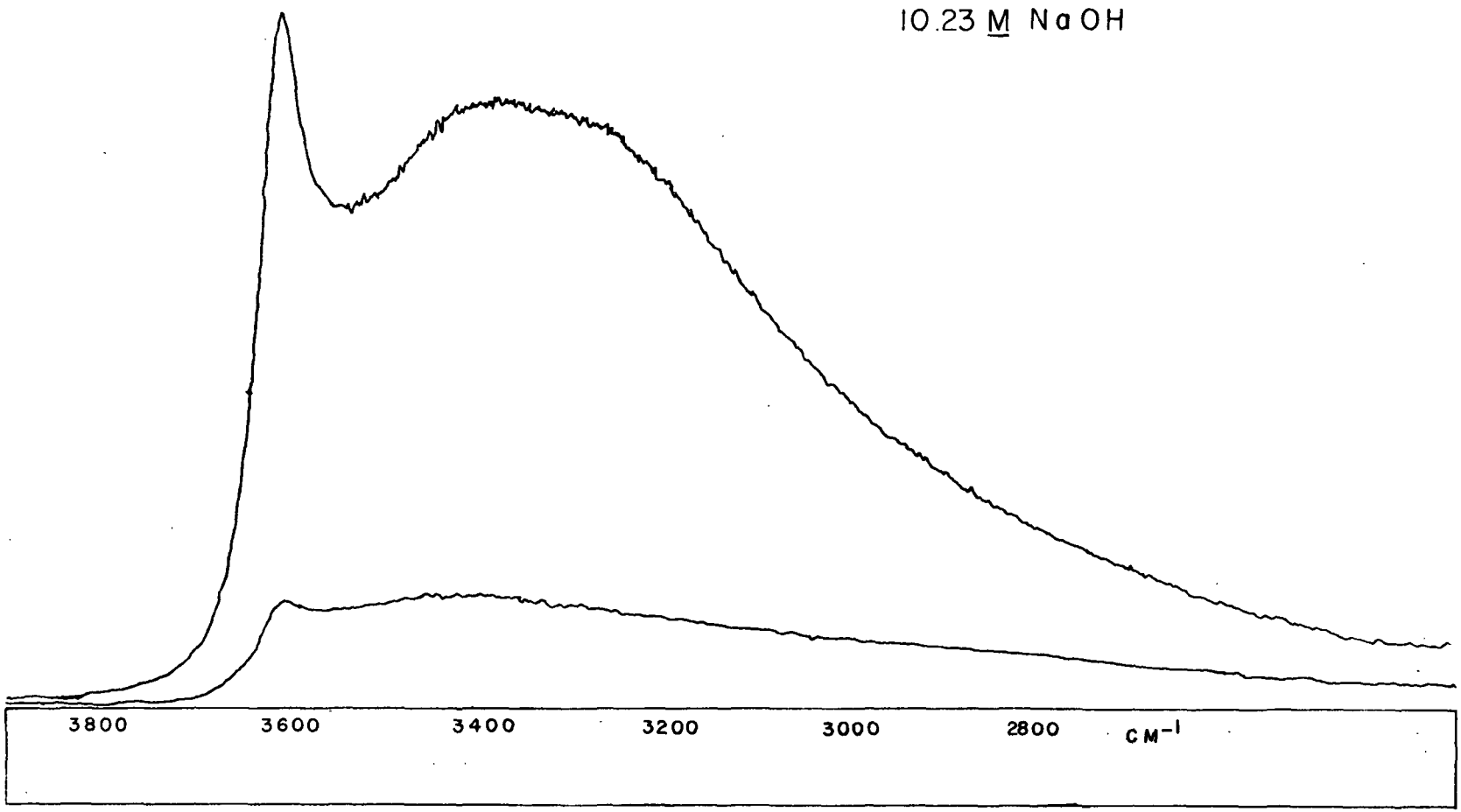

Figure 27. Raman Spectrum of a Mercerizing Solution Demonstrating that the Band at 3610 cm^{-1} and the Intramolecular Vibrational Bands of Water are Highly Polarized

and a broad, low, residual located at approximately 3060 cm^{-1}. Walrafen's band resolution strongly suggests that the high frequency symmetric and the antisymmetric modes of water are influenced by two distinct environments. The mixture model first proposed by Frank and Wen (25) predicts that on the molecular level liquid water exhibits two environments: tetrahedrally hydrogen-bonded water and nonhydrogen-bonded monomeric water. Walrafen found that as the temperature increased, the integrated intensities of the two high frequency components increased whereas the integrated intensity of the two low frequency components decreased. The pairs of high and low frequency components were assigned to nonhydrogen-bonded and hydrogen-bonded species, respectively.

Clarke and Glew (78) resolved the infrared spectrum of water in this region into four Gaussian bands and came to similar conclusions about the structure of water from their analysis. At 10°C they found the band centers to be located at 3296, 3391, 3496, and 3595 cm^{-1}. Increases in temperature always had the effect of increasing the frequency of all the bands.

Band Resolution of the Raman Spectra

The Raman spectra of all the alkali metal hydroxide solutions were resolved into four bands using a nonlinear least squares computer program written by Fraser and Suzuki (79,80) for a C.D.C. 3600 computer and extensively modified by the author to run on an IBM 360 under RAX. Appendix V includes the theoretical development behind the program, operating instructions, a flow diagram, a copy of the program, and some sample output. The raw data for the program were obtained by having the Raman spectra reduced photographically without measurable distortion. Relative intensity values were punched directly onto IBM cards every 10 cm^{-1} using a microcomparator.

Figures 28 and 29 are computer plotted band resolutions of a low and a high concentration alkali metal hydroxide. Initially the spectra were resolved into five bands. However, this resolution was not satisfactory as the band between the two prominent water bands and the band at 3610 cm^{-1} was not sufficiently restrained and would tend to become unreasonably large during the computer refinement. Thus the assumption had to be made that the band could be ignored. No attempt was made to try to resolve the band at 3610 cm^{-1} into two components. One of these components would have been the hydroxide ion stretch which is, of course, the main contribution, and the other component would be the other nonhydrogen-bonded vibrational mode of water which Walrafen (77) placed at 3640 cm^{-1} and Clark and Glew (78) placed at 3595 cm^{-1} in the infrared. Any attempt to resolve these two bands would have been quite artificial. The two mentioned approximations (neglecting the water bands at 3565 and 3640 cm^{-1}) were believed to have a negligible effect on the overall analysis, as the two bands which were not accounted for are quite small.

Interpretation of the Results of the Band Resolution

The pertinent results of the band resolution analysis are embodied in Appendix VI. These results include the height, center, and width at half height of each peak as well as the relative integrated intensity or area. The band at 3610 cm^{-1} was normalized as a ratio of the integrated intensities according to the following equation:

$$\text{Intensity Ratio} = I_{3610\ cm^{-1}}/(I_{3265\ cm^{-1}} + I_{3610\ cm^{-1}}) \qquad (29)$$

The band at 3265 cm^{-1} was included in the normalization scheme as it and the band at 3610 cm^{-1} are the two best resolved bands in the spectrum.

The band centered at 3610 cm^{-1} was normalized in order to facilitate quantitative comparisons among the three hydroxides. Relative, rather than

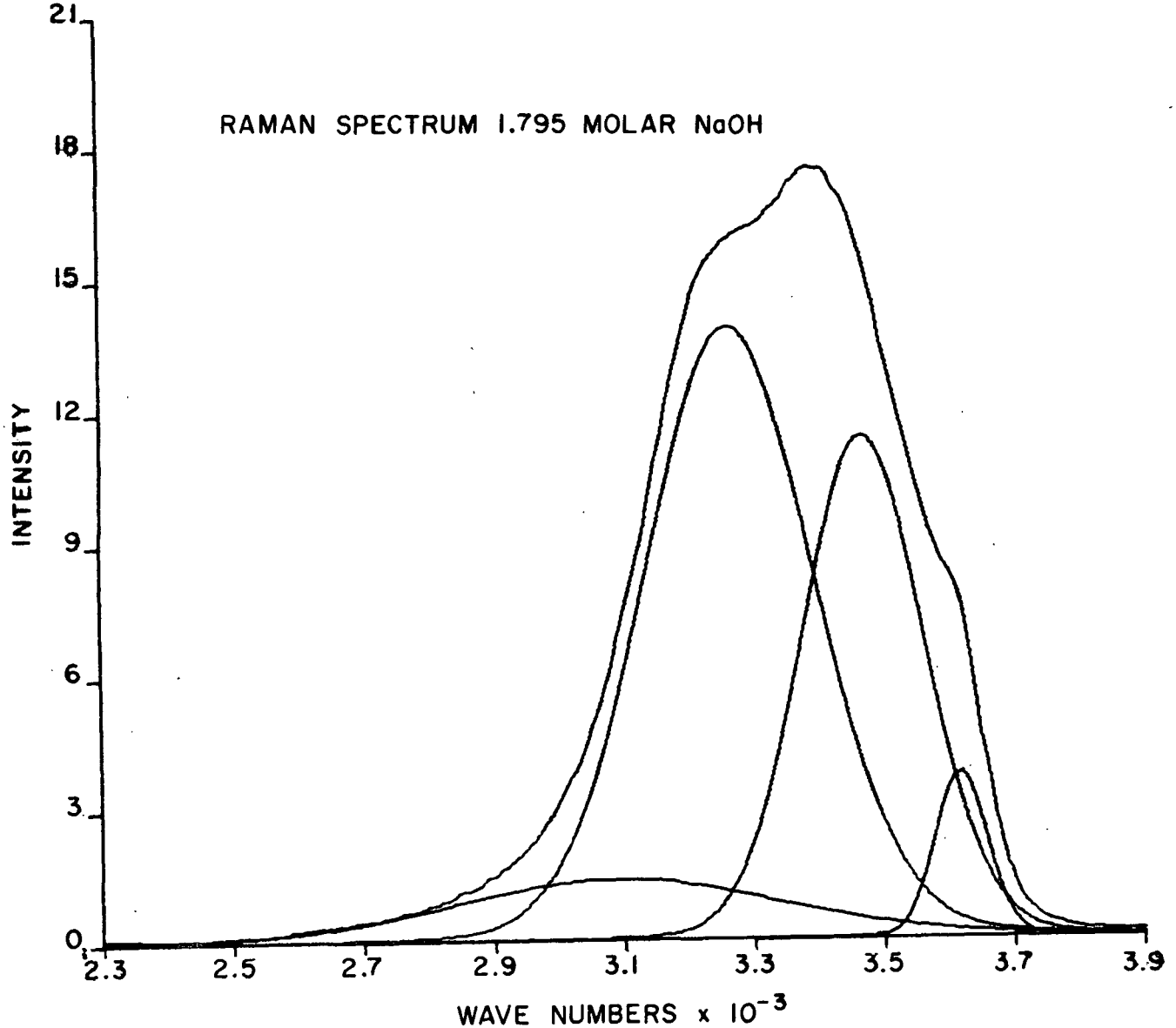

Figure 28. Four Band Computer Analysis of the Raman Spectrum of a Low Concentration Alkali Metal Hydroxide Solution

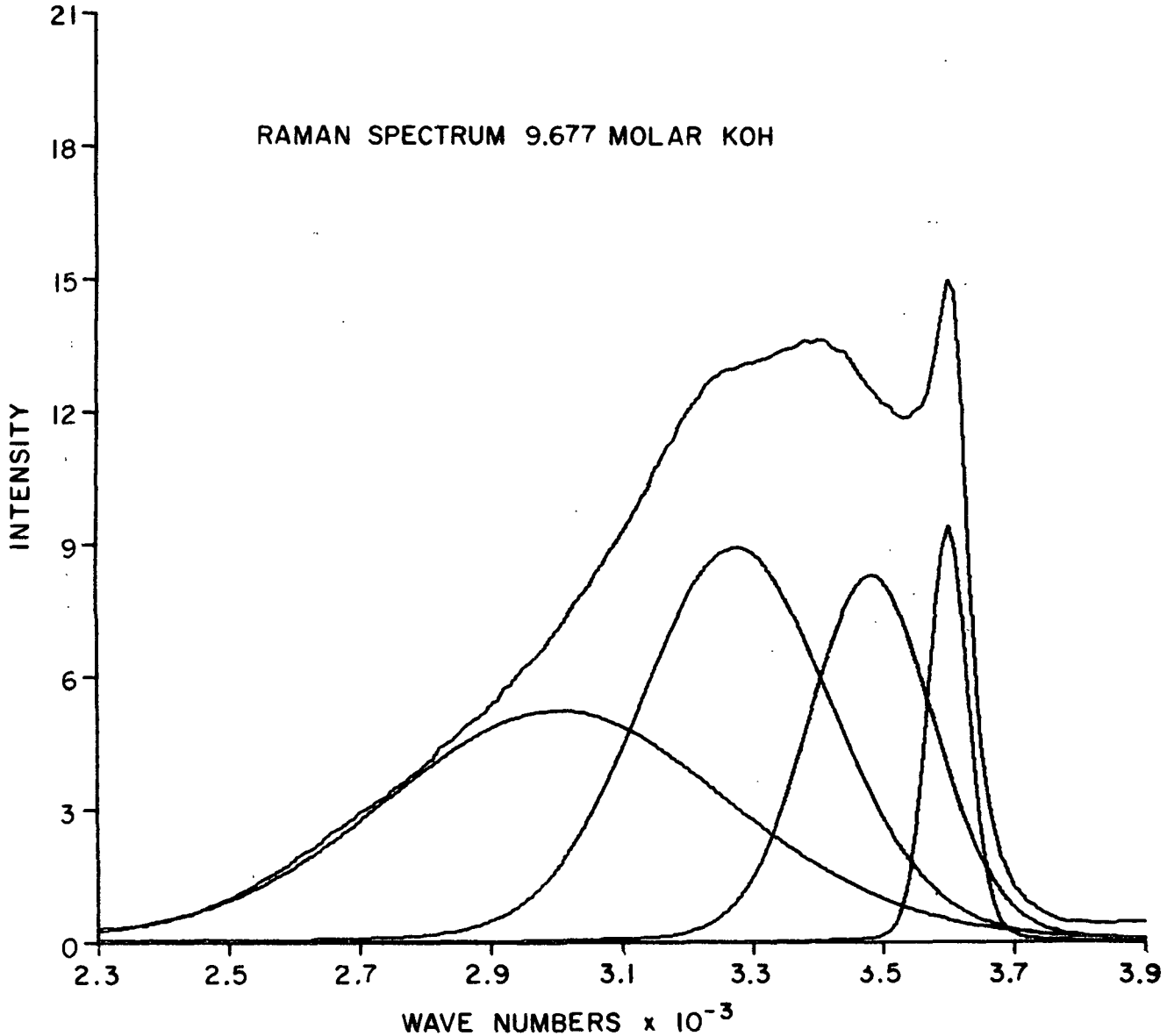

Figure 29. Four Band Computer Analysis of the Raman Spectrum of a High Concentration Alkali Metal Hydroxide Solution

absolute integrated intensities were sufficient for this study, because the objective was to get a relative measure of the free hydroxide ion concentration. It was believed that any OH^- M^+ ion pairs would be shifted to a lower frequency; therefore, the band at 3610 cm^{-1} could be used as a measure of the free hydroxide ion concentration. The work of Irish and Chen (81-83) supported this approach. They conducted an extensive Raman spectral investigation of the bisulfate-sulfate equilibrium for several bisulfate salts over a wide range of concentrations. They found that the ion pair H_3O^+ SO_4^{2-} lowered the symmetric stretch of SO_4^{2-} from 981 to 948 cm^{-1}. Nelson and Irish (84) have noted similar trends in their study of the nitrate ion which they also attributed to ion pairing.

Figure 30 is a plot of the normalized integrated relative intensity of the band at 3610 cm^{-1} vs. concentration for each of the three hydroxides.

The solid lines shown in the figure are the results of a linear regression analysis on each of the data sets. The R^2 values for the linear regression were 0.71 for lithium hydroxide, 0.97 for sodium hydroxide, and 0.97 for potassium hydroxide. (An R^2 value of 1.0 would indicate that the data are fit perfectly by the indicated equation and deviations from 1.0 indicate scatter in the data which cannot be explained.) The results illustrated in Fig. 30 are consistent with the work done on the dissociation constants of the alkali metal hydroxides (60,61). As was discussed previously, potassium hydroxide is believed to be completely dissociated in aqueous solution, sodium hydroxide is slightly associated, and lithium hydroxide is the most highly associated of the alkali metal hydroxides with a dissociation constant of about 0.65. Sodium and potassium hydroxides are well fit by the assumption of linearity while lithium hydroxide is not. Since lithium hydroxide is appreciably more associated than the other two hydroxides, the hydroxide ion concentration should not be a linear function of the concentration.

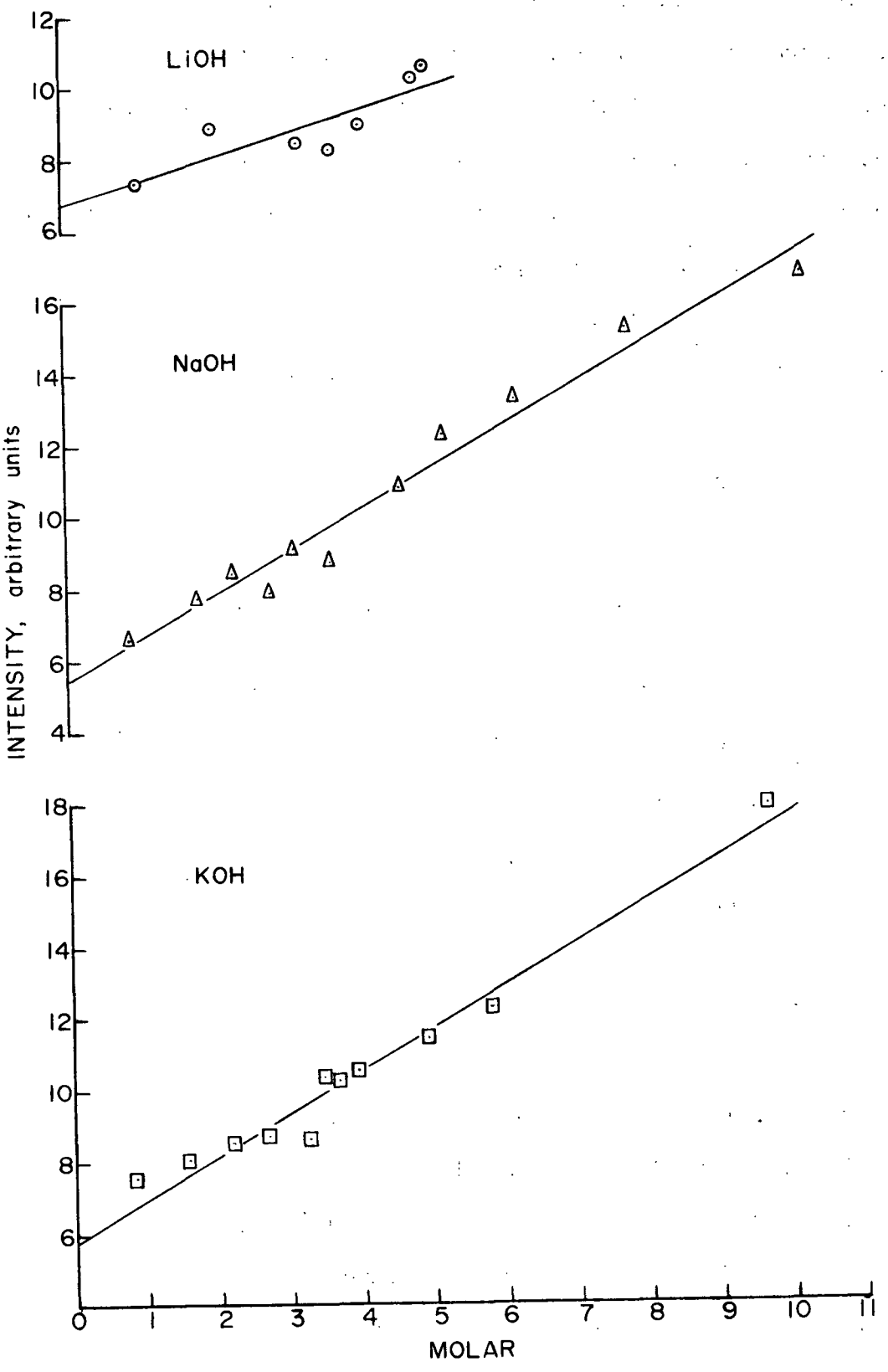

Figure 30. The Integrated Intensity of the Band at 3610 cm^{-1} as a Function of Concentration for the Three Alkali Metal Hydroxides

The linear regression lines for the three hydroxides are directly compared in Fig. 31. The relative ranking of the hydroxides, as well as the differences in magnitude among them, correlate quite well with their effectiveness as mercerizing agents (see, for example, Fig. 19). This constitutes strong evidence that the hydroxide ion concentration is the key factor in the decrystallization step of mercerization. The lithium hydroxide regression line crosses the other two regression lines. This is probably due to the greater uncertainty and scatter of the data at low concentrations and the assumption of linearity imposed on the lithium hydroxide system.

The width at half height of the band at 3610 cm^{-1} also proved to be of considerable interest. The band became narrower as the concentration increased for all three hydroxide systems. Figure 32 exhibits the relationship between the width at half height and concentration for sodium and potassium hydroxide. The data for lithium hydroxide demonstrate a similar trend and could have been included in Fig. 32. As can be seen in Fig. 32, there is a definite change in the rate of decrease of the width at half height at about 3.5 to 4.0M. Since there are no great differences between the potassium and sodium hydroxides with respect to the band at 3610 cm^{-1} and two populations were lumped together for statistical purposes. The two intersecting lines represent linear regressions of the low and the high concentration points. Each of the two populations arbitrarily contained 11 data points. The R^2 value for the low concentration line was 0.83 and the value for the high concentration line was 0.85; their slopes were -6.27 and -1.97, respectively.

The significance of Fig. 32 has been interpreted to be related to changes in the hydration of the hydroxide ion. Gluekauf (85) has concluded (through a theoretical study of activity data) that the hydration number of the hydroxide ion should be 4.0 at a concentration of 1.0M. Other estimates of the hydration

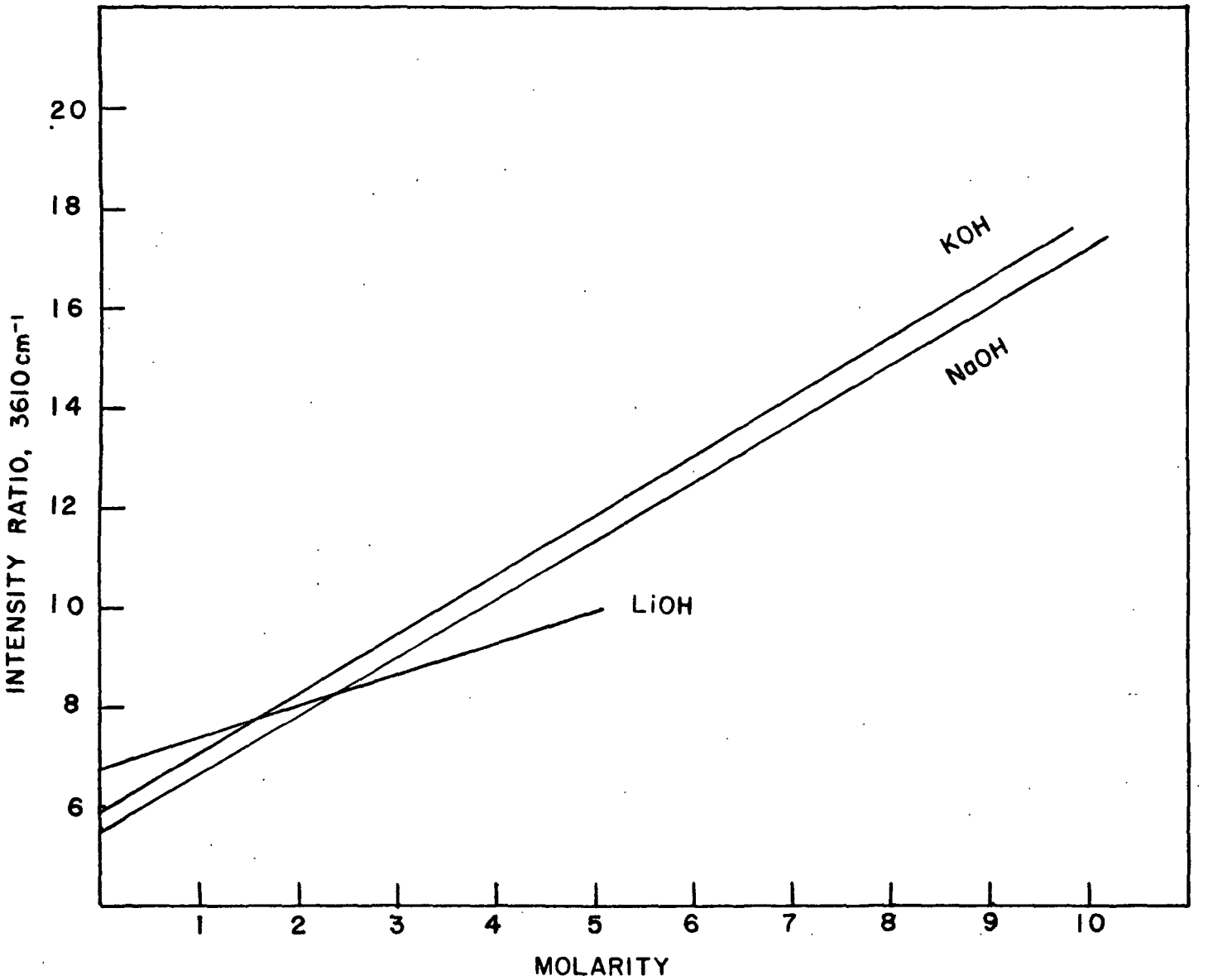

Figure 31. The Three Linear Regression Lines of the Normalized Intensity Ratio of the Band at 3610 cm^{-1} as a Function of Concentration. The Intensity Units are Arbitrary

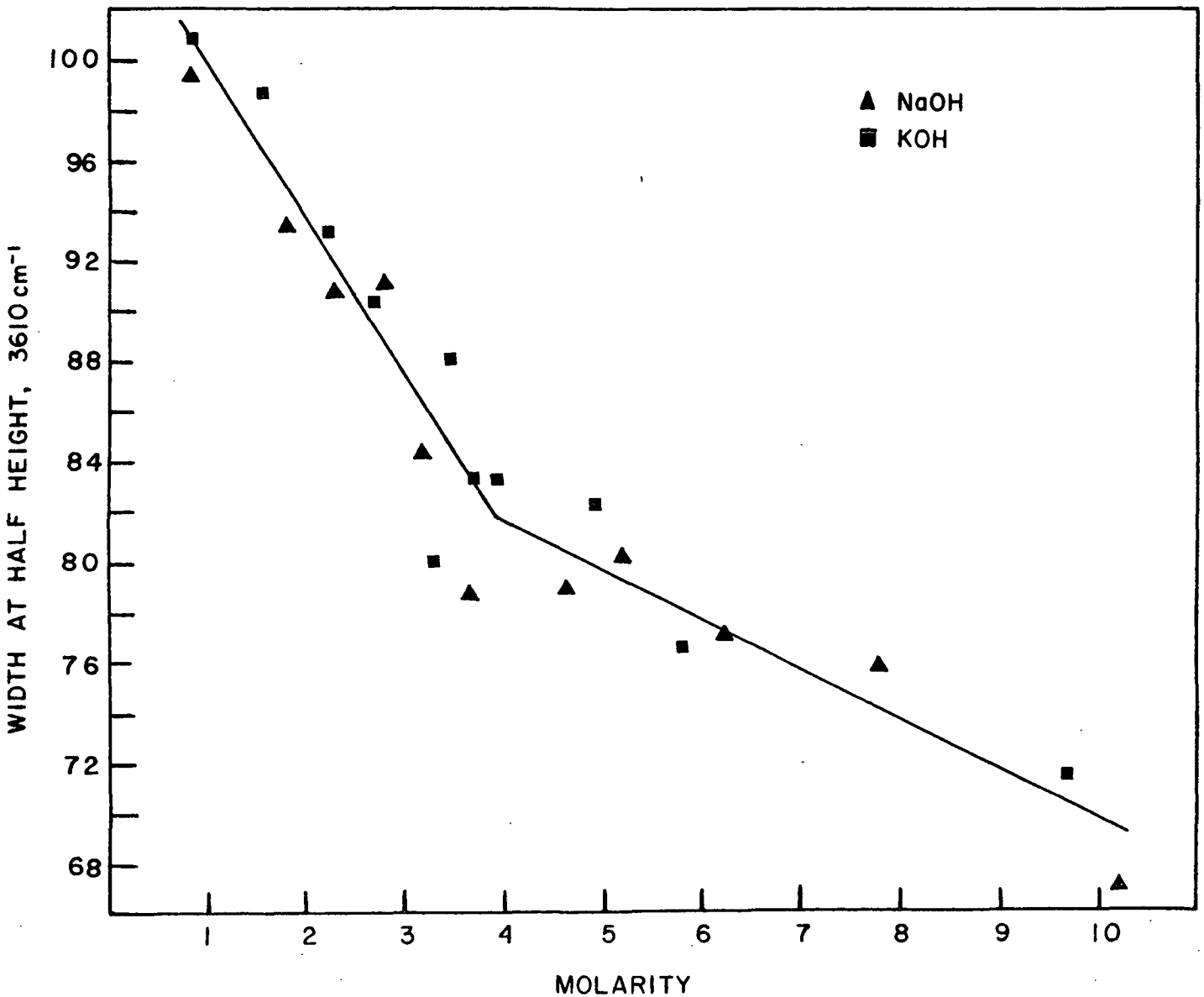

Figure 32. The Width at Half Height of the Fundamental Stretching Frequency of the Hydroxide Ion as a Function of Concentration

number range from 8.0 to 0.0 (23). At low concentrations the hydroxide ion would be expected to be fully hydrated. The hydration sphere would provide a variety of interactions and perturbations with the hydroxide ion which would tend to broaden the band. The amount of free water available for hydrating the hydroxide ion would diminish as the concentration of electrolyte increases. The interpretation of Fig. 32 is that the hydroxide ion is only marginally hydrated at concentrations beyond the inflection point shown in the diagram.

As was mentioned previously, Turnbull (74) found the width at half height of the band associated with the unhydrated hydroxide ion to be between 60 and 80 cm^{-1}. The inflection point in Fig. 32 corresponds to a width at half height of about 82 cm^{-1}.

The most exciting aspect of these findings is how they relate to the mercerization curves presented previously. The inflection point of Fig. 32 indicates that a concentration close to 4.0M must be reached before the hydration sphere of the hydroxide ion is completely (or almost completely) lost. This concentration closely corresponds to the end of the transition region of the mercerization curves of sodium and potassium shown in Fig. 19. This observation suggests that the hydroxide ion must be nearly unhydrated before it has the ability to disrupt the cellulose lattice. One possible interpretation of the aforementioned observation is that the fully hydrated hydroxide ion may not be able to penetrate and disrupt the cellulose lattice due to a size restriction. Once the hydroxide ion becomes dehydrated it would be smaller and it could penetrate the lattice more easily.

It will be shown in subsequent sections that a theoretical interpretation of the activity data of the alkali metal hydroxides is consistent with and

supports the interpretation of the change in the width at half height of the fundamental frequency of the hydroxide ion.

In order to find out whether the nonion paired cation has any role in the decrystallization process, Fig. 33 was constructed. This figure is a plot of the normalized intensity of the band at 3610 cm^{-1} *vs.* the percent conversion to cellulose II in the transition region for each of the three hydroxides.

The solid lines represent linear regressions for each of the three hydroxides. The R^2 values were found to be 0.97 for lithium, 0.95 for sodium, and 0.94 for potassium hydroxide.

Figure 33 indicates that at equal hydroxide ion concentrations the order of effectiveness of the three cations in promoting lattice conversion is: $Li^+ > Na^+ > K^+$. The ranking of the effectiveness of the cations is in the same order as their hydration numbers (23). This is an indication that the Donnan mechanism may be of some importance in the decrystallization step of mercerization. The more highly hydrated the cation, the greater the osmotic pressure which it can exert which in turn should be more effective in disrupting the crystal lattice. The cations would be expected to retain their hydration spheres even though they may associate with or form ion pairs with the deprotonated hydroxyls on the cellulose chains (86).

The differences among the three alkali metal hydroxides at equal anion concentrations are certainly not great as is apparent from the figure. There is certainly a possibility that these small differences are merely the result of a secondary effect which has not been accounted for.

There were several other aspects of the band resolution which, while not as relevant to an understanding of the mercerization process as those discussed in the preceding discussion, are nevertheless interesting. Figures 34 and 35

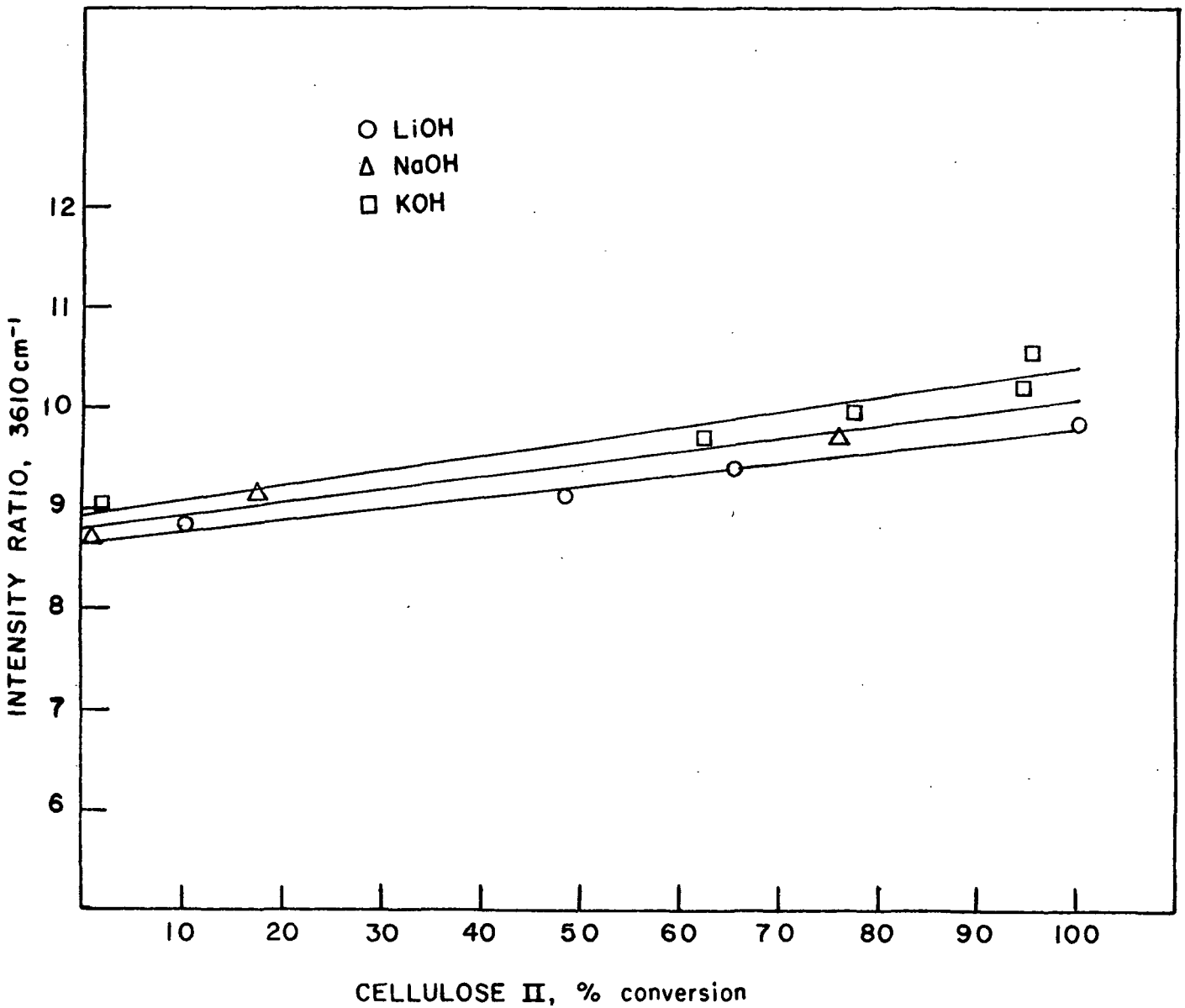

Figure 33. The Normalized Intensity of the Band at 3610 cm^{-1} vs. the Percent Conversion to Cellulose II. The solid lines represent linear regressions for each of the hydroxides

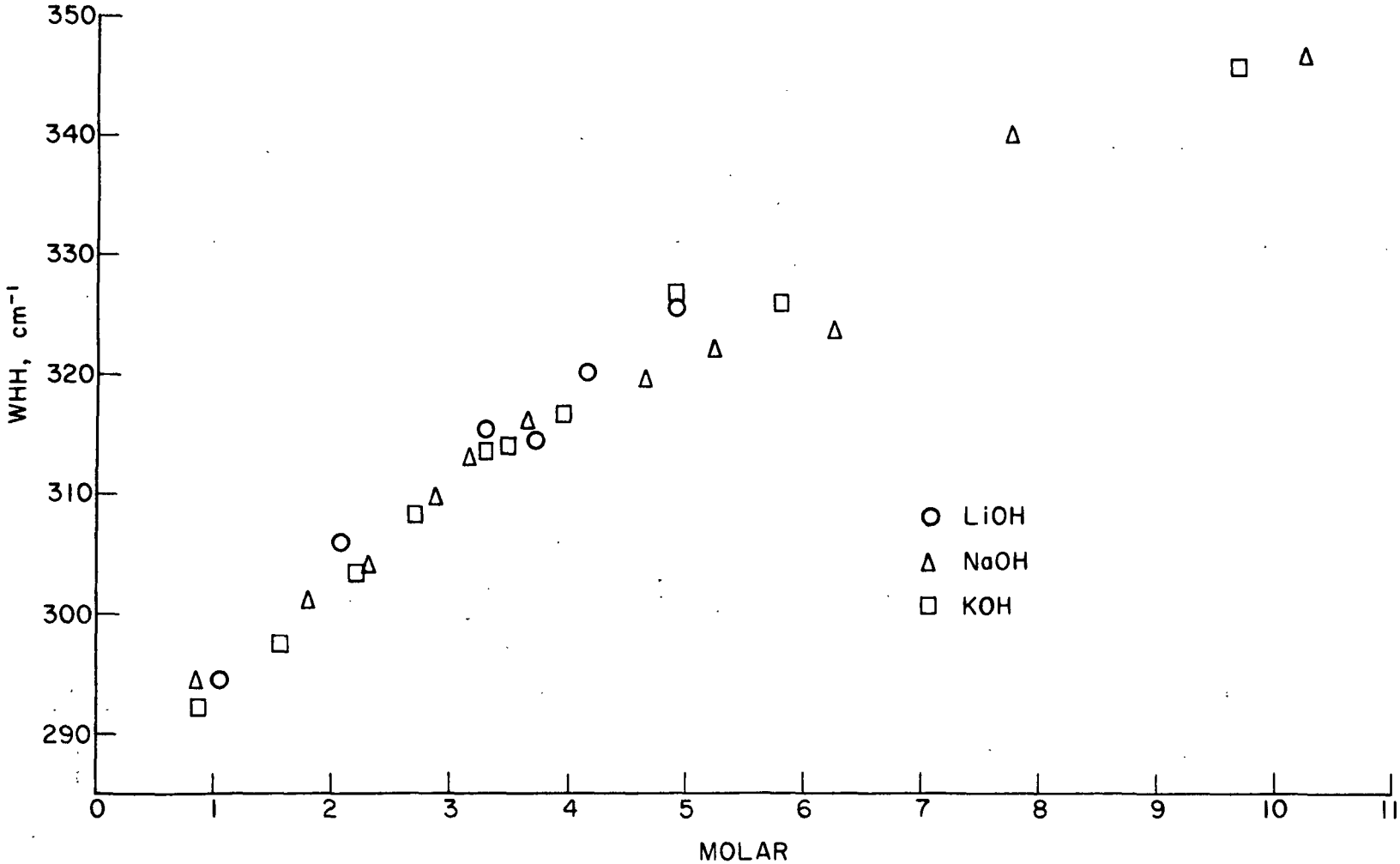

Figure 34. Width at Half Height of the Water Band at 3265 cm^{-1} vs. Concentration

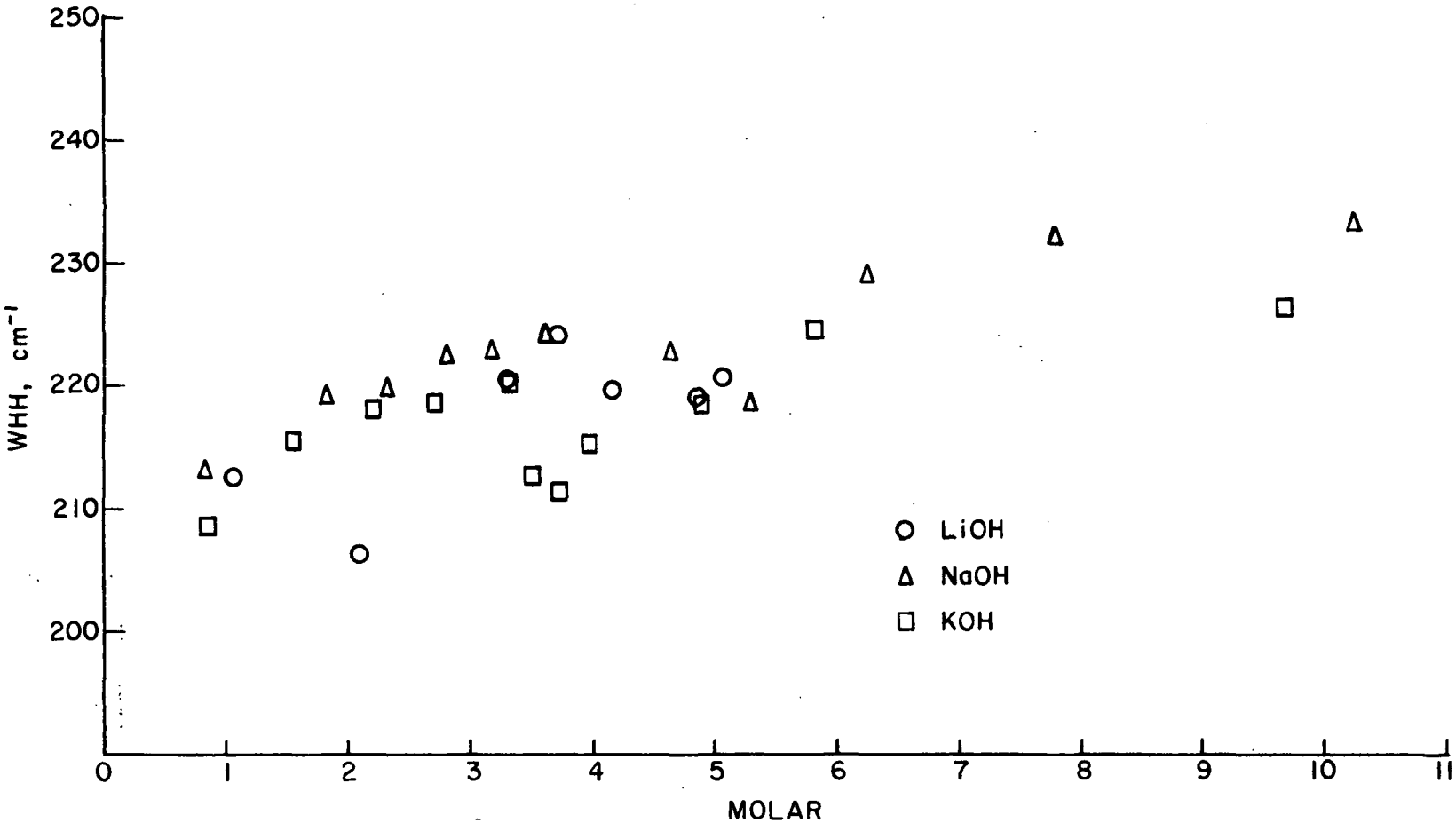

Figure 35. Width at Half Height of the Water Band at 3470 cm^{-1} vs. Concentration

illustrate the width at half height of the major symmetric and antisymmetric bands, respectively, of water as a function of concentration. The band at 3265 cm^{-1} clearly increases in width as the molarity of the alkali increases. The band at 3470 cm^{-1} appears to broaden, but less appreciably, and there is more scatter in the data since this band cannot be as well resolved as the others.

The function parameter, which indicates the linear ratio of the proportion of Gaussian and Cauchy functions used to fit the data, also was found to be a function of concentration. As the concentration increased, the Cauchy component of the band increased.

These trends just mentioned appear to be consistent with observations made on other aqueous systems, although the emphasis has generally been on the solute, not the solvent.

Irish and Davis (87) found a strong concentration dependence of band positions, intensities, and widths at half height for aqueous alkali metal nitrate solutions. The authors related changes in the width at half height of the nitrate ion to the hydrated radii of the cations.

Collision broadening is reported (88) to be the main factor with respect to band broadening in the liquid state. Also, solute-solvent interactions may foster a complex set of equilibrium conditions which should also broaden bands (88). Certainly a plausible interpretation for the band broadening of the two water bands is that an increasing fraction of the solvent would be involved in hydration of the ions with increasing concentration.

In general, the shape of bands in the liquid state have been found to be intermediate between those of the Gaussian and Cauchy functions. Collision broadening can be described by a Cauchy function (88); therefore, the results

reported here, in which the Cauchy contribution increased with increasing concentration, are consistent with previous studies.

There was one significant factor in the band analysis related to concentration which has evaded explanation. This is the significant increase in integrated intensity and width at half height of the broad residual centered near 3085 cm^{-1}. Walrafen (77) gave no explanation for the origin of this band and none can be offered here.

THERMODYNAMIC CONSIDERATIONS

Activity Coefficients of the Alkali Metal Hydroxides

Figure 36 compares the activity coefficients of lithium, sodium, and potassium hydroxide as a function of concentration. The experimental data used in constructing Fig. 36 were taken from NBS Report 1002 (89).

The differences in relative magnitude of the activity coefficients among the hydroxides at equal concentrations reflects, in part, the relative degree of ion pairing. The activity coefficients are based on the stoichiometric concentration; that is, they are not corrected for ion pairing.

The fact that the activity coefficients of sodium and potassium hydroxide increase at high concentrations and actually exceed a value of 1.0 must be rationalized (90).

> "A qualitative explanation of the activity coefficients that increase with concentration and even become greater than unity can be given in terms of the solvation of the ions. As the ions tie up solvent molecules, the effective concentration, i.e., the moles solute per mole of free solvent, becomes greater than the concentration calculated as moles of solute per mole of solvent. The solute in the apparently more concentrated solution has a higher free energy than would be expected, and this shows up as an increased activity coefficient."

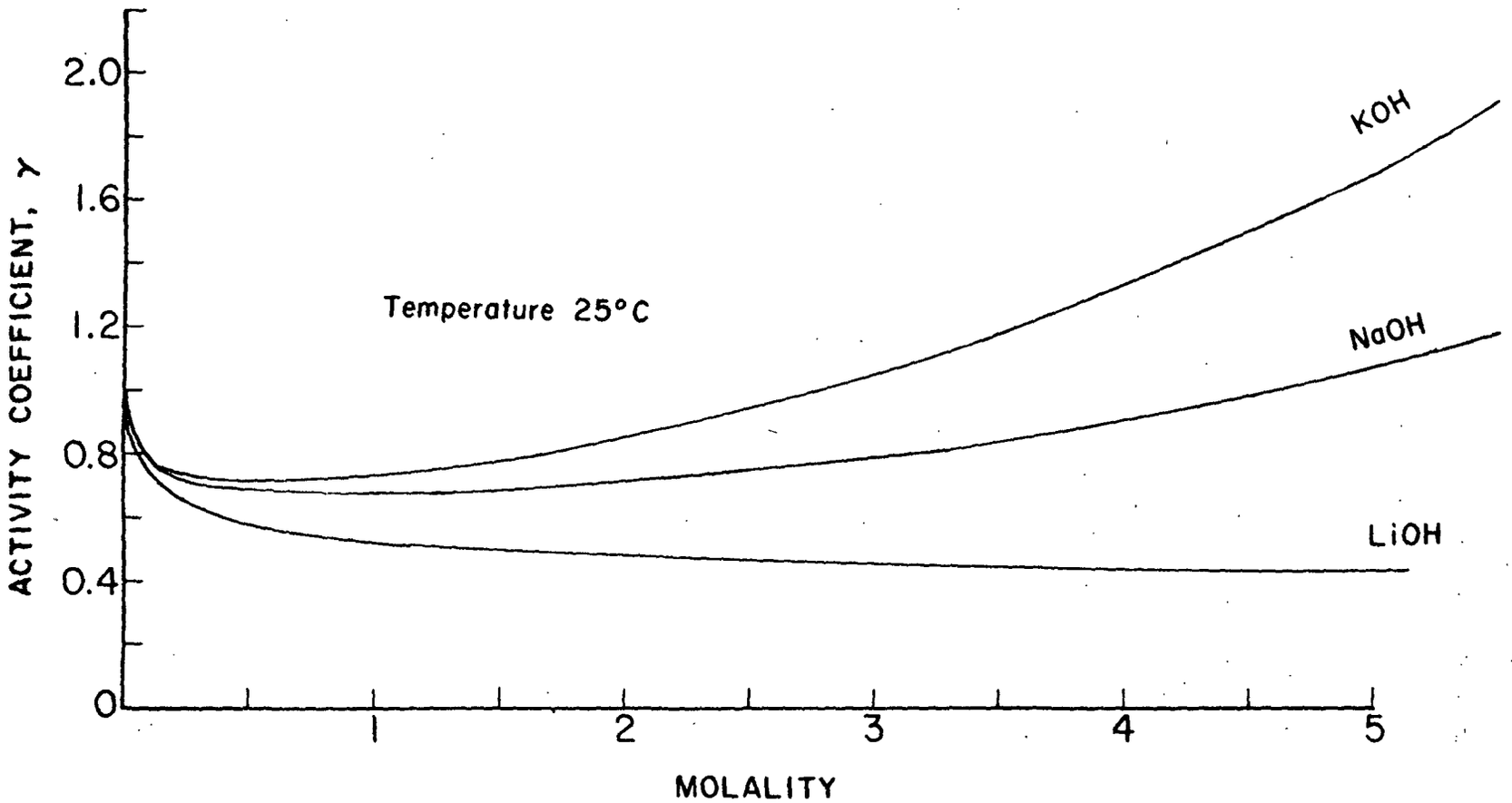

Figure 36. The Activity Coefficients of the Alkali Metal Hydroxides are Compared

Robinson and Stokes (91,92) and more recently Bockris and Reddy (93) have dealt quantitatively with modifying the basic Debye-Huckel expression for activity coefficients to take into account the solvent removed for hydration of the ions. Since the hydration state of the hydroxide ion had been implicated as being important to the decrystallization step of mercerization, the water removal theory of activity coefficients was examined.

The Water Removal Theory of Activity Coefficients

Any discussion of ionic activity coefficients generally commences with the Debye-Huckel expression which is quite successful at low concentrations.

$$\log \gamma\pm = -AZ_1Z_2\sqrt{\mu}/(1 + B\mathring{a}\sqrt{\mu}) \qquad (30)$$

where $\gamma\pm$ = mean activity coefficient

A,B = Debye-Huckel constants

Z_1, Z_2 = ionic charges

μ = ionic strength = $1/2(M_1Z_1^2 + M_2Z_2^2 \ldots)$

$\mathring{a}$ = mean distance of closest approach

The only arbitrary parameter in this equation is $\mathring{a}$, the mean distance of closest approach of the ions. This parameter is generally larger than the crystallographic radii of the ions, which is consistent with the fact that the ions are hydrated.

A derivation of the Debye-Huckel theory will not be presented here, but the basic postulates are listed below (93):

1. The central ion sees the surrounding ions in the form of a smoothed-out charge density and not as discrete charges.
2. All the ions in the electrolytic solution are free to contribute to the charge density. Ion pairing does not exist.
3. Only long-range coulombic forces are relevant to ion-ion interactions; short-range noncoulombic forces, such as dispersion forces, play a negligible role.

4. The solution is sufficiently dilute that the Boltzmann distribution equation may be linearized.

5. The only role of the solvent is to provide a dielectric medium for the operation of interionic forces.

To increase the range of applicability of the Debye-Huckel theory, various higher order terms have been added such as that shown in Equation (31).

$$\log \gamma\pm = -AZ_1Z_2\sqrt{\mu}/(1 + B\mathring{a}\sqrt{\mu}) + DC \qquad (31)$$

The term DC has little or no theoretical significance; neither do other higher power of concentration terms which one sometimes sees associated with the Debye-Huckel expression.

The water of hydration must be taken into account at high concentration because the "true" molality of the solute is altered by the removal of water molecules into the hydration spheres of the ions. These water molecules are no longer effectively part of the solvent. As an example of the magnitude of this effect, if a 3.0 molal solution of potassium hydroxide had a hydration number of 6.5, the "true" molality should be 4.62 molal where the "true" molality, $\underline{m}'$, is calculated according to the following equation:

$$m' = 55.51\ m/(55.51 - hm) \qquad (32)$$

where $\underline{m}$ = molality, not taking hydration into consideration

$\underline{h}$ = hydration number: number of moles of water/mole of solute

In deriving an expression for the activity coefficient which would take into account the importance of hydration, the following basic principles were used by Robinson and Stokes (91,92):

1. The chemical potential of a solute considered as a solvated species will be different from its value when considered as unsolvated.

2. The total Gibbs free energy, G, of a fixed amount of solution is fixed, regardless of the method used in expressing composition.

3. The chemical potential of the solvent, $\bar{G}_W = (\partial G/\partial n_W)_{n_B,T,P}$ is unaffected by the method of expressing n_B.

Now consider an ionic solution containing a total of ν moles of solute which dissociates into ν_1 moles of cations and ν_2 moles of anions. There are P moles of solvent W. Let h be the moles of solvent which are used in hydrating the ν moles of solute. The Gibbs free energy of this solution can be expressed in two equivalent ways. In Equation (33) hydration is neglected while in Equation (34) hydration is taken into account. In all cases primes indicate a reference to the solvated state.

$$G = P\bar{G}_W + \nu_1\bar{G}_1 + \nu_2\bar{G}_2 \tag{33}$$

$$G = (P-h)\bar{G}_W + \nu_1\bar{G}_1' + \nu_2\bar{G}_2' \tag{34}$$

For the general case the following is the proper expression for the chemical potential. The symbol a refers to the activity which is a product of the concentration, c, and the activity coefficient f.

$$G - G^\circ = RT \ln a$$

$$G = RT \ln cf + G^\circ$$

$$G = RT \ln c + RT \ln f + G^\circ$$

Thus for the solvent W, H_2O, the following relationship applies.

$$\bar{G}_W = RT \ln a_W + \bar{G}_W^\circ \tag{35}$$

And for $\bar{G}_1$

$$\bar{G}_1 = RT \ln c_1 + RT \ln f_1 + \bar{G}_1^\circ$$

$$\bar{G}_1 = RT \ln \frac{\nu_1}{P + \nu} + RT \ln f_1 + \bar{G}_1^\circ$$

$$\bar{G}_1 = RT(\ln \nu_1 + \ln \frac{1}{P + \nu} + \ln f_1) + \bar{G}_1^\circ \tag{36}$$

Likewise:

$$\bar{G}_2 = RT(\ln \nu_2 + \ln \frac{1}{P + \nu} + \ln f_2) + \bar{G}_2^\circ \qquad (37)$$

And for the hydrated case

$$\bar{G}_1' = RT(\ln \nu_1 + \ln \frac{1}{P-h+\nu} + \ln f_1') + \bar{G}_1'^\circ \qquad (38)$$

$$\bar{G}_2' = RT(\ln \nu_2 + \ln \frac{1}{P-h+\nu} + \ln f_2') + \bar{G}_2'^\circ \qquad (39)$$

Now equate Equations (33) and (34) to get:

$$P\bar{G}_W + \nu_1\bar{G}_1 + \nu_2\bar{G}_2 = (P-h)\bar{G}_W + \nu_1\bar{G}_1' + \nu_2\bar{G}_2' \qquad (40)$$

If the chemical potential values from Equations (35)-(39) are substituted into Equation (40) and simplified, Equation (41) results:

$$\nu_1(\bar{G}_1^\circ - \bar{G}_1'^\circ)/RT + \nu_2(\bar{G}_2^\circ - \bar{G}_2'^\circ)/RT + h\bar{G}_W^\circ/RT + h \ln a_W +$$

$$\nu \ln \frac{P-h+\nu}{P+\nu} + \nu_1 \ln f_1 + \nu_2 \ln f_2 = \nu_1 \ln f_1' + \nu_2 \ln f_2' \qquad (41)$$

Now at infinite dilution all the activity coefficients approach unity and a_W approaches unity. Thus the sum of the first three terms in the above equation must be zero as all the logarithmic terms would be zero under these conditions. Thus, Equation (41) simplifies to the following (mean ionic acitivity coefficients have been introduced):

$$\ln f'\pm = \ln f\pm + (h/\nu)(\ln a_W) + \ln(P-h+\nu)/(P+\nu) \qquad (42)$$

Now the Debye-Huckel term for ln f± is substituted in, and if the solvent is water, Equation (43) results:

$$\ln \gamma\pm = -AZ_1Z_2\sqrt{\mu}/(1 + B\mathring{a}\sqrt{\mu}) - (h/\nu)(\ln a_W) - \ln [1 - 0.018(h-\nu)m] \qquad (43)$$

where $\gamma\pm$ = mean molal activity coefficient

$f\pm = \gamma\pm(1 + 0.018\ \nu\underline{m})$

$\underline{P} = 1000/W_{\underline{A}}\underline{m}$

$W_{\underline{A}}$ = molecular weight of solvent

In this case ν equals the number of ions from the dissociation of one molecule of solute.

This derivation has been based on the assumption that $\underline{h}$, the hydration number, is independent of concentration which is probably not true at high concentrations.

The second term in Equation (43) can be evaluated from an experimental knowledge of the osmotic coefficient according to the following relationship which can be derived from the Gibbs-Duhem relationship.

$$\phi = -1000/\nu W_A m\ (\ln a_W) \tag{44}$$

This equation further simplifies to the following:

$$-1/\nu\ (\log a_W) = 0.007824\ m\phi$$

ϕ = osmotic coefficient (45)

Two computer programs were written with regard to Equation (43). Program DEH3 theoretically calculates the activity coefficient of a solute according to Equation (43) up to 6 molal. Also, the experimental activity coefficients are generated from empirical equations and parameters from Reference (89). The data input include the mean distance of closest approach parameter in the Debye-Huckel term and the hydration number as well as the five empirical parameters from the National Bureau of Standards report. The values for A and B in the Debye-Huckel term were obtained from another National Bureau of Standards

report (94). The data output include the following at each of the concentrations for which a calculation is made: The molality, the value of the Debye-Huckel term at that concentration, the osmotic coefficient, the experimental activity coefficient, the theoretical activity coefficient as calculated from Equation (43), the difference between the experimental and theoretical calculation, the water not bound up in hydration, termed free water, and the "true" molality calculated on the basis of Equation (32). The output may also be stored on disk File 1 for use by the plotting program, DEH4.

Program DEH4 is a simple plotting program which uses a Calcomp plotter to plot the activity coefficient as a function of molality. The experimental activity coefficient is plotted as a continuous curve while the theoretical activity coefficient is represented by an annotated curve. Both of these programs, as well as some sample output, are incorporated in Appendix VII.

Essentially what was done with these programs was to adjust the distance of closest approach parameter, $\underline{\mathring{a}}$, and the hydration number until a good fit between the theoretical and experimental values was achieved. The study was limited to the potassium hydroxide system in order to avoid the complications of incomplete dissociation. A value of $\underline{\mathring{a}}$ for potassium hydroxide was not found in the literature, but the following table [Table IX (95)] does indicate that the proper value for $\underline{\mathring{a}}$ should be in the neighborhood of 3.5 to 4.0.

There is little sense using experimental values from the literature for the hydration parameter as these numbers are extremely method dependent (23). The hydration parameter was arbitrarily varied in order to improve the fit. At low concentrations, where the Debye-Huckel term predominates, the distance of closest approach parameter could be adjusted almost independently of the hydration parameter. The hydration parameter was then adjusted until the fit was optimized.

Figure 37 compares the theoretical and experimental activity coefficients for what was considered to be the optimum fit. Since the hydration parameter was treated as a constant when it is most likely a decreasing function with respect to concentration, the two curves begin to diverge at a molality of about 3.0.

TABLE IX

SEVERAL SELECTED HYDRATED IONIC DIAMETERS

Ion	$\mathring{a}$	Ion	$\mathring{a}$
H^+	9	OH^-	3.5
Na^+	4	F^-	3.5
Mg^{++}	8	Cl^-	3
Ca^{++}	6	Br^-	3
Ba^{++}	5	$SO_4^=$	4
Ag^+	2.5	NO_3^-	3
Fe^{++}	6	BrO_3^-	3.5
Fe^{+++}	9		

Another way of approaching this problem would have been to force a fit between the experimental and theoretical activity coefficients by allowing the hydration parameter to be a concentration-dependent variable. If this had been done the hydration number would have remained essentially constant up to about 3.0M. Beyond that concentration, the value of the hydration parameter would have decreased.

This investigation presents evidence that the hydration number of potassium hydroxide commences to decrease at approximately 3.0M. This is in the same concentration range that potassium hydroxide commences to decrystallize cellulose I (see Fig. 20). These findings complement the interpretation of the Raman spectra of the mercerizing solutions with regard to the width at half height of the band located at 3610 cm^{-1}. The interpretation of the Raman spectra was

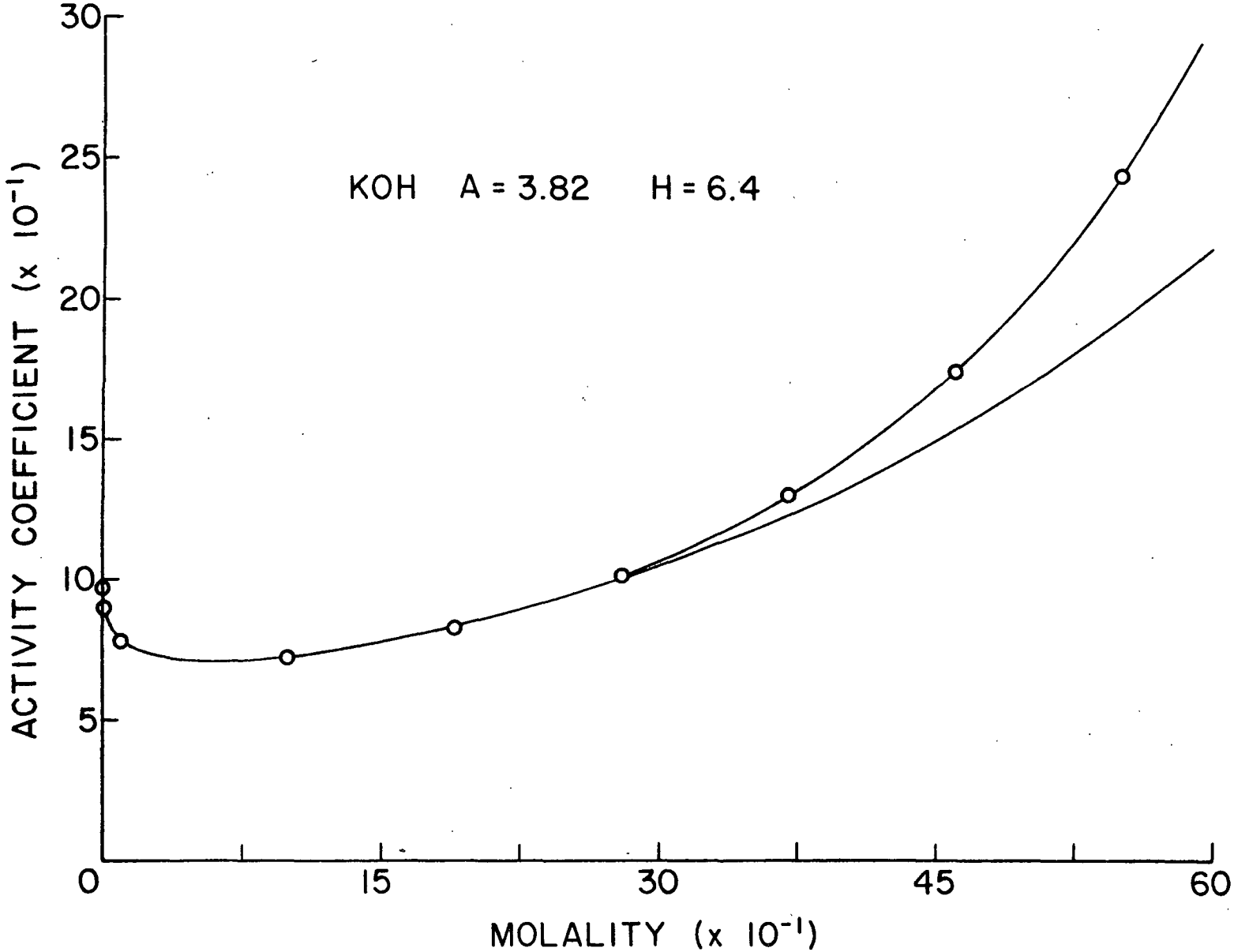

Figure 37. Comparison of Experimental and Theoretical Activity Coefficients for Potassium Hydroxide. The annotated line represents the theoretical curve

that the hydroxide ion must be nearly dehydrated before it can participate in decrystallizing the native lattice.

A TEST OF THE PROPOSED THEORY

The theory developed in this thesis that the key species in the decrystallization of cellulose I is the dehydrated hydroxide ion is a radical departure from previous ideas on mercerization. This theory can be experimentally probed from a number of vantage points in order to insure its validity or to reject it.

One qualitative test of the theory would be to add neutral electrolyte to a mercerizing solution in the transition region. The neutral electrolyte would be expected to decrease the amount of free water available for the hydration of the hydroxide ion. Therefore, the solution should be more effective in decrystallizing cellulose I than a solution of the same concentration of hydroxide ion, but without the added neutral electrolyte, if the theory is valid.

A test of the above hypothesis was run in the following manner. The standard mercerization procedure was followed using a solution which was 3.19M sodium hydroxide and 1.30M sodium chloride. A 3.19M solution of sodium hydroxide without added salt would be expected to convert the cellulose I about 24% to cellulose II. The measured conversion using the solution containing the added sodium chloride was 65%. This was interpreted to mean that the added electrolyte had helped to dehydrate the hydroxide ion and enhance the potential of the hydroxide ion to disrupt the cellulose lattice.

EFFECT OF TEMPERATURE ON THE LATTICE TYPE ASSUMED BY CELLULOSE PRECIPITATED FROM SOLUTION

As mentioned previously it has been concluded that mercerization at elevated temperatures is not as successful as it is at lower temperatures due to tempera-

ture-dependent changes associated with the mercerizing solution (17). An alternative hypothesis which had yet to be explored is the possibility that the crystallographic form which cellulose assumes upon recrystallization is a function of temperature. Atalla and Nagel (27,96) have done a series of experiments which indicate that this may be true. They found that they could precipitate cellulose IV from a phosphoric acid solution at elevated temperatures. They also were able to precipitate cellulose I from solution at 170°C.

Since x-ray diffraction is most commonly employed in following the mercerization process, a misinterpretation of the results may occur if polymorphs of cellulose other than I and II are present. This misinterpretation may occur as the mercerization process is generally followed by observing the transition from cellulose I to II using relative intensity values. If another polymorph is present in small amounts it may alter the relative intensity ratios as the diffraction peaks of the four polymorphs of cellulose overlap considerably.

Cellulose treated with alkali of a concentration beyond the transition region is not transformed into a solution. However, the polymeric chains must have substantial mobility in this swollen, gelatinous phase. Therefore, temperature effects associated with changes in the crystal structure of cellulose precipitated from solution would also be operative during the recrystallization step of mercerization. The clear advantage of precipitating cellulose from solution in order to investigate the relationship between temperature and crystal structure is that there would be no ambiguity about residual crystalline material being present in mixed lattice samples. Solvent effects were ignored.

The x-ray diffractograms of the precipitation series from the DMSO-PF solvent system are exhibited in Fig. 38. The precipitation temperature for each sample is indicated. The anticipated temperature effect is obviously

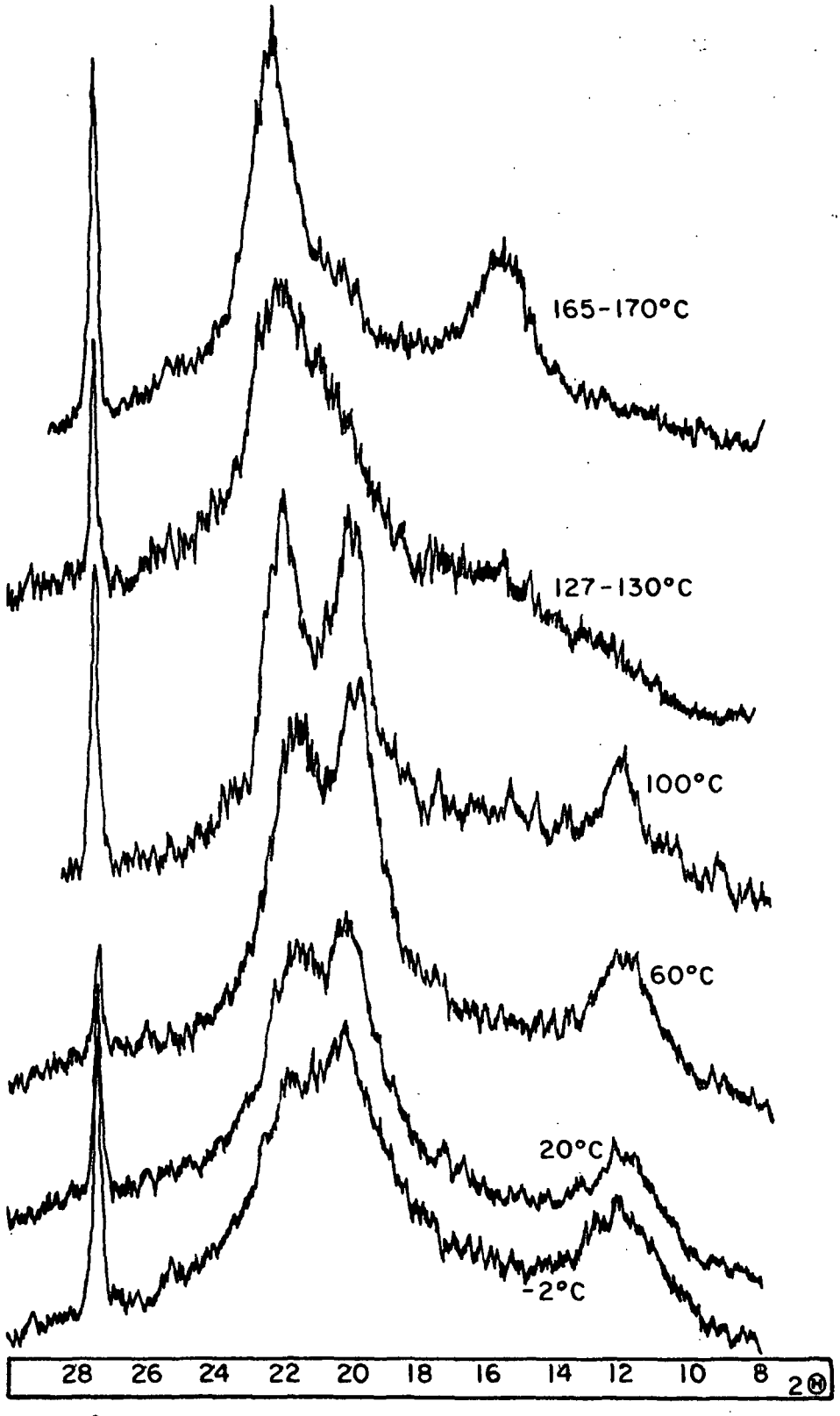

Figure 38. X-ray Diffractograms of the Precipitation Series from 3% Cellulose in the DMSO-PF Solvent System

operative. The two diffractograms of samples precipitated at -2 and 20°C are typical of low crystallinity cellulose II. The diffractogram of the sample precipitated at 60°C is also indicative of a wholly cellulose II lattice, but the crystallinity has improved. At 100°C there is definitely a mixed lattice. Note the change in relative intensities of the (002) and $(10\bar{1})$ peaks. There is also a hint of a peak between the $(10\bar{1})$ and (101) peaks of the major constituent. The sample precipitated at 127-130°C appears to be a mixed lattice of cellulose II and cellulose IV, and the sample precipitated at 165-175°C is almost totally a cellulose IV.

The sample precipitated at 100°C is of special interest since Jeffries and Warwicker (17) washed their mercerized samples at that temperature. It is easy to perceive how they may have interpreted a diffractogram similar to the one presented here as containing a residue of cellulose I. If it is assumed for comparative purposes that the sample shown here is a mixture of cellulose I and II, the residual cellulose I is calculated to be 18% using the standards developed in this thesis.

The evidence presented in Fig. 38 suggests that there is an evolution from the cellulose II lattice to cellulose IV, and that this evolution is a function of temperature. The Raman spectra of these samples, which are shown in Fig. 39, should aid in explaining why this polymorphic change is a function of temperature.

The more significant changes among the Raman spectra of these precipitated celluloses are found in the low frequency region below 600 cm^{-1}. In an earlier section it was mentioned that changes in this region of the vibrational spectrum have been shown to be associated with changes in conformation. (In this context changes in conformation refer to changes in the spatial relationship between adjoining anhydroglucose units.)

From their computerized study of the Van der Waals interactions about the glycosidic linkage, Rees and Skerrett (97) have concluded that there are two free energy minima which would indicate that there are two plausible conformations for the cellulose chain. The changes in the Raman spectra in the low frequency region also indicate that there are two conformations. Cellulose I is associated with one conformation while cellulose II is found in the alternative conformation. Celluloses III and IV appear to incorporate unspecified distributions of both conformations (98).

As is apparent from Fig. 39, the relative intensity ratio of the bands at 350 and 375 cm^{-1} appear to be a continuous function of temperature. The band located at 375 cm^{-1}, which is indicative of the conformation associated with cellulose I, is just a shoulder of the band at 350 cm^{-1} at -2°C, but the two bands, although badly overlapped, are of almost equal intensity at a precipitation temperature of 165-170°C. Atalla and Nagel (96) noted a similar trend in their precipitation work from phosphoric acid.

The Raman spectra and x-ray diffractograms of these precipitated celluloses suggest the following hypothesis: the chain conformation of cellulose in solution is a function of temperature. Elevated temperatures promote an increase in the population of the glycosidic linkages that are in the conformation associated with cellulose I. Upon precipitation from solution the conformation of the chain is frozen in the crystalline areas. Since the various lattice types of cellulose are a function of the chain conformation, it is suggested that the equilibrium chain conformation in solution plays a major role in determining the type of lattice which will result upon precipitation.

The precipitation work presented here does not, of course, prove the above hypothesis. But it is certainly consistent with it. Other precipitation and

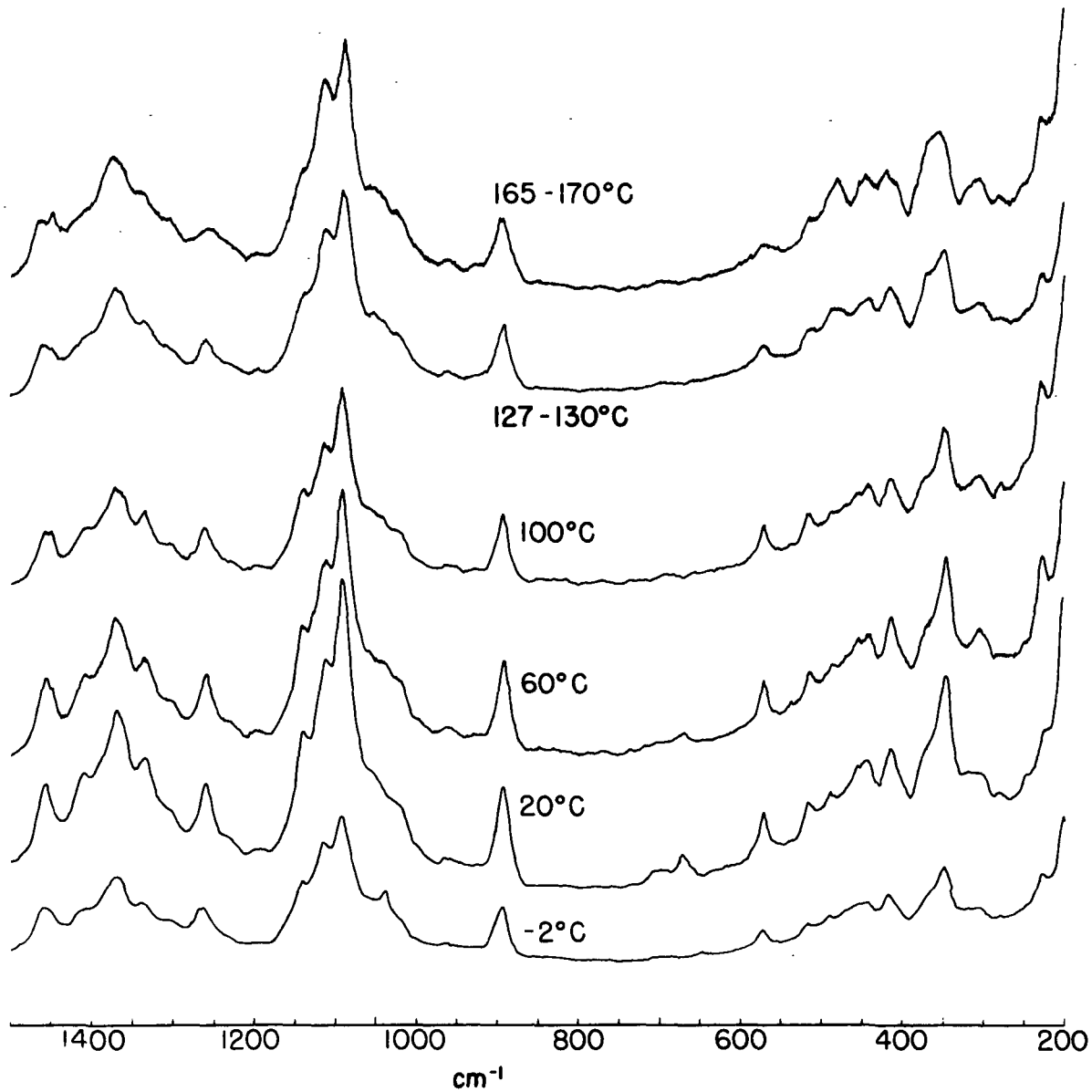

Figure 39. Raman Spectra of the Precipitation Series from 3% Cellulose in the DMSO-PF Solvent System

annealing work presented in Appendix III are consistent with the experimental findings presented here. It was discovered, for instance, that when the precipitating conditions were altered such that an essentially amorphous cellulose would result, annealing such samples at 150°C in glycerine for two weeks would convert them to cellulose IV. Apparently, the cellulose chains in the plasticized amorphous cellulose have enough mobility to change conformation.

There are several other considerations which suggest that there is more to the interrelationship among chain conformation, temperature of precipitation, and lattice type than what has been hypothesized here. The Raman spectra of cellulose III is one example. Atalla and Nagel (96) have prepared cellulose III at temperatures near -50°C using liquid ammonia. The Raman spectra of some of these samples appear to have a band at 375 cm^{-1} which is as prominent or more prominent than is the case with some cellulose IV samples. However, some cellulose III samples appear to have no trace of a band at 375 cm^{-1} and in several instances the original cellulose I lattice was not completely disrupted. This suggests that the band at 375 cm^{-1} in cellulose III may represent a residue of the original lattice. Work is continuing in this area which will clarify this point.

A second and more fundamental criticism of the hypothesis is that it may be interpreted to imply a phenomenon that is thermodynamically impossible. If the two conformations of the cellulose chain represent two free energy states that are in thermodynamic equilibrium, the population of the conformation in the higher energy state could never exceed 50%. It could only reach 50% at infinite temperature. As already mentioned, Atalla and Nagel (27) have recovered cellulose I from solution at 170°C. The cellulose I conformation is by implication the conformation of higher free energy as it is stabilized by high temperatures. Therefore, it would appear that there may be a cooperative effect between the

crystallization process and the final conformation of the cellulose chain in some cases, or there is not a true thermodynamic equilibrium between the two conformations.

EFFECT OF WASHING MERCERIZED SAMPLES AT HIGH TEMPERATURE

Two samples were treated with 6.0M sodium hydroxide using the standard mercerization procedures. One sample was washed at 100°C in H_2O and the other at 165°C in glycerol. This was done to see if the same trends observed with the precipitated cellulose would manifest themselves with completely decrystallized, mercerized cellulose. X-ray diffractograms of the two samples are shown in Fig. 40. The sample washed at 165°C is a mixture of cellulose II and IV, but the expected trend is less apparent with the sample washed at 100°C. The cellulose chains do not have as much mobility in mercerized cellulose as they do in solution. Therefore, crystallization was probably initiated before the chains could reach their equilibrium conformation.

SUMMARY OF RESULTS AND CONCLUSIONS

The mercerization process involves the swelling and decrystallization of the native fiber and the recrystallization of the swollen gel as the mercerizing solution is removed.

This thesis work has demonstrated that the decrystallization of highly crystalline cellulose I is quite different from the swelling of accessible cellulose. The concentration of alkali metal hydroxide must reach a certain minimum before any effect on the lattice is observed using x-ray diffraction measurements. The Donnan theory does not predict a threshold effect, but it adequately explains the swelling of accessible cellulose.

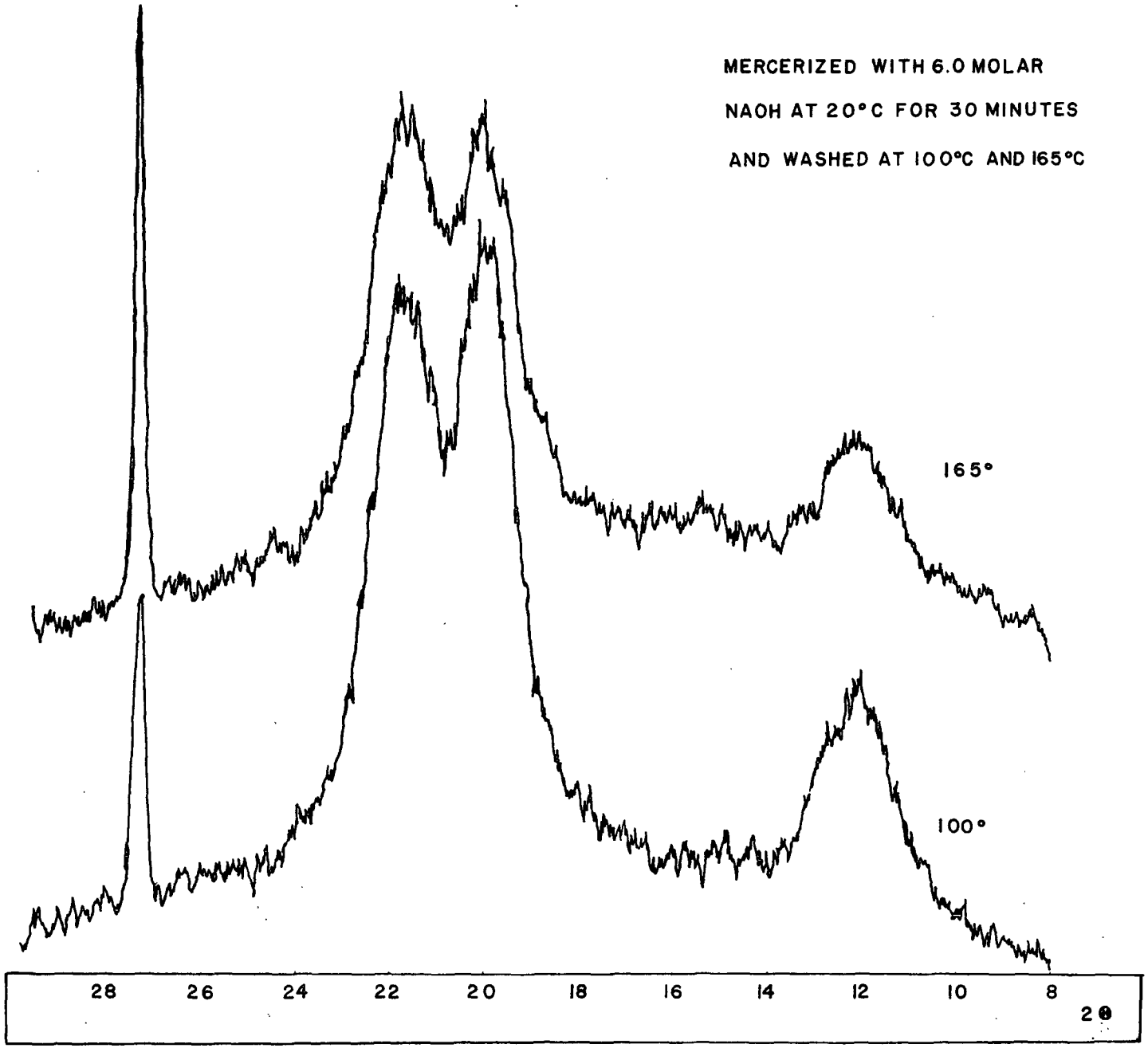

Figure 40. X-ray Diffractograms of Two Mercerized Samples Washed at High Temperature

The three alkali metal hydroxides studied are able to disrupt the native lattice; the relative effectiveness at equal concentrations in the transition region is: KOH≥NaOH>LiOH. This sequence is the same as their dissociation order; potassium hydroxide is believed to be completely dissociated in aqueous solutions, whereas lithium hydroxide has a dissociation constant of 0.65.

The order predicted by the dissociation constants was experimentally verified. An analysis of the Raman spectra of the alkali metal hydroxide mercerizing solutions revealed that the integrated intensity of a band located at 3610 cm^{-1} could be used as a relative measure of the nonion-paired hydroxide ion concentration. The band was identified as the fundamental stretching vibration of the free hydroxide ion.

The width at half height of the band at 3610 cm^{-1} decreased as the alkali metal hydroxide concentration increased. The rate of decrease was found to go through a definite transition at about 3.5 to 4.0M and the width at half height at the inflection point was 82 cm^{-1}. This value nearly equals what has been found to be the width at half height of the unhydrated hydroxide ion (74). An investigation of the water removal theory of activity coefficients also indicated that the hydration number of the hydroxide ion is decreased near a concentration which corresponds closely to the beginning of the transition region.

The Raman spectra of the mercerizing solutions allowed for a comparison of the three alkali metal hydroxides at equal free hydroxide ion concentrations. Under these circumstances it was found that the order of effectiveness of the alkali metal hydroxides in decrystallizing cellulose I is LiOH>NaOH>KOH. However, on this basis, the differences among the three hydroxides were found to be quite modest and perhaps insignificant. This order of effectiveness is the same as the hydration order of the cations with the lithium ion being the most highly hydrated of the three.

These considerations lead to the formulations of the following theory about the decrystallization of the native lattice with alkali metal hydroxides: the most important parameter in the decrystallization process is the activity of the hydroxide ion. The concentration of electrolyte must be sufficient to promote competition among the ionic species for water of hydration. The hydroxide ions have the ability to penetrate and disrupt the native lattice only after their hydration spheres are depleted.

The data indicate that the cations may play a secondary role which may be explained in terms of the Donnan equilibrium theory. Decrystallization is thus envisioned as a synergism of hydrogen bond disruption and swelling pressure.

The Raman spectra of the alkali treated cellulose indicated that there are some minor changes in the crystal lattice prior to the transition region, but that the cellulose chains do not achieve sufficient mobility to assume the cellulose II conformation until the transition region is reached.

The Raman spectra and x-ray diffractograms of the precipitated celluloses indicated that the lattice form assumed by cellulose is a function of temperature. There are two stable conformations of the cellulose chain. On conformation is associated with the cellulose I crystal structure and the other with cellulose II. Cellulose IV incorporates both conformations in the unit cell. The conformation of the cellulose chain in solution which has been associated with the cellulose I lattice is favored by increasing temperature. The lattice type of precipitated cellulose is then a function of the chain conformation or relative populations of the two possible conformations.

SUGGESTIONS FOR FUTURE RESEARCH

The theory of mercerization presented in this thesis is substantially different from what has been previously believed. It should be explored further from several different perspectives in order to increase its credibility and to modify it if that proves to be necessary.

One interesting investigation would be to increase the dissociation of lithium hydroxide at intermediate mercerizing concentrations and see if that enhances the lattice conversion at that concentration. This could be done using Kryptofix 211* which is one of a family of bicyclic rings with two nitrogen end atoms. These compounds bind specific cations and increase their solubility. Another possibility would be to use Kryptofix 222 to solvate potassium hydroxide in dimethyl sulfoxide.

It would prove informative to determine the relative importance of hydrated cationic size in the decrystallization of cotton fibers. Perhaps a mixture of lithium and potassium hydroxide would exhibit a synergistic effect.

Much more work needs to be done on the relationship between cellulose chain conformation, precipitating temperature, and lattice structure. Probably, the first step should be to quantify on a relative basis the percent of each chain conformation present in the precipitated series. This could be accurately done using the computer program presented in Appendix V and the Raman bands located at 350 and 375 cm^{-1}. By doing this one could find out if the relative amounts of each conformation are a true continuous function of temperature.

Future precipitation work should also include altering the DP of the cellulose to see what effect that has.

* Kryptofix is distributed by PCR, Incorporated, P.O. Box 1466, Gainesville, Florida, 32602.

ACKNOWLEDGMENTS

The most creative individual that I have ever had the pleasure of working with is Dr. R. H. Atalla, the Chairman of my Thesis Advisory Committee. Dr. Atalla has been a constant source of inspiration and ideas during the course of this research. I am grateful for his help and interest.

Drs. D. G. Williams and R. A. Stratton served on my Thesis Advisory Committee and contributed ideas and pertinent criticisms. I wish to thank both of these men for their contributions.

I wish to extend my appreciation to Dr. M. Nicholson for discovering the DMSO-PF solvent system and spending many hours discussing it with me.

I have received assistance and advice from almost every member of the Institute staff while engaged in this research, and I am especially indebted to Mr. J. D. Hultman for acquainting me with the x-ray diffraction equipment and techniques, and Mr. S. C. Nagel for numerous experimental techniques. Mr. Nagel also taught me how to run the Raman spectrometer. Without the help of Messrs. J. J. Bachhuber and J. O. Church, I would probably still be trying to debug the major computer program used in this research. Messrs. M. C. Filz, Jr. and P. F. Van Rossum contributed time and ideas which assisted me both directly and indirectly in completing this thesis.

My wife Doreen has spent many hours doing the typing throughout the course of this work. I wish to thank her for all the help and encouragement she has given me. My daughters Sarah and Rebekah have helped me keep this thesis work in its proper perspective.

LITERATURE CITED

1. Nicoll, W. D., Cox, N. L., and Conway, R. F. Alkali and other metal derivatives. In Ott and Spurlin's Cellulose and cellulose derivatives. 2nd ed. Part II. p. 825. New York, Interscience, 1954.

2. Warwicker, J. O., Jeffries, R., Colbran, R. L., and Robinson, R. N. A review of the literature on the effect of caustic soda and other swelling agents on the fine structure of cotton. Shirley Institute Pamphlet No. 93. Didsbury, Manchester, Shirley Institute, 1966. 247 p.

3. Warwicker, J. O. Swelling. In Bikales and Segal's Cellulose and cellulose derivatives. 2nd ed. Part 4. p. 369. New York, Wiley-Interscience, 1971.

4. Billmeyer, F. W. Textbook of polymer science. New York, Interscience, 1970. 601 p.

5. Flory, P. J. Principles of polymer chemistry. p. 577-93. Ithaca, New York, Cornell University Press, 1953.

6. Donnan, F. G., and Harris, A. B., Trans. Chem. Soc. (99):1554-77(1911).

7. Chedin, J., and Marsaudon, A., Die Makromolekulare Chemie 33:195-221(1959).

8. Neale, S. M., J. Textile Inst. 20:T373-400(1929); 21:T225-30(1930); 22: T320-38(1931).

9. Pennings, A. J., and Prins, W., J. Polymer Sci. 58:229-48(1962).

10. Barrow, G. M. Physical chemistry. 2nd ed. p. 809-10. New York, McGraw-Hill, 1966.

11. Morrison, J. L., Campbell, W. B., and Maass, O., Can. J. Res. 16:195-202 (June, 1938).

12. Vigo, T. L., Wade, R. H., Mitcham, O., and Welch, C. M., Textile Res. J. 39:305-16(April, 1969).

13. Vigo, T. L., Mitcham, O., and Welch, C. M., J. Polymer Sci. (B. Polymer Letters) 8:385-93(1970).

14. Chedin, J., and Marsaudon, A., Die Makromolekulare Chemie 15:115-60(1955).

15. Chedin, J., and Marsaudon, A., Die Makromolekulare Chemie 20:57-82(1956).

16. Warwicker, J. O., J. Polymer Sci., Part A-1, 5:2579-93(1967).

17. Jeffries, R., and Warwicker, J. O., Textile Res. J. 39:548-59(June, 1969).

18. Warwicker, J. O., and Wright, A. C., J. Appl. Polymer Sci. 11:659-71(1967).

19. Liang, C. Y., and Marchessault, R. H., J. Polymer Sci. 35(129):529-31; 37(132):385-95; 39(135):269-78(1959).

20. Denoyelle, G., Svensk Papperstid. 62:390-406(1959).

21. Ranby, B. G., Acta Chem. Scand. 6:101-15; 116-27; 128-38(1952).

22. Cabradilla, K. E., and Zeronian, S. H. The effect of crystal form on the thermal properties of cotton cellulose. 169th ACS National Meeting, Philadelphia, PA, April 6-11, 1975.

23. Hinton, J. F., and Amis, E. S., Chem. Rev. 71:627-74(1971).

24. Dobbins, R. J., Tappi 53:2284-90(1970).

25. Frank, H. S., and Wen, W. Y., Discn. Faraday Soc. 24:133-40(1957).

26. Atalla, R. H. Proceedings of the Eighth Cellulose Conference. J. Polymer Sci. (C. Polymer Symp.), in press.

27. Atalla, R. H., and Nagel, S. C., Science 185:522-3(1974).

28. Battista, O. A., Hill, D., and Smith, P. A. Level-off D. P. cellulose products. U.S. pat. 2,978,446(April 4, 1961).

29. Battista, O. A., Chem. Eng. News 40:77-8(June 18, 1962).

30. Nelson, M. L., and O'Connor, R. T., J. Appl. Polymer Sci. 8:1325-41(1964).

31. Sharples, A., Trans. Faraday Soc. 53:1003-13(1956).

32. Ant-Wuorinen, O., and Visapaa, A., Norelco Rept. 9:48-52(1962).

33. Skoog, D. A., and West, D. M. Analytical chemistry. 1st ed. p. 300. New York, Holt, Rinehart, and Winston, 1965.

34. Hindeleh, A. M., and Johnson, D. J., Polymer 13:423-30(1972).

35. Atalla, R. H. Personal communication, 1973.

36. Atalla, R. H., and Nagel, S. C., JCS Chem. Comm. 1972:1049-50.

37. Atalla, R. H. Unpublished work, 1970.

38. Schonland, D. S. Molecular symmetry. p. 288. New York, Van Nostrand Reinhold Co., 1965.

39. Tobin, M. C. Laser Raman spectroscopy. p. 68-70. New York, Wiley-Interscience, 1971.

40. Nicholson, M. D. Investigation of reactions in the dimethyl sulfoxide/paraformaldehyde (DMSO/PF) cellulose solvent. Doctor's Dissertation. Appleton, WI, The Institute of Paper Chemistry, 1976. 101 p.

41. Swenson, H. A. In Proceedings of the Eighth Cellulose Conference. (J. Polymer Sci., Part C).

42. Tripp, V. W. Measurement of crystallinity. In Cellulose and cellulose derivatives. Vol. 5. Part 4. p. 305-24. New York, Wiley-Interscience, 1971.

43. Kakudo, M., and Kasai, N. X-Ray diffraction by polymers. p. 139. Tokyo, Kodansha Ltd., 1972.

44. Kakudo, M., and Kasai, N. X-Ray diffraction by polymers. p. 362. Tokyo, Kodansha Ltd., 1972.

45. Wakelin, J. H., Virgin, H. S., and Crystal, E., J. Appl. Phys. 30:1654-62(Nov., 1959).

46. Ellefsen, Ø., Lund, E. W., Tønnesen, B. A., and Øien, K., Norsk Skogind. 8:284-93; 9:349-55(1957).

47. Kakudo, M., and Kasai, N. X-Ray diffraction by polymers. p. 125-33. Tokyo, Kodansha Ltd., 1972.

48. Kulshreshtha, A. K., Sweltz, N. E., and Radhadkrishnan, T. Fourier analysis of the meridional profiles of paracrystalline x-ray diffraction from a polynosic viscose fibre. Proceedings of the Twelfth Technological Conference. p. 221. Bombay, T. V. Ananthan, 1971.

49. Gjonnes, J., Norman, N., and Vierroll, H., Acta Chem. Scand. 12:489-94(1958).

50. Gjonnes, J., and Norman, N., Acta Chem. Scand. 12:2028-33(1958).

51. Segal, L., Creely, J. J., Mart, A. E., Jr., and Conrad, C. M., Textile Res. J. 29:786-94(1959).

52. Nelson, M. L., and O'Connor, R. T., J. Appl. Polymer Sci. 8:1311-24(1964).

53. Silverstein, R. M., and Bassler, G. C. Spectrometric identification of organic compounds. 2nd ed. p. 73. New York, John Wiley and Sons, 1967.

54. Gjonnes, J., and Norman, N., Acta Chem. Scand. 14:683-8(1960).

55. Gjonnes, J., and Norman, N., Acta Chem. Scand. 14:689-91(1960).

56. Alexander, L. E. X-Ray diffraction methods in polymer science. p. 140. New York, Wiley-Interscience, 1959.

57. Sisson, W. A., and Saner, W. R., J. Phys. Chem. 45:717-30(1941).

58. Ranby, B. G., and Mark, H. F., Svensk Papperstid. 58:374-82(1958).

59. Zeronian, S. H., and Cabradilla, K. E., J. Appl. Polymer Sci. 16:113-28 (1972).

60. Gimblett, F. G. R., and Monk, C. B., Trans. Faraday Soc. 50:965-72(1954).

61. Douglas, B. E., and McDaniel, D. H. Concepts and models of inorganic chemistry. p. 199. Waltham, MA, 1965.

62. Atalla, R. H., and Dimick, B. E., Carbohyd. Res. 39:C1-3(1975).

63. Pitzner, L. J. An investigation of the vibrational spectra of the 1,5-anhydropentitols. Doctor's Dissertation. Appleton, WI, The Institute of Paper Chemistry, 1973. 402 p.

64. Watson, G. M. An investigation of the vibrational spectra of the pentitols and erythritol. Doctor's Dissertation. Appleton, WI, The Institute of Paper Chemistry, 1974. 178 p.

65. Phillips, B., and Busing, W. R., J. Phys. Chem. 61:502(1957).

66. Jones, L. H., J. Chem. Phys. 22:217-19(1954).

67. Naikamoto, K. Infrared spectra of inorganic and coordination compounds. 2nd ed. p. 81. New York, Wiley-Interscience, 1970.

68. Krishnamurti, P., Indian J. Phys. 5:651(1930).

69. Busing, W. R., J. Chem. Phys. 23:933-6(1955).

70. Krishnamurti, P., Proc. Indian Acad. Sci. 50:223(1959).

71. Ibers, J. A., Kumamoto, J., and Snyder, R. G., J. Chem. Phys. 33:1164-77 (1950).

72. Buchanan, R. A., Kinsey, E. L., and Caspers, H. H., J. Chem. Phys. 36: 2665-75(1962).

73. Walrafen, G. E., J. Chem. Phys. 52:4176-98(1970).

74. Turnbull, A. G., Austral. J. Chem. 24:2213-22(1971).

75. Schonland, D. S. Molecular symmetry. p. 172-3. New York, Van Nostrand Reinhold Co., 1965.

76. Barrow, G. M. Physical chemistry. 2nd ed. p. 350. New York, McGraw-Hill, 1966.

77. Walrafen, G. E. Raman and infrared spectral investigations of water structure. In Frank's Water a comprehensive treatise. 1st ed. Vol. 1. p. 151-214. New York, Plenum Press, 1972.

78. Clarke, E. C. W., and Glew, D. N., Can. J. Chem. 50:1655-65(1972).

79. Fraser, R. D. B., and Suzuki, E., Anal. Chem. 38:1770-3(1966).

80. Fraser, R. D. B., and Suzuki, E., Anal. Chem. 41:37-9(1969).

81. Irish, D. E., and Chen. H., J. Phys. Chem. 74:3796-801(1970).

82. Chen, H., and Irish, D. E., J. Phys. Chem. 75:2672-81(1971).

83. Chen. H., and Irish, D. E., J. Phys. Chem. 75:2681-4(1971).

84. Nelson, D. L., and Irish, D. E., J. Chem. Phys. 54:4479-89(1971).

85. Glueckauf, E., Trans. Faraday Soc., 51:1235-44(1955).

86. Tan, J. S., Fisher, L. W., and Marcus, P. 169th National Meeting of ACS, Philadelphia, PA, April, 1975.

87. Irish, D. E., and Davis, A. R., Can. J. Chem. 46:943-51(1968).

88. Seshadri, K. S., and Jones, R. N., Spectrochim. Acta 19:1013-85(1963).

89. Wu, Y., and Hamer, W. J. Electrochemical data, Part XIII. Osmotic coefficients and mean activity coefficients of a series of univalent electrolytes in aqueous solutions at 25°C. NBS Report 1002. Washington, D.C., U.S. Government Printing Office, February, 1969. 44 p.

90. Barrow, G. M. Physical chemistry. 2nd ed. p. 707. New York, McGraw-Hill, 1966.

91. Stokes, R. H., and Robinson, R. A., J. Am. Chem. Soc. 70:1870-8(1948).

92. Robinson, R. A., and Stokes, R. H. Electrolytic solutions. 2nd ed. p. 238-48. London, Butterworth's Scientific Publications, 1959.

93. Bockris, J. O'M., and Reddy, A. K. N. Modern electrochemistry. 1st ed. Vol. 1. p. 175-285. New York, Plenum/Rosetta, 1973.

94. Hamer, W. J. Theoretical mean activity coefficients of strong electrolytes in aqueous solutions from 0 to 100°C. NSRDS-NBS 24. Washington, D.C., U.S. Government Printing Office, December, 1968. 271 p.

95. Stratton, W. J. Chemistry 46. Richmond, IN, Earlham College, 1966.

96. Atalla, R. H., and Nagel, S. C. Unpublished work, 1974.

97. Rees, D. A., and Skerrett, R. J., Carbohyd. Res. 7:334-48(1968).

98. Atalla, R. H. To be published.

99. Venkateswaran, A., Tappi 48:191-2(March, 1965).

100. Corbett, W. M. Purification of cotton cellulose. In Whistler's Methods in carbohydrate chemistry. Vol. 3. p. 3. New York, Academic Press, 1963.

101. Atalla, R. H., and Nagel, S. C., J. Polymer Sci. (Polymer Letters) Ed. 12: 565-8(1974).

102. Ward, K. Personal communication, 1975.

APPENDIX I

PREPARATION OF CRYSTALLINE CELLULOSE I SAMPLES

The purpose of this appendix is to add experimental details about each of the celluloses examined for crystallinity.

Sample Number	Origin and Preparation[1]
1	Avicel-PH-101, Lot 1033-342 Used as received after conditioning in a constant temperature-constant humidity room at 50% RH and 20°C for a minimum of 24 hours
2	Avicel Refluxed 1 hour with 2.4N HCl in polyethylene. Filtered, washed, dried via solvent exchange: acetone, ethanol, diethylether, vacuum dried
3	Avicel Refluxed 4 hours with 2.4N HCl. All else the same as Sample 2
4	Avicel Refluxed 8 hours with 2.4N HCl. All else the same as Sample 2
5	Padua nonsterile cotton[2] Prepared in much the same manner as is specified in the Avicel patent (28). Thirty grams of the product were refluxed in 2.5N HCl for 15 minutes at 105°C. The resulting particulate solution was filtered, washed with distilled water, washed with 1% ammonium hydroxide, and again washed with water. The material was then slurried at 5% consistency by weight and vigorously agitated in a Waring blendor for 50 minutes. The resulting colloidal suspension was diluted to 1.5% consistency and placed in a 2000 ml separatory funnel. After 25 minutes the first 700 ml were discarded and the rest of the material was reclaimed through centrifugation. The resulting hydrocellulose was freeze-dried and then dried in a vacuum oven at 55°C for approximately 4 hours

[1] All the celluloses examined were conditioned in the same manner as Sample 1.

[2] Padua nonsterile cotton is a commercial preparation.

6	Padua Nonsterile Cotton Prepared in much the same manner as Sample 5 with the following exceptions: the cotton was hydrolyzed for 2 hours and condensed through filtration rather than centrifugation. None of the product was discarded, as it appeared quite homogenous after being allowed to settle for 12 hours
7	Avicel Otherwise unaltered, was freeze-dried
8	Avicel Otherwise unaltered, was dried using the solvent exchange technique: acetone, 100%, ethanol, diethylether, and vacuum dried
10	Ramie fiber Purified in the following manner which is a synthesis of the procedures suggested by Venkateswaren (99) and Corbett (100). Ramie roving which contained leaves and other debris was carded with carding combs and the remaining extraneous material was removed with forceps. The fibers were then extracted with $CHCl_3$ for 18 hours followed by a further extraction of the same duration with 95% ethanol. These extractions were done to remove the natural waxes. The pectins were removed by vigorously boiling the fibers for 8 hours in 1% NaOH under an atmosphere of N_2. After washing with hot H_2O, the fibers were hydrolyzed with 2.5N HCl for 30 minutes and further processed in the same manner as Sample 6.
11	Stoneville 2B cotton fibers Purified using the same procedures as were used in purifying the Ramie fibers. The sample was hydrolyzed in 4N HCl for 30 minutes, filtered, washed, and freeze-dried
12	Whatman CF1 long fiber cellulose powder Hydrolyzed for 15 minutes in boiling 2.5N HCl. The hydrocellulose was then filtered and washed with H_2O and 1% NH_4OH. The final product was freeze-dried and conditioned in a vacuum oven for 4 hours at 55°C
13	Whatman CF1 long fiber cellulose powder Hydrolyzed for 30 minutes in 4N HCl. The hydrocellulose was further prepared in the same manner as Sample 12

APPENDIX II

MOLARITIES AND MOLALITIES OF MERCERIZING SOLUTIONS

The molarities and molalities as well as the numbering code are given below for the lithium, sodium, and potassium hydroxide mercerizing solution.

Solution Code	Molarity	Molality
	LiOH	
1-Li	1.059	1.057
2-Li	2.083	2.080
4-Li	3.296	3.300
7-Li	3.732	3.739
8-Li	4.159	4.175
10-Li	4.882	4.914
9-Li	5.061	5.099
	NaOH	
1-Na	0.851	0.851
2-Na	1.795	1.796
3-Na	2.297	2.300
4-Na	2.793	2.808
5-Na	3.163	3.172
7-Na	3.644	3.664
8-Na	4.631	4.691
9-Na	5.228	5.624
10-Na	6.243	6.399
11-Na	7.771	8.120
12-Na	10.233	11.035
	KOH	
1-K	0.862	0.868
2-K	1.572	1.596
3-K	2.126	2.268
4-K	2.692	2.778
5-K	3.282	3.418
6-K	3.492	3.641
7-K	3.695	3.865
8-K	3.959	4.164
9-K	4.919	5.310
10-K	5.808	6.412
11-K	9.677	11.459

APPENDIX III

PREPARATION OF PRECIPITATED CELLULOSES FROM THE DMSO-PF SOLVENT SYSTEM

The purpose of this appendix is to supplement the Experimental section with details about the preparation of precipitated samples from the DMSO-PF solvent system.

SAMPLE 21 — AMORPHOUS CELLULOSE

One gram of cellulose (Whatman CF1) was dissolved in 50 ml DMSO with approximately 3 g of paraformaldehyde at a temperature of about 120°C. The solution was frozen and freeze-dried. After freeze drying the sample appeared fibrillar and horny. An x-ray diffractogram of the material, Fig. 41, indicated that it was quite amorphous at this stage. A fraction of this sample was placed in water at 20°C. The material degassed what was probably formaldehyde and lost its physical integrity. This fraction was frozen and freeze-dried. A diffractogram of this material is also included in Fig. 41.

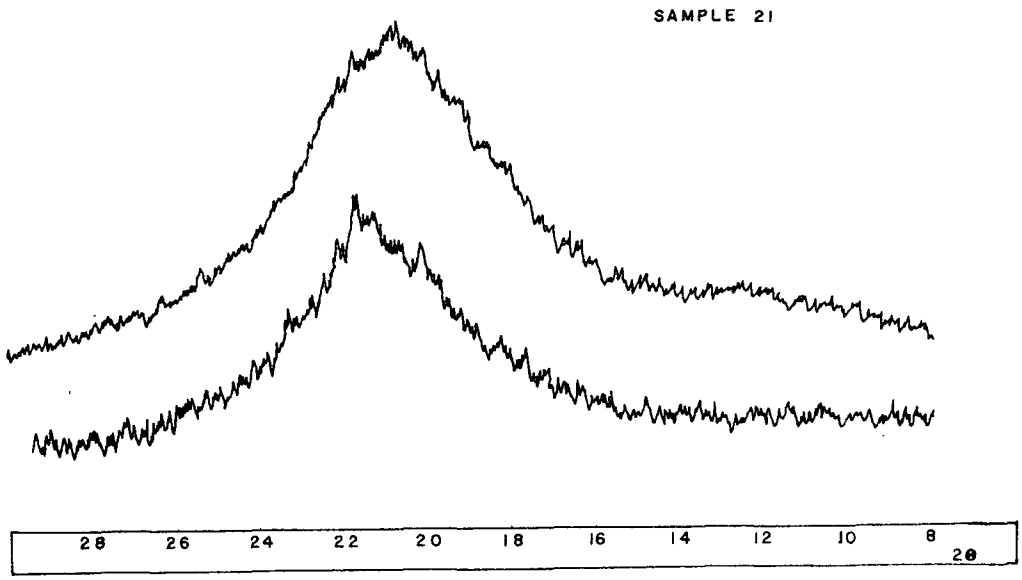

Figure 41. Top: X-Ray Diffractogram of Methylol Cellulose After Treatment with Water. Bottom: Before Treatment with Water

SAMPLE 22 — LOW CRYSTALLINITY CELLULOSE II

A low crystallinity cellulose II was needed as an x-ray standard; therefore, this sample was developed. Six g of cellulose (Whatman CF1) were dissolved in 600 ml of DMSO and enough paraformaldehyde to cause complete solubilization of the cellulose. Three hundred ml of the cellulose solution were precipitated in 500 ml of methanol, filtered, and subjected to 5.228M NaOH for 30 minutes at 20°C. The cellulose slurry was then diluted, neutralized with HCl, filtered, washed, and freeze-dried using the same procedures that were used for all the mercerized samples. Figure 42 includes a diffractogram of the material at this point. The crystallinity of the cellulose II was somewhat lower than anticipated; therefore, a portion of it was annealed in glycerine at 150°C for 3 days, as Atalla and Nagel had found that this type of procedure increases the degree of order of cellulose II samples (101). A diffractogram of this slightly improved

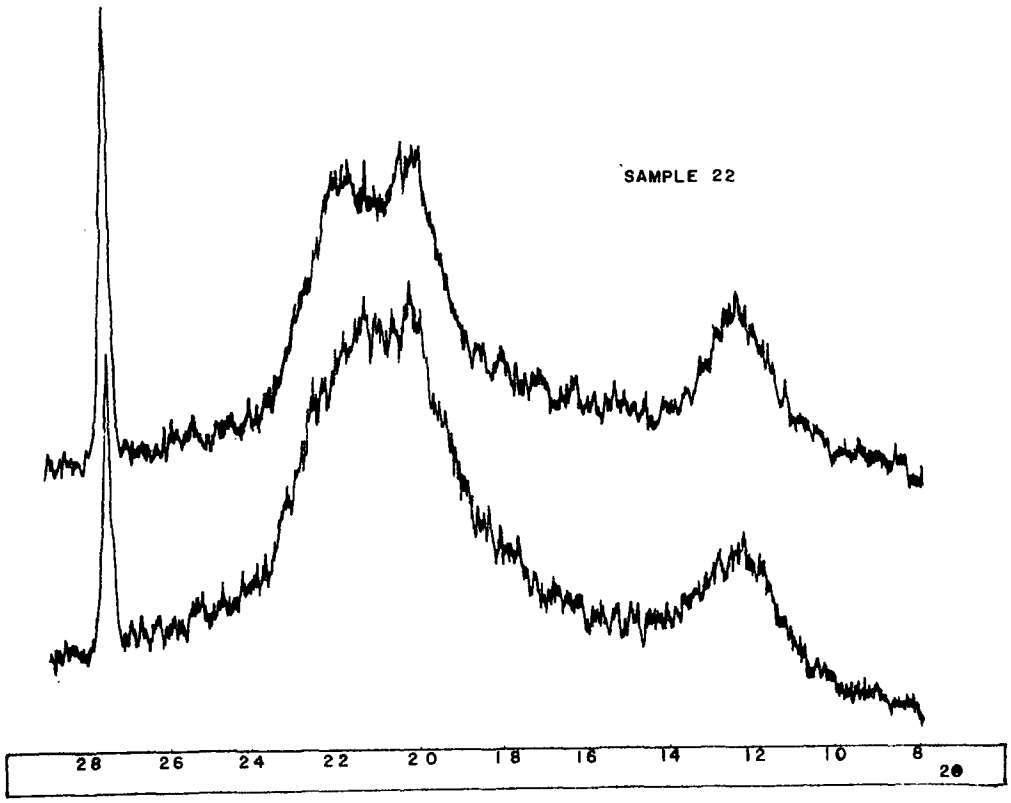

Figure 42. X-ray Diffractograms of Low Crystallinity Cellulose II. Top: Annealed. Bottom: Before Annealing

material is also shown in Fig. 42. This annealed cellulose II is still significantly less crystalline than the cellulose resulting from the standard mercerization procedure used in this work. This annealed material was referred to as 22-B.

SAMPLE 24 — HIGH CRYSTALLINITY CELLULOSE II

Freeze-dried, amorphous cellulose (Sample 21) was treated with 100 ml 5.228M NaOH for 3.5 hours at 20°C. The slurry was then transferred to a larger closed vessel and heated to 80°C under N_2. The slurry was then slowly diluted with 2000 ml of distilled water which had been pretreated with N_2 to remove dissolved O_2. The slurry was then filtered, washed, freeze-dried, and annealed with glycerine at 150°C for 5 days. Again the sample was filtered, washed, and freeze-dried. An x-ray diffractogram of the sample at this point indicated that there was an orientation effect due to the flaky character of the sample which had persisted from the original freeze drying from solution. The (101) plane was proportionately too intense. Therefore, the sample was hydrolyzed for 11 hours in 2.5N HCl in order to reduce it to a crystalline powder. The powder was filtered, washed, and freeze-dried. An x-ray diffractogram of this highly ordered material is shown in Fig. 43. The sample probably is not entirely cellulose II for the reasons discussed elsewhere. It was, therefore, not used as a cellulose II standard.

SAMPLE 28 — LOW TEMPERATURE PRECIPITATION

Three hundred ml of 1% cellulose-DMSO-PF solution were cooled to 0°C in a salted ice water bath. Two hundred ml of methanol were added in order to lower the freezing point of the solution sufficiently . The solution was slowly precipitated with 400 ml of water at 0°C. Gas evolved during the precipitation.

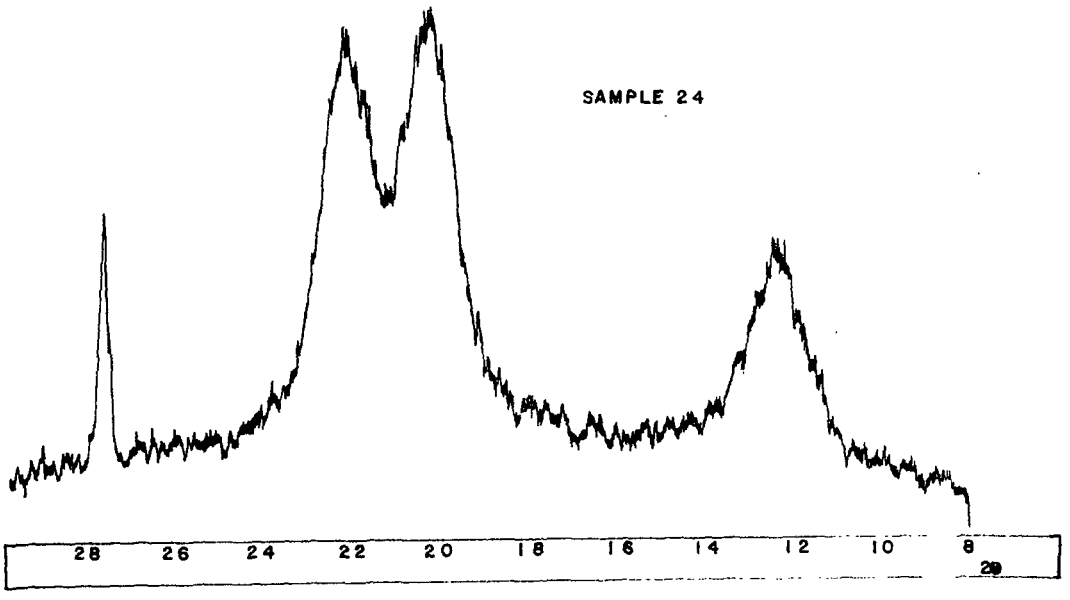

Figure 43. X-ray Diffractogram of a High Crystallinity Cellulose II

The resulting gelatinous mixture was dumped into 800 ml of water at 0°C and condensed through centrifugation. It was then washed and freeze-dried. Figure 44 shows two x-ray diffractograms of Sample 28. The top scan was run before the precipitate was annealed while the bottom scan was taken after the cellulose had been annealed for 2 weeks at 150°C in glycerine. The figure suggests that the annealing treatment did enhance the crystallinity.

SAMPLES 29, 30, AND 31 — ROOM TEMPERATURE PRECIPITATION

Samples 29, 30, and 31 were precipitated at room temperature (approximately 23°C) from 1% cellulose-DMSO-PF using different precipitating procedures. All three samples appeared to be amorphous which, when annealed for 2 weeks at 150°C in glycerine, assumed essentially the cellulose IV lattice. Figures 45, 46, and 47 are x-ray diffractograms of the samples. The top scans were taken before annealing while the bottom scans were taken after the annealing process. Since acid was used in the precipitating solutions, the possibility of cross-linking does exist (102).

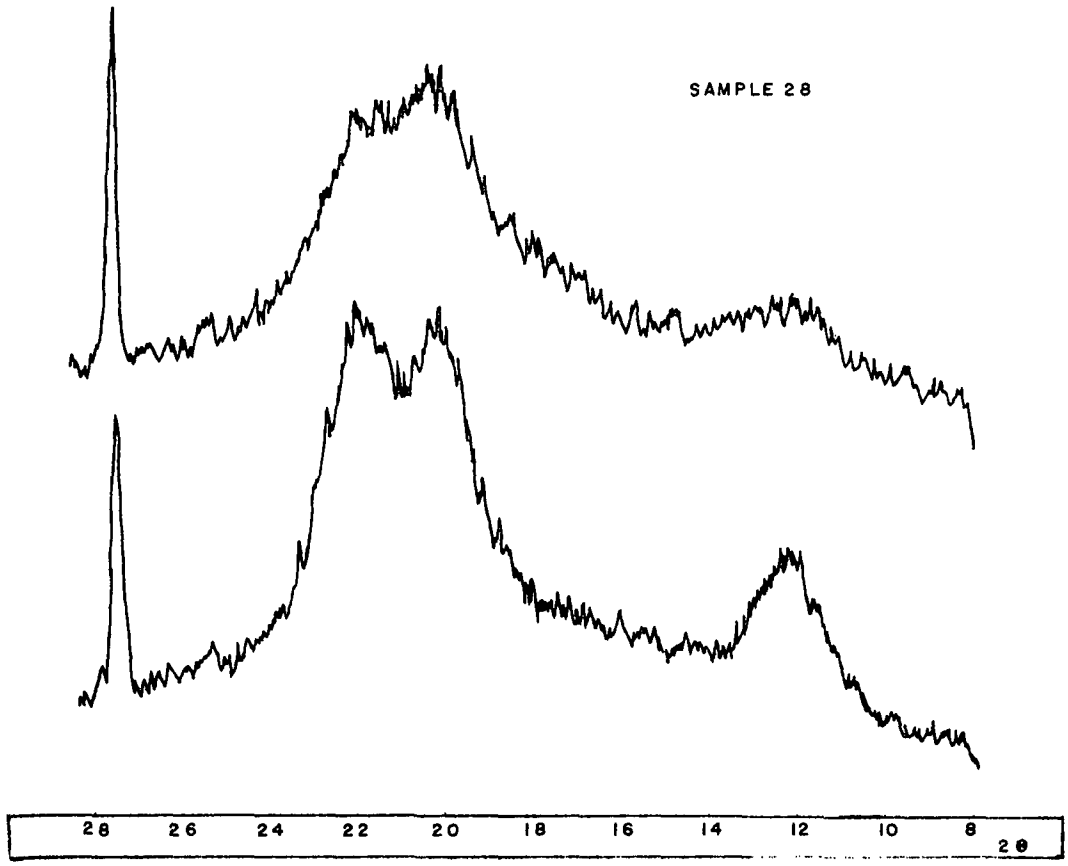

Figure 44. X-ray Diffractograms of a Low Temperature Precipitation. Top: Before Annealing. Bottom: After Annealing

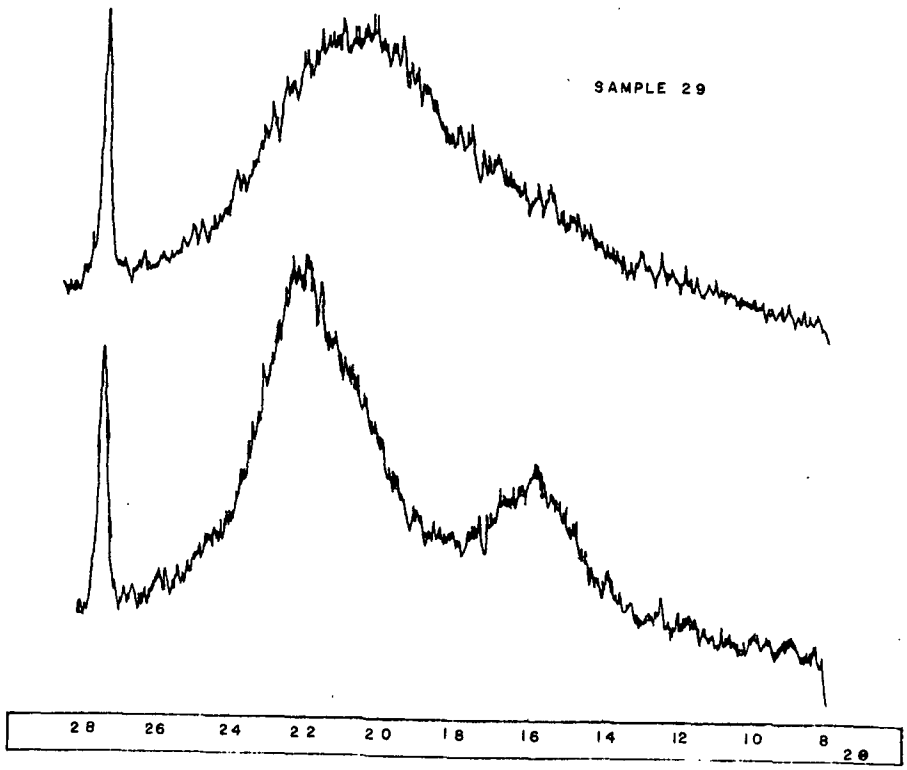

Figure 45. X-Ray Diffractograms of a Room Temperature Precipitation. Top: Before Annealing. Bottom: After Annealing

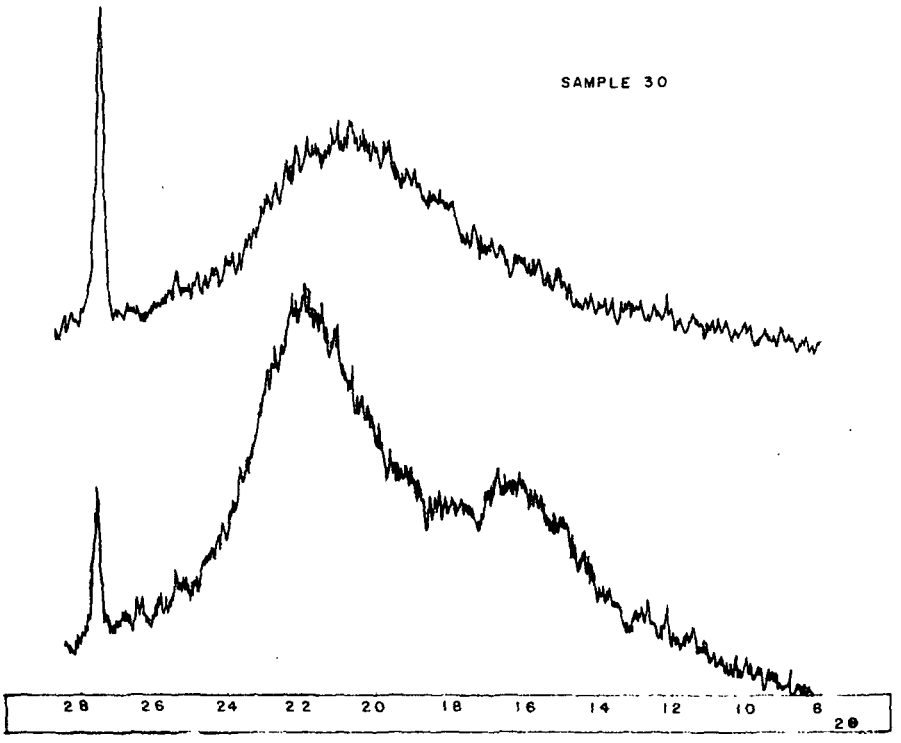

Figure 46. X-Ray Diffractograms of a Room Temperature Precipitation. Top: Before Annealing. Bottom: After Annealing

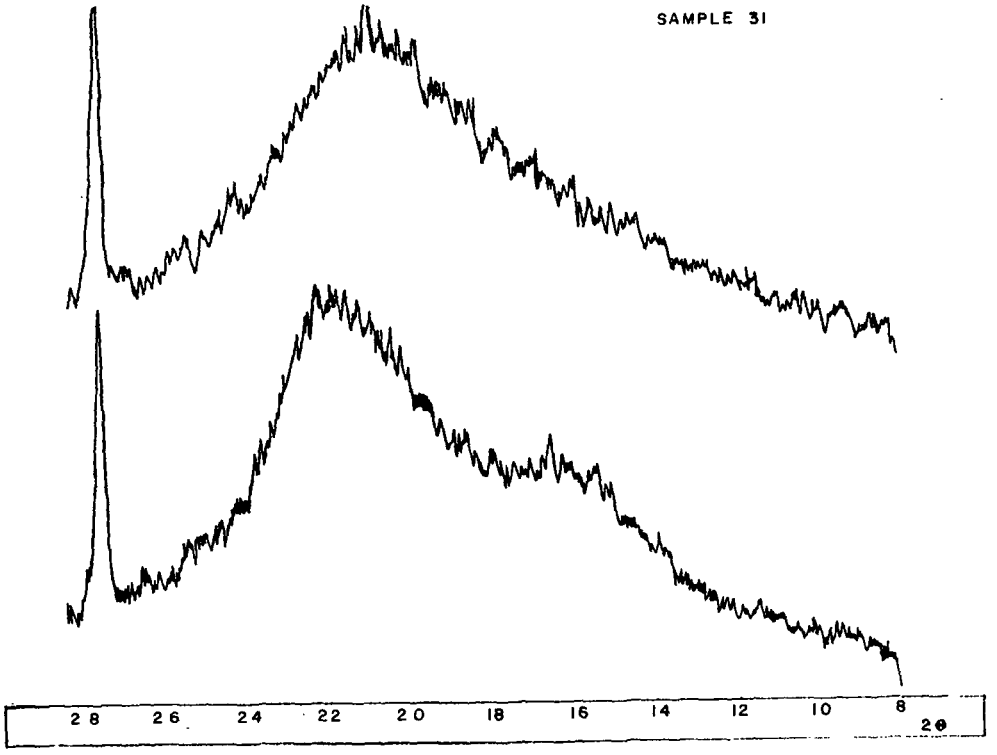

Figure 47. X-Ray Diffractograms of a Room Temperature Precipitation. Top: Before Annealing. Bottom: After Annealing

SAMPLE 29

To 200 ml of 1% solution were added 100 ml of water which failed to promote nucleation. Two ml of concentrated HCl were added which caused some nucleation. 2-Propanol was found to be somewhat effective in further promoting nucleation. To complete the precipitation, 600 ml of ethanol were added. The rather gelatinous precipitate was condensed with centrifugation and added to 800 ml of distilled water at 20° with stirring. The material was filtered, washed, freeze-dried, and a portion of it was annealed.

SAMPLE 30

To 200 ml of 1% cellulose-DMSO-PF solution were added 400 ml of a solution which was prepared from 600 ml of isopropanol, 40 ml of water and had a pH of 2 as adjusted with HCl. The gelatinous material was then worked up in a manner similar to Sample 29.

SAMPLE 31

To 200 ml of 1% cellulose-DMSO-PF solution were added 50 ml of a solution which had been prepared from 500 ml of isopropanol and 100 ml of concentrated HCl. This gelatinous precipitate was also worked up in a manner similar to Sample 29.

SAMPLE 32 — 80°C PRECIPITATION

Two hundred ml of 1% cellulose-DMSO-PF solution were heated to 80°C with stirring. The cellulose was precipitated with a solution prepared from 500 ml of isopropanol and 100 ml of concentrated HCl. After filtration the precipitate was kept at 80°C with stirring for approximately 6 hours in 800 ml of water. The sample was then washed, freeze-dried, and annealed for 2 weeks at 150°C in glycerine. A diffractogram of this sample is shown in Fig. 48.

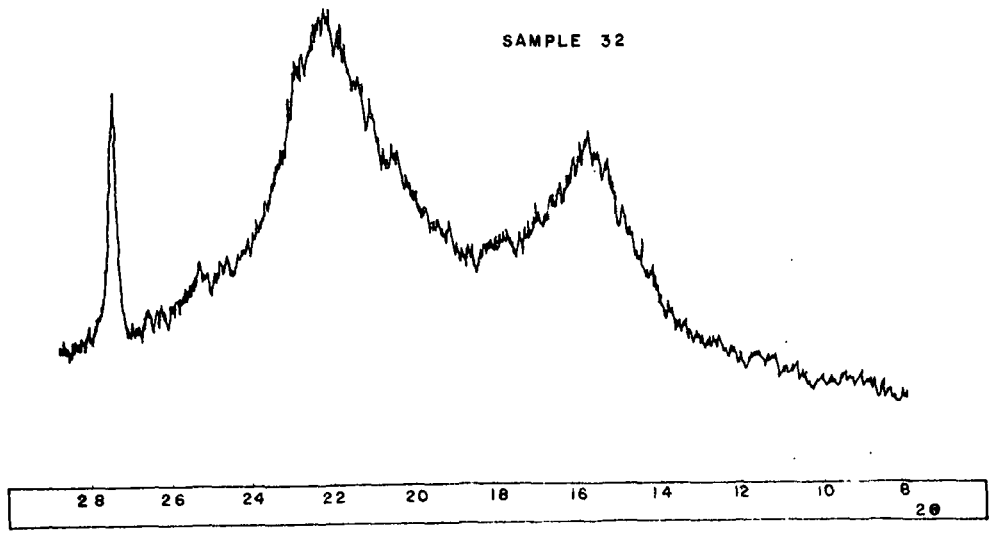

Figure 48. X-Ray Diffractogram of a Sample Precipitated at 80°C and Annealed

SAMPLE 33 — 135°C PRECIPITATION

Two hundred ml of 1% cellulose-DMSO-PF solution were heated to 135°C. Precipitation occurred due to the breakdown of the hemiacetal over a period of 2 hours. This sample was not annealed. Its highly crystalline, predominantly cellulose IV diffractogram is shown in Fig. 49.

SAMPLES 37, 38, 40-43 — HOMOGENEOUS PRECIPITATING CONDITIONS OVER A RANGE OF TEMPERATURES

These samples were all precipitated under approximately the same conditions with the only major variable being the temperature of precipitation. Unlike the previously discussed precipitated celluloses, these samples were produced by slowly dripping 3% cellulose-DMSO-PF solution into the precipitating media. The other samples had all been precipitated by adding the precipitating media to the cellulose solutions. This method produced better crystals and the temperature control was more accurate. The major criticism of this approach is that crystallization may have commenced as the drops of cellulose solution hit the precipitating solution before the cellulose chains came to the temperature of the

precipitating solution. The x-ray diffractograms and Raman spectra of these samples are not shown here; they are presented in the Results and Discussion section.

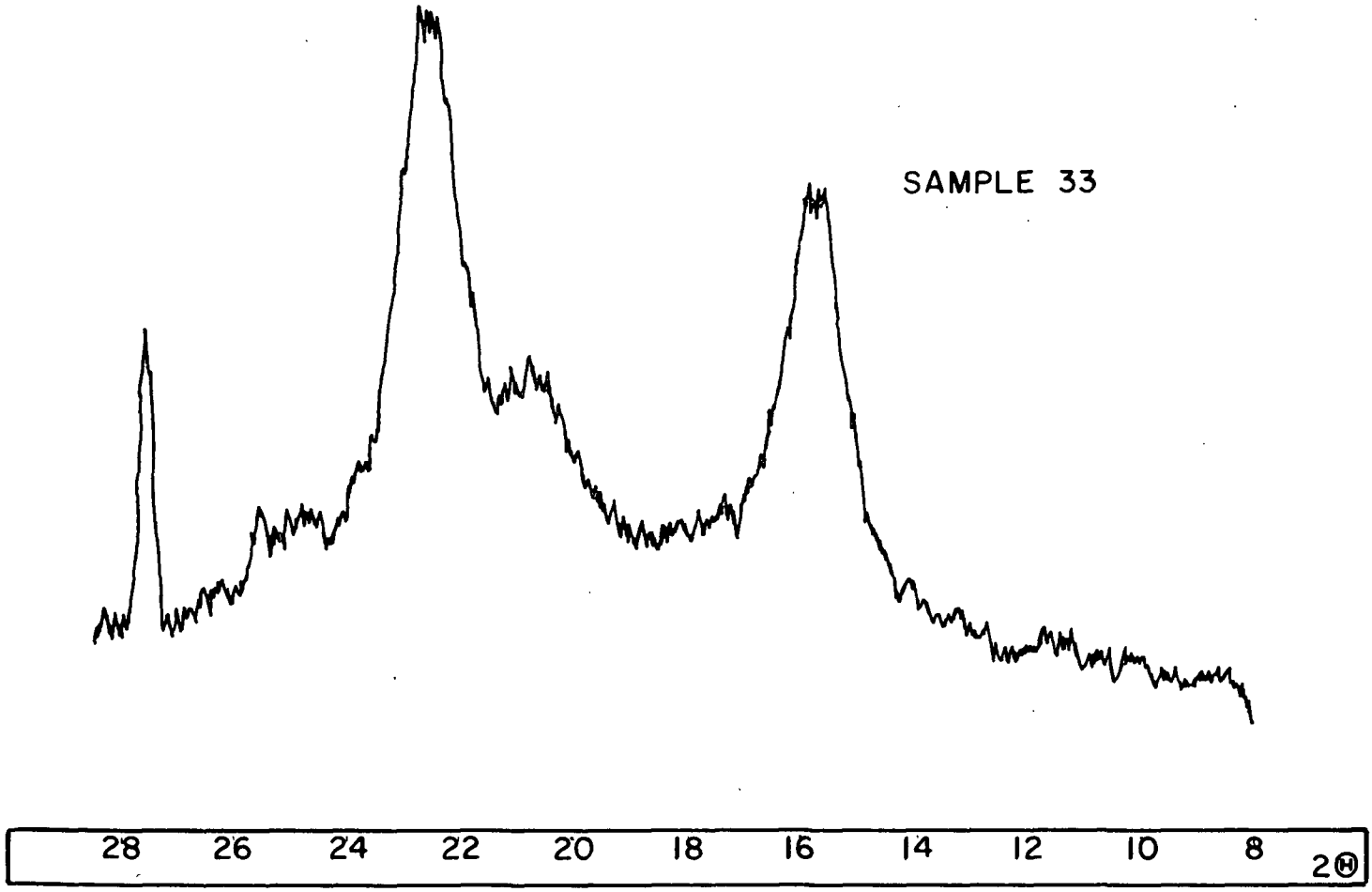

Figure 49. X-ray Diffractogram of a Sample Precipitated with Heat at 135°C

SAMPLE 37

Two hundred fifty ml of 3% cellulose solution were slowly dripped into a stirred precipitating solution made up of 1500 ml of water and 100 ml of methanol. The temperature was -2°C. The resulting crystals were washed and freeze-dried.

SAMPLE 38

Two hundred fifty ml of 3% cellulose were slowly dripped into 1500 ml of stirred water at 20°C. The crystalline precipitate was filtered, washed, and freeze-dried.

SAMPLE 40

Two hundred fifty ml of 3% cellulose solution were slowly dripped into glycerol at 165-170°C with agitation and under N_2 to preclude oxidation. The final slurry was quite discolored at the end of the 3 hours precipitation, but the crystals filtered easily on an M fritted glass filter and were washed without difficulty with hot water. Apparently, the discoloration was associated with the liquid phase entirely. The crystals were freeze-dried.

SAMPLE 41

Two hundred fifty ml of 3% cellulose solution slowly dripped into 600 ml of agitated water at 60°C under N_2. The cellulose crystals were filtered, washed, and freeze-dried.

SAMPLE 42

The temperature was 100°C. Everything else was the same as Sample 41.

SAMPLE 43

Two hundred ml of 3% cellulose solution were slowly added to 473 ml of glycerol and 50 ml of water at 127-130°C under N_2. The sample was worked up in the usual manner.

APPENDIX IV

X-RAY DIFFRACTOGRAMS OF THE LABORATORY STANDARDS

Figures 50, 51, and 52 contain the x-ray diffractograms of the laboratory standards. The pertinent x-ray parameters are reported in Table III.

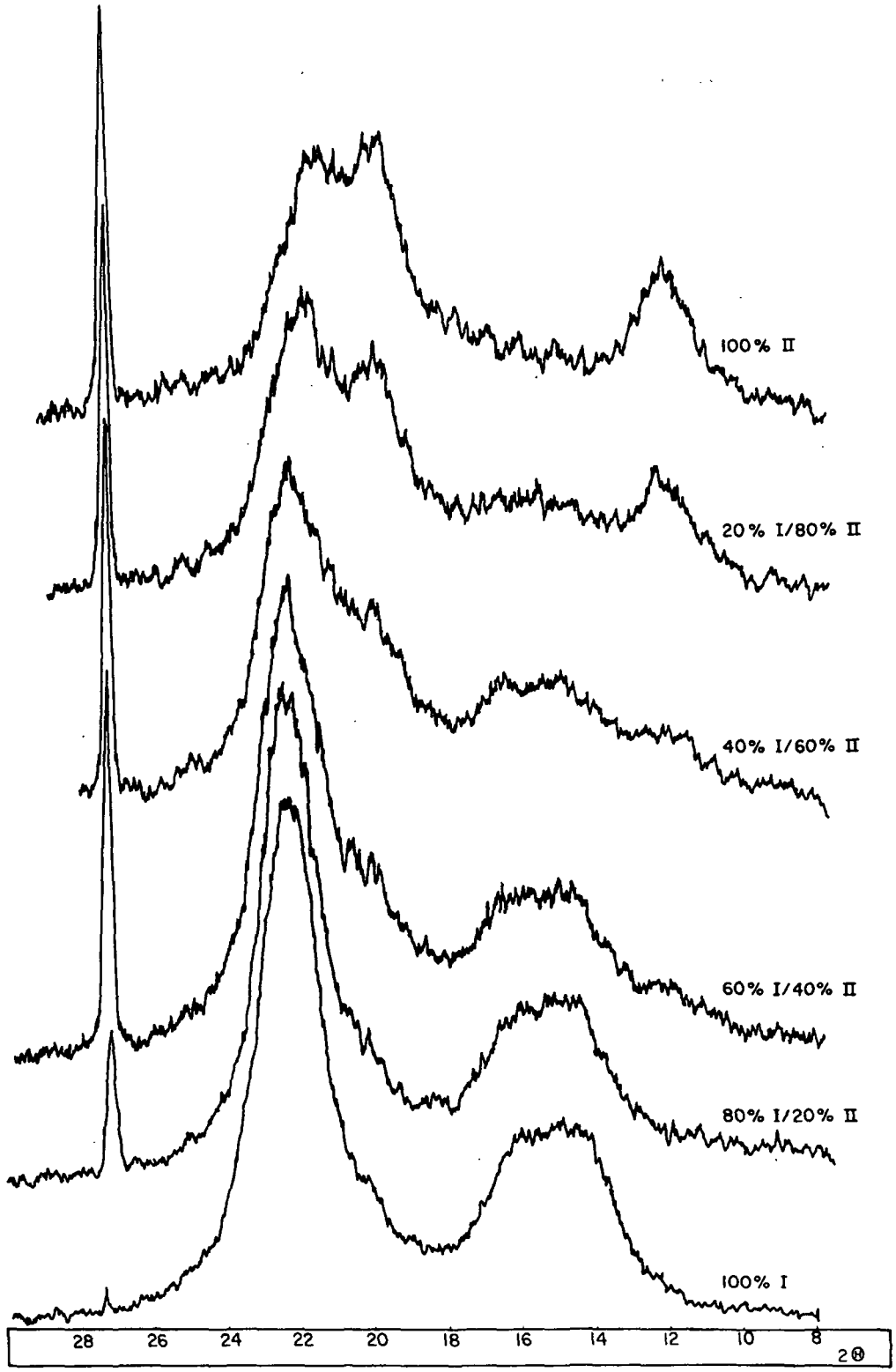

Figure 50. Laboratory Standards of Low Crystallinity Cellulose I and II

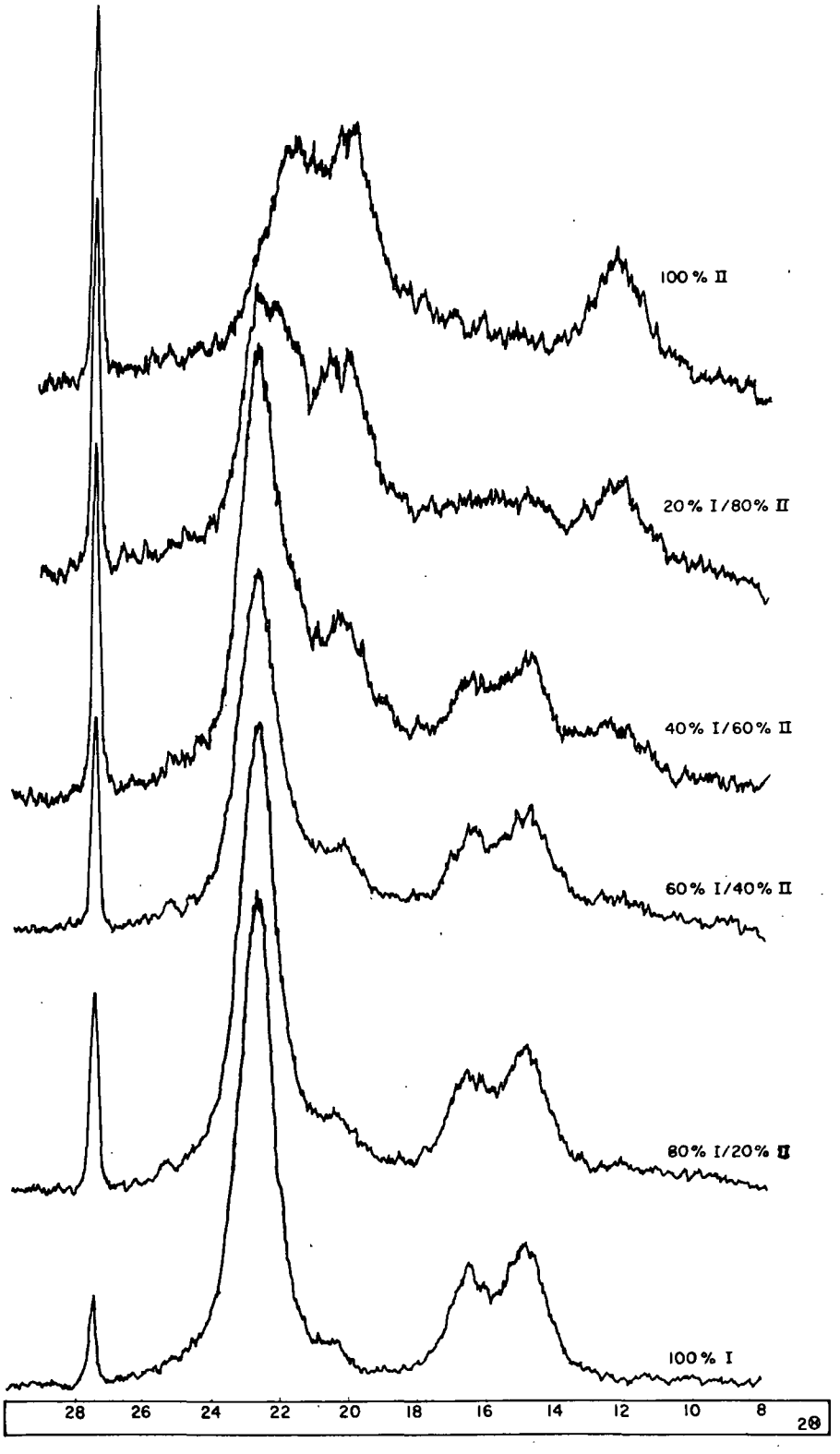

Figure 51. Laboratory Standards of High Crystallinity Cellulose I and Low Crystallinity Cellulose II

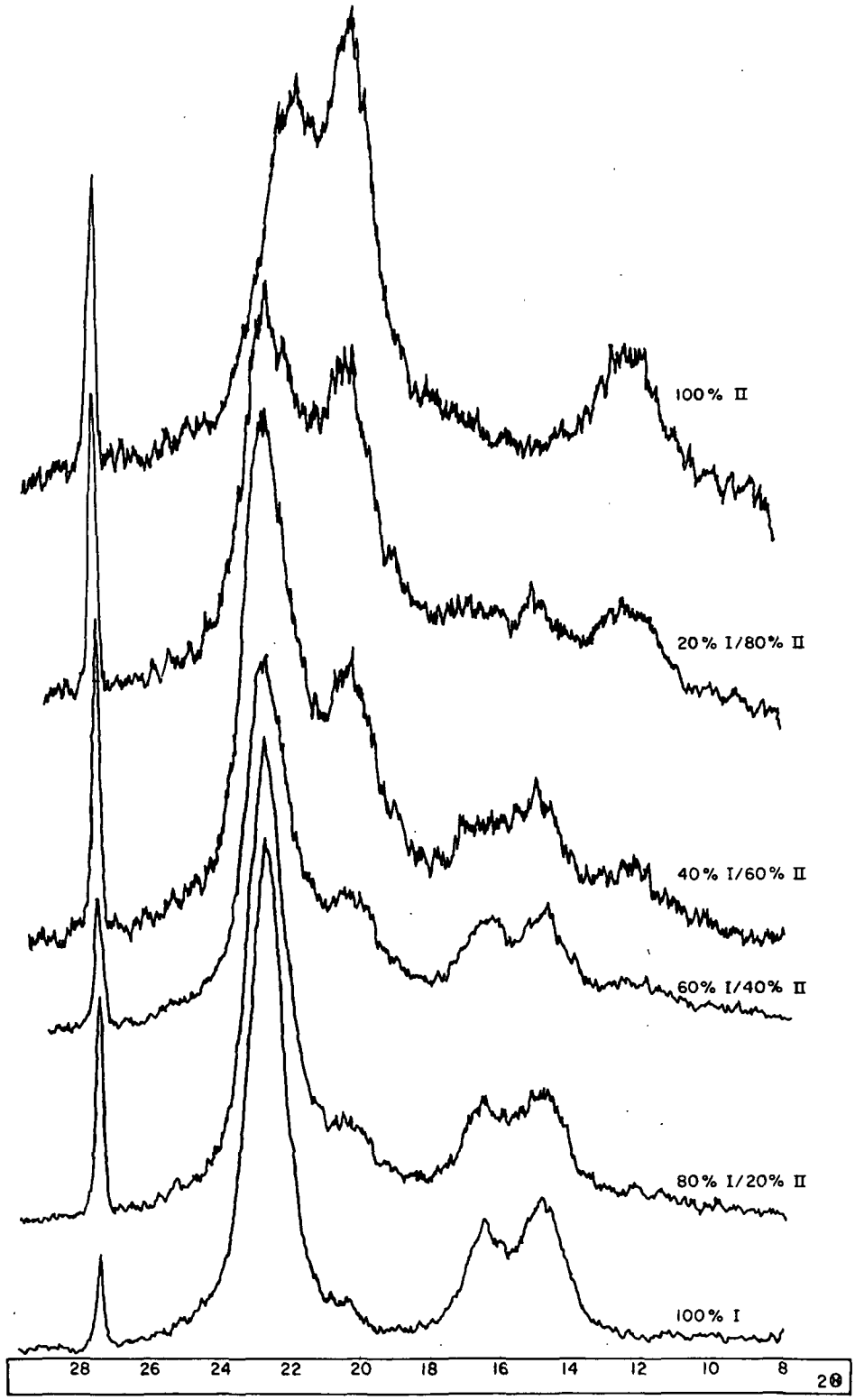

Figure 52. Laboratory Standards of High Crystallinity Cellulose I and II

APPENDIX V

PROGRAM BAND — A COMPUTER PROGRAM TO RESOLVE OVERLAPPING BANDS USING A NONLINEAR LEAST-SQUARES PROCEDURE

INTRODUCTION

There are many areas of analytical chemistry in which one is interested in band heights, widths at half height, and peak locations. Also, the integrated intensities are often of value when one is involved in areas such as chromatography and analytical Raman spectroscopy.

Quite often the bands of interest are overlapped. Approximate procedures for separating bands are generally quite unreliable.

There are now available various sophisticated methods for resolving overlapping bands. The computer program described here is among them. This program can resolve bands even when the overlap is quite extensive.

THEORY

Consider a series of bands as drawn by a chart recorder. For this program the experimental data would consist of $\underline{N}$ observations which would be the intensity values as a function of $\underline{x}$ ($\underline{x}$ being wavelength, time, or some other linear function). Thus we would have:

$$Y_1, Y_2, \ldots Y_i \ldots Y_n \text{ where } Y_i = Y(X_i),$$

which are to be fitted to a function

$$F(X, P_1, \ldots, P_m), \tag{46}$$

where $\underline{P}_1, \ldots, \underline{P}_m$ are the M parameters defining the component bands and the base line. A Gaussian or Cauchy function can be described by three parameters: the

height, the peak center or location, and the band width at half height. The best fit is obtained when the following function is minimized.

$$S = \sum_{i=1}^{N} W_i(F_i - Y_i)^2 \tag{47}$$

W_i is a weighting function whose value is generally 1 and:

$$F_i = F(X_i, P_1, \ldots, P_m) \tag{48}$$

F is not a linear function of the M parameters. Therefore, optimum values of the M parameters, $P_1, \ldots, P_m$, cannot readily be calculated from Equation (47). However, if approximate values $P_1', \ldots, P_m'$ can be "guessed," F_i can be taken as a linear function of the adjustments to the true parameters, $P_j = P_j - P_j'$ ($j=1, \ldots, M$) required to optimize the parameters. A Taylor's expansion is used and second order and higher terms are neglected.

$$F_i = F_i' + \sum_{j=1}^{m} (\alpha F_i/\alpha P_j)' \, \Delta P_j \quad (i=1, \ldots, N) \tag{49}$$

The prime here and throughout this derivation means that the primed function is to be evaluated for the approximate values of the parameters $P_1', \ldots, P_m'$.

The condition that S in Equation (47) is a minimum requires $\delta S = 0$ and together with Equation (49) a set of M simultaneous equations is obtained for the required parameter adjustments.

$$\sum_{j=1}^{N} \Delta P_j \sum_{i=1}^{N} W_i(\alpha F_i/\alpha P_j)' \, (\alpha F_i/\alpha P_k)' =$$

$$\sum_{i=1}^{N} W_i(Y_i - F_i') \, (\alpha F_i/\alpha P_k)' \quad (k=1, \ldots, M) \tag{50}$$

The function F in Equation (46) may be expressed in the form

$$F = \sum_{i=1}^{N} A_i + B \tag{51}$$

where $\underline{A}_1$, ..., $\underline{A}_N$ are functions, such as Gaussian or Cauchy functions or a linear combination of the two, each of which generates a single bank and $\underline{B}$ generates the base line.

The form of the Gaussian function in which the three aforementioned parameters are used is:

$$A_i = P_{3i-3} \exp\{-\ln 2[2(X-P_{3i-2})/P_{3i-1}]^2\} \tag{52}$$

P_{3i-3} = peak height

P_{3i-2} = peak center

P_{3i-1} = band width at half height

And similarly, the form of a Cauchy function is:

$$A_i = P_{3i-3}/\{1 + [2(X-P_{3i-2})/P_{3i-1}]^2\} \tag{53}$$

In this program the bands are assumed to be a linear combination of the Cauchy and Gaussian functions. The percentage of each is one of the variables that is solved for. The area beneath one of these composite bands is given by Equation (54).

$$A = \frac{1}{2} P_{3i-3} P_{3i-1} \{P_1(\pi/\ln 2)^{1/2} + (1-P_1)\pi\} \tag{54}$$

P_1 = function parameter $0 \leq P_1 \leq 1$

0 yields 100% Cauchy

1 yields 100% Gaussian

Using the values of the trial parameters $\underline{P}_1'$, ..., $\underline{P}_m'$, the coefficients

$$\sum_{i=1}^{N} (\alpha F_i/\alpha P_j)' (\alpha F_i/\alpha P_k)'$$

of the $\underline{\Delta P}_j$'s are calculated. The constant term

$$\sum_{i=1}^{N} (Y_i - F_i') (\alpha F_i / \alpha P_k)',$$

in Equation (50), can be computed for each of the M equations and the values of the ΔP_j's are solved for by matrix inversion. An MXM symmetric matrix is produced. Since it is symmetric only a triangular matrix is created and inverted. Thus almost half the core space is saved which can be important if the program is expanded beyond its present dimensions.

The solution cannot be found after only one iteration. In fact, if the initial "guess" parameters were poor approximations, it may take hundreds of cycles before the solution is found. Each iteration uses the adjusted parameters as its new set of trial parameters.

In many cases the least-squares procedure must be damped. Otherwise the solutions will tend to diverge instead of converge. In this method the parameter adjustments are introduced as extra terms in Equation (47) giving:

$$S' = \sum_{i=1}^{N} W_i (F_i - Y_i)^2 + d^2 \sum_{j=1}^{M} C_j (P_j - P_j')^2 \qquad (55)$$

The only casualty of damping the least-squares procedure is that it converges more slowly the bigger the damping factor.

Another design feature of the program is that certain parameters may be fixed. If they are fixed they are removed from the least-squares refinement. Therefore, their values are not altered. This is an especially attractive feature as will become apparent.

This theoretical discussion closely parallels the two papers on the subject by Fraser and Suzuki (79,80).

OPERATION OF THE PROGRAM AND DATA PREPARATION

The program has been written so that it will run on an IBM 360 under RAX, but if the dimensions are expanded very much it will have to be run on OS.

The best way to handle the data is to store it on library disk so that it can be easily updated. The data form which immediately follows this section can be used in the proper preparation and formulating of the data. The following data description should also be of assistance.

1. Record 1. A one card alphanumeric heading. This is the title of the data set and will also appear as the heading on the graph.

2. Record 2. One card with the x and y axis labels. These labels are for the plot. This card must be included even if a plot is not desired.

3. Record 3. This card holds three numbers: N is the number of observations or data points from the spectrum, X(1) is the initial X value, and DX is the increment for X. The X values are generated within the program using this information.

4. Record 4. This is a series of cards which read in the N observation. The N observations could be hand calculated from the spectra, chromatogram, etc., but a far more satisfactory method is to have the raw spectra reduced photographically. The negative can then be used in conjunction with the microcomparator which is cabled to an IBM key punch. A special format board was constructed with 16F5 format just for this purpose. Only y values are recorded. The spectra should be reduced so that they are no more than 2 inches high in the y direction or more than 4 inches in the x direction. The spectra should be marked prior to photo reduction at each point where a data point will be taken.

5. Record 5. If a graph of the component bands enclosed in the band envelope is desired, the value is 1, otherwise 0. The plotting subroutine GRAFC will have to be updated slightly for different x and y axis demarcation. Also this card must have an integer 1 if the base line is flat or a zero if it is sloped.

6. Record 6. Three numbers are contained here. The first is the number of parameters, M, which equals (3 x number of bands +3). The second is the number of cycles of refinement desired, and the third is the damping factor. The proper value of the damping factor for a given situation can only be determined by experimentation. Values have ranged from 0 to 50 have been used, depending upon the circumstances.

7. Record 7. The function parameter, $0 \leq f \leq 1$. Since this is simple a guess and the true function parameter will be found by the computer, a good place to start would be 1.0 for IR spectra, Raman spectra, and gas chromatography. For x-ray powder patterns of semicrystalline polymers a good guess might be 0.7. A function parameter of 1 signifies that the band is 100% Gaussian, while a value of 0 indicates that the band is 100% Cauchy.

8. Records 8-12. These cards contain the initial guess parameters for each of the bands, the peak heights, peak centers, and peak widths at half height. Each card has the three values for a single peak. The cards must be in the following order:

$P_2 = I_{max}$(band 1) P_3 = center (band 1) P_4 = width (band 1)
$P_5 = I_{max}$(band 2) P_6 = center (band 2) P_7 = width (band 2)

.
.
.

P_{m-4} = I_{max}(last band) P_{m-3} = center (last band) P_{m-2} = width (last band)

9. Record 13. The values of the base line at X(1) and X(N) are entered here. The base line is described by these two parameters, thus we have

   P_{m-1} = base line at X(1) and P_m = base line at X(N)

10. Records 14-21. The next series of cards contains zeros and ones for the M parameters in the same order as the M parameters. A zero signifies that the parameter is to be adjusted by the computer program while a one means that the parameter is not to be tampered with.

HINTS ON HOW TO MAKE THE PROGRAM WORK

If the band overlap is not too serious and the initial "guess" parameters are fairly accurate, the program will generally converge on a solution in about 10 or 20 cycles. But if the bands overlap badly, the initial guess parameters will naturally be poor. Under these circumstances the program may diverge or the matrix inversion routing will fail because the matrix is singular. In this case the program will print SINGULAR MATRIX, and stop.

If there is a good chance that the initial guess parameters for a certain peak are poor, and this is causing the program to fail, fix all the parameters which represent good estimates and let the program work on just a few parameters. After the program has refined these parameters as much as it can under the constrained circumstances, substitute the refined values for your initial guess parameters in the data set. Next fix those parameters which were previously refined and unleash several other parameters and repeat the process.

After each cycle the program prints out the standard deviation and CV, an empirical statistical parameter. Thus one has a record of the rate of convergence

or divergence as the case may be. In the case of extensive overlapping of peaks it is a good idea to use a large damping factor; 50 seems to work well.

PROGRAM BAND — DATA FORM

Record	Definition	Format
1	A one card alphanumeric heading	(20A4)
2	One card with the x and y axis labels. Each label is allotted 12 alphanumeric characters _WAVELENGTH INTENSITY (example)	(20A4)
3	N = number of observations, X(1)= the initial X value, DX = the increment for X	(I3,2F10.0)
4	A series of cards reading in the N observations y	(16F5.3)
5	Graph of final data 1, No Graph 0 Flat Base line 1 Not Flat 0	(2I1)
6	Number of Parameters Number of Cycles of Refinement Damping Factor	(I2,I4,F10.0)
7	P_1; Function Parameter $0 \leq f \leq 1$	(F10.0)
8	Parameters for PEAK one $P_2 = I_{max}$, P_3 = BAND Center, P_4 = width at half height	(3F10.0)
9	Peak Two P_5 P_6 P_7	(3F10.0)
10	Peak Three P_8 P_9 P_{10}	(3F10.0)
11	Peak Four P_{11} P_{12} P_{13}	(3F10.0)
12	Peak Five P_{14} P_{15} P_{16}	(3F10.0)
13	P_{17} = BASELINE at X(1) P_{18} = BASELINE at X(N)	(3F10.0)

Record	Definition			Format
14	If the above parameters are fixed 1. No fix; 0; for P_1			(I1)
15	P_2	P_3	P_4	(3I1)
16	P_5	P_6	P_7	(3I1)
17	P_8	P_9	P_{10}	(3I1)
18	P_{11}	P_{12}	P_{13}	(3I1)
19	P_{14}	P_{15}	P_{16}	(3I1)
20	P_{17}	P_{18}		(3I1)

PROGRAM BAND FLOW DIAGRAM

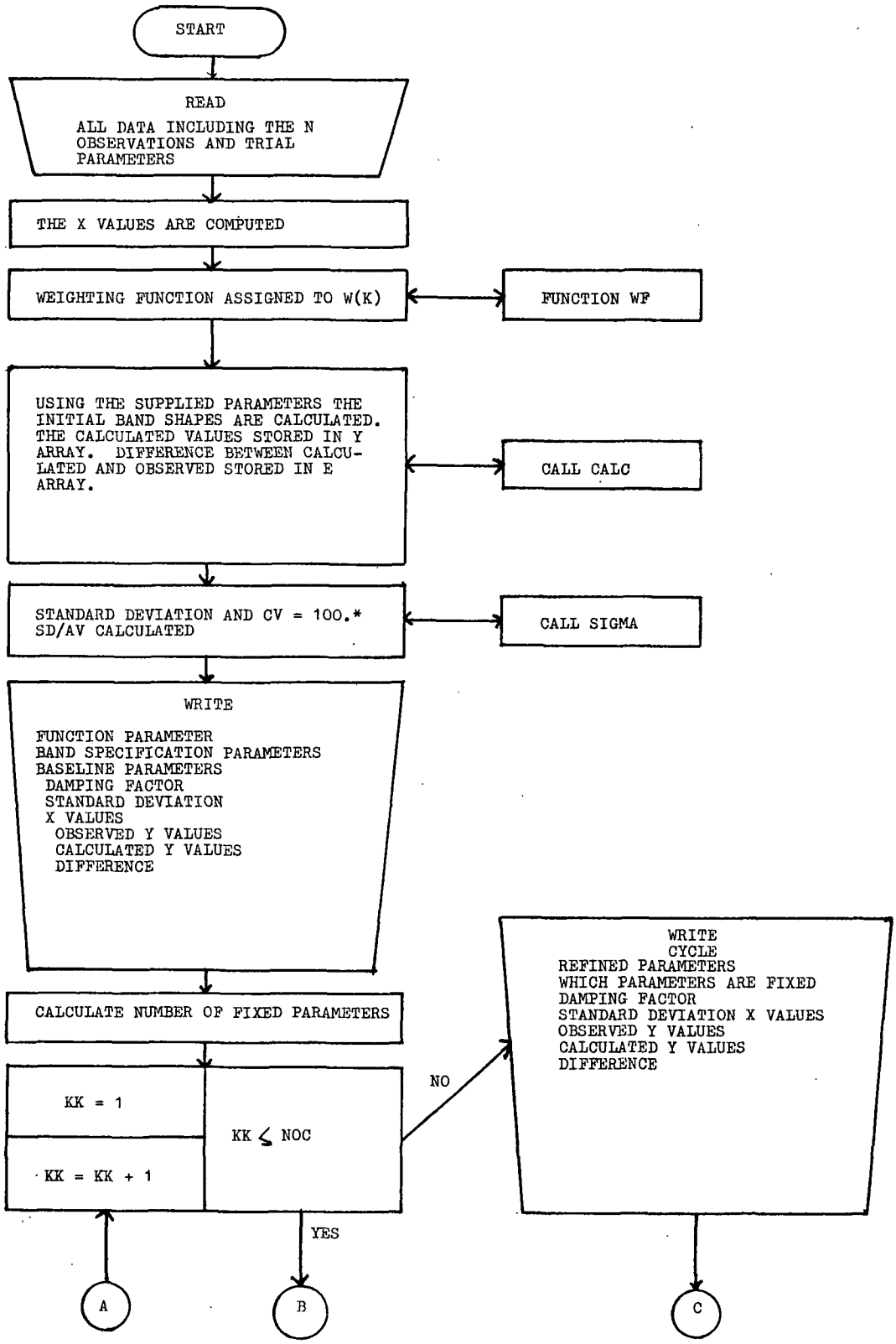

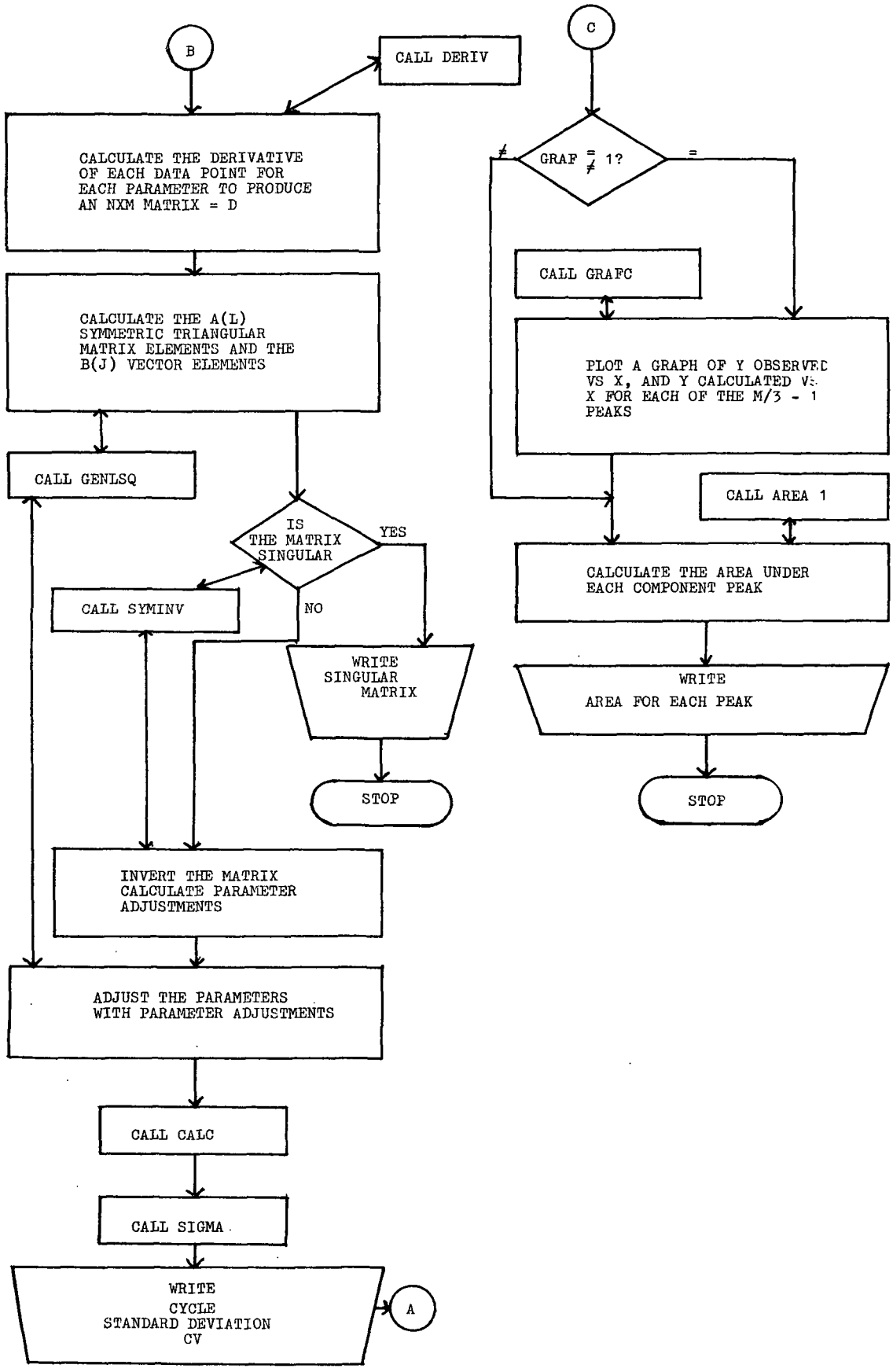
B
CALL DERIV
CALCULATE THE DERIVATIVE OF EACH DATA POINT FOR EACH PARAMETER TO PRODUCE AN NXM MATRIX = D
CALCULATE THE A(L) SYMMETRIC TRIANGULAR MATRIX ELEMENTS AND THE B(J) VECTOR ELEMENTS
CALL GENLSQ
IS THE MATRIX SINGULAR
YES
NO
CALL SYMINV
WRITE SINGULAR MATRIX
STOP
INVERT THE MATRIX CALCULATE PARAMETER ADJUSTMENTS
ADJUST THE PARAMETERS WITH PARAMETER ADJUSTMENTS
CALL CALC
CALL SIGMA
WRITE CYCLE STANDARD DEVIATION CV
A
C
GRAF = 1?
≠
=
CALL GRAFC
PLOT A GRAPH OF Y OBSERVED VS X, AND Y CALCULATED VS X FOR EACH OF THE M/3 - 1 PEAKS
CALL AREA 1
CALCULATE THE AREA UNDER EACH COMPONENT PEAK
WRITE AREA FOR EACH PEAK
STOP

```
C       PROGRAM BAND
C      A LEAST SQUARES FIT OF UP TO  5 (1-P)*CAUCHY + P*GAUSS FUNCTIONS
C      AND A LINEAR BASELINE. THE ORIGINAL PROGRAM WAS WRITTEN BY FRASER
C      AND SUZUKI AND WAS ADAPTED BY DIMICK TO RUN ON AN IBM 360 UNDER
C      RAX
C*************************************************************************
C      DEFINITION OF VARIABLES AND ARRAYS
C      HEAD = ALPHANUMERIC HEADING LIMIT 80 CHARACTERS
C      IX = X AXIS CAPTION FOR THE GRAPH, 12 CHARACTERS
C      IY = Y AXIS CAPTION FOR THE GRAPH, 12 CHARACTERS
C      N =   NUMBER OF EXPERIMENTAL OBSERVATIONS
C      X(1) =    INITIAL X VALUE
C      DX  =    THE INCREMENT USED FOR X, THE X VALUES ARE GENERATED
C      INTERNALLY
C      O   =  ARRAY IN WHICH THE RAW Y DATA , THE N OBSERVATIONS, ARE STORED
C      GRAF =    INTEGER, 1 IF A PLOT IS DESIRED, 0 NO PLOT
C      FLAT = INTEGER, 1 IF THE BASELINE IS FLAT, 0 NOT FLAT
C        M = NUMBER OF PARAMETERS DEFINING THE M/3 - 1 PEAKS
C        NOC = NUMBER OF CYCLES OF REFINEMENT TYPICALLY ABOUR 20
C        DF =  DAMPING FACTOR VALUES BETWEEN 0 AND 100. FOR BADLY
C        OVERLAPPED PEAKS IN WHICH THE PROGRAM DIVERGES INSTEAD OF
C        CONVERGING IT IS SUGGESTED THAT A DF OF ABOUT 50 BE USED
C        T = ARRAY STORING THE PARAMETERS M
C        IG = ARRAY HOLDING 1 OR 0 FOR EACH PARAMETER  1 FOR FIXED
C        PARAMETERS 0 OTHERWISE
C
C
C
C
S.0001          DIMENSION X(170), Y(170), W(170), C(170), E(170), D(170,20),
               1T(18), WO(10), IG(20), HEAD(20),B(20),IX(3), IY(3)
S.0002          INTEGER GRAF, FLAT
S.0003          COMMON DUMMY(820),D
C      READ IN THE HEADING AND PRINT IT OUT ALSO READ IN X AND Y AXIS CAPTIONS
C      FOR THE PLOT
```

```
S.0004          IRR=0
S.0005          READ (5, 301) HEAD
S.0006          READ (5, 301) IX,IY
S.0007    301   FORMAT (20A4)
S.0008          WRITE (6, 302) HEAD
S.0009    302   FORMAT(1H1, 20A4)
          C     READ IN NUMBER OF OBSERVATIONS, STARTING X VALUE AND INCREMENT OF X
S.0010          READ (5, 303) N,X(1),DX
S.0011    303   FORMAT (I3, 2F10.0)
          C     READ IN THE N OBSERVED Y VALUES AND PUT THEM IN ARRAY O
S.0012          READ (5, 304) (O(I), I = 1, N)
S.0013    304   FORMAT(16F5.3)
          C     DETERMINE WHETHER A PLOT IS DESIRED AND WHETHER THE BASELINE
          C     IS FLAT. NEXT THE NUMBER OF PARAMETERS, CYCLES OF REFINEMENT
          C     DAMPING FACTOR
S.0014          GRAF = 0
S.0015          FLAT = 0
S.0016          DF = 0
S.0017          READ (5, 305) GRAF,FLAT
S.0018    305   FORMAT (2I1)
S.0019          READ (5, 306) M,NOC,DF
S.0020    306   FORMAT (I2,I4,F10.0)
          C     THE M PARAMETERS ARE NOW STORED IN THE ARRAY T. THE ARRAY
          C     IG HOLD 1 FOR FIXED PARAMETERS, 0 OTHERWISE. THE FIRST
          C     PARAMETER READ IN IS THE FUNCTION PARAMETER
S.0021          READ (5, 307) T(1)
S.0022    307   FORMAT (F10.0)
S.0023          DO 181 I = 1, M
S.0024    181   IG(I) = 0
S.0025          MM = M
S.0026          READ (5, 308) (T(I), I = 2, MM)
S.0027    308   FORMAT (3F10.0)
S.0028          READ (5, 309) IG(1)
S.0029    309   FORMAT (I1)
S.0030          READ (5, 310) (IG(I), I = 2, MM)
S.0031    310   FORMAT (3I1)
          C     THE X VALUES ARE COMPUTED
S.0032    205   DO 25 K = 1, N
S.0033     25   X(K) = X(1) + DX*FLOAT(K - 1)
S.0034          DO 26 K = 1, N
S.0035     26   W(K) = WF(X, O, K, N)
S.0036          CALL CALC(Y, X, T, N, M, O, E, FLAT)
S.0037          CALL SIGMA(SD, CV, O, Y, N, W)
S.0038          MM = M - 2
S.0039          WRITE (6,103) T(1)
S.0040          WRITE (6,111) (T(I), I = 2, MM)
S.0041          MM = M - 1
S.0042          WRITE (6, 109) (T(I), I = MM, M),DF
S.0043          WRITE (6, 104) SD,(X(I),O(I),Y(I),E(I),I = 1,N)
S.0044          NOG = 0
S.0045          DO 263 I = 1, M
S.0046    263   NOG = NOG + IG(I)
S.0047          IF (FLAT) 265,265,264
S.0048    264   NOG = NOG + 1
S.0049    265   CONTINUE
S.0050          DO 29 KK = 1, NOC
S.0051          CALL DERIV(X, T, N, M, FLAT)
S.0052    274   CALL GENLSQ(O, Y, N, T, M, IG ,    NOG, W, DF, IRR)
S.0053          IF (IRR) 51,51,50
S.0054     50   GO TO 325
S.0055    51    CALL CALC(Y, X, T, N, M, O, E, FLAT)
S.0056          CALL SIGMA(SD, CV, O, Y, N, W)
S.0057    29    WRITE (6, 110) KK,SD,CV
S.0058          MM = M - 2
S.0059          WRITE (6, 105) NOC,T(1)
S.0060          WRITE (6, 111) (T(I), I = 2, MM)
```

```
S.0061              IF (NOG) 397,397,396
S.0062      396     WRITE (6, 113)
S.0063              DO 400 I = 1, M
S.0064              IF (IG(I)) 398,400,398
S.0065      398     WRITE(6, 117) I
S.0066      400     CONTINUE
S.0067      397     IF (FLAT) 403,403,402
S.0068      402     WRITE (6, 112)
S.0069      403     WRITE (6, 109) T(M -1),T(M),DF
S.0070              WRITE (6, 106) SD,(X(I),O(I),Y(I),E(I), I = 1, N)
S.0071              IF (GRAF) 291,291,290
S.0072      290     CALL GRAFC(X, O, T, HEAD, IX, IY, M, N)
S.0073      291     WRITE (6, 114)
S.0074              CALL AREA1(M, T)
S.0075      103     FORMAT (19H INITIAL PARAMETERS//1H F10.3)
S.0076      104     FORMAT (//19H INITIAL DATA    SD=F10.7///1H 4X, 1HX9X, 2HYO8X,
                   12HYC8X, 1HE/(1H F10.3, 3F10.5))
S.0077      105     FORMAT (1H , 25H1REFINED PARAMETERS CYCLEI3//
                   124H      FUNCTION PARAMETER=F7.3)
S.0078      106     FORMAT (//19H REFINED DATA    SD=F10.7///1H , 4X,
                   11HX9X, 2HYO8X, 2HYC8X, 1HE/(1H , F10.3, 3F10.5))
S.0079      109     FORMAT (/21H BASE LINE INTERCEPTS2F10.3, 5H  DF=F10.3)
S.0080      110     FORMAT(/6H CYCLEI4, 4H SD=F10.6, 4H CV=F10.6)
S.0081      111     FORMAT (1H , 3F10.3)
S.0082      112     FORMAT (/14H FLAT BASELINE/)
S.0083      113     FORMAT (19H SPECIAL CONDITIONS/)
S.0084      114     FORMAT (1H1)
S.0085      117     FORMAT (1H , 11H PARAMETERSI3, 6H FIXED)
S.0086      325     STOP 325
S.0087              END
                       SIZE OF COMMON  16880     PROGRAM  07090


END OF COMPILATION MAIN

BPS FORTRAN D COMPILER
            C       BAN1
S.0001              FUNCTION WF(X, O, K, N)
S.0002              DIMENSION X(200), O(200)
S.0003              WF =   1.00
S.0004              RETURN
S.0005              END
                       SIZE OF COMMON  00000     PROGRAM  00202
END OF COMPILATION  WF

BPS FORTRAN D COMPILER
            C       BAN2
S.0001              SUBROUTINE CALC(Y,X,T,N,M,O,E,FLAT)
            C       USING THE SUPPLIED PARAMETERS THE BAND SHAPES ARE CALCULATED
            C       ACCORDING TO THE SPECIFIED FUNCTION PARAMETER T(1). THE CALCULATED
            C       VALUES ARE STORED IN Y. E HOLDS THE DIFFERENCE BETWEEN THE SUM OF
            C       THE CALCULATED AND THE EXPERIMENTAL OBSERVATIONS.
S.0002              DIMENSION Y(200), X(200), T(33), O(200), E(200)
S.0003              INTEGER FLAT
S.0004              P = T(1)
S.0005              MM = M - 2
S.0006              DO 2 K = 1, N
S.0007              G = 0
S.0008              DO 1 I = 2, MM, 3
S.0009              A1 = T(I)
S.0010              A2 = T(I + 1)
S.0011              A3 = T(I + 2)
S.0012              C = 2.*(A2 - X(K))/A3
S.0013              G = G + A1*(1. - P)/(1. + C*C)
S.0014              D = -ALOG(2.)*C*C
```

```
 S.0015     1      G = G + A1*P*EXP(D)
 S.0016            IF(FLAT) 4, 4, 3
 S.0017       3    G = G + T(M - 1)
 S.0018            GO TO 5
 S.0019       4    G = G + T(M -1) + (X(K) - X(1))*(T(M) - T(M -1))/(X(N) - X(1))
 S.0020     5      Y(K) = G
 S.0021     2      E(K) = G - O(K)
 S.0022            RETURN
 S.0023            END
                      SIZE OF COMMON   00000     PROGRAM  00914
END OF COMPILATION  CALC

BPS FORTRAN D COMPILER
           C      BAN3
 S.0001            SUBROUTINE SIGMA(SD, CV, O, Y, N, W)
           C A STATISTICAL PROGRAM WHICH CALCULATES THE SUM OF SQUARES
           C TOP, THE STANDARD DEVIATION, SD, AND AN EMPIRICAL
           C STATISTICAL PARAMETER, CV.
 S.0002            DIMENSION O(200), Y(200), W(200)
 S.0003            TOT = 0
 S.0004            TOP = 0
 S.0005            DO 1 K = 1, N
 S.0006            TOP = TOP + W(K)*(Y(K) - O(K))**2
 S.0007     1      TOT = TOT + O(K)*W(K)
 S.0008            AV = TOT/FLOAT(N)
 S.0009            SD = SQRT(TOP/FLOAT(N))
 S.0010            CV = 100.*SD/AV
 S.0011            RETURN
 S.0012            END
                      SIZE OF COMMON   00000     PROGRAM  00662
END OF COMPILATION  SIGMA

BPS FORTRAN D COMPILER
           C      BAN4
 S.0001            SUBROUTINE DERIV(X, T, N, M, FLAT)
           C      COMPUTES THE DERIVATIVE OF THE PARAMETERS AT EACH POINT N
           C      FOR EACH OF THE I PARAMETERS AND STORES IT IN THE ARRAY D
 S.0002            DIMENSION D(170,20), X(170), T(33)
 S.0003            COMMON DUMMY(820),D
 S.0004            INTEGER FLAT
 S.0005            MM = M - 2
 S.0006            P = T(1)
 S.0007            PP = 1. - P
 S.0008            DO 2 K = 1, N
 S.0009            D(K,1) = 0
 S.0010            DO 1 I = 2, MM, 3
 S.0011            A1 = T(I)
 S.0012            A2 = T(I + 1)
 S.0013            A3 = T(I + 2)
 S.0014            C = 2.*(A2 - X(K))/A3
 S.0015            B = 1./(1. + C*C)
 S.0016            B1 = PP*B
 S.0017            B2 = -4.*A1*C*B*B1/A3
 S.0018            B3 = -C*B2/2.
 S.0019            CC = -ALOG(2.)*C*C
 S.0020            D(K,I) = P*EXP(CC)
 S.0021            D(K,I + 1) = -4.*C*A1*D(K,I)*ALOG(2.)/A3
 S.0022            D(K,I + 2) = -C*D(K,I + 1)/2.
 S.0023            D(K,I) = D(K,I) + B1
 S.0024            D(K,I + 1) = D(K,I + 1) + B2
 S.0025            D(K,I + 2) = D(K,I + 2) + B3
 S.0026     1      D(K,1) = D(K,1) - A1/(1. + C*C) + A1*EXP(CC)
 S.0027            IF(FLAT) 4, 4, 3
 S.0028     3      D(K,M -1) = 0
 S.0029            D(K,M) = 0
 S.0030            GO TO 2
```

```
S.0031     4      C = (X(K) - X(1))/(X(N) - X(1))
S.0032            D(K,M - 1) = 1. - C
S.0033     2      D(K,M) = C
S.0034            RETURN
S.0035            END
                     SIZE OF COMMON   16880     PROGRAM  01202


END OF COMPILATION DERIV

BPS FORTRAN D COMPILER
           C      BAN12
           C      THE MATRIX ELEMENTS WHICH ARE INVERTED AND THE B VECTOR ARE
           C      COMPUTED IN THIS ROUTINE.  THE PARAMETERS ARE CORRECTED BY CALLING
           C      THE MATRIX INVERSION ROUTINE BAN7.
S.0001             SUBROUTINE GENLSQ(O, FC, NOF, P, NOP, IG, NOG, W, DF, IRR)
S.0002             DIMENSION O(200), FC(200), P(33), W(200), A(820),  B(67),IG(34)
S.0003             COMMON DUMMY(820),FD(170,20)
S.0004             EQUIVALENCE (DUMMY(1), A(1))
S.0005             K = 0
S.0006             L = 0
S.0007             DO 80 J = 1, NOP
S.0008             IF(IG(J)) 401,401,80
S.0009     401     K = K + 1
S.0010             B(K) = 0.
S.0011             DO 8 I = 1, NOF
S.0012             B(K) = B(K) - W(I)*FD(I,J)*(FC(I) - O(I))
S.0013      8      CONTINUE
S.0014     80      CONTINUE
S.0015             DO 30 J = 1, NOP
S.0016             IF(IG(J)) 404,404,30
S.0017     404     DO 35 M = J, NOP
S.0018             IF(IG(M)) 405,405,35
S.0019     405     L = L + 1
S.0020             A(L) = 0.
S.0021             DO 1 I = 1, NOF
S.0022     1       A(L) = A(L) + W(I)*FD(I,J)*FD(I,M)
S.0023             IF(DF) 301,3,301
S.0024     301     IF(M - J) 3,2,3
S.0025     2       A(L) = A(L)*(1 + DF)
S.0026     3       CONTINUE
S.0027     35      CONTINUE
S.0028     30      CONTINUE
S.0029             CALL SYMINV(A, NOP - NOG, B, IRR)
S.0030             IF(IRR) 11,11,10
S.0031     10      WRITE(6, 101)
S.0032     101     FORMAT (1H , 16H SINGULAR MATRIX//)
S.0033             RETURN
S.0034     11      K = 0
S.0035             DO 12 J = 1, NOP
S.0036             IF(IG(J)) 410,410,411
S.0037     410     K = K + 1
S.0038             P(J) = P(J) + B(K)
S.0039             GO TO 12
S.0040     411     P(J) = P(J)
S.0041     12      CONTINUE
S.0042             RETURN
S.0043             END
                     SIZE OF COMMON   16880     PROGRAM  01676


END OF COMPILATION GENLSQ

BPS FORTRAN D COMPILER
```

```
      C     BAN7
      C     THIS SUBROUTINE WILL INVERT THE TRIANGULAR MATRIX PRODUCED IN
      C     BAN12 AND RETURNS THE DELTA P(J) WHICH ARE ADDED TO THE PARAMETERS.
      C     THE  PROGRAM SOLVES AS MANY SIMULTANEOUS EQUATIONS AS THERE ARE
      C     UNFIXED PARAMETERS
S.0001      SUBROUTINE SYMINV(A,N,B,IRR)
S.0002      DIMENSION A(820),  B(67), IP(67)
S.0003      DET = 1.0
S.0004      DO 220 I = 1, N
S.0005      AMAX = 0.
S.0006      II = N*(I - 1) - I*(I - 3)/2
S.0007      K = II
S.0008      DO 20 J = I, N
S.0009      IF(ABS(A(K)) - AMAX) 20,20,10
S.0010   10 JJ = K
S.0011      IP(I) = J
S.0012      AMAX = ABS(A(K))
S.0013   20 K = K + N -J + 1
S.0014      IF(AMAX - 1.0E-20) 30,30,40
S.0015   30 IRR = 1
S.0016      RETURN
S.0017   40 DET = DET*A(JJ)
S.0018      JI = IP(I) - I
S.0019      IF(JI) 110,110,42
S.0020   42 K = II
S.0021      KK = K + N - I + JI
S.0022      DO 90 L = 1, JI
S.0023      K = K + 1
S.0024      AMAX = A(K)
S.0025      A(K) = A(KK)
S.0026      A(KK) = AMAX
S.0027   90 KK = KK + N - I - L
S.0028      JU = I
S.0029      K = I
S.0030      IF(JU) 55,55,45
S.0031   45 DO 50 J = 1, JU
S.0032      KK = K + JI
S.0033      AMAX = A(K)
S.0034      A(K) = A(KK)
S.0035      K = K + N - J
S.0036   50 A(KK) = AMAX
S.0037   55 K = II + JI
S.0038      KK = JJ
S.0039      JU =II + N - I
S.0040      IF(JU - K) 80,60,60
S.0041   60 DO 70 L = K, JU
S.0042      AMAX = A(L)
S.0043      A(L) = A(KK)
S.0044      A(KK) = AMAX
S.0045   70 KK = KK + 1
S.0046   80 K = IP(I)
S.0047      AMAX = B(I)
S.0048      B(I) = B(K)
S.0049      B(K) = AMAX
S.0050  110 A(II) = 1.0/A(II)
S.0051      JU = I - 1
S.0052      K = 1
S.0053      IF(JU) 170,170,115
S.0054  115 DO 160 J = 1, JU
S.0055      AMAX = A(K)*A(II)
S.0056      LL = K - I + J
S.0057      LU = K - 1
S.0058      KK = J - 1
S.0059      JI = K
S.0060      DO 120 L = LL, LU
S.0061      KK = KK + 1
```

```
 S.0062           A(L) = A(L) + A(JI)*AMAX
 S.0063     120   JI = JI + N -KK
 S.0064           A(K) = AMAX
 S.0065           LL = K + 1
 S.0066           LU = K + N - I
 S.0067           KK = II
 S.0068           IF(LU -LL) 150,125,125
 S.0069     125   DO 130 L = LL, LU
 S.0070           KK = KK + 1
 S.0071     130   A(L) = A(L) - A(KK)*AMAX
 S.0072     150   B(J) = B(J) + B(I)*AMAX
 S.0073     160   K = K + N - J
 S.0074     170   JU = N - I
 S.0075           KK = II + N - I
 S.0076           LL = N*(N + 1)/2
 S.0077           IF(JU) 220,220,175
 S.0078     175   DO 200 JJ = 1, JU
 S.0079           J = N + 1 - JJ
 S.0080           AMAX = A(KK)*A(II)
 S.0081           K = KK
 S.0082           KK = KK - 1
 S.0083           LU = LL + N - J
 S.0084           DO 180 L = LL, LU
 S.0085           A(L) = A(L) - A(K)*AMAX
 S.0086     180   K = K + 1
 S.0087           B(J) = B(J) - B(I)*AMAX
 S.0088     200   LL = LL - N + J - 2
 S.0089           LL = II + 1
 S.0090           LU = II + N - I
 S.0091           DO 210 L = LL, LU
 S.0092     210   A(L) = - A(L)*A(II)
 S.0093     220   B(I) = B(I)*A(II)
 S.0094           DO 270 I = 1, N
 S.0095           L = N - I + 1
 S.0096           K = IP(L)
 S.0097           AMAX = B(L)
 S.0098           B(L) = B(K)
 S.0099     270   B(K) = AMAX
 S.0100           IRR = 0
 S.0101           RETURN
 S.0102           END
                     SIZE OF COMMON   00000     PROGRAM  02568
END OF COMPILATION  SYMINV

BPS FORTRAN D COMPILER
           C       BAN15
           C       THIS SUBROUTINE WILL PLOT A GRAPH OF THE OBSERVED DATA
           C       AND EACH OF THE COMPONENT PEAKS.
 S.0001           SUBROUTINE GRAFC(X, O, T, HEAD, IX, IY, M, N)
 S.0002           DIMENSION X(170), O(170), T(20),            HEAD(20),
                 1IX(3), IY(3),R(170)
 S.0003           JMAX = M/3. - 1.
 S.0004           CALL ITLZ
 S.0005           CALL DPT(1,4)
 S.0006           CALL PLOT(0.,-11.,3)
 S.0007           CALL PLOT(0.,-9.5,-3)
           C      DRAW THE X AND Y AXIS WITH ANNOTATION
 S.0008           X(N + 1) = 2300.
 S.0009           X(N + 2) = 200.
 S.0010           R(N + 1) = 0.0
 S.0011           R(N + 2) = 4.0
 S.0012           CALL AXIS(0.,0.,IX,-12,8.,0.,X(N + 1),X(N + 2))
 S.0013           CALL AXIS(0.,0.,IY,+12,7.,90.,R(N + 1),R(N + 2))
 S.0014           DO 2 K = 1, N
 S.0015     2     R(K) = O(K) - T(M -1) - (T(M) - T(M - 1))*
                 1((X(K) - X(1))/(X(N) - X(1)))
```

```
S.0016            CALL LINE(X, R, N, 1, 0, 4)
S.0017            P = T(1)
S.0018            MM = M - 2
S.0019            DO 53 I = 2,MM,3
S.0020            DO 51 K = 1, N
S.0021            G = 0
S.0022            A1 = T(I)
S.0023            A2 = T(I + 1)
S.0024            A3 = T(I + 2)
S.0025            C = 2.*(A2 - X(K))/A3
S.0026            G = A1*(1. - P)/(1. + C*C)
S.0027            D = - ALOG(2.)*C*C
S.0028            G = G + A1*P*EXP(D)
S.0029      51    R(K) = G
S.0030            CALL LINE(X, R, N, 1, 0, 4)
S.0031      53    CONTINUE
            C     WRITE THE HEADING
S.0032            CALL SYMBOL(1.,6.,.14,HEAD,0,+30)
S.0033            CALL PLOT(9.5,0.,-3)
S.0034            CALL FINAL
S.0035            RETURN
S.0036            END
                     SIZE OF COMMON  00000     PROGRAM  02194
END OF COMPILATION  GRAFC

BPS FORTRAN D COMPILER
            C     BAN9
            C     THIS SUBROUTINE CALCULATES THE AREA UNDER EACH PEAK USING THE
            C     REFINED PARAMETERS
S.0001            SUBROUTINE AREA1(M, T)
S.0002            REAL PI
S.0003            DIMENSION T(33)
S.0004            P = T(1)
S.0005            MM = M - 2
S.0006            PI = 3.14159265
S.0007            DO 1 I = 2, MM, 3
S.0008            A1 = T(I)
S.0009            A2 = T(I + 2)
S.0010            A3 = T(I + 1)
S.0011              AR = .5*A1*A2*(P*(SQRT(PI/ALOG(2.))) + (1. - P)*PI)
S.0012            WRITE (6, 102) A3, AR
S.0013      102   FORMAT (1H0, 14HBAND CENTER = , F6.1, 5X, 12HBAND AREA = ,
                 1 F12.5)
S.0014      1     CONTINUE
S.0015            RETURN
S.0016            END
                     SIZE OF COMMON  00000     PROGRAM  00588
END OF COMPILATION  AREA1
```

RAMAN SPECTRUM 3.641 MOLAL KOH
INITIAL PARAMETERS

0.838		
1.727	3087.897	624.468
9.134	3265.771	309.981
7.485	3472.000	202.023
3.800	3610.738	81.000

BASE LINE INTERCEPTS 40.522 40.176 DF= 50.000

INITIAL DATA SD= 0.2942752

X	YO	YC	E
2300.000	40.63799	40.62416	-0.01382
2310.000	40.63799	40.62582	-0.01216
2320.000	40.62500	40.62776	0.00276
2330.000	40.62500	40.62999	0.00499
2340.000	40.62500	40.63252	0.00752
2350.000	40.62500	40.63538	0.01038
2360.000	40.62500	40.63860	0.01360
2370.000	40.62500	40.64220	0.01720
2380.000	40.62500	40.64619	0.02119
2390.000	40.62500	40.65062	0.02562
2400.000	40.63599	40.65549	0.01950
2410.000	40.63599	40.66087	0.02489
2420.000	40.64099	40.66676	0.02577
2430.000	40.65900	40.67319	0.01419
2440.000	40.65900	40.68019	0.02119
2450.000	40.65900	40.68782	0.02882
2460.000	40.65900	40.69609	0.03709
2470.000	40.65900	40.70503	0.04604
2480.000	40.67499	40.71469	0.03970
2490.000	40.70499	40.72508	0.02010
2500.000	40.71899	40.73625	0.01726
2510.000	40.72800	40.74823	0.02023
2520.000	40.72800	40.76108	0.03308
2530.000	40.73999	40.77478	0.03479
2540.000	40.76500	40.78940	0.02440
2550.000	40.78000	40.80496	0.02496
2560.000	40.81999	40.82150	0.00151
2570.000	40.83400	40.83902	0.00502
2580.000	40.85599	40.85759	0.00160
2590.000	40.88599	40.87721	-0.00877
2600.000	40.92599	40.89790	-0.02809
2610.000	40.94199	40.91969	-0.02229
2620.000	40.94800	40.94261	-0.00539
2630.000	40.96199	40.96666	0.00467
2640.000	40.97400	40.99185	0.01785
2650.000	41.02599	41.01820	-0.00778
2660.000	41.03799	41.04575	0.00775
2670.000	41.05899	41.07445	0.01546
2680.000	41.09000	41.10432	0.01433
2690.000	41.14899	41.13541	-0.01358
2700.000	41.17599	41.16766	-0.00833
2710.000	41.21999	41.20111	-0.01888
2720.000	41.24500	41.23575	-0.00925
2730.000	41.32599	41.27159	-0.05440
2740.000	41.34000	41.30865	-0.03134
2750.000	41.34799	41.34694	-0.00105
2760.000	41.39999	41.38647	-0.01352
2770.000	41.41800	41.42732	0.00932
2780.000	41.43399	41.46953	0.03554
2790.000	41.51700	41.51315	-0.00385
2800.000	41.52899	41.55833	0.02934
2810.000	41.58400	41.60518	0.02118
2820.000	41.64299	41.65387	0.01088
2830.000	41.66899	41.70462	0.03563
2840.000	41.73799	41.75772	0.01973
2850.000	41.81400	41.81348	-0.00052
2860.000	41.84999	41.87228	0.02229
2870.000	41.92200	41.93463	0.01263
2880.000	42.02599	42.00104	-0.02495
2890.000	42.11400	42.07214	-0.04185
2900.000	42.21999	42.14867	-0.07132
2910.000	42.32700	42.23143	-0.09557
2920.000	42.39499	42.32132	-0.07367
2930.000	42.51799	42.41931	-0.09868
2940.000	42.59299	42.52650	-0.06648
2950.000	42.73000	42.64398	-0.08601
2960.000	42.86400	42.77298	-0.09102
2970.000	42.96999	42.91467	-0.05531
2980.000	43.14999	43.07033	-0.07967
2990.000	43.29099	43.24112	-0.04987
3000.000	43.48399	43.42818	-0.05582
3010.000	43.64099	43.63255	-0.00844
3020.000	43.84299	43.85515	0.01216
3030.000	44.08899	44.09665	0.00766
3040.000	44.34900	44.35756	0.00856
3050.000	44.60500	44.63806	0.03307
3060.000	44.88599	44.93799	0.05200
3070.000	45.19199	45.25685	0.06487
3080.000	45.52100	45.59372	0.07272
3090.000	45.84200	45.94724	0.10524
3100.000	46.25899	46.31557	0.05658
3110.000	46.59000	46.69643	0.10643
3120.000	47.00200	47.08708	0.08508
3130.000	47.45200	47.48425	0.03226
3140.000	47.82799	47.88434	0.05635
3150.000	48.31499	48.28331	-0.03168
3160.000	48.66699	48.67682	0.00983
3170.000	49.09698	49.06023	-0.03676
3180.000	49.60100	49.42885	-0.17215
3190.000	49.92899	49.77791	-0.15108
3200.000	50.33800	50.10278	-0.23521
3210.000	50.57399	50.39917	-0.17482
3220.000	50.84499	50.66330	-0.18169
3230.000	51.09499	50.89221	-0.20277
3240.000	51.30699	51.08391	-0.22308
3250.000	51.45200	51.23775	-0.21425
3260.000	51.54599	51.35452	-0.19147
3270.000	51.58899	51.43658	-0.15240
3280.000	51.67599	51.48790	-0.18810
3290.000	51.72198	51.51382	-0.20816
3300.000	51.78200	51.52084	-0.26115
3310.000	51.86699	51.51611	-0.35088
3320.000	51.91299	51.50694	-0.40605
3330.000	51.97099	51.50024	-0.47075
3340.000	52.11499	51.50192	-0.61307
3350.000	52.24599	51.51637	-0.72961
3360.000	52.34698	51.54604	-0.80095
3370.000	52.50600	51.59106	-0.91493
3380.000	52.50200	51.64903	-0.85297
3390.000	52.59099	51.71495	-0.87604
3400.000	52.75000	51.78128	-0.96872
3410.000	52.63199	51.83807	-0.79391
3420.000	52.63899	51.87340	-0.76559
3430.000	52.53299	51.87384	-0.65915
3440.000	52.37799	51.82532	-0.55267
3450.000	52.06099	51.71425	-0.34674
3460.000	51.86800	51.52913	-0.33887
3470.000	51.47899	51.26225	-0.21674
3480.000	51.03400	50.91135	-0.12265
3490.000	50.65199	50.48093	-0.17107
3500.000	50.35100	49.98320	-0.36780
3510.000	49.81599	49.43889	-0.37711
3520.000	49.45999	48.87776	-0.58223
3530.000	49.02699	48.33871	-0.68828
3540.000	48.79700	47.86708	-0.92992
3550.000	48.41199	47.50745	-0.90454
3560.000	48.13499	47.29071	-0.84428
3570.000	47.80199	47.21832	-0.58366
3580.000	47.58400	47.24936	-0.33464
3590.000	47.44199	47.29739	-0.14459
3600.000	47.42599	47.24200	-0.18399
3610.000	47.50000	46.96307	-0.53693
3620.000	47.12000	46.40196	-0.71803
3630.000	46.15799	45.60326	-0.55473
3640.000	45.08400	44.68292	-0.40108
3650.000	43.91800	43.76593	-0.15207
3660.000	43.21999	42.94806	-0.27193
3670.000	42.57899	42.28218	-0.29681
3680.000	42.04599	41.77951	-0.26648
3690.000	41.69600	41.42155	-0.27444
3700.000	41.29999	41.17566	-0.12433
3710.000	41.12799	41.00826	-0.11974
3720.000	40.89999	40.89201	-0.00798
3730.000	40.82599	40.80786	-0.01813
3740.000	40.72400	40.74385	0.01985
3750.000	40.65500	40.69296	0.03796
3760.000	40.58899	40.65108	0.06209
3770.000	40.56000	40.61571	0.05571
3780.000	40.56099	40.58528	0.02429
3790.000	40.55299	40.55870	0.00571
3800.000	40.51999	40.53516	0.01517
3810.000	40.49899	40.51404	0.01505
3820.000	40.49500	40.49490	-0.00009
3830.000	40.49199	40.47742	-0.01457
3840.000	40.49199	40.46129	-0.03070
3850.000	40.48599	40.44633	-0.03966
3860.000	40.48599	40.43239	-0.05360
3870.000	40.47899	40.41936	-0.05963
3880.000	40.47899	40.40709	-0.07190
3890.000	40.47899	40.39554	-0.08345
3900.000	40.47899	40.38461	-0.09438

CYCLE 1 SD= 0.274003 CV= 0.616467
CYCLE 2 SD= 0.256184 CV= 0.576378
CYCLE 3 SD= 0.240545 CV= 0.541191
CYCLE 4 SD= 0.226837 CV= 0.510352
CYCLE 5 SD= 0.214837 CV= 0.483352
CYCLE 6 SD= 0.204335 CV= 0.459725
CYCLE 7 SD= 0.195147 CV= 0.439052
CYCLE 8 SD= 0.187101 CV= 0.420950
CYCLE 9 SD= 0.180052 CV= 0.405091
CYCLE 10 SD= 0.173861 CV= 0.391163
CYCLE 11 SD= 0.168417 CV= 0.378913
CYCLE 12 SD= 0.163614 CV= 0.368107
CYCLE 13 SD= 0.159360 CV= 0.358538
CYCLE 14 SD= 0.155582 CV= 0.350038
CYCLE 15 SD= 0.152214 CV= 0.342461
CYCLE 16 SD= 0.149196 CV= 0.335670
CYCLE 17 SD= 0.146481 CV= 0.329561
CYCLE 18 SD= 0.144027 CV= 0.324039
CYCLE 19 SD= 0.141801 CV= 0.319032
CYCLE 20 SD= 0.139770 CV= 0.314463
CYCLE 21 SD= 0.137912 CV= 0.310283
CYCLE 22 SD= 0.136206 CV= 0.306443
CYCLE 23 SD= 0.134633 CV= 0.302904
CYCLE 24 SD= 0.133177 CV= 0.299630
CYCLE 25 SD= 0.131828 CV= 0.296593
CYCLE 26 SD= 0.130570 CV= 0.293764
CYCLE 27 SD= 0.129395 CV= 0.291120
CYCLE 28 SD= 0.128300 CV= 0.288656
CYCLE 29 SD= 0.127271 CV= 0.286342
CYCLE 30 SD= 0.126306 CV= 0.284171
CYCLE 31 SD= 0.125398 CV= 0.282128
CYCLE 32 SD= 0.124542 CV= 0.280201
CYCLE 33 SD= 0.123733 CV= 0.278381
CYCLE 34 SD= 0.122971 CV= 0.276666
CYCLE 35 SD= 0.122249 CV= 0.275044
CYCLE 36 SD= 0.121566 CV= 0.273507
CYCLE 37 SD= 0.120920 CV= 0.272054
CYCLE 38 SD= 0.120307 CV= 0.270674
CYCLE 39 SD= 0.119726 CV= 0.269367
CYCLE 40 SD= 0.119174 CV= 0.268125
CYCLE 41 SD= 0.118649 CV= 0.266943
CYCLE 42 SD= 0.118150 CV= 0.265821
CYCLE 43 SD= 0.117678 CV= 0.264758
CYCLE 44 SD= 0.117224 CV= 0.263738
CYCLE 45 SD= 0.116795 CV= 0.262771
CYCLE 46 SD= 0.116385 CV= 0.261850
CYCLE 47 SD= 0.115995 CV= 0.260973
CYCLE 48 SD= 0.115624 CV= 0.260138
CYCLE 49 SD= 0.115269 CV= 0.259339
CYCLE 50 SD= 0.114931 CV= 0.258579
CYCLE 51 SD= 0.114608 CV= 0.257852
CYCLE 52 SD= 0.114299 CV= 0.257157
CYCLE 53 SD= 0.114004 CV= 0.256493
CYCLE 54 SD= 0.113721 CV= 0.255857
CYCLE 55 SD= 0.113452 CV= 0.255250
CYCLE 56 SD= 0.113192 CV= 0.254666
CYCLE 57 SD= 0.112946 CV= 0.254112
CYCLE 58 SD= 0.112710 CV= 0.253581
CYCLE 59 SD= 0.112481 CV= 0.253066
CYCLE 60 SD= 0.112264 CV= 0.252577
CYCLE 61 SD= 0.112056 CV= 0.252111
CYCLE 62 SD= 0.111855 CV= 0.251658
CYCLE 63 SD= 0.111662 CV= 0.251223
CYCLE 64 SD= 0.111477 CV= 0.250807
CYCLE 65 SD= 0.111300 CV= 0.250410
CYCLE 66 SD= 0.111128 CV= 0.250023
CYCLE 67 SD= 0.110964 CV= 0.249653
CYCLE 68 SD= 0.110806 CV= 0.249297
CYCLE 69 SD= 0.110654 CV= 0.248955
CYCLE 70 SD= 0.110507 CV= 0.248625
CYCLE 71 SD= 0.110365 CV= 0.248306
CYCLE 72 SD= 0.110230 CV= 0.248001
CYCLE 73 SD= 0.110098 CV= 0.247704
CYCLE 74 SD= 0.109971 CV= 0.247418
CYCLE 75 SD= 0.109848 CV= 0.247143
CYCLE 76 SD= 0.109730 CV= 0.246878
CYCLE 77 SD= 0.109615 CV= 0.246619
CYCLE 78 SD= 0.109504 CV= 0.246369
CYCLE 79 SD= 0.109398 CV= 0.246129
CYCLE 80 SD= 0.109294 CV= 0.245896
CYCLE 81 SD= 0.109194 CV= 0.245670
CYCLE 82 SD= 0.109096 CV= 0.245450
CYCLE 83 SD= 0.109002 CV= 0.245240
CYCLE 84 SD= 0.108910 CV= 0.245033
CYCLE 85 SD= 0.108822 CV= 0.244834
CYCLE 86 SD= 0.108736 CV= 0.244640
CYCLE 87 SD= 0.108652 CV= 0.244452
CYCLE 88 SD= 0.108570 CV= 0.244267
CYCLE 89 SD= 0.108492 CV= 0.244092
CYCLE 90 SD= 0.108415 CV= 0.243919
CYCLE 91 SD= 0.108340 CV= 0.243749
CYCLE 92 SD= 0.108268 CV= 0.243588
CYCLE 93 SD= 0.108197 CV= 0.243427
CYCLE 94 SD= 0.108129 CV= 0.243274
CYCLE 95 SD= 0.108061 CV= 0.243123
CYCLE 96 SD= 0.107995 CV= 0.242974
CYCLE 97 SD= 0.107932 CV= 0.242832
CYCLE 98 SD= 0.107870 CV= 0.242691
CYCLE 99 SD= 0.107809 CV= 0.242555
CYCLE 100 SD= 0.107750 CV= 0.242421
CYCLE 101 SD= 0.107693 CV= 0.242293
CYCLE 102 SD= 0.107637 CV= 0.242167
CYCLE 103 SD= 0.107581 CV= 0.242042
CYCLE 104 SD= 0.107527 CV= 0.241920
CYCLE 105 SD= 0.107474 CV= 0.241802
CYCLE 106 SD= 0.107422 CV= 0.241684
CYCLE 107 SD= 0.107372 CV= 0.241571
CYCLE 108 SD= 0.107322 CV= 0.241459
CYCLE 109 SD= 0.107274 CV= 0.241350
CYCLE 110 SD= 0.107227 CV= 0.241245
CYCLE 111 SD= 0.107181 CV= 0.241141
CYCLE 112 SD= 0.107135 CV= 0.241039
CYCLE 113 SD= 0.107090 CV= 0.240936

CYCLE 114 SD= 0.107045 CV= 0.240836
CYCLE 115 SD= 0.107004 CV= 0.240744
CYCLE 116 SD= 0.106962 CV= 0.240648
CYCLE 117 SD= 0.106921 CV= 0.240557
CYCLE 118 SD= 0.106880 CV= 0.240465
CYCLE 119 SD= 0.106839 CV= 0.240373
CYCLE 120 SD= 0.106802 CV= 0.240289
CYCLE 121 SD= 0.106763 CV= 0.240201
CYCLE 122 SD= 0.106724 CV= 0.240114
CYCLE 123 SD= 0.106688 CV= 0.240032
CYCLE 124 SD= 0.106651 CV= 0.239949
CYCLE 125 SD= 0.106614 CV= 0.239867
CYCLE 126 SD= 0.106581 CV= 0.239793
CYCLE 127 SD= 0.106544 CV= 0.239709
CYCLE 128 SD= 0.106511 CV= 0.239635
CYCLE 129 SD= 0.106477 CV= 0.239558
CYCLE 130 SD= 0.106444 CV= 0.239483
CYCLE 131 SD= 0.106411 CV= 0.239409
CYCLE 132 SD= 0.106379 CV= 0.239337
CYCLE 133 SD= 0.106346 CV= 0.239264
CYCLE 134 SD= 0.106316 CV= 0.239195
CYCLE 135 SD= 0.106285 CV= 0.239126
CYCLE 136 SD= 0.106254 CV= 0.239057
CYCLE 137 SD= 0.106224 CV= 0.238990
CYCLE 138 SD= 0.106195 CV= 0.238923
CYCLE 139 SD= 0.106166 CV= 0.238857
CYCLE 140 SD= 0.106137 CV= 0.238794
CYCLE 141 SD= 0.106109 CV= 0.238731
CYCLE 142 SD= 0.106080 CV= 0.238666
CYCLE 143 SD= 0.106053 CV= 0.238604
CYCLE 144 SD= 0.106025 CV= 0.238541
CYCLE 145 SD= 0.105998 CV= 0.238481
CYCLE 146 SD= 0.105972 CV= 0.238421
CYCLE 147 SD= 0.105944 CV= 0.238359
CYCLE 148 SD= 0.105919 CV= 0.238302
CYCLE 149 SD= 0.105892 CV= 0.238243
CYCLE 150 SD= 0.105868 CV= 0.238188
CYCLE 151 SD= 0.105842 CV= 0.238128
CYCLE 152 SD= 0.105817 CV= 0.238073
CYCLE 153 SD= 0.105793 CV= 0.238018
CYCLE 154 SD= 0.105767 CV= 0.237961
CYCLE 155 SD= 0.105745 CV= 0.237912
CYCLE 156 SD= 0.105720 CV= 0.237855
CYCLE 157 SD= 0.105697 CV= 0.237804
CYCLE 158 SD= 0.105675 CV= 0.237753
CYCLE 159 SD= 0.105651 CV= 0.237699
CYCLE 160 SD= 0.105628 CV= 0.237647
CYCLE 161 SD= 0.105605 CV= 0.237597
CYCLE 162 SD= 0.105583 CV= 0.237546
CYCLE 163 SD= 0.105560 CV= 0.237496
CYCLE 164 SD= 0.105539 CV= 0.237447
CYCLE 165 SD= 0.105517 CV= 0.237398
CYCLE 166 SD= 0.105495 CV= 0.237349
CYCLE 167 SD= 0.105474 CV= 0.237302
CYCLE 168 SD= 0.105452 CV= 0.237253
CYCLE 169 SD= 0.105431 CV= 0.237206
CYCLE 170 SD= 0.105411 CV= 0.237160
CYCLE 171 SD= 0.105391 CV= 0.237115
CYCLE 172 SD= 0.105371 CV= 0.237069
CYCLE 173 SD= 0.105351 CV= 0.237024
CYCLE 174 SD= 0.105330 CV= 0.236978
CYCLE 175 SD= 0.105311 CV= 0.236935
CYCLE 176 SD= 0.105291 CV= 0.236891
CYCLE 177 SD= 0.105272 CV= 0.236846
CYCLE 178 SD= 0.105253 CV= 0.236804
CYCLE 179 SD= 0.105234 CV= 0.236761
CYCLE 180 SD= 0.105214 CV= 0.236717
CYCLE 181 SD= 0.105196 CV= 0.236675
CYCLE 182 SD= 0.105178 CV= 0.236635
CYCLE 183 SD= 0.105159 CV= 0.236592
CYCLE 184 SD= 0.105140 CV= 0.236549
CYCLE 185 SD= 0.105121 CV= 0.236508
CYCLE 186 SD= 0.105104 CV= 0.236468
CYCLE 187 SD= 0.105086 CV= 0.236428
CYCLE 188 SD= 0.105068 CV= 0.236388
CYCLE 189 SD= 0.105051 CV= 0.236350
CYCLE 190 SD= 0.105034 CV= 0.236312
CYCLE 191 SD= 0.105017 CV= 0.236272
CYCLE 192 SD= 0.105000 CV= 0.236234
CYCLE 193 SD= 0.104981 CV= 0.236193
CYCLE 194 SD= 0.104965 CV= 0.236156
CYCLE 195 SD= 0.104948 CV= 0.236119
CYCLE 196 SD= 0.104930 CV= 0.236079
CYCLE 197 SD= 0.104915 CV= 0.236044
CYCLE 198 SD= 0.104898 CV= 0.236005
CYCLE 199 SD= 0.104881 CV= 0.235968
CYCLE 200 SD= 0.104866 CV= 0.235933
CYCLE 201 SD= 0.104849 CV= 0.235896
CYCLE 202 SD= 0.104833 CV= 0.235859
CYCLE 203 SD= 0.104817 CV= 0.235824
CYCLE 204 SD= 0.104802 CV= 0.235789
CYCLE 205 SD= 0.104785 CV= 0.235751
CYCLE 206 SD= 0.104770 CV= 0.235718
CYCLE 207 SD= 0.104754 CV= 0.235682
CYCLE 208 SD= 0.104739 CV= 0.235647
CYCLE 209 SD= 0.104724 CV= 0.235614
CYCLE 210 SD= 0.104708 CV= 0.235579
CYCLE 211 SD= 0.104695 CV= 0.235548
CYCLE 212 SD= 0.104679 CV= 0.235512
CYCLE 213 SD= 0.104663 CV= 0.235478
CYCLE 214 SD= 0.104649 CV= 0.235444
CYCLE 215 SD= 0.104634 CV= 0.235411
CYCLE 216 SD= 0.104619 CV= 0.235378
CYCLE 217 SD= 0.104605 CV= 0.235347
CYCLE 218 SD= 0.104590 CV= 0.235314
CYCLE 219 SD= 0.104576 CV= 0.235280
CYCLE 220 SD= 0.104562 CV= 0.235249
CYCLE 221 SD= 0.104547 CV= 0.235215
CYCLE 222 SD= 0.104533 CV= 0.235185
CYCLE 223 SD= 0.104518 CV= 0.235152
CYCLE 224 SD= 0.104506 CV= 0.235123
CYCLE 225 SD= 0.104492 CV= 0.235092

CYCLE 226 SD= 0.104477 CV= 0.235059
CYCLE 227 SD= 0.104464 CV= 0.235029
CYCLE 228 SD= 0.104449 CV= 0.234996
CYCLE 229 SD= 0.104437 CV= 0.234968
CYCLE 230 SD= 0.104423 CV= 0.234937
CYCLE 231 SD= 0.104409 CV= 0.234906
CYCLE 232 SD= 0.104396 CV= 0.234876
CYCLE 233 SD= 0.104382 CV= 0.234845
CYCLE 234 SD= 0.104369 CV= 0.234816
CYCLE 235 SD= 0.104357 CV= 0.234788
CYCLE 236 SD= 0.104343 CV= 0.234757
CYCLE 237 SD= 0.104330 CV= 0.234728
CYCLE 238 SD= 0.104317 CV= 0.234698
CYCLE 239 SD= 0.104304 CV= 0.234669
CYCLE 240 SD= 0.104292 CV= 0.234641
CYCLE 241 SD= 0.104279 CV= 0.234612
CYCLE 242 SD= 0.104265 CV= 0.234581
CYCLE 243 SD= 0.104252 CV= 0.234552
CYCLE 244 SD= 0.104242 CV= 0.234529
CYCLE 245 SD= 0.104229 CV= 0.234499
CYCLE 246 SD= 0.104215 CV= 0.234468
CYCLE 247 SD= 0.104203 CV= 0.234441
CYCLE 248 SD= 0.104190 CV= 0.234413
CYCLE 249 SD= 0.104178 CV= 0.234385
CYCLE 250 SD= 0.104166 CV= 0.234359
CYCLE 251 SD= 0.104153 CV= 0.234329
CYCLE 252 SD= 0.104142 CV= 0.234304
CYCLE 253 SD= 0.104131 CV= 0.234279
CYCLE 254 SD= 0.104118 CV= 0.234251
CYCLE 255 SD= 0.104107 CV= 0.234225
CYCLE 256 SD= 0.104095 CV= 0.234199
CYCLE 257 SD= 0.104083 CV= 0.234173
CYCLE 258 SD= 0.104071 CV= 0.234145
CYCLE 259 SD= 0.104060 CV= 0.234119
CYCLE 260 SD= 0.104049 CV= 0.234095
CYCLE 261 SD= 0.104037 CV= 0.234069
CYCLE 262 SD= 0.104026 CV= 0.234043
CYCLE 263 SD= 0.104014 CV= 0.234016
CYCLE 264 SD= 0.104002 CV= 0.233991
CYCLE 265 SD= 0.103991 CV= 0.233965
CYCLE 266 SD= 0.103980 CV= 0.233939
CYCLE 267 SD= 0.103969 CV= 0.233916
CYCLE 268 SD= 0.103957 CV= 0.233889
CYCLE 269 SD= 0.103947 CV= 0.233866
CYCLE 270 SD= 0.103936 CV= 0.233841
CYCLE 271 SD= 0.103925 CV= 0.233816
CYCLE 272 SD= 0.103914 CV= 0.233791
CYCLE 273 SD= 0.103904 CV= 0.233769
CYCLE 274 SD= 0.103893 CV= 0.233744
CYCLE 275 SD= 0.103882 CV= 0.233719
CYCLE 276 SD= 0.103871 CV= 0.233696
CYCLE 277 SD= 0.103860 CV= 0.233671
CYCLE 278 SD= 0.103849 CV= 0.233646
CYCLE 279 SD= 0.103839 CV= 0.233622
CYCLE 280 SD= 0.103828 CV= 0.233598
CYCLE 281 SD= 0.103817 CV= 0.233573
CYCLE 282 SD= 0.103807 CV= 0.233552
CYCLE 283 SD= 0.103797 CV= 0.233527
CYCLE 284 SD= 0.103787 CV= 0.233505
CYCLE 285 SD= 0.103776 CV= 0.233482
CYCLE 286 SD= 0.103766 CV= 0.233458
CYCLE 287 SD= 0.103755 CV= 0.233435
CYCLE 288 SD= 0.103745 CV= 0.233412
CYCLE 289 SD= 0.103735 CV= 0.233389
CYCLE 290 SD= 0.103726 CV= 0.233368
CYCLE 291 SD= 0.103715 CV= 0.233343
CYCLE 292 SD= 0.103706 CV= 0.233323
CYCLE 293 SD= 0.103695 CV= 0.233298
CYCLE 294 SD= 0.103684 CV= 0.233275
CYCLE 295 SD= 0.103675 CV= 0.233254
CYCLE 296 SD= 0.103665 CV= 0.233231
CYCLE 297 SD= 0.103655 CV= 0.233210
CYCLE 298 SD= 0.103646 CV= 0.233188
CYCLE 299 SD= 0.103636 CV= 0.233166
CYCLE 300 SD= 0.103627 CV= 0.233145
CYCLE 301 SD= 0.103616 CV= 0.233122
CYCLE 302 SD= 0.103608 CV= 0.233103
CYCLE 303 SD= 0.103597 CV= 0.233079
CYCLE 304 SD= 0.103588 CV= 0.233059
CYCLE 305 SD= 0.103578 CV= 0.233037
CYCLE 306 SD= 0.103569 CV= 0.233016
CYCLE 307 SD= 0.103560 CV= 0.232994
CYCLE 308 SD= 0.103550 CV= 0.232973
CYCLE 309 SD= 0.103541 CV= 0.232952
CYCLE 310 SD= 0.103531 CV= 0.232930
CYCLE 311 SD= 0.103522 CV= 0.232910
CYCLE 312 SD= 0.103512 CV= 0.232887
CYCLE 313 SD= 0.103504 CV= 0.232868
CYCLE 314 SD= 0.103495 CV= 0.232849
CYCLE 315 SD= 0.103485 CV= 0.232826
CYCLE 316 SD= 0.103476 CV= 0.232805
CYCLE 317 SD= 0.103467 CV= 0.232786
CYCLE 318 SD= 0.103457 CV= 0.232764
CYCLE 319 SD= 0.103449 CV= 0.232745
CYCLE 320 SD= 0.103438 CV= 0.232720
CYCLE 321 SD= 0.103429 CV= 0.232701
CYCLE 322 SD= 0.103422 CV= 0.232684
CYCLE 323 SD= 0.103411 CV= 0.232659
CYCLE 324 SD= 0.103403 CV= 0.232643
CYCLE 325 SD= 0.103394 CV= 0.232621
CYCLE 326 SD= 0.103385 CV= 0.232601
CYCLE 327 SD= 0.103376 CV= 0.232580
CYCLE 328 SD= 0.103367 CV= 0.232562
CYCLE 329 SD= 0.103358 CV= 0.232540
CYCLE 330 SD= 0.103349 CV= 0.232521
CYCLE 331 SD= 0.103340 CV= 0.232500
CYCLE 332 SD= 0.103332 CV= 0.232482
CYCLE 333 SD= 0.103322 CV= 0.232459
CYCLE 334 SD= 0.103314 CV= 0.232443
CYCLE 335 SD= 0.103306 CV= 0.232425
CYCLE 336 SD= 0.103296 CV= 0.232401
CYCLE 337 SD= 0.103289 CV= 0.232385

```
CYCLE 338 SD=  0.103279 CV=  0.232363
CYCLE 339 SD=  0.103270 CV=  0.232343
CYCLE 340 SD=  0.103264 CV=  0.232328
CYCLE 341 SD=  0.103253 CV=  0.232305
CYCLE 342 SD=  0.103245 CV=  0.232286
CYCLE 343 SD=  0.103236 CV=  0.232267
CYCLE 344 SD=  0.103228 CV=  0.232248
CYCLE 345 SD=  0.103219 CV=  0.232229
CYCLE 346 SD=  0.103212 CV=  0.232212
CYCLE 347 SD=  0.103204 CV=  0.232195
CYCLE 348 SD=  0.103195 CV=  0.232174
CYCLE 349 SD=  0.103187 CV=  0.232156
CYCLE 350 SD=  0.103179 CV=  0.232139
IREFINED PARAMETERS CYCLE350

    FUNCTION PARAMETER=   0.882
     1.766  3087.897    636.293
     9.235  3269.962    313.926
     7.655  3472.000    212.847
     3.806  3610.929     87.959
SPECIAL CONDITIONS

 PARAMETERS  3 FIXED
 PARAMETERS  9 FIXED

BASE LINE INTERCEPTS     40.513     40.213  DF=     50.000

REFINED DATA   SD= 0.1031793

        X          YO          YC           E
  2300.000   40.63799   40.60049   -0.03749
  2310.000   40.63799   40.60248   -0.03551
  2320.000   40.62500   40.60475   -0.02025
  2330.000   40.62500   40.60733   -0.01767
  2340.000   40.62500   40.61024   -0.01476
  2350.000   40.62500   40.61353   -0.01147
  2360.000   40.62500   40.61717   -0.00783
  2370.000   40.62500   40.62123   -0.00377
  2380.000   40.62500   40.62572    0.00072
  2390.000   40.62500   40.63066    0.00566
  2400.000   40.63599   40.63609    0.00011
  2410.000   40.63599   40.64204    0.00606
  2420.000   40.64099   40.64854    0.00755
  2430.000   40.65900   40.65564   -0.00336
  2440.000   40.65900   40.66333    0.00433
  2450.000   40.65900   40.67165    0.01265
  2460.000   40.65900   40.68065    0.02165
  2470.000   40.65900   40.69037    0.03137
  2480.000   40.67499   40.70082    0.02583
  2490.000   40.70499   40.71205    0.00706
  2500.000   40.71899   40.72409    0.00510
  2510.000   40.72800   40.73695    0.00896
  2520.000   40.72800   40.75069    0.02269
  2530.000   40.73999   40.76534    0.02534
  2540.000   40.76500   40.78090    0.01590
  2550.000   40.78000   40.79744    0.01744
  2560.000   40.81999   40.81496   -0.00504
  2570.000   40.83400   40.83350   -0.00050
  2580.000   40.85599   40.85306   -0.00293
  2590.000   40.88599   40.87367   -0.01231
  2600.000   40.92599   40.89537   -0.03062
  2610.000   40.94199   40.91815   -0.02383
  2620.000   40.94800   40.94206   -0.00594
  2630.000   40.96199   40.96707    0.00508
  2640.000   40.97400   40.99321    0.01921
  2650.000   41.02599   41.02046   -0.00552
  2660.000   41.03799   41.04886    0.01086
  2670.000   41.05899   41.07840    0.01941
  2680.000   41.09000   41.10907    0.01907
  2690.000   41.14899   41.14087   -0.00812
  2700.000   41.17599   41.17380   -0.00220
  2710.000   41.21999   41.20784   -0.01215
  2720.000   41.24300   41.24300   -0.00200
  2730.000   41.32599   41.27928   -0.04671
  2740.000   41.34000   41.31670   -0.02330
  2750.000   41.34799   41.35526    0.00726
  2760.000   41.39999   41.39497   -0.00502
  2770.000   41.41800   41.43588    0.01788
  2780.000   41.43399   41.47806    0.04407
  2790.000   41.51700   41.52156    0.00456
  2800.000   41.52899   41.56650    0.03751
  2810.000   41.58400   41.61304    0.02904
  2820.000   41.64299   41.66132    0.01833
  2830.000   41.66899   41.71155    0.04256
  2840.000   41.73799   41.76405    0.02606
  2850.000   41.81400   41.81912    0.00513
  2860.000   41.84999   41.87720    0.02721
  2870.000   41.92200   41.93874    0.01674
  2880.000   42.02599   42.00432   -0.02167
  2890.000   42.11400   42.07454   -0.03946
  2900.000   42.21999   42.15018   -0.06981
  2910.000   42.32700   42.23203   -0.09497
  2920.000   42.39499   42.32103   -0.07396
  2930.000   42.51799   42.41817   -0.09982
  2940.000   42.59299   42.52454   -0.06845
  2950.000   42.73000   42.64127   -0.08873
  2960.000   42.86400   42.76956   -0.09444
  2970.000   42.96999   42.91066   -0.05933
  2980.000   43.14999   43.06580   -0.08420
  2990.000   43.29099   43.23618   -0.05481
  3000.000   43.48399   43.42294   -0.06105
  3010.000   43.64099   43.62718   -0.01381
  3020.000   43.84299   43.84975    0.00676
  3030.000   44.08899   44.09137    0.00238
  3040.000   44.34900   44.35255    0.00356
  3050.000   44.60500   44.63347    0.02847
  3060.000   44.88599   44.93401    0.04802
  3070.000   45.19199   45.25366    0.06168
  3080.000   45.52100   45.59152    0.07053
  3090.000   45.84200   45.94623    0.10423
  3100.000   46.25899   46.31604    0.05705
  3110.000   46.59000   46.69868    0.10869
  3120.000   47.00200   47.09149    0.08949
  3130.000   47.45200   47.49136    0.03937
  3140.000   47.82799   47.89479    0.06680
  3150.000   48.31499   48.29796   -0.01703
  3160.000   48.66699   48.69678    0.02979
  3170.000   49.09698   49.08701   -0.00998
  3180.000   49.60100   49.46436   -0.13664
  3190.000   49.92899   49.82455   -0.10443
  3200.000   50.33800   50.16357   -0.17442
  3210.000   50.57399   50.47774   -0.09625
  3220.000   50.84499   50.76387   -0.08112
  3230.000   51.09499   51.01958   -0.07541
  3240.000   51.30699   51.24332   -0.06367
  3250.000   51.45200   51.43459   -0.01741
  3260.000   51.54599   51.59413    0.04814
  3270.000   51.58899   51.72383    0.13484
  3280.000   51.67599   51.82683    0.15083
  3290.000   51.72198   51.90727    0.18529
  3300.000   51.78200   51.97011    0.18811
  3310.000   51.86699   52.02069    0.15370
  3320.000   51.91299   52.06441    0.15141
  3330.000   51.97099   52.10614    0.13515
  3340.000   52.11499   52.14984    0.03485
  3350.000   52.24599   52.19820   -0.04779
  3360.000   52.34698   52.25215   -0.09483
  3370.000   52.50600   52.31076   -0.19524
  3380.000   52.50200   52.37106   -0.13094
  3390.000   52.59099   52.42805   -0.16293
  3400.000   52.75000   52.47475   -0.27525
  3410.000   52.63199   52.50252   -0.12947
  3420.000   52.63899   52.50145   -0.13754
  3430.000   52.53299   52.46078   -0.07220
  3440.000   52.37799   52.36967   -0.00832
  3450.000   52.06099   52.21817    0.15718
  3460.000   51.86800   51.99826    0.13026
  3470.000   51.67899   51.70528    0.22629
  3480.000   51.03400   51.33922    0.30522
  3490.000   50.65199   50.90608    0.25409
  3500.000   50.35100   50.41895    0.06795
  3510.000   49.81599   49.89890    0.08290
  3520.000   49.45999   49.37523   -0.08476
  3530.000   49.02699   48.88387   -0.14313
  3540.000   48.79700   48.46318   -0.33382
  3550.000   48.41199   48.14592   -0.26607
  3560.000   48.13499   47.94827   -0.18672
  3570.000   47.80199   47.85912    0.05713
  3580.000   47.58400   47.83383    0.24983
  3590.000   47.44199   47.79654    0.35455
  3600.000   47.42599   47.65326    0.22726
  3610.000   47.50000   47.31828   -0.18172
  3620.000   47.12000   46.75194   -0.36806
  3630.000   46.15799   45.98415   -0.17384
  3640.000   45.08400   45.09784    0.01384
  3650.000   43.91800   44.19142    0.27342
  3660.000   43.21999   43.35002    0.13004
  3670.000   42.57899   42.63028    0.05128
  3680.000   42.04599   42.05630    0.01031
  3690.000   41.69600   41.62451   -0.07149
  3700.000   41.29999   41.31358    0.01360
  3710.000   41.12799   41.09543   -0.03256
  3720.000   40.89999   40.94304    0.04305
  3730.000   40.82599   40.83484    0.00885
  3740.000   40.72400   40.75552    0.03152
  3750.000   40.65500   40.69507    0.04007
  3760.000   40.58899   40.64729    0.05830
  3770.000   40.56000   40.60838    0.04839
  3780.000   40.56099   40.57594    0.01495
  3790.000   40.55299   40.54839   -0.00461
  3800.000   40.51999   40.52461    0.00462
  3810.000   40.49899   40.50381    0.00482
  3820.000   40.49500   40.48537   -0.00963
  3830.000   40.49199   40.46883   -0.02316
  3840.000   40.49199   40.45384   -0.03815
  3850.000   40.48599   40.44012   -0.04587
  3860.000   40.48599   40.42747   -0.05852
  3870.000   40.47899   40.41574   -0.06325
  3880.000   40.47899   40.40480   -0.07419
  3890.000   40.47899   40.39455   -0.08444
  3900.000   40.47899   40.38492   -0.09407

BAND CENTER = 3087.9      BAND AREA =   1263.56348
BAND CENTER = 3270.0      BAND AREA =   3259.13672
BAND CENTER = 3472.0      BAND AREA =   1831.68066
BAND CENTER = 3610.9      BAND AREA =    376.39648
STOP      00325
```

APPENDIX VI

RESULTS OF THE BAND RESOLUTION OF THE ALKALI METAL HYDROXIDE SOLUTIONS

The results of the computerized analysis of the Raman spectra of all the alkali metal hydroxide mercerizing solutions are listed below. The spectra have not been normalized; therefore, comparisons between solutions with respect to height and integrated intensity (area) are not valid. The area of the peak at 3610 cm^{-1} was normalized as discussed earlier in the section entitled "Band Resolution of the Raman Spectra." The intensity ratios listed below refer to this normalization.

LIOH
MOLARITY = 1.059
MOLALITY = 1.057
STANDARD DEVIATION = 0.1373
FUNCTION PARAMETER = 0.998
INTENSITY RATIO = 7.39117

HEIGHT	CENTER	WIDTH	AREA
0.894	3088.9	527.7	502.777
13.252	3259.0	294.3	4155.805
10.515	3467.2	212.4	2380.248
3.091	3617.3	100.7	331.677

LIOH
MOLARITY = 2.083
MOLALITY = 2.080
STANDARD DEVIATION = 0.1536
FUNCTION PARAMETER = 0.994
INTENSITY RATIO = 8.83236

HEIGHT	CENTER	WIDTH	AREA
2.529	3082.2	525.2	1417.698
17.696	3265.1	306.4	5788.004
13.487	3468.7	206.3	2969.524
5.261	3614.0	99.8	560.744

LIOH
MOLARITY = 3.296
MOLALITY = 3.300
STANDARD DEVIATION = 0.1254
FUNCTION PARAMETER = 0.923
INTENSITY RATIO = 8.44806

HEIGHT	CENTER	WIDTH	AREA
1.866	3084.1	650.1	1338.345
10.920	3265.6	315.3	3799.071
8.408	3471.3	220.1	2041.641
3.675	3615.5	86.4	350.563

LIOH
MOLARITY = 3.732
MOLALITY = 3.739
STANDARD DEVIATION = 0.1349
FUNCTION PARAMETER = 0.901
INTENSITY RATIO = 8.27124

HEIGHT	CENTER	WIDTH	AREA
2.360	3089.6	643.9	1694.023
11.641	3265.9	314.5	4079.916
8.878	3471.3	224.3	2219.180
4.045	3611.8	81.6	367.889

LIOH
MOLARITY = 4.159
MOLALITY = 4.175
STANDARD DEVIATION = 0.1415
FUNCTION PARAMETER = 0.888
INTENSITY RATIO = 8.93087

HEIGHT	CENTER	WIDTH	AREA
2.927	3078.0	659.2	2163.341
13.568	3266.2	320.1	4868.816
10.238	3471.5	219.4	2518.078
5.246	3612.4	81.2	477.470

LIOH
MOLARITY = 4.882
MOLALITY = 4.914
STANDARD DEVIATION = 0.1243
FUNCTION PARAMETER = 0.925
INTENSITY RATIO = 10.23702

HEIGHT	CENTER	WIDTH	AREA
2.906	3080.9	676.8	2167.910
10.968	3267.6	325.6	3936.389
8.203	3472.2	219.2	1981.781
4.833	3611.6	84.3	448.926

LIOH
MOLARITY = 5.061
MOLALITY = 5.099
STANDARD DEVIATION = 0.1682
FUNCTION PARAMETER = 0.932
INTENSITY RATIO = 10.54500

HEIGHT	CENTER	WIDTH	AREA
3.457	3079.0	662.6	2517.239
12.285	3267.7	327.7	4424.410
9.376	3472.6	220.6	2272.958
5.844	3610.7	81.2	521.552

NAOH
MOLARITY = 0.851
MOLALITY = 0.851
STANDARD DEVIATION = 0.1877
FUNCTION PARAMETER = 1.000
INTENSITY RATIO = 6.61588

HEIGHT	CENTER	WIDTH	AREA
0.767	3090.9	567.5	463.087
15.426	3259.3	294.6	4838.234
12.410	3468.8	213.0	2813.673
3.242	3620.9	99.3	342.769

NAOH
MOLARITY = 1.795
MOLALITY = 1.796
STANDARD DEVIATION = 0.1385
FUNCTION PARAMETER = 0.946
INTENSITY RATIO = 7.72927

HEIGHT	CENTER	WIDTH	AREA
1.388	3083.7	585.9	887.648
13.898	3264.7	301.1	4568.504
11.387	3469.4	219.1	2724.085
3.751	3616.9	93.4	382.691

NAOH
MOLARITY = 2.297
MOLALITY = 2.300
STANDARD DEVIATION = 0.1134
FUNCTION PARAMETER = 0.922
INTENSITY RATIO = 8.48965

HEIGHT	CENTER	WIDTH	AREA
1.343	3083.4	595.8	883.549
11.192	3263.5	303.7	3752.640
9.598	3469.7	219.8	2329.317
3.472	3613.3	90.8	348.142

NAOH
MOLARITY = 2.793
MOLALITY = 2.808
STANDARD DEVIATION = 0.1302
FUNCTION PARAMETER = 0.915
INTENSITY RATIO = 7.80472

HEIGHT	CENTER	WIDTH	AREA
1.902	3083.7	646.4	1361.589
12.948	3265.7	309.5	4438.379
10.634	3470.2	222.5	2620.029
3.723	3611.1	91.1	375.728

NAOH
MOLARITY = 3.163
MOLALITY = 3.172
STANDARD DEVIATION = 0.1313
FUNCTION PARAMETER = 0.909
INTENSITY RATIO = 9.15661

HEIGHT	CENTER	WIDTH	AREA
2.199	3083.6	645.8	1577.298
12.417	3266.9	312.8	4312.855
10.462	3471.7	222.7	2587.706
4.651	3611.1	84.2	434.717

NAOH
MOLARITY = 3.644
MOLALITY = 3.664
STANDARD DEVIATION = 0.1319
FUNCTION PARAMETER = 0.898
INTENSITY RATIO = 8.77637

HEIGHT	CENTER	WIDTH	AREA
2.487	3088.0	660.6	1833.326
11.913	3267.8	315.8	4198.422
9.974	3471.5	224.5	2499.282
4.598	3608.9	78.7	403.918

NAOH
MOLARITY = 4.631
MOLALITY = 4.691
STANDARD DEVIATION = 0.1129
FUNCTION PARAMETER = 0.928
INTENSITY RATIO = 10.81461

HEIGHT	CENTER	WIDTH	AREA
2.639	3102.1	673.9	1958.074
9.654	3273.1	319.4	3394.203
8.220	3473.6	222.8	2016.614
4.737	3609.8	78.9	411.581

NAOH
MOLARITY = 5.228
MOLALITY = 5.624
STANDARD DEVIATION = 0.1480
FUNCTION PARAMETER = 0.900
INTENSITY RATIO = 12.30066

HEIGHT	CENTER	WIDTH	AREA
3.624	3074.5	673.2	2720.540
11.111	3274.3	322.0	3989.912
9.467	3474.3	218.4	2305.581
6.256	3607.4	80.2	559.623

NAOH
MOLARITY = 6.243
MOLALITY = 6.399
STANDARD DEVIATION = 0.1672
FUNCTION PARAMETER = 0.868
INTENSITY RATIO = 13.28619

HEIGHT	CENTER	WIDTH	AREA
3.482	3035.8	651.3	2565.407
10.203	3268.1	323.2	3730.012
9.346	3471.7	228.9	2420.436
6.559	3606.5	77.0	571.508

NAOH
MOLARITY = 7.771
MOLALITY = 8.120
STANDARD DEVIATION = 0.2225
FUNCTION PARAMETER = 0.832
INTENSITY RATIO = 15.28506

HEIGHT	CENTER	WIDTH	AREA
4.908	3026.5	648.2	3657.044
11.669	3275.0	340.6	4568.391
10.725	3473.8	232.7	2869.146
9.449	3605.9	75.9	824.271

NAOH
MOLARITY = 10.233
MOLALITY = 11.035
STANDARD DEVIATION = 0.3485
FUNCTION PARAMETER = 0.866
INTENSITY RATIO = 16.73018

HEIGHT	CENTER	WIDTH	AREA
5.695	2996.8	610.2	3935.190
11.023	3276.7	346.6	4325.879
9.726	3482.5	233.3	2569.235
11.432	3603.3	67.1	869.135

KOH
MOLARITY = 0.862
MOLALITY = 0.868
STANDARD DEVIATION = 0.2091
FUNCTION PARAMETER = 0.991
INTENSITY RATIO = 7.57241

HEIGHT	CENTER	WIDTH	AREA
0.911	3082.9	495.3	482.158
15.383	3260.5	292.2	4804.750
12.206	3466.5	208.6	2721.496
3.651	3617.8	100.8	393.644

KOH
MOLARITY = 1.572
MOLALITY = 1.596
STANDARD DEVIATION = 0.1316
FUNCTION PARAMETER = 0.936
INTENSITY RATIO = 8.06231

HEIGHT	CENTER	WIDTH	AREA
1.081	3083.7	552.7	655.185
11.906	3264.0	297.5	3884.946
9.926	3467.6	215.4	2345.446
3.153	3615.0	98.5	340.683

KOH
MOLARITY = 2.216
MOLALITY = 2.268
STANDARD DEVIATION = 0.1206
FUNCTION PARAMETER = 0.939
INTENSITY RATIO = 8.53746

HEIGHT	CENTER	WIDTH	AREA
1.425	3078.9	599.1	935.350
11.079	3263.5	303.3	3680.719
9.314	3468.9	217.9	2222.671
3.364	3614.4	93.2	343.573

KOH
MOLARITY = 2.692
MOLALITY = 2.778
STANDARD DEVIATION = 0.1393
FUNCTION PARAMETER = 0.914
INTENSITY RATIO = 8.74032

HEIGHT	CENTER	WIDTH	AREA
1.858	3084.0	649.5	1336.762
12.900	3264.8	308.1	4403.578
10.738	3469.7	218.6	2600.559
4.214	3613.0	90.3	421.749

KOH
MOLARITY = 3.282
MOLALITY = 3.418
STANDARD DEVIATION = 0.1711
FUNCTION PARAMETER = 0.901
INTENSITY RATIO = 8.60397

HEIGHT	CENTER	WIDTH	AREA
2.727	3083.7	647.2	1967.441
14.633	3268.6	313.7	5116.004
12.158	3471.1	220.2	2984.589
5.398	3610.5	80.0	481.618

KOH
MOLARITY = 3.492
MOLALITY = 3.641
STANDARD DEVIATION = 0 1030
FUNCTION PARAMETER = 0.882
INTENSITY RATIO = 10.38161

HEIGHT	CENTER	WIDTH	AREA
1.770	3086.2	636.2	1266.061
9.227	3270.0	314.1	3258.755
7.658	3471.7	212.4	1828.678
3.818	3610.9	88.0	377.502

KOH
MOLARITY = 3.695
MOLALITY = 3.865
STANDARD DEVIATION = 0.1182
FUNCTION PARAMETER = 0.882
INTENSITY RATIO = 10.28501

HEIGHT	CENTER	WIDTH	AREA
1.970	3085.7	656.0	1453.220
9.510	3270.4	313.0	3346.781
7.916	3471.7	211.3	1880.927
4.097	3610.1	83.3	383.678

KOH
MOLARITY = 3.959
MOLALITY = 4.164
STANDARD DEVIATION = 0.1281
FUNCTION PARAMETER = 0.911
INTENSITY RATIO = 10.58388

HEIGHT	CENTER	WIDTH	AREA
2.539	3091.2	654.6	1844.164
10.852	3271.5	316.7	3813.688
9.103	3472.3	215.0	2171.897
4.881	3608.9	83.3	451.413

KOH
MOLARITY = 4.919
MOLALITY = 5.310
STANDARD DEVIATION = 0.1354
FUNCTION PARAMETER = 0.906
INTENSITY RATIO = 11.48576

HEIGHT	CENTER	WIDTH	AREA
3.118	3068.6	683.8	2370.540
10.700	3275.0	327.4	3895.480
8.905	3472.2	218.7	2165.937
5.532	3605.6	82.2	505.484

KOH
MOLARITY = 5.808
MOLALITY = 6.412
STANDARD DEVIATION = 0.1183
FUNCTION PARAMETER = 0.848
INTENSITY RATIO = 12.16217

HEIGHT	CENTER	WIDTH	AREA
2.628	3066.7	660.1	1980.234
7.881	3273.1	326.5	2936.580
7.099	3475.3	224.6	1820.019
4.649	3607.7	76.6	406.604

KOH
MOLARITY = 9.677
MOLALITY = 11.459
STANDARD DEVIATION = 0.2517
FUNCTION PARAMETER = 0.872
INTENSITY RATIO = 17.92421

HEIGHT	CENTER	WIDTH	AREA
5.240	2999.2	623.7	3690.762
8.932	3274.2	345.7	3486.667
8.305	3482.1	226.0	2119.615
9.420	3599.9	71.6	761.440

APPENDIX VII

CALCULATION OF THEORETICAL ACTIVITY COEFFICIENTS — PROGRAMS DEH3 AND DEH4

This program, which is stored on disk under the RAX system as DEH3, can be used to calculate the theoretical activity coefficient from 0.001 to 6 molal according to the following equation:

$$\ln \gamma\pm = -AZ_1Z_2\sqrt{\mu}/(1 + B\mathring{a}\sqrt{\mu}) - (h/\nu)(\ln a_w) - \ln[1 - 0.018(h-\nu)m] \qquad (43)$$

The program computes and prints the Debye-Huckel term, the experimental osmotic coefficient, the theoretical mean activity coefficient, the experimental mean activity coefficient, the difference between the two activity coefficients, the free water not bound in hydration, and the "true molality," based on the assumption that water of hydration is no longer effectively solvent.

The data input include P, which is the mean hydrated ion diameter, or distance of closest approach parameter $\mathring{a}$, in the Debye-Huckel term. The units of P are in angstroms; H is the hydration number defined as moles of water/mole of solute. These two parameters are the only parameters which are used in the theoretical calculation.

The parameters BM, Beta, C, D, and E are empirical parameters from a National Bureau of Standards Report (89) and are used in regenerating the experimental activity coefficient and osmotic coefficient data used in this program. These parameters are referred to as B_M^*, β, C, S_ϕ, and S_γ in the NBS report. The program is set up to store the results on disk, Sysfl 1, so that they may be plotted by Program DEH4.

```
C DEH3(1BED) A PROGRAM SIMILIAR TO DEH2 TO CALCULATE THE SAME
C PARAMETERS AND STORE THEM IN A FILE FOR PLOTTER USE
C*************************************************************
C PROGRAM DEH2(1BED) A PROGRAM TO THEORETICALLY CALCULATE ACTIVITY COEFFICIENTS
C WHICH INCLUDES THE DEBYE HUCKEL TERM AS WELL AS TWO TERMS WHICH TAKE INTO
C ACCOUNT THE EFFECTS OF HYDRATION.  THE BASIS FOR THIS APPROACH WAS DEVELOPED
C BY ROBINSON AND STOKES.  THE DEFINITION OF THE VARIABLES INVOLVED FOLLOWS
C A = THE A PARAMETER IN THE DEBYE HUCKEL THEORY, TEMPERATURE DEPENDENT
C B = THE B PARAMETER IN THE DEBYE HUCKEL THEORY, TEMPERATURE DEPENDENT
C P = THE ION SIZE PARAMETER OR DISTANCE OF CLOSEST APPROACH
C M = MOLALITY
C GAMDH = LOG OF THE ACTIVITY COEFFICIENT AS CALCULATED FROM DEBYE HUCKEL
C AGDH = ACTIVITY COEFFICIENT CALCULATED FROM DEBYE HUCKEL
C BM = EMPIRICAL COEFFICIENT FROM NBS
C BETA = EMPERICAL COEFFICIENT FROM NBS
C C = EMPERICAL COEFFICIENT C,NBS
C D = SAME
C E = SAME
C OS = OSMOTIC COEFFICIENT AS CALCULATED FROM NBS
C Q =  -1/VLOG ACTIVITY OF H2O
C LMAC = LOG MEAN ACTIVITY COEFFICIENT
C MAC = MEAN ACTIVITY COEFFICIENT
C FREEW = FREE WATER NOT BOUND UP IN HYDRATION

C H  = THE HYDRATION NUMBER
C EAC =  EXPERIMENTAL ACTIVITY COEFFICIENT
C DIFF =  DIFFERENCE BETWEEN EAC AND MAC
C TM = TRUE MOLALITY
C
      REAL A, B, P, M, GAMDH, AGDH, BM, BETA, C, D, E, OS
      REAL Q, LMAC, MAC, FREEW, TM, LEAC, EAC, DIFF, H
      READ (5, 20) P, H
20    FORMAT (2F10.3)
      WRITE (6, 21) P, H
21    FORMAT (1H1, 4HP = , F5.2, 10X, 4HH = , F5.2///)
C OSMOTIC COEFFICIENT PARAMETERS READ IN HERE
      READ (5, 22) BM, BETA, C, D, E
22    FORMAT (5F10.0)
      WRITE (6, 23)
23    FORMAT (1H , 33HMOLAL DEBYE HU  OSCOEF  ACT COEF ,
     1 40H   EAC          DIFF  FREEWATER   TM     ///)

C THIS SECTION COMPUTES THE DEBYE HUCKEL TERM
      M = 0.001
25    A = 0.5108
      B = 0.3287
      GAMDH = 0
      AGDH = 0

      GAMDH = (-A*(SQRT(M)))/(1 + B*P*(SQRT(M)))
      AGDH = 1.0/(10.0**(ABS(GAMDH)))
C NOW THE OSMOTIC COEFFICIENT IS CALCULATED USING EXPERIMENTAL DATA FROM
C NBS
      OS = 0
      Q = C
      OS = 1.0 - ((2.302585*A)/((BM**3)*M))*(1.00 + BM*SQRT(M) -
     1  2*ALOG(1 + BM*SQRT(M)) - 1.0/(1.0 + BM*SQRT(M))) +
     1  (2.302585)*(BETA*M/2.0 + (2*C*(M**2))/3 + (3*D*(M**3))/4
     1  + (4*E*(M**4))/5)
26    Q = 0.007824*M*OS

      LMAC = GAMDH + (M*Q) - ALOG10(1.0 -0.018*(M - 2)*M)
      IF (LMAC - 0.0) 27, 29, 29
27    MAC = 1.0/(10.0**(ABS(LMAC)))
      GO TO 28
29    MAC = 10.0**LMAC
28    FREEW = 55.51 - M*M
      LEAC = -(A*SQRT(M))/(1 + BM*SQRT(M)) + BETA*M + C*(M**2) +
     1  D*(M**3) + E*(M**4)
      IF (LEAC) 30, 31, 31
30    EAC = 1.0/(10.0**(ABS(LEAC)))
      GO TO 32
31    EAC = 10.0**LEAC
32      DIFF = EAC - MAC
      TM = (55.51*M)/(55.51 - (H*M))
      WRITE (6, 401) M, AGDH, OS, MAC, EAC, DIFF, FREEW, TM
401   FORMAT (F7.3, 2F8.4, 5F10.4)
      WRITE (1, 9001) M, AGDH, OS, MAC, EAC, DIFF, FREEW, TM
9001  FORMAT (8A4)
      IF (M - 0.009) 40, 50, 50
40    M = M + 0.001
      GO TO 25
50    IF (M - 0.09) 51, 52, 52
51    M = M + 0.01

      GO TO 25
52    M = M + 0.100



      IF (M - 6.00) 25, 25, 60
60    END FILE 1
      STOP
      END
```

SAMPLE OUTPUT FOR KOH

P = 3.82 H = 6.40

MOLAL	DEBYE HU	OSCOEF	ACT COEF	EAC	DIFF	FREEWATER	TM
0.001	0.9649	0.9883	0.9650	0.9650	-0.0000	55.5036	0.0010
0.002	0.9514	0.9840	0.9518	0.9517	-0.0001	55.4972	0.0020
0.003	0.9415	0.9808	0.9420	0.9420	-0.0001	55.4908	0.0030
0.004	0.9334	0.9782	0.9341	0.9340	-0.0001	55.4844	0.0040
0.005	0.9265	0.9760	0.9273	0.9272	-0.0002	55.4780	0.0050
0.006	0.9203	0.9741	0.9214	0.9212	-0.0002	55.4716	0.0060
0.007	0.9148	0.9723	0.9160	0.9158	-0.0002	55.4652	0.0070
0.008	0.9098	0.9708	0.9111	0.9109	-0.0002	55.4588	0.0080
0.009	0.9051	0.9693	0.9067	0.9064	-0.0002	55.4524	0.0090
0.010	0.9008	0.9680	0.9025	0.9022	-0.0003	55.4460	0.0100
0.020	0.8683	0.9584	0.8716	0.8712	-0.0004	55.3820	0.0200
0.030	0.8459	0.9522	0.8507	0.8503	-0.0005	55.3180	0.0301
0.040	0.8286	0.9477	0.8345	0.8344	-0.0005	55.2540	0.0402
0.050	0.8144	0.9443	0.8221	0.8215	-0.0005	55.1900	0.0503
0.060	0.8023	0.9415	0.8114	0.8108	-0.0005	55.1260	0.0604
0.070	0.7917	0.9393	0.8022	0.8016	-0.0005	55.0620	0.0706
0.080	0.7823	0.9376	0.7942	0.7936	-0.0005	54.9980	0.0807
0.090	0.7739	0.9361	0.7871	0.7866	-0.0005	54.9340	0.0909
0.100	0.7663	0.9349	0.7808	0.7803	-0.0004	54.8700	0.1012
0.200	0.7140	0.9309	0.7413	0.7416	0.0003	54.2300	0.2047
0.300	0.6827	0.9340	0.7223	0.7237	0.0014	53.5900	0.3107
0.400	0.6606	0.9401	0.7124	0.7150	0.0025	52.9500	0.4193
0.500	0.6437	0.9480	0.7079	0.7116	0.0037	52.3100	0.5306
0.600	0.6301	0.9569	0.7068	0.7117	0.0049	51.6700	0.6446
0.700	0.6188	0.9666	0.7083	0.7144	0.0061	51.0300	0.7615
0.800	0.6093	0.9768	0.7118	0.7190	0.0072	50.3900	0.8813
0.900	0.6010	0.9875	0.7169	0.7252	0.0083	49.7500	1.0042
1.000	0.5937	0.9985	0.7234	0.7327	0.0093	49.1100	1.1303
1.100	0.5872	1.0098	0.7311	0.7413	0.0102	48.4700	1.2598
1.200	0.5814	1.0214	0.7399	0.7509	0.0110	47.8300	1.3927
1.300	0.5761	1.0331	0.7498	0.7615	0.0117	47.1900	1.5292
1.400	0.5713	1.0451	0.7606	0.7729	0.0123	46.5500	1.6695
1.500	0.5669	1.0573	0.7724	0.7851	0.0127	45.9100	1.8137
1.600	0.5628	1.0695	0.7851	0.7981	0.0130	45.2700	1.9619
1.700	0.5591	1.0820	0.7987	0.8118	0.0131	44.6300	2.1144
1.800	0.5556	1.0945	0.8132	0.8262	0.0130	43.9900	2.2714
1.900	0.5523	1.1072	0.8286	0.8413	0.0127	43.3500	2.4330
2.000	0.5492	1.1200	0.8449	0.8571	0.0122	42.7100	2.5994
2.100	0.5464	1.1328	0.8622	0.8735	0.0114	42.0700	2.7709
2.200	0.5436	1.1458	0.8804	0.8907	0.0103	41.4300	2.9477
2.300	0.5411	1.1589	0.8996	0.9086	0.0089	40.7900	3.1300
2.400	0.5387	1.1721	0.9199	0.9271	0.0072	40.1500	3.3181
2.500	0.5364	1.1853	0.9412	0.9463	0.0052	39.5100	3.5124
2.600	0.5342	1.1986	0.9635	0.9662	0.0027	38.8701	3.7130
2.700	0.5321	1.2120	0.9871	0.9869	-0.0002	38.2301	3.9204
2.800	0.5301	1.2254	1.0118	1.0082	-0.0035	37.5901	4.1348
2.900	0.5282	1.2389	1.0377	1.0303	-0.0074	36.9501	4.3566
3.000	0.5264	1.2525	1.0649	1.0531	-0.0118	36.3101	4.5863
3.100	0.5247	1.2662	1.0934	1.0767	-0.0167	35.6701	4.8242
3.200	0.5230	1.2799	1.1234	1.1011	-0.0223	35.0301	5.0708
3.300	0.5214	1.2936	1.1548	1.1262	-0.0286	34.3901	5.3266
3.400	0.5199	1.3074	1.1878	1.1521	-0.0357	33.7501	5.5921
3.500	0.5184	1.3212	1.2224	1.1789	-0.0435	33.1101	5.8678
3.600	0.5170	1.3351	1.2587	1.2065	-0.0522	32.4701	6.1544
3.700	0.5156	1.3491	1.2967	1.2349	-0.0618	31.8301	6.4526
3.800	0.5143	1.3630	1.3367	1.2642	-0.0725	31.1901	6.7629
3.900	0.5130	1.3770	1.3787	1.2944	-0.0843	30.5501	7.0863
4.000	0.5117	1.3911	1.4227	1.3256	-0.0972	29.9101	7.4235
4.100	0.5105	1.4052	1.4690	1.3576	-0.1114	29.2701	7.7755
4.200	0.5094	1.4193	1.5176	1.3907	-0.1269	28.6301	8.1432
4.300	0.5083	1.4334	1.5687	1.4247	-0.1440	27.9901	8.5277
4.400	0.5072	1.4476	1.6224	1.4597	-0.1626	27.3501	8.9302
4.500	0.5061	1.4618	1.6788	1.4958	-0.1830	26.7101	9.3520
4.600	0.5051	1.4760	1.7381	1.5329	-0.2052	26.0701	9.7945
4.700	0.5041	1.4902	1.8005	1.5711	-0.2294	25.4301	10.2593
4.800	0.5031	1.5045	1.8662	1.6104	-0.2558	24.7901	10.7481
4.900	0.5021	1.5187	1.9354	1.6509	-0.2845	24.1501	11.2628
5.000	0.5012	1.5330	2.0082	1.6925	-0.3157	23.5101	11.8055
5.100	0.5003	1.5473	2.0849	1.7354	-0.3495	22.8701	12.3786
5.200	0.4995	1.5616	2.1657	1.7794	-0.3863	22.2302	12.9846
5.300	0.4986	1.5759	2.2510	1.8247	-0.4263	21.5902	13.6266
5.400	0.4978	1.5902	2.3409	1.8713	-0.4696	20.9502	14.3079
5.500	0.4970	1.6045	2.4357	1.9192	-0.5165	20.3102	15.0321
5.600	0.4962	1.6189	2.5359	1.9685	-0.5674	19.6702	15.8033
5.700	0.4954	1.6332	2.6416	2.0192	-0.6225	19.0302	16.6265
5.800	0.4946	1.6475	2.7534	2.0712	-0.6821	18.3902	17.5070
5.900	0.4939	1.6619	2.8715	2.1248	-0.7467	17.7502	18.4509
6.000	0.4932	1.6762	2.9964	2.1798	-0.8166	17.1102	19.4655
STOP	00000						

PROGRAM DEH4

This program is used in conjunction with DEH3. The program plots the theoretical activity coefficient as an annotated line and the experimental activity coefficient as a solid line.

The activity data are read from disk, Sysfl 1, and the heading and x and y axis labels are read from cards.

```
C DEH4 PROGRAM USED TO PLOT ACTIVITY COEFFICIENT DATA GENERATED
C IN DEH3 AND STORED IN DISK FILE SYSFL1
C
C
      INTEGER HEAD(20), IX(20), IY(20)
      REAL M(80), AGDH(80), OS(80), MAC(80), EAC(80),DIFF(80)
      REAL FREEW(80), TM(80)
      KOUNT = 78
      DO 1 I = 1, KOUNT
1     READ (1, 9002) M(I), AGDH(I), OS(I), MAC(I), EAC(I), DIFF(1),
     1 FREEW(I), TM(I)
9002  FORMAT (8A4)
      CALL ITLZ
      CALL DPT(1, 4)
      CALL PLOT(0.,-11.,3)
      CALL PLOT(0.,-9.5,-3)
C     READ THE HEADING FOR THE PLOT FROM A DATA CARD
      READ(5, 9003) HEAD
9003  FORMAT (20A4)
      READ (5, 9003) IX
      READ (5, 9003) IY

C SCALE BOTH THE X AND Y AXIS
      CALL SCALE(M,8.,KOUNT,1)
      CALL SCALE(EAC,6.,KOUNT,1)
C DRAW THE X AND Y AXIS WITH ANNOTATION
      M(KOUNT + 1) = 0
      M(KOUNT + 2) = 0.75
      CALL AXIS(0.,0.,IX,-30,8.,0.,M(KOUNT + 1),M(KOUNT + 2))
      EAC(KOUNT + 1) = 0
      EAC(KOUNT + 2) = .5
      CALL AXIS(0.,0.,IY,30,6.,90., EAC(KOUNT + 1),EAC(KOUNT + 2))

C PLOTT EAC VS MOLALITY
      CALL LINE(M,EAC,KOUNT,1,0,0)
      MAC(KOUNT + 1) = 0
      MAC(KOUNT + 2) = .5
      CALL LINE(M,MAC,KOUNT,1,9,4)
C WRITE THE HEADING ON THE PLOT
      CALL SYMBOL(2.,5.,.14,HEAD,0.,30)
      CALL FINAL
      CALL EXIT
      END
```